

The sediment capture efficiency of a managed realignment polder

Master Civil Engineering - Hydraulic Engineering
Tijmen Hilgersom



The sediment capture efficiency of a managed realignment polder

by

Tijmen Hilgersom

to obtain the degree of Master of Science
at the Delft University of Technology,
to be defended publicly on Tuesday March 8, 2023 at 15:30 AM.

Student number:	4388720	
Project duration:	March 1, 2022 – March 8, 2023	
Thesis committee:	Prof. dr. ir. S.G.J. Aarninkhof,	Delft University of Technology
	Dr. D.S. van Maren,	Delft University of Technology & Deltares
	Ir. R.J.A. van Weerdenburg,	Deltares
	Dr. ir. B.C. van Prooijen,	Delft University of Technology

Cover:	Artist impression inner-dike intertidal area (ED2050, 2017: Hydro-morfologische verbetering, voorstel voor vervolg. Versie 1.0)
Style:	TU Delft Report Style, with modifications by Daan Zwaneveld

An electronic version of this thesis is available at <http://repository.tudelft.nl/>.

Abstract

The Ems Dollart estuary is facing high levels of turbidity, which hinders the growth of algae and impacts the entire ecosystem. In recent years, turbidity has increased here with 0.5 to 3% per year between 1990 and 2010, corresponding to a doubling of suspended sediment concentration (SSC) within 24 years for the upper bound of 3% (van Maren et al., 2016). This trend is mainly attributed to a decrease in the amount of sediment sinks (van Maren et al., 2016). The Ems-Dollart 2050 program aims to address this issue by exploring various solutions, aiming to extract one million tons of dry matter from the estuary per year. This study investigates the potential of creating additional sediment sinks by scaling up managed realignment polders. The aim of the research is:

To investigate the important factors of influence for sediment capturing efficiency in a managed realignment polder, to make the mud extraction from a turbid estuary as efficient as possible while creating new natural and agricultural value.

Using the Delft3D FM numerical model, the study focuses on two key factors that influence sediment capturing, namely the effects of the surface area and the effect of the tidal prism (i.e. the volume of water that flows into an area during a tidal cycle), with the goal of making sediment extraction from the turbid estuary as efficient as possible. The study finds that the general concept of using a managed realignment polder to extract sediment is viable. However, the calibration process using Polder Breebaart revealed that the model struggled to accurately replicate some of the accumulation patterns in the low-dynamic system in this polder. While the model seems more appropriate for the project area, significant uncertainty remains due to the sensitivity of the results to sediment properties and calibration parameters.

The study's results suggest that a smaller tidal range can result in a more uniform sediment distribution across the area. This can be achieved by implementing a submerged weir behind the open entrance to the area. An even distribution of sediment could enhance the natural values in the intertidal area, which is a key goal of the Ems-Dollart 2050 program. In addition, wind-generated waves appear to have a major influence on the distribution of sediment over the area. Due to the extra shear stresses, waves provide more resuspension, which transports the sediment further.

Furthermore, the study observes a significant accumulation of sediment in a side-basin near the entrance. The high sediment accumulation in this area, compared to adjacent areas without accumulation, may be attributed to local low energetic conditions. This finding has potential implications for raising agricultural land using transitional polders.

In conclusion, this study provides insights into the effectiveness of using managed realignment as a method for extracting sediment from a turbid estuary. While it highlights some important aspects and influences, it also underscores the need for further research to confirm the findings and reduce the uncertainty in the results. Nevertheless, the potential benefits for both natural and agricultural values make this an intriguing avenue for future exploration.

Preface

The master thesis “The sediment capture efficiency of a managed realignment polder”. This thesis concludes the Master of Science program in Hydraulic Engineering at the Delft University of Technology. The research was carried out at the Deltares research institute. I am grateful for the opportunity to conduct my thesis research in such a professional environment and I look back with pride on the pleasant experience of the past year.

During the specialization courses during my Master’s study I developed a huge interest in the ‘Building with Nature’ approach; an approach to hydraulic engineering that harnesses the forces of nature to benefit environment, economy and society. I am grateful to Mindert de Vries for helping me find an opportunity to graduate in this field. By being able to delve into this further, I have only become more convinced of this approach. I also learned a lot about the approach of an investigation. Looking back, I would start writing my report earlier and feel more confident in asking questions throughout the process. During my research I gained a lot of experience with the coastal modeling software Delft3D FM. Delft3D FM is a powerful numerical modeling software used to simulate hydrodynamics, sediment transport, and morphology in a range of water environments. With this skill I have developed a valuable skill that will probably be of great use to me. In conclusion, this thesis has been a rich learning experience for me, both personally and professionally.

This thesis would not have been possible without the help of my graduation committee. That’s why I want to thank Bas van Maren for the regular help. Your constructive feedback, extensive knowledge of the processes and interest in the results was very helpful throughout the process. Also Roy van Weerdenburg for your daily help and accessibility. I really appreciate that you always made time when I got stuck and/or asked questions. The investigation has gained momentum since you became involved. Thank you also for your help with the models, especially when the results were once again inexplicable. Thank you Stefan Aarninkhof for chairing the committee and guiding the project. In addition, thanks for the creative ideas during the various committee meetings and the feedback on the report. Thank you Bram van Prooijen for the feedback and help in the last phase of the project, some of your comments were very valuable for building the report.

I would also like to thank Peter Esselink for making the data about Polder Breebaart available. Without this data I would not have been able to calibrate the model. Thank you Albert Vos and Matthijs Buurman for initiating the research and helping to define the outer limits of the realignment project area. This research was financially supported by the EU project REST-COAST.

Finally, I would like to thank my family and friends for their support, enthusiasm or just a listening ear. I had a great time, not only during my graduation, but also during the past years studying at Delft University of Technology.

*Tijmen Hilgersom
Delft, February 2023*

Contents

Abstract	ii
Preface	iv
Nomenclature	ix
1 Introduction	1
1.1 Background and problem statement	1
1.2 Relevance of research	2
1.3 Aim and research approach	2
1.4 Outline	3
2 Building the conceptual model	4
2.1 The Ems Dollart estuary	4
2.1.1 Historical development of Ems Dollart	4
2.1.2 Turbidity in the Ems Dollart	5
2.2 Managed realignment polders	6
2.2.1 General concept of managed realignment	6
2.2.2 Polder Breebaart	8
2.3 Relevant processes	8
2.3.1 Erosion and deposition	9
2.3.2 Transport	10
2.3.3 Flocculation	10
2.3.4 Tidal forcing	10
2.3.5 Tidal asymmetry	10
2.3.6 Settling lag	12
2.3.7 Scour lag	13
2.3.8 Tidal basin area	13
2.3.9 Waves	13
2.3.10 Consolidation	14
2.3.11 Vegetation	15
2.3.12 Other environmental factors	15
2.4 Tidal flats and salt marshes	15
2.4.1 Tidal flat food web	16
2.4.2 Tidal flat and salt marsh morphodynamics	16
2.5 The conceptual model	16
2.5.1 Reduction of high turbidity level	17
2.5.2 Sediment import in polder	17
2.5.3 Effect of hydrodynamic forcing on resuspension of sediment	17
2.5.4 Factors influencing sediment accumulation and distribution	17
2.5.5 Additional benefits	17
2.5.6 Neglected processes	17
2.5.7 Polder Breebaart for calibration	18
2.5.8 Important parameters for calibration	18
2.5.9 Research questions	19
3 Methodology	20
3.1 Data analysis	20
3.2 Model set-up calibration: Polder Breebaart	20
3.2.1 Grid and bathymetry	21
3.2.2 Forcing conditions	22

3.2.3	Design choices	23
3.2.4	Performance evaluation	23
3.3	Model set-up application: Realignment project area	25
3.3.1	Grid schematization	26
3.3.2	Bathymetry	26
3.3.3	External forcing conditions	27
3.3.4	Design choices	28
3.3.5	Model scenarios	30
3.3.6	Wave effect	31
3.4	Assessment of application results	31
3.4.1	Total sediment extraction	31
3.4.2	Spatial sediment distribution	31
4	Results	32
4.1	Insights from data analysis	32
4.1.1	General accumulation pattern	32
4.1.2	Total sediment import	32
4.1.3	Distribution between northern part and southern part of Polder Breebaart	32
4.1.4	Distribution between tidal flat and channel	33
4.2	Calibration phase of the model: Polder Breebaart	33
4.2.1	Parthediades-Krone parameters	34
4.2.2	Only tide effect	34
4.2.3	Wind effect	35
4.2.4	Wave effect	35
4.2.5	Increased tidal energy	35
4.2.6	Parameters from calibration	35
4.2.7	Assessment during calibration	37
4.2.8	Overall assessment	38
4.3	Application phase: realignment project area	38
4.3.1	Sediment extraction	38
4.3.2	Spatial accumulation distribution	39
4.3.3	Elevation distribution of accumulation	46
4.3.4	Wave effect	49
4.3.5	Key findings	50
5	Discussion	54
5.1	Uncertainty in the approach	54
5.1.1	Suitability of calibration location	54
5.1.2	Possible limiting factors in Polder Breebaart model	54
5.1.3	Simplifications	55
5.2	Optimization of the design	56
5.2.1	Reliability of the model results	56
5.2.2	Elevations are dependent on spatial location	56
5.2.3	Important neglected complex processes	56
5.2.4	Ecological benefits	57
5.3	Generalizing the results	57
6	Conclusions	58
6.1	The general concept of sediment extraction with a managed realignment polder	58
6.2	Effect of surface area of the managed realignment polder	58
6.3	Influence of shape of the managed realignment polder	58
6.4	Effect of incoming tidal energy	59
6.5	Impact of waves	59
6.6	Additional natural and agricultural value	59
7	Recommendations	60
7.1	Recommendation for further research on this project	60
7.1.1	Calibration	60

7.1.2 Application	60
7.2 General research recommendations	61
References	62
A Methodology overview	72
B Literature study	74
B.1 Historical development of Ems Dollart	74
B.2 observed changes in turbidity and biomass in the Ems Dollart	74
B.2.1 The increase of turbidity	74
B.2.2 The decrease in algae biomass	78
B.3 Causes of turbidity increase in Ems Dollart	80
B.3.1 Decrease of sinks	80
B.3.2 Turbidity of Ems River	80
B.3.3 Increase in suspended sediment in the Wadden	83
B.3.4 Dredging activities	83
B.3.5 Channel Deepening	83
B.4 managed realignment	84
B.4.1 The Medway Estuary	84
B.4.2 The Hedwige-Prosper Polder	84
B.5 Tidal flat and salt marsh morphodynamics	86
C Calibration findings	88
C.1 Settling velocity	88
C.2 Critical shear stress	88
C.3 Erosion Parameter	89
C.4 Wave-stirring parameter	89
C.5 One or two sediment fractions	89
C.6 Breaker index	90
D Model results project area	96
E SSC measuring stations	107
F The conceptual model	109
G Creation tidal boundary Polder Breebaart	111
H Meteorological forcing condition	113
I Main calibration problems and solutions	115
J Assessment methods	117
J.1 Sediment import	117
J.2 Mean absolute error	117
J.3 Brier Skill Score	118
J.4 The python function	118
K Creation bed level change map Polder Breebaart	120
L Numerical model choice	123
L.1 Numerical coastal model	123
L.1.1 Model calibration	123
L.1.2 Polder Breebaart for calibration	124
L.1.3 Grid and bed schematization	124
L.2 Rectangular grid vs. triangular grid	124
M Domain boundary of realignment project area	126
N Impact of coordinate system on Polder Breebaart model	129

Nomenclature

Abbreviations

Abbreviation	Definition
AHN	Actueel Hoogtebestand Nederland
BSS	Briar Skill Score
D3D	Delft3D
DFM	Delft3D Flexible Mesh
HW	High water
KNMI	Royal Netherlands Meteorological Institute
LW	Low water
MAE	Mean Absolute Error
MHT	Mean high tide
MLT	Mean low tide
MSL	Mean Sea Level
MTR	Mean Tidal Range
NAP	Normaal Amsterdams Peil
RWS	Rijkswaterstaat
SSC	Suspended sediment concentration
SPM	Suspended Particle Matter
WCI	Wave-current interaction

Symbols

Symbol	Definition	Unit
A_c	Cross sectional area	$[m^2]$
a	Coefficient for O'brien inlet calculation	$[-]$
C	Concentration	$[kg/m^3]$
D	Deposition flux	$[kg/m^2/s]$
E	Erosion flux	$[kg/m^2/s]$
H_b	Wave height at breaking	$[m]$
H_{RMS}	Root mean square wave height	$[m]$
h_b	Water depth at breaking	$[m]$
M	Erosion parameter	$[kg/m^2/s]$
m	Coefficient for O'brien inlet calculation	$[-]$
n	Manning's roughness coefficient (= 0.015)	$[s/m^{1/3}]$
P	Prism	$[m^3]$
w_s	Settling velocity	$[m/s]$
γ_b	Breaker index	$[-]$
ρ_s	Specific density mud (= 2650)	$[kg/m^3]$
ρ_b	Dry bed density mud (= 500)	$[kg/m^3]$
τ_b	Occurring bed shear stress	$[N/m^2]$
τ_c	Current induced bed shear stress	$[N/m^2]$
τ_{cr}	Critical (threshold) bed shear stress	$[N/m^2]$
τ_{max}	Maximum bed shear stress	$[N/m^2]$
τ_w	Wave induced bed shear stress	$[N/m^2]$

Introduction

The goal of the Ems-Dollart 2050 program is to reduce the turbidity. This chapter provides background information and the problem statement regarding the turbidity in the Ems Dollart estuary. In addition, the relevance of the research is explained, the aim is stated and the research method is presented.

1.1. Background and problem statement

The estuary of the Ems Dollart has been suffering from high turbidity levels for years. The high suspended sediment concentration (SSC) reduces light penetration in the water, which limits the growth of algae (Colijn and Cadée, 2003). This also effects the rest of the ecology, because algae are the base of the food web in the Ems Dollart (de Jonge and Schückel, 2019). In the Netherlands, the Ems Dollart estuary and the Western Scheldt are the last open connections to the sea. As a result, the Ems Dollart has a unique ecological function with characteristic estuarine nature such as salt marshes and mudflats. This landscape is home to salt-tolerant plants, birds, seals, and many small benthic animals that play an important role in the entire food web of the Wadden Sea. Besides the ecologic function, this estuary has an important economic function for the three ports of Eemshaven, Delfzijl and Emden.

The estuary between Groningen (NL) and East Frisia (GE) is naturally already very turbid, but various studies have shown that this turbidity has increased considerably (de Jonge et al., 2014; van Maren et al., 2015). This increase has several causes, but is mainly attributed to the decrease in sediment sinks in the system (van Maren et al., 2020). At the same time, a significant decrease in algae (especially the floating phytoplankton) biomass has been observed (de Jonge and Schückel, 2019).

In 2014, the decline in ecology was the reason for a partnership between the national government, the province of Groningen, the business community, and environmental organizations. Together they came to the Ems-Dollart 2050 program plan. This program aims to bring ecology and economy back into balance. It works on ecological recovery through various projects and pilots. The second phase of this plan started in 2021. In this phase, the focus is more on scaling up different strategies to structurally work on an improved ecology (van Es, 2021).

Before the correct measures can be taken against the turbidity, it is important to understand the causes of the turbidity. There are various causes for the increased turbidity, but an important one is the decrease in sediment sinks in the estuary (Taal et al., 2015; van Maren et al., 2016). Because the number of sediment sinks has decreased, less sediment can settle down and more sediment remains in suspension in the estuary. By creating a new location where the sediment can settle, the sediment can be extracted from the water body. A potential way to create sediment sinks is by restructuring agricultural land into intertidal areas. This way of restructuring is called managed realignment and has been successfully applied in several places (Clapp, 2009; Esteves, 2013; Morris, 2012). This creates space for nature development and at the same time increases flood safety. Not much is known about its effectiveness in capturing sediment in such an area.

In the vicinity of the Ems Dollart, the ground level has subsided by draining the agricultural land. This water extraction and subsidence cause peat oxidation, which releases a lot of CO₂, and thereby accelerates the subsidence process (Hoogland et al., 2012). As a result, the agricultural sector must

deal with salinization of the soil and much of the area is below sea level. The large amounts of suspended sediment in the Ems Dollart can possibly be used to raise agricultural land and thus make it future-proof but also more productive. Accumulated sediment can also be used for dike reinforcements or it can be used to compress bio building elements (van Es, 2021). Finally, the estuary provides an important ecological function through its gradual transition between the fresh inland area and the salty sea. More intertidal areas would strengthen the ecological value of the estuary.

In summary, the Ems Dollart estuary is facing high turbidity levels that have negative impacts on its ecology and economy. Using managed realignment areas as sediment sinks is a potential solution to address this issue, but there is limited knowledge on the efficiency of this approach. This research aims to investigate the potential of an managed realignment polder as sediment sink in the Ems Dollart estuary and contributes to the ongoing efforts to balance ecology and economy in the area.

1.2. Relevance of research

As part of the Ems-Dollart 2050 program, several pilot initiatives have been launched with the aim of enhancing the ecological value of the region. One goal is to extract 1 million tons of dry mud from the estuary per year (van Es, 2021). The 'Kleine polder', 'Dubbele Dijk' and 'Groote polder/Eemshilten' pilot projects are testing the feasibility of sediment capture in inner dike areas (Schmidt et al., 2021). The inner dike tidal area, Polder Breebaart, established in 2001, has been largely silted up (with a speed of 5 to 10 cm/year, Tydeman (2005)) in the first 10 years after opening to tidal exposure (Schmidt et al., 2019). Although these tidal areas are small, they have the potential to be scaled up, as is being explored (van Paridon x de Groot | abe veenstra landschapsarchitect, 2020). However, much is yet unknown about the challenges that such scaling may entail. To maximize mud capture efficiency, factors affecting sedimentation and accumulation in the polders should be studied and optimized.

1.3. Aim and research approach

The aim of this research is:

To investigate the important factors of influence for sediment capturing efficiency in a managed realignment polder, to make the mud extraction from a turbid estuary as efficient as possible while creating new natural and agricultural value.

To achieve the aim of the research, the main question is:

How to optimize the efficiency of extracting sediment from a turbid estuary with a managed realignment polder?

The research starts with a literature review. This review provides a theoretical foundation for the research and with this knowledge the conceptual model of the mud extraction in a managed realignment polder is developed. The conceptual model is made to gather background information, identify gaps in current knowledge, and it helps in formulating research questions. The research questions are formulated in Section 2.5.9, after setting up the conceptual model.

The main tool used in this research is the numerical model Delft3d FM to simulate the relevant processes for sedimentation in the project area. The parameters in this model are calibrated to local conditions using observations from an area where similar circumstances to the project location are present. This calibration process ensures that the model accurately simulates the processes.

Once the model is calibrated, it is applied to the project area. By comparing and analyzing the results of the created scenarios in the project area, it is determined which factors are important. These results contribute to the understanding of the different processes of interest. The model results are assessed on the basis of sediment import and sediment distribution within the polder.

It is important to note that throughout the research, the link between the numerical model and the theoretical background is emphasized. The numerical model is used as a tool to support the conceptual model, but the theoretical background is always taken into account to ensure the validity of the results. The results of the numerical model are integrated with the conceptual model, in order to answer the research questions.

1.4. Outline

The report begins by developing the conceptual model in Chapter 2, where the background of the problem is discussed, relevant processes are explained and the general concept is presented. Based on the gaps in knowledge that are identified in the conceptual model, research questions are formulated.

In Chapter 3, the research methodology is explained and the design choices are briefly discussed. Chapter 4 presents the results of the data analysis, calibration, and the research model. In Chapter 5, the results are discussed and various aspects of the research are analyzed. The conclusions of the research are presented in Chapter 6 and recommendations are provided in Chapter 7.

2

Building the conceptual model

The conceptual model is the framework for understanding the system that is studied, identifying the key processes to include and it provides the concept of the solution to the problem. To come to this conceptual model, a literature review is conducted to the background of the system (Section 2.1), to similar cases (Section 2.2) and key processes (Section 2.3). With this background knowledge and a good system understanding, the conceptual model is developed (Section 2.5), resulting in the research questions in the last section. The theoretical steps to come to the conceptual model are explained in Appendix F.

2.1. The Ems Dollart estuary

The Ems Dollart estuary lies between Groningen in the northeast of the Netherlands and East Frisia in the northwest of Germany. Several rivers flow into the sea in this estuary, such as the Westerwoldse Aa and the Knockster Tief, but the most important is the Ems river. This estuary has an important economic function with the three ports of Eemshaven, Delfzijl and Emden. This estuary is together with the Western Scheldt, the last open connection to the sea in the Netherlands. As a result, the Ems Dollart also has a unique ecological function with characteristic estuarine nature such as salt marshes and mudflats. This landscape is home to salt-tolerant plants, birds, seals and many small benthic animals that form the basis of the entire food web of the Wadden Sea.

Unfortunately, the ecology of the Ems Dollart estuary is under pressure. This is mainly due to a too high suspended sediment concentration (SSC). The high SSC reduces light penetration in the water column, which limits the growth of algae (Colijn and Cadée, 2003). The algae in the water column (Phytoplankton), together with the microalgae on the tidal flats (Microphytobenthos) and the resuspended microphytobenthos (Tychoplankton) are the base of the food web in the Ems Dollart (de Jonge and Schückel, 2019).

The Ems Dollart is naturally very turbid, but various studies have shown that this turbidity has increased considerably (de Jonge et al., 2014; van Maren et al., 2015). This increase has several causes but is mainly attributed to man-made changes in the system (van Maren et al., 2020). At the same time, a significant decrease in algae (especially Phytoplankton) biomass has been observed (de Jonge and Schückel, 2019).

In 2014, the decline in ecology was the reason for a partnership between the national government, the province, the business community, and environmental organizations. Together they came to the Ems-Dollart 2050 program plan. This program aims to bring ecology and economy back into balance. This program works on ecological recovery through various projects and pilots. The second phase of this plan started in 2021. In this 2nd tranche, among other things, the focus is on scaling up in order to structurally work on an improved ecology.

2.1.1. Historical development of Ems Dollart

In order to understand the current mud dynamics in the Ems Dollart, it is important to consider the origin of the shape of the Ems Dollart Estuary. Until the 15th century, the estuary had a completely different shape. The Ems delta was much more narrow, and the Dollart did not yet exist (Figure 2.1A).

The land surrounding the Ems delta mainly consisted of peat (the brown areas in Figure 2.1A). Before humans started working the land, the ground level was well above sea level with salt marshes on the coast (the green areas in Figure 2.1A). Since the peat land has been drained with ditches for agriculture purposes in the Middle Ages, this area subsided, which led to an increased flood risk. The Ems delta was embanked, but large-scale erosion following two major floods (in 1412 and 1509) created the Dollart. Around 1550 the Dollart had reached its maximum size (Figure 2.1B). From then on, the Dollart was increasingly reclaimed until it took its current shape in 1924.

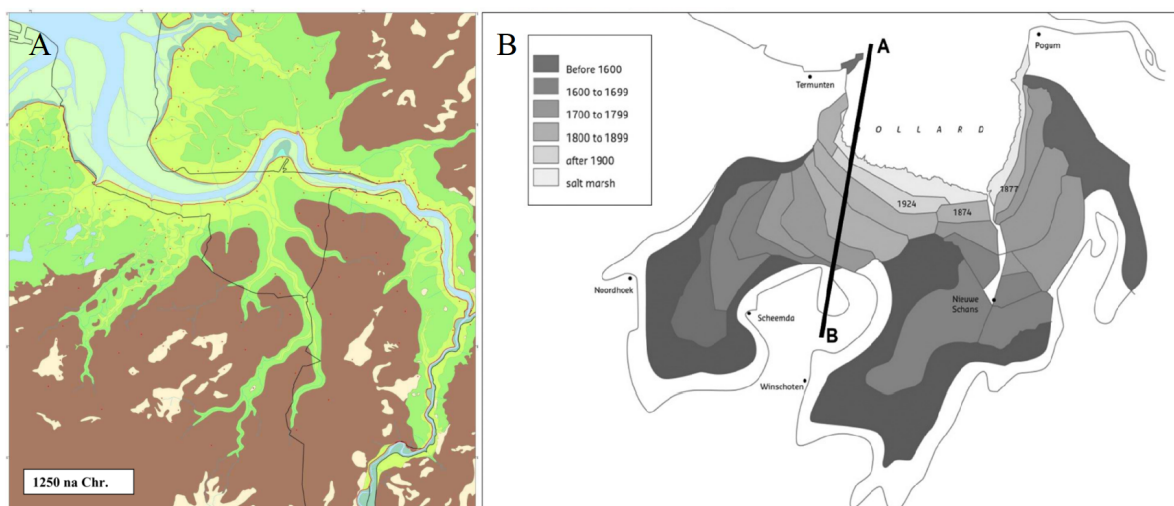


Figure 2.1: A: The Ems estuary around 1250 AD. All brown areas are peat, the green areas are embanked salt marshes with the red lines along the ems representing some of the first dikes. Due to the absence of the Dollart, the Ems estuary was much more narrow than it is today (P. Vos and Knol, 2013a). B: The development of the Dollart since its largest size. Since 1550, the surface of the Dollart has been greatly reduced. (van Maren et al., 2016)

In Section B.1 of Appendix B the development of the Ems Dollart is described in more detail. The bottom development across cross-section A-B in Figure 2.1B is also visualised in Section B.1.

2.1.2. Turbidity in the Ems Dollart

Turbidity processes

The most important processes which affect the Suspended Particle Matter (SPM) levels are shown in Figure 2.2. The human influence on the SPM levels becomes very visible here, there is human interference on almost all facets. Humans have influenced the forcing over the past several decades, as a result of which the sediment is no longer extracted from the system. At the same time, new sediment is steadily being supplied from the Ems and via the Wadden Sea. This together results in higher levels of SPM.

As already indicated in the introduction of this section, the Ems Dollart has been suffering with high turbidity. The estuary is naturally already very turbid, but various studies have shown that this turbidity has increased considerably (de Jonge et al., 2014; van Maren et al., 2015). As mentioned in the introduction, there is a relationship between the turbidity and the biomass of algae (Colijn and Cadée, 2003). It therefore is useful to look at the changes over time of both aspects.

Increase of turbidity

As mentioned above, various studies have shown that the turbidity has increased in recent years. This increase in turbidity amounts to an increase of between 0.5 and 3 percent per year between 1990 and 2010, corresponding to a doubling of SSC within 24 years for the upper bound of 3% (van Maren et al., 2016). In Section B.2.1 of Appendix B the conclusions of several studies are described in more detail.

Decrease of biomass

The high SSC reduces light penetration in the water column, which limits the growth of algae (Colijn and Cadée, 2003). This has also effect on the rest of the ecology because the algae are the base of the food web in the Ems Dollart. There has been a significant decrease in algae (especially the floating

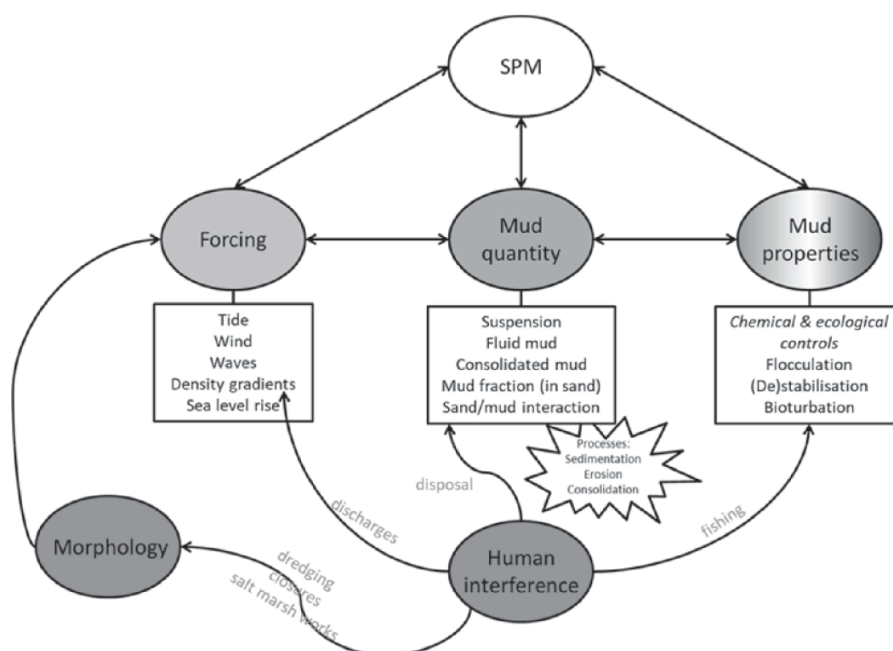


Figure 2.2: Schematic diagram with the most important processes affecting SPM levels. Human influence affects all facets. (Winterwerp et al., 2022)

Phytoplankton) biomass observed (de Jonge and Schückel, 2019). In Section B.2.2 of Appendix B the conclusions of studies with respect to the biomass are described in more detail.

measures aimed at improving the ecology by reducing SSC require an in-depth understanding of the reason for the high SSC.

Causes of turbidity increase in Ems Dollart

There are several causes of the increase in turbidity possible. They were listed and described in Appendix B. The vast majority of the increase in turbidity can be explained by the decrease of sediment sinks (Taal et al., 2015). As described in Section 2.1.1, much land reclamation took place in the past in the entire Ems Dollart Estuary. In addition, there used to be a lot of room for natural accretion in salt marshes and in the past 100 years a lot of dredging has been done in the estuary and in the Ems River. A large part of the dredging work took place in the port of Emden (1.5 million m³/year was extracted; van Maren et al., 2015), but here they stopped extracting dredging sludge in 1994 and started regular re-aeration of the mud layer to prevent consolidation and keep it navigable. Another 0.8 million m³/year deposited in channels.

Taken together, until 1994 a total volume of 2.3 million m³/year of sediment was extracted from or deposited in the Dollart. Since 1994 this has reduced to 1.3 m³/year (which is mainly extracted in the Ems-river) (van Maren et al., 2016). Reducing in sediment sinks leads to an increase in the amount of suspended sediments in the estuary.

2.2. Managed realignment polders

2.2.1. General concept of managed realignment

Managed realignment is a coastal management technique that involves actively reshaping the coastline in order to protect against flooding and erosion. This is typically achieved by breaching or removing existing sea defenses, such as dikes or seawalls, and allowing the sea to naturally reclaim and reshape the land behind them (Esteves, 2014). This controlled inundation of land creates a wider and more natural coastal floodplain, which can better absorb the energy of incoming waves and tides (Finkl, 2015).

One benefit of managed realignment is that it can help to reduce the risk of flooding in coastal communities. By creating a wider floodplain, managed realignment can help to dissipate the energy of incoming waves and tides, reducing the likelihood of flooding. In addition, managed realignment can



Figure 2.3: The concept of a managed realignment polder. (Ketelaars M.B.G., 2022)

help to reduce the risk of coastal erosion, which can cause land to be lost to the sea and can damage important infrastructure, such as roads and buildings (Morris, 2012).

Another benefit of managed realignment is that it can provide a more sustainable and natural approach to coastal defense. Traditional sea defenses, such as seawalls, can be effective at protecting against flooding and erosion, but they can also have negative impacts on the natural environment. A gentle transition between fresh and water is important because it helps to support a diverse and healthy ecosystem by allowing different species of plants and animals to adapt and thrive in different environments, and by helping to maintain the balance of nutrients and chemicals in the water. Freshwater and saltwater ecosystems often have very different chemical and physical properties, and many species are adapted to thrive in one or the other, but not both. A gentle transition zone allows for a mixing of these two types of water, which can support a greater variety of species and create a more diverse and resilient ecosystem. In addition, a gradual transition helps to minimize disruptions in the local ecosystem and allows the water to naturally adapt and balance itself over time. By allowing the sea to reclaim and reshape the land, managed realignment can create more diverse and dynamic coastal habitats, which can support a greater variety of flora and fauna (Cox et al., 2006).

Despite these benefits, managed realignment is not without its challenges. One of the key challenges is that it is expensive and time-consuming to implement, especially in areas with complex coastal environments (Jongepier et al., 2015). In addition, managed realignment can sometimes result in reduced biodiversity in small realignment sites, poor ecosystem services provision, and the loss of existing coastal habitats such as salt marshes or mudflats, which can be important for wildlife and ecosystem health (Esteves, 2013). A good system understanding is therefore of great importance when creating new managed realignment sites.

Models can be used in the planning and implementation of managed realignment projects. Numerical models simulate the movement and behavior of sediment in a coastal environment allowing engineers and planners to predict how the coastline will respond to the removal of sea defenses and optimize managed realignment designs.

In conclusion, managed realignment is a technique that involves actively reshaping the coastline and whereby the outer dike rings are retreated. Overall, it is a valuable technique for protecting against flooding and erosion in coastal areas. Moreover, it can provide a more sustainable and natural approach to coastal defense, creating more diverse and dynamic coastal habitats that support a greater variety



Figure 2.4: Polder Breebaart, a small polder, open to the tide in the Dollart through a culvert, indicated by the red line. (courtesy of Rijkswaterstaat, 2022)

of flora and fauna. However, it can be expensive and time-consuming to implement and may result in reduced biodiversity and the loss of existing habitats in some cases. Modeling is a tool used in the planning and implementation of managed realignment projects, helping to prevent negative outcomes and ensure the success of the project.

There are many successful implementations of managed realignment, some of them are described in Appendix B, but one of them is described below.

2.2.2. Polder Breebaart

Polder Breebaart is a long polder connected to the Dollart estuary, where sea water has been flowing in and out since 2001. The polder was constructed in 1979, and was the last piece of land that was reclaimed in the region of Groningen. In 1991, the polder was transformed into a nature reserve and has become a home to many different bird species. With an area of 63 hectares, the polder has been specifically designed to create a brackish water area that accommodates a gentle transition between fresh and salt water. This design helps to ensure that fish migration between the Dollart and the hinterland of the Breebaart polder is restored. To achieve this, a culvert was installed to connect the polder to the Dollart, a creek was excavated to allow the tide to flow through the area, and a fish passage was created for fish migration (Tydeman, 2005). The maximum water level in the culvert can be managed with slides, and the small opening to the culvert results in a much smaller tidal amplitude in the polder compared to the adjacent Dollart. However, since the opening, the polder has experienced significant sedimentation and has almost completely silted up in about 10 years. From September 2018 to the end of 2020, 70,000 cubic meters of sludge was dredged from the polder (Schmidt et al., 2021). In the early years after the opening, experiments were carried out with the position of the gates in order to maximize the tidal difference in the polder, as described in more detail in Appendix G. In 2022, the tidal range in the polder is estimated to be approximately 20 cm (Esselink, 2022).

2.3. Relevant processes

Before starting research on the most important factors to promote sedimentation, it is crucial to understand the relevant processes regulating the erosion, transport and deposition of fine-grained sediments.

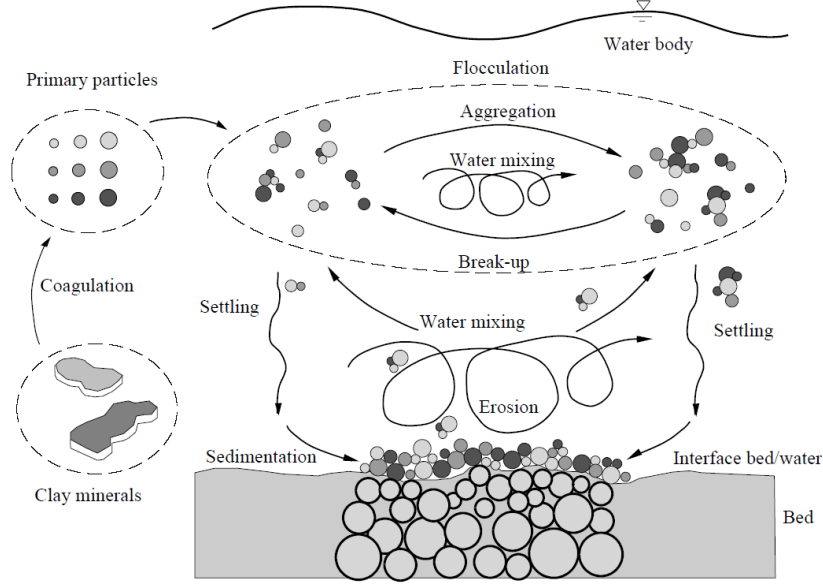


Figure 2.5: Cycle of deposition and resuspension of clay particles (Maggi, 2005)

2.3.1. Erosion and deposition

The first and most important processes of interest are the general processes of erosion and sedimentation. Figure 2.5 shows schematically the deposition flux (*Settling* in the figure) to the bed and an erosion flux from the bed. Partheniades and Krone have extensively studied these fluxes in the 1970's and they have developed a mathematical description of these processes. They are based on the physical principles of sediment transport, including the balance of forces acting on sediment particles, such as the forces of gravity, buoyancy, drag, and turbulence. The deposition flux D can be determined with Krone's equation (equation 2.1) and the erosion flux E can be determined with the Partheniades' equation (equation 2.2) (Winterwerp et al., 2022).

$$\begin{aligned} D &= w_s C (1 - \tau_b / \tau_{cr,d}) \quad \text{with } \tau_{cr,d} = \infty \\ D &= w_s C \end{aligned} \quad (2.1)$$

$$E = M \left(\frac{\tau_b - \tau_{cr}}{\tau_{cr}} \right) \quad \text{for } \tau_b > \tau_{cr} \quad (2.2)$$

The deposition is dependent on the gravity driven sediment settling velocity to the bed w_s , the near-bed suspended sediment concentration C and the acting bed shear stress τ_b compared to the critical shear stress for deposition $\tau_{cr,d}$. Due to doubts about the resistance against deposition, it is assumed that the critical shear stress for deposition is infinite and permanent deposition takes place (van Maren, e-mail, 8 February 2023). This makes deposition only dependent on the settling velocity and the SSC. The erosion is the result of the acting bed shear stress τ_b on a mud layer with a specific resistance against erosion τ_{cr} , multiplied by a erosion flux parameter M . The difference between τ_b and τ_{cr} is also called the *excess bed shear stress* (Winterwerp et al., 2022). The resultant of these two equations forms the net erosion or accumulation, 2.3.

$$dz = D - E \quad (2.3)$$

The Partheniades-Krone equations can be used to calculate the sediment transport rate, the bed elevation, the effects of changes in currents, sediment size and concentration. They have been widely used to model sediment transport in rivers, estuaries and coastal areas, especially in muddy environments. However, it is important to keep in mind that the Partheniades-Krone equations are empirical with vary site-specific (but often unknown) parameter values, and their results should be used with caution and in conjunction with field observations.

2.3.2. Transport

The suspended mud particles are carried along by the current. In the area of interest, the current is usually caused by tides. Deposited mud is highly susceptible to erosion. This means that accumulation will occur particularly in areas with low bed shear stress. When the bed shear stress is lower in one location than in another, the majority of the accumulation will occur in that location. This creates a net transport to the location with the lowest bed shear stress.

2.3.3. Flocculation

On particle level Flocculation also an important process to understand influencing SSC values in the estuary. Flocculation of mud refers to the natural process where small particles of mud suspended in water aggregate together to form larger, flocculated particles. This process occurs when the small particles of mud come into contact with each other and stick together, forming clumps. These larger particles then settle out of the suspension more easily, making the water clearer.

In natural environments such as mudflats, flocculation of mud can have a significant effect on turbidity and sedimentation. The formation of flocculated particles can reduce the amount of suspended mud particles in the water, leading to lower turbidity (Maggi, 2005). This process is visualised in Figure 2.5.

2.3.4. Tidal forcing

Sediment transport by tidal currents

The primary force driving sediment transport in an intertidal area is tidal forcing. The regular movement of water in and out of the area, known as the tide, is typically transports sediment in a landward direction. The impact of sediment transport caused by waves will be discussed later in Section 2.3.9. Tides bring water and sediment into the area, but the resulting currents and bed shear stresses can also lead to erosion. Thus, tides have both positive and negative effects on the sedimentation within the intertidal area, both bringing in new sediment and eroding existing sediment. Understanding the role of tidal forcing in sediment transport is crucial for managing an intertidal area. When channels are present in the intertidal area, the strongest currents will typically occur in those channels. In the right conditions, this can cause sediment to accumulate and the tidal flats to grow.

Current-induced bed shear stresses

Current-induced bed shear stresses refers to the force exerted by flowing water on the bottom. It plays a crucial role in determining the dynamics of sediment transport and it affects both erosion and sedimentation processes. When the bed shear stress is higher than a the critical shear stress for erosion, it can cause erosion by scouring and removing sediment particles from the bottom. When the bed shear stress is low sediment particles deposit on the bottom. The magnitude of the bed shear stress is determined by the velocity of the fluid and the roughness of the bottom surface.

2.3.5. Tidal asymmetry

There are many different causes and types of tidal asymmetry. The main two are explained below; slack tide asymmetry and velocity asymmetry.

Slack tide asymmetry

Slack tide is the period of minimal tidal flow that occurs twice a tidal cycle. In a closed basin, this occurs when the waterlevel is high or low. During slack tide, the water is not flowing as strongly, so sediment transport is reduced. Asymmetry in slack tide occurs when the duration of the high tide and low tide are not equal. When the duration of high tide slack is larger then the low tide slack, more sedement can settle during the high tide slack period. This can cause a difference in the amount of sediment transport that occurs during each tide.

Velocity asymmetry

Probably the most important asymmetry in tide is the velocity asymmetry, which refers to the difference in the strength of the tidal currents within a tidal cycle. Tidal asymmetry can have a significant impact on the transport of sediment. A flood dominant tidal cycle (with a higher flow velocity during flood) tends to transport more sediment in landward direction. This is because of the non-linear relation between sediment transport and the flow velocity, see Figure 2.6. The sediment only moves after a

certain critical bed shear stress (induced by a critical flow velocity) is exceeded. In the case of a flood dominant tide, the volume of transported sediment during flood is larger than the volume of transported sediment during ebb, even though if the second phase would take longer (Friedrichs, 2011).

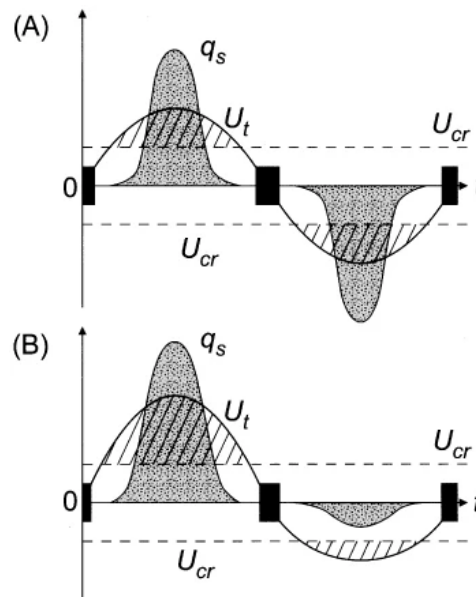


Figure 2.6: Bed load transport of sediment in a symmetrical tidal current (A) and an asymmetrical current (B). In the asymmetrical case is the volume of transported sediment lower in the second phase of the tide (with lower flow velocities) than in the first phase of the tide, due to the required critical flow velocity for erosion. Even if the second phase would take longer. (Dalrymple et al., 2003)

Due to higher flow velocities, the current is more turbulent. This higher turbulence creates a higher bed shear stress, which leads to the formation of larger and more flocs. Due to the higher turbulence, the larger flocs are also dispersed higher in the water column. This increases the transport of flocs because the flow velocity is larger in higher water layers (Winterwerp, 2011), see Figure 2.7.

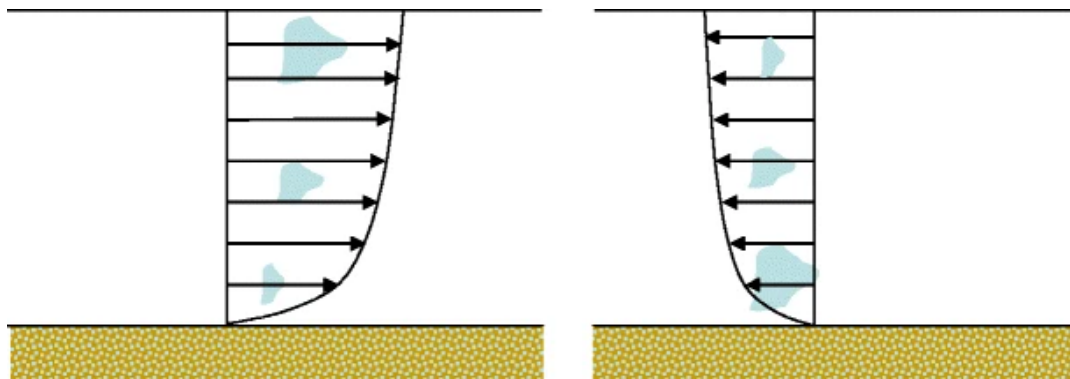


Figure 2.7: Mud flocs transported during flood (left) and during ebb (right). As a result of higher flow velocities, the water is more turbulent, which leads to the formation of larger and more flocs that are dispersed higher in the water column. This increases the transport of flocs. (Winterwerp, 2011)

Influence on mudflats

Studies have shown that tidal asymmetry can also affect the distribution and transport of sediment on mudflats in a number of ways.

In a symmetric tidal cycle, the transported sediment is equal for both ebb and flood tide. This symmetric situation does not exist on mudflats. Above mudflats the tidal flow is always asymmetric, even if the tidal flow is spatially uniform through time, the peak flow is asymmetric in direction of the upper intertidal zone (Van Maren and Winterwerp, 2013), initiating a residual transport in that direction.

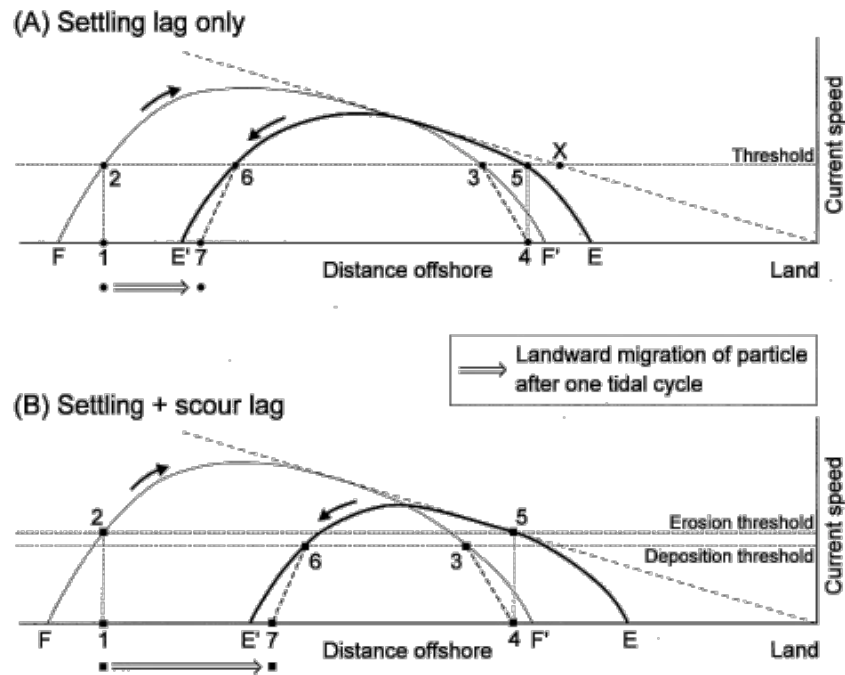


Figure 2.8: Effect of only settling lag (A) and combined settling lag with scour lag (B). The maximum current speeds decrease toward the land (dashed diagonal line). A sediment travels from 1) (where threshold velocity is exceeded) to 4) (after the threshold velocity becomes below the threshold at 3) during flood. The particle travels back to point 7 during ebb. This creates a landward migration of the particle due to the inequality between the time it needs to reach the threshold velocity due to the landward decreasing current velocities. Due to the scour lag, this effect becomes even larger (Dalrymple et al., 2003).

Pronounced tidal asymmetry can lead to greater scouring of the mudflat surface and more efficient transport of sediment by tidal currents. This can result in the accumulation of sediment in certain areas of the mudflat and erosion in others, leading to a more complex and variable sedimentary environment (Dronkers, 1986). Especially spatial variation in flow velocity has an important influence on the transport of fine sediment (Van Maren and Winterwerp, 2013). Weak tidal asymmetry can lead to weaker tidal currents and less scouring and residual sediment transport. This can result in a more stable sedimentary environment, with less variation in the distribution of sediment across the mudflats and less accretion of mudflats.

Overall, the effect of tidal asymmetry on sedimentation on mudflats is largely dependent on the specific conditions present in a given location, including the strength, direction and spatial variability of the tidal currents, in combination with sediment properties and other characteristics of the mudflats.

2.3.6. Settling lag

Settling lag refers to the delay between the time sediment particles are initially transported and the time they deposit on the bottom. It is highly dependent on the settling velocity, caused by a variety of factors such as the size and shape of the particles, the viscosity and turbulence of the fluid, and the presence of other particles that may interfere with settling, but especially on a landward decreasing maximum flow velocity. Sediment particles or mud flocs only erode after a certain critical shear stress is created by the current (point 1 in Figure 2.8A). From that moment on wards, particles are eroded and transported by the tidal current. When the current speed decreases to a current speed where the bed shear stress is below the critical shear stress for erosion, the suspended particles start to settle again (point 3 in Figure 2.8A). Because current is still present, the location where a particle ends up will be further than the location where the critical flow velocity was reached (point 4 in Figure 2.8A). The difference between these is called the settling lag. This process takes place both during flood tide and during ebb tide, but because the flow velocity during ebb tide is weaker than during flood (because it decreases in the landward direction), the distance a sediment particle travels due to settling is smaller during ebb tide than during flood tide. This creates a residual flow in landward direction (Dalrymple et al., 2003). Tidal asymmetry even enhances this process.

2.3.7. Scour lag

Scour lag, refers to the delay between the time when sediment particles or mud flocs are exposed to high flow velocities and the time when the scour or erosion process starts to occur. Scour lag can be caused by factors such as the characteristics of the sediment, the presence of vegetation or other structures that may inhibit erosion, and the initial state of the channel or riverbed. A decent scour lag occurs, when the critical erosion stress is higher than the critical deposition stress. This can be caused by consolidation of the mud layers. Figure 2.8 shows that the effect of the scour lag reinforces the effect of the settling lag.

A study by van Maren et al (2013) shows that in the intertidal area, the settling lag is more important for the residual transport than the scour lag (Van Maren and Winterwerp, 2013).

2.3.8. Tidal basin area

When designing an intertidal area, it is important to carefully consider the dimensions of the entrance channel in relation to the size of the entire area. The entrance channel should be designed to maintain an equilibrium cross-sectional area, according to O'Brien's model, that allows the tidal prism to flow through efficiently and without restrictions (O'Brien, 1969). Having an entrance channel that is too small would impede the natural flow of water and cause the tidal prism to back up, which can lead to a range of negative impacts such as erosion and sedimentation issues. It is essential that the channel dimensions are large enough to allow for the smooth flow of water and efficient exchange between the intertidal area and the surrounding body of water.

Equilibrium cross-sectional area of flow channel

As mentioned above, O'Brien has described a relationship between the cross-sectional area of a channel and the tidal prism flowing through the channel. This relationship was first described in 1969. O'Brien has developed the following relationship for several American inlet channels (O'Brien, 1969).

$$A_c = aP^m \quad (2.4)$$

In this equation is A the cross-sectional area of the entrance (relative to MSL), P the tidal prism and a and m are coefficients, depending on the location. For the Eastern Dutch Wadden Sea, the value for $a = 7.75 \cdot 10^{-5}$ and the value for $m = 1$ (Stive and Rakhorst, 2008).

2.3.9. Waves

Impact of waves on erosion

Waves can have a significant impact on sedimentation and erosion in a muddy estuary with mudflats and salt marshes. Waves generated by wind and their near-bed orbital velocities may lead to both erosion and sedimentation.

Waves can erode the surface of the mudflat, initiating resuspended sediments being transported offshore. Smaller sediment particles take longer to settle due to their increased settling time, particularly the smallest particles tend to remain suspended longer due to the waves impact. This can result in the finest sediment being carried away by the tide. In areas where wave activity is low, the average diameter of sediment particles is likely to be smaller due to this process (Dronkers, 1986).

In salt marshes, waves can also cause erosion by scouring and removing vegetation. The loss of vegetation can lead to further erosion as the roots of the plants help to hold the sediment in place. Additionally, waves can also cause sediment to be transported into salt marshes, leading to sedimentation. Sediment deposited in a salt marsh can change the vegetation, and changes in vegetation can change the topography of the marsh leading to a less favorable habitat for the marsh inhabitants.

Overall, waves can have both positive and negative effects on sedimentation and erosion in a muddy estuary with mudflats and salt marshes. While they can lead to erosion and loss of sediment, they can also transport sediment and cause sedimentation. However, a wave impact that is too large should be avoided, because then the erosive effects will prevail. Wave-induced erosion and sedimentation in estuaries can be an ongoing process that can lead to various changes in habitats and ecosystems, it is important to understand how waves interact with these environments and what factors determine the magnitude of their impact.

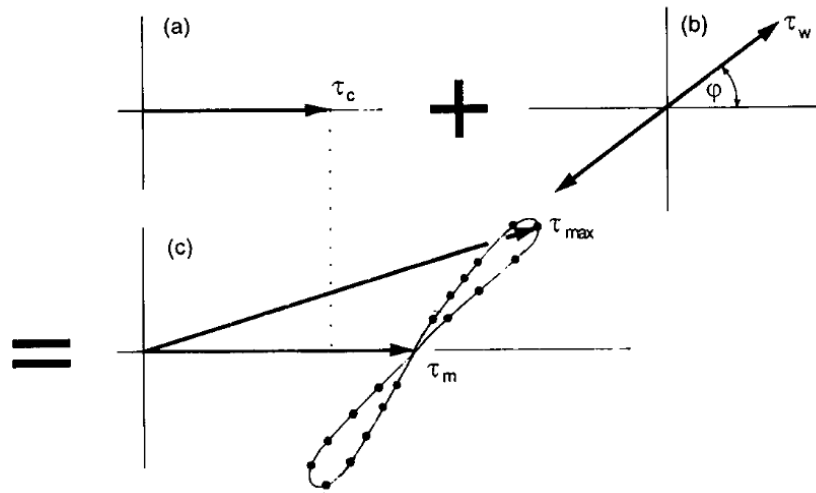


Figure 2.9: schematic representation of bed shear stress with non-linear Wave-current interaction. The bed shear stress of the current (τ_c) in (a), the bed shear stress of the waves (τ_w) in (b) and the combined mean bed shear (τ_m) and combined maximum bed shear (τ_{max}) in (c) (Soulsby et al., 1993).

Wave-induced bed shear stresses

In Section 2.3.4, the concept of current-induced bed shear stress was introduced. However, another important factor to consider are wave-induced bed shear stresses. It plays a crucial role in determining the dynamics of sediment transport and its magnitude is determined by wave properties such as height, period, and direction.

Waves and currents can interact in a nonlinear manner, which can generate new waves and currents and have an impact on the bed shear stresses. The nonlinear interaction of wind waves and currents in muddy shallow waters can lead to complex patterns of erosion, sediment transport, and deposition. This is because the combined action of wind waves and currents can create stronger bed shear stresses than the sum of their individual stresses (Soulsby et al., 1993), leading to extra erosion of the bed. On the other hand, if the wind waves and currents move in opposite directions, they can cancel each other out, reducing the bed shear stresses, and leading to extra sediment deposition. In Figure 2.9 is the non-linear wave current interaction visualised.

Overall, the nonlinear interaction between waves and currents in muddy shallow waters can lead to a dynamic and constantly changing bathymetry. It has complex and unpredictable effects on the bed shear stress which can be difficult to predict and model accurately. Therefore, it is essential to study and understand this interaction to better understand and manage the effects of waves and currents on the bed shear stresses.

2.3.10. Consolidation

Consolidation, which refers to the process of compaction and hardening of sediment in an intertidal area during low tide, can have a significant impact on the erodibility of mudflats.

On one hand, consolidation can make mudflats more resistant to erosion. As the mudflat hardens and compacts, it becomes more difficult for wave and current-induced erosion to remove sediment particles. This can lead to a stabilization of the mudflat surface and an overall reduction in erosion. Also, as the sediment's granular structure compacts, it can support a greater load and resist better to shear forces (Berlamont et al., 1993a).

On the other hand, consolidation can also make mudflats more susceptible to erosion. When the surface becomes less permeable, water that penetrates the surface during high tide can't drain as easily, and this can cause water to build up, weaken the mudflat surface, and make it more prone to failure and erosion.

Overall, the effect of consolidation on the erodibility of mudflats is complex and context-dependent. It is important to consider the time frame of consolidation, as well as other factors such as the specific sediment composition of the mudflat, the intensity and duration of the consolidation process, and the presence of other erosive forces such as waves and currents.

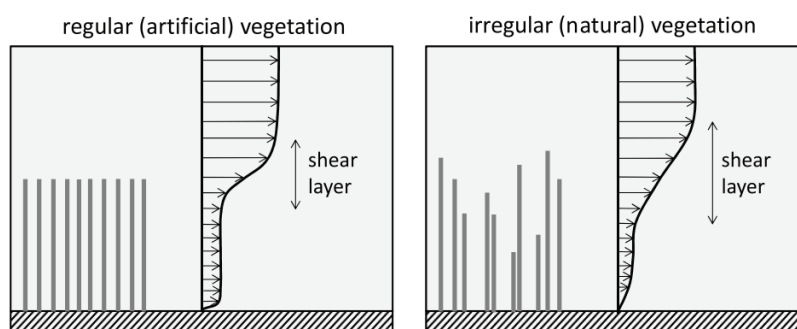


Figure 2.10: The reduction of flow velocity over regular (left) and irregular (right) vegetation. (Winterwerp et al., 2022)

2.3.11. Vegetation

Vegetation can have a positive effect on sedimentation of mud in intertidal areas and therefore reduce the amount of suspended sediment in the water. The leaves and stems of vegetation can physically trap sediment by helping to decrease the flow velocity. Due to the decreased flow velocity, the bed shear stresses are lower, which promotes sedimentation. Furthermore, the roots of vegetation can help to create a more stable surface, reduce erosion and the building up of marsh elevation over time, this effect is known as "vegetative stabilization" (Chirol et al., 2021; Knutson et al., 1981).

Vegetation can play a critical role in elevating the marsh surface, by trapping and retaining sediment over time, making the marsh surface above the tidal zone. This is crucial for the survival of the marsh as a whole, as it allows the marsh to keep pace with sea level rise (Kearney and Fagherazzi, 2016).

An irregular field of vegetation may be best for reducing flow velocities (Poggi et al., 2004). Figure 2.10 shows that with irregular vegetation the flow velocities decrease even further towards the bottom.

Vegetation can also help to create a more diverse habitat and increase biodiversity by providing food and shelter for a wide range of organisms. In this way, as many different ecotopes as possible can be realized, which also benefits biodiversity (Baptist et al., 2019). This in turn can increase the organic matter input to the system, making sediment more cohesive and further enhancing sediment accumulation (D'Alpaos et al., 2007).

Overall, vegetation plays a vital role in promoting sedimentation in salt marshes and mudflats, it can trap sediment particles and create a more stable surface, lead to an increase in sediment accumulation (Price, 2016), promote biodiversity and help the marsh keep pace with sea level rise.

2.3.12. Other environmental factors

Another important environmental factor are the human activities such as dredging, coastal development, and coastal engineering. These activities can greatly affect sedimentation by altering the natural sediment transport patterns and changing the physical characteristics of the intertidal area.

Finally, there are environmental factors that have a significant impact on the microorganisms in an intertidal area. These microorganisms, also known as microbiota, can play a key role in sedimentation, erosion resistance, and turbidity. The growth and activity of the microbiota can be influenced by factors such as nutrient levels, oxygen levels, pollution, and water quality. These factors can either promote the growth and proliferation of the microorganisms or inhibit it, thus affecting the sedimentation, erosion resistance and turbidity in the intertidal zone.

2.4. Tidal flats and salt marshes

Tidal flats and salt marshes are important coastal ecosystems that are highly influenced by the movement of water with the tides. Tidal flats are flat, muddy areas that are covered by water at high tide and exposed at low tide, and are typically found in areas with low wave energy and a large tidal range. Salt marshes are wetlands that are characterized by their salt-tolerant vegetation, which includes grasses, shrubs, and other plants that are adapted to survive in both wet and dry conditions (Adam, 1993). These ecosystems provide a range of ecological and economic benefits, such as acting as a buffer against storms and coastal erosion and providing habitat for a diverse range of plants and animals.

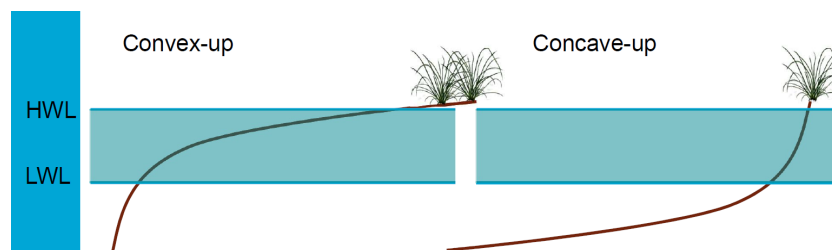


Figure 2.11: Convex-up and concave-up tidal flats. Convex-up tidal flats have a larger area within the tidal range, where the most ecologic value is present. Convex-up tidal flats are therefore preferable for nature development. Additionally, more creek development occurs in convex-up tidal flats, which is also preferable for nature development (Hanssen et al., 2022).

2.4.1. Tidal flat food web

Tidal flats and salt marshes have a very important ecologic function. Research suggests that middle and upper tidal flats have disproportionately high ecological value, particularly in terms of biomass production and supporting local wildlife populations (Drylie et al., 2018; Mu and Wilcove, 2020; Zhou et al., 2022). Areas with convex-up tidal flats are especially beneficial for nature development, as they have a larger surface area within the tidal range (Figure 2.11) and support more creek development (Hanssen et al., 2022). Strong ecosystems contribute to coastal flood defenses by providing biogeomorphic controls for a stronger coast (Reed et al., 2018). In this way the coast can be more effective against changes such as sea level rise or storm surges.

2.4.2. Tidal flat and salt marsh morphodynamics

Understanding the processes and factors that influence tidal flat and salt marsh morphodynamics is important for predicting and managing the changes that these ecosystems may undergo over time. Tidal flat morphodynamics are driven by several processes, including tidal flat erosion and accretion, settling lag, and tidal asymmetry. These processes are described in more detail in Section 2.3. Other factors that influence tidal flat and salt marsh morphodynamics are described in Appendix B.

Sediment (especially mud) tends to move net from areas of high energy to areas of low energy (Friedrichs, 2011). When waves are small, mud tends to deposit on the upper intertidal flats. This ensures that intertidal flats are more convex-up in a muddier environment (Zhou et al., 2015). Waves create high bed shear stresses in shallow areas, resulting in a net sediment flux towards the deeper channels. Therefore, the formation of convex-up tidal flats is promoted in muddy areas, influenced by tides and with low wave energy.

The presence of vegetation can also have a significant impact on salt marsh morphodynamics. The vegetation mainly gives a positive feedback on the amount of sediment that is fixed in a salt marsh. Due to the presence of pioneer vegetation, the wave energy and current energy are dissipated. This creates an area with little energy which increases net sedimentation. The growth of salt marsh vegetation also contributes to the formation of a channel network. The formation of this channel network involves not only the salt marshes, but also the mudflats and the rest of the intertidal area (Kearney and Fagherazzi, 2016). The formation of a salt marsh area along the edge of the intertidal zone therefore contributes to a dynamic and varied ecosystem (Cox et al., 2006).

2.5. The conceptual model

The conceptual model is a summary of all essential knowledge about the processes that occur in the model. It provides a framework for understanding the system that is studied, identifying the key processes to include, and determining the necessary validation methods. It forms the theoretical foundation of the research, and the results must be interpreted in light of the theory presented in the conceptual model. The numerical model can provide valuable insights and contribute to refining the conceptual model, but it should not be considered as the sole source of truth or the final answer to the research questions.

The main concept is to extract suspended mud from a turbid estuary in a managed realignment polder. Every tidal cycle, a part of the incoming suspended mud is deposited in the polder and thereby extracted from the estuary. The various important aspects are briefly explained below.

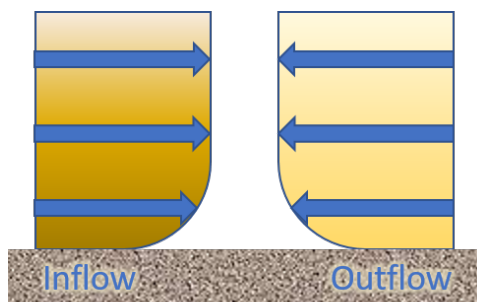


Figure 2.12: The concept of the sediment import in the managed realignment polder. The tidal inflow in the polder has a higher SSC than the outflow because a part of the suspended mud particles settles.

2.5.1. Reduction of high turbidity level

The turbidity in the Ems Dollart estuary is currently too high. The high turbidity hinders light penetration in the water column, restricting the growth of algae and impacting the overall ecosystem. The turbidity has increased as a result of a decrease in the amount of sediment sinks (Section 2.1.2). To address this issue, a new sediment sink is created by creating a managed realignment polder in the Ems Dollart, which extract sediment from the estuary. The Ems-Dollart 2050 program is aiming to extract one million tons of dry matter from the estuary per year

2.5.2. Sediment import in polder

Suspended sediment is transported into the managed realignment polder by the tidal currents. In this intertidal area, a part of the suspended sediment settles, resulting in more sediment being transported into the area than being transported out (Figure 2.12). This is facilitated by low erosion rates in the intertidal area. However, it is crucial that the tidal current is not too strong, as this would cause the sediment to erode away and be carried out of the polder.

2.5.3. Effect of hydrodynamic forcing on resuspension of sediment

Erosion can be affected by various factors such as tide-driven currents, wind-driven currents, and wind-generated waves. Particularly the wind-generated waves can cause additional shear stresses due to their orbital motion. When these extra shear stresses occur during an incoming tide, it can result in resuspended sediment being transported further into the polder, before settling again. Conversely, when they occur during outgoing tides, it can cause sediment to be transported out of the polder.

2.5.4. Factors influencing sediment accumulation and distribution

The spatial distribution of sediment accumulation and the rate of filling in the realigned intertidal area are determined by both the forcing factors and sediment properties. Factors such as the SSC in the Ems Dollart and the tidal prism entering the managed realignment polder influences the amount of sediment that is being imported. Sediment properties such as the settling velocity w_s and critical shear stress for erosion τ_{cr} are important for both the sediment import and the spatial distribution of accumulation.

2.5.5. Additional benefits

Allowing the managed realignment polder to silt up has additional benefits. Firstly, it creates large space for nature development, providing an important transition zone between freshwater and saltwater for a diverse range of species, resulting in significant ecological value. The additional ecological values can be maximized by creating as much mudflats between the tidal range as possible and stimulate the creation of creeks. Secondly, silting up allows to raise agricultural land to adapt for sea level rise, as the silted-up area can over time be repurposed for agricultural land or by relocating the accumulated sediment to other areas.

2.5.6. Neglected processes

In Section 2.3, several key processes related to mud dynamics and accumulation on mudflats were discussed. The most significant processes mentioned include erosion, deposition, transport, tidal forcing

and the impact of waves. Other factors such as consolidation, flocculation, scour lag, vegetation, and other environmental factors have been omitted for the sake of simplicity. They are difficult to implement in the numerical model and they are considered to have a lesser impact on overall sediment import and distribution. Some of these processes are explained below

Consolidation

Consolidation of mud is a complex process that can be difficult to accurately account for in numerical models due to its non-linear, time-dependent behavior. Accurately modeling consolidation requires a detailed understanding of the physical and chemical properties of the sediment and the underlying processes that govern its behavior. At this moment, this is not yet possible to implement into the model.

Flocculation

Flocculation, the process of clumping fine mud particles together, is a complex phenomenon that is influenced by factors such as sediment chemistry, microorganisms, and flow. It is difficult to include in coastal models due to its dynamic and unpredictable nature, as well as a lack of data and understanding of its mechanisms in muddy environments. Coastal models often rely on simplifying assumptions, but the challenges associated with accurately predicting flocculation behavior make it a difficult process to model.

Vegetation

Implementing vegetation in coastal numerical models is challenging due to the complexity of plant morphology, hydrodynamic effects, and the interplay between vegetation and sediment transport. Vegetation can alter the flow and sediment dynamics in coastal areas, but the exact mechanisms are not well understood, and can be influenced by factors such as plant density, morphology, and species composition. The lack of accurate and consistent data on these factors makes it difficult to incorporate vegetation into numerical models accurately.

Microbiotics

Incorporating microbiotics into coastal models is challenging due to the complexity and dynamic nature of microbial activity. The composition of microbial communities, environmental conditions, and interactions between microbes and their surroundings can all affect the process, which can change rapidly and unpredictably. Additionally, the lack of data and understanding of microbiological mechanisms in muddy environments makes it difficult to model accurately.

2.5.7. Polder Breebaart for calibration

The location deemed most suitable for calibration is Polder Breebaart. As mentioned in Section 2.2.2, Polder Breebaart is in the Ems Dollart estuary, and therefore is assumed that the mud characteristics and other important parameters of Polder Breebaart correspond to the parameters of the project location. Some important data are available for polder Breebaart, such as height measurements, sediment samples and water levels (Esselink and Berg, 2004; Peletier et al., 2004; Tydeman, 2005).

2.5.8. Important parameters for calibration

Of the important processes, the main parameters that require calibration are in the Morphological processes. The hydrodynamic parameters of the model do not require calibration as the viscosity and specific density of water are (almost) constant. The only location-dependent parameter is the tidal forcing, which does not require calibration and is determined using data.

The morphological processes in the model are mainly calculated using the Partheniades-Krone equations. Therefore, the most important parameters to calibrate are those that influence these equations. These include the settling velocity w_s , the critical shear stress for erosion τ_{cr} , and the erosion parameter M . Additionally, during the calibration process, it was discovered that the bed shear stress due to wave action was overestimated compared to the bed shear stress due to currents. As a result, it was found that calibrating the wave stirring scaling factor $f_{\tau_{auw}}$, which limits the wave-induced bed shear stress, is also crucial.

2.5.9. Research questions

The conceptual model outlines the general concept of how and why sediment is removed from the estuary. However, some processes within this model are not fully understood. These gaps in understanding have led to the formulation of several research questions. These research questions aim to increase understanding of the system and aid in addressing the main research question:

- *How to optimize the efficiency of extracting sediment from a turbid estuary with a managed realignment polder?*

To answer this question, a number of supporting research questions have been formulated:

- *What is the influence of domain shape on the sediment distribution in the managed realigned polder?*
- *What is the influence of wind and waves on the erosion in an intertidal area?*
- *What surface area of a managed realignment polder is the most efficient in capturing sediment?*
- *At what bed level elevation relative to the tidal range does most accumulation take place?*
- *What is the influence of the tidal range on the spatial sediment distribution?*
- *Is it possible to increase the total net sediment import by increasing the settlement time?*
- *How can additional ecological values be stimulated?*

3

Methodology

In this research, the numerical model Delft3D FM is used for this research. There are different types of coastal models, including empirical models, process-based models, and coupled models, which can focus on hydrodynamics, waves and morphodynamics. Delft3D FM is a process-based combined hydrodynamic-morphodynamic numerical model and is used to simulate the behavior of the coastal system in a comprehensive and physically-realistic way. The choice of the numerical model is explained in more detail in Appendix L.

The calibration of the model is important as it improves the accuracy of the predictions and identifies any limitations or biases in the model. Model calibration is the process of adjusting the model parameters and inputs to better match the observed data from the real-world system being modeled. Additionally, identifying any limitations or biases in the model through calibration allows for improvements to be made, making the model more useful and reliable for a variety of applications. To calibrate the model, a comparable location to the project location is required. Polder Breebaart is found suitable for this. It must be noted that the main goal of Polder Breebaart's design is to create a nature reserve, while the project area aims to reduce turbidity through mud extraction.

The data to calibrate is obtained by a data analysis, described in Section 3.1. This includes the methods used to collect and analyze data for the calibration process. The calibration is further described in Section 3.2 that outlines the methods used and the parameters being tested. Once the calibration is completed, the application model is developed. The application model serves to answer the remaining research questions and to achieve the overall research goal. With the settings determined during calibration, different scenarios can be simulated to determine the effects of the adjustments and increase understanding of the system. The application of the calibrated model on the project area is described in Section 3.3. An overview of the methodology is illustrated in Appendix A, in Figure A.1.

3.1. Data analysis

As already described in Section 2.2.2, Polder Breebaart is been deepened between 2018 and 2020 (Schmidt et al., 2021). The bathymetry of the area is measured in 40 cross-section profiles in March 2020 (Esselink et al., 2020). After this, the area was measured in August 2020 and August 2021 with an RTK-drone and with echo sounding (P. Esselink, e-mail, 15 august 2022). The different bed level elevation maps are shown in Figure 3.1. Details on the data processing are discussed in Appendix K.

3.2. Model set-up calibration: Polder Breebaart

The aim of the calibration process is to determine parameters that govern sedimentation dynamics in the intertidal area, such as the erosion parameter (M), the settling velocity (w_s), and the critical shear stress for erosion (τ_{cr}). It is crucial to determine realistic values for these parameters in order to accurately simulate the sedimentation patterns in the study area. This is achieved by comparing the results of the Delft3D FM simulation to the data of the measured sedimentation patterns in the Polder Breebaart, with the goal of achieving as close a match as possible.

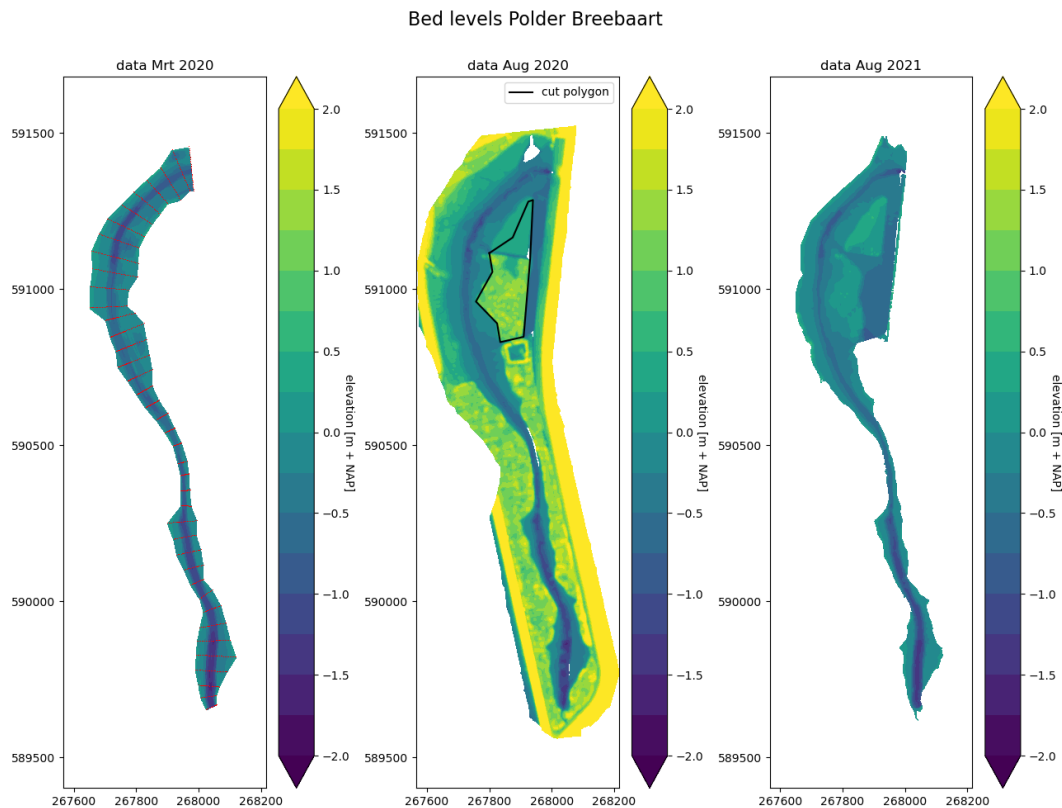


Figure 3.1: The bed levels in Mrt 2020 (with measurement cross-sections in red), Aug 2020 and Aug 2021. The black polygon represents the data which is not included in the data analysis due to differences in reed height.

3.2.1. Grid and bathymetry

Calibration model domain

The dikes of Polder Breebaart can easily be adopted as outer edges in the model domain. The location of polder Breebaart can be seen in Figure 3.5. In this figure, the location of Polder Breebaart can also be seen relative to the project location.

Topographic data Polder Breebaart

In Section 3.1, the available bed level data of Polder Breebaart is described. For the numerical model of Polder Breebaart, use is made of the data from the RTK drone. The two data sets obtained by the RTK-drone are more similar and therefore better comparable and useful for the calibration. The bed level change during the first 5 months since the completion of the deepening project will therefore not be taken into account for the calibration and the data of August 2020 is the starting point for the morphological development in the calibration area Polder Breebaart. This bed levels are shown in the upper middle figure in Figure 3.1. Where data is missing, this is supplemented with height data from AHN. If there are still gaps in the data, this is completed by triangular interpolation.

Computational grid Polder Breebaart

The computational grid of Polder Breebaart is designed such that the rectangular grid cells follow approximately the direction of the flow profile in the polder. The rectangular grid cells have, due to a better orthogonality and easier smoothness, a slightly faster computation time than the triangular grid cells. On the other hand, triangular grid cells are more flexible when filling irregular surfaces. The shape of the grid is therefore determined on the hand of the topographic data. The size of the grid cells has been chosen such that there are always several grid cells in the width of the flow profile. The grid schematization and processing of topographic data in the grid are shown in Figure 3.2.

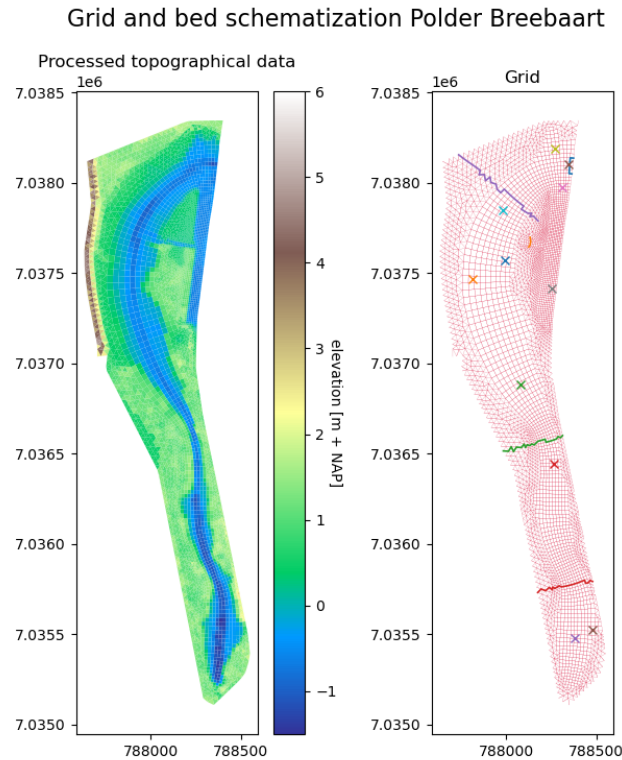


Figure 3.2: Projected topographic data of Polder Breebaart (left) and grid schematisation (right). The crosses in the right figure show the model measurement stations and the lines show the model measurement cross sections.

3.2.2. Forcing conditions

The forcing conditions consist of tide, wind and sediment concentration at the model boundary. All of these play a role in shaping the behavior of the intertidal area over time. In this case there are only locally generated wind waves, as the propagation of waves into the domain is limited by a culvert.

Tide

The main external forcing in the system is the tides. The tide is the cause that ensures that water, and thereby suspended sediment, flows in and out of the polder. As already described in Section 2.2.2, Polder Breebaart has a damped tidal range. The water flows in and out of the polder through a culvert with dimensions of 1 by 2 meters (Peletier et al., 2004), such that the tidal range can be influenced. The tidal range in 2022 is 20 cm (Esselink, 2022). By combining different harmonic components, a tidal signal which corresponds to the tidal signal in Polder Breebaart is simulated. This resulting tidal signal is shown in Figure 3.3. The creation of this tidal signal is described in more detail in Appendix G.

Wind

Because it has been established that wind-generated waves have an important influence on bed shear stresses, and thereby on the re-suspension of sediment, wind must also be included in the simulation. The wind data has been obtained from the KNMI (KNMI, 2022). For the calibration model the used wind data starts on August 2020. Appendix H further discusses how this data was obtained and processed.

Sediment concentration at boundary

The SSC that enters the boundary is an important forcing condition that determines the total volume of sediment that enters the area. However, the SSC in the Ems Dollart can vary a lot in both time and space, making it challenging to establish accurate values. For the Polder Breebaart, a constant SSC value of 0.2 kg/m^3 was chosen, based on the yearly average SSC reported by van Maren et al. (2015)

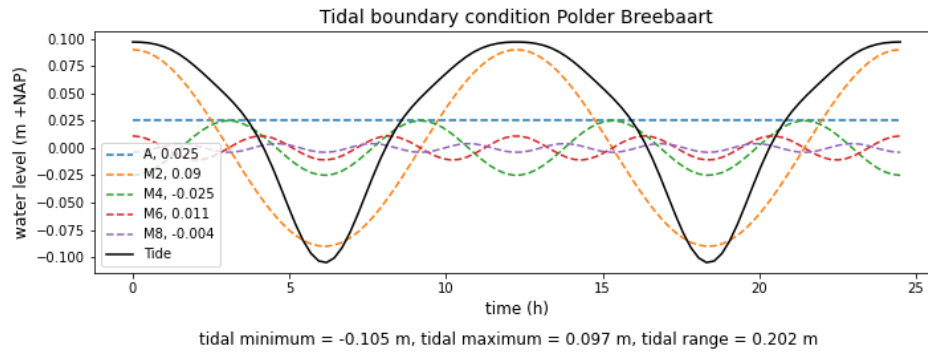


Figure 3.3: Tidal forcing in Polder Breebaart on open boundary

in the Ems Dollart at the measuring station closest to Polder Breebaart taken together with the value in the map with the computed yearly averaged SSC (station S5, see Appendix E for the location and the map). This value is considered to be a reasonable approximation of the SSC at the open boundary of polder Breebaart.

3.2.3. Design choices

Bed roughness

The bed roughness can be defined in different ways. In this study, the roughness is defined with Manning's formula. Due to a lack of data on roughness, it is decided to perform the simulations with a uniform Manning's roughness coefficient of $n = 0.015 \text{ s/m}^{1/3}$. This is a fairly average value for mud flats (Arcement and Schneider, 1989)

Bottom thickness

The initial bed thickness is based on the maximum erosion depth seen in the data. Making this thickness about twice as thick as the maximum erosion, it is assumed to have no impact on morphology.

One or more sediment fractions

Because the bottom in Delft3D FM consists of a uniform layer, settled sediment mixes uniformly with the sediment in the bottom layer. This disrupts the erosion process of easily erodible sediment. So calculations are based on 1 sediment fraction. For more explanation about this, see Appendix C.

3.2.4. Performance evaluation

Evaluating the results obtained from the numerical models is an essential part of developing a credible morphological model. In Section 3.1 is described how the data is collected and analysed. This data forms the starting point for the calibration, described in Section 3.2. The data is used to create the starting conditions (section 3.2.1), but also to compare the model results with, to determine whether the model gives reliable results. It must be determined how the model results will be evaluated to see if they correspond sufficiently with the observation from Section 3.1.

This evaluation must be done on a reliable basis and may not be done just subjectively. Sutherland et al. (2004) have compared how different model quantification methods which are used in meteorology, can be used to quantify morphological models. In their paper they show that the quality of a morphodynamic model can be judged on the basis of bias, accuracy and skill. They define *bias* as a measure of the difference in the overall tendency, e.g. the overall mean. This shows whether a model underestimates or overestimates the results on average. *Accuracy* is defined as a measure of the mean difference between predictions and measurements and *skill* as a non-dimensional measure of the accuracy of a prediction relative to the accuracy of a base prediction (Sutherland et al., 2004). In this research study, it is attempted to assess the quality of the calibration in all three ways.

But first, before evaluating the morphodynamic model results, it must be checked whether the hydrodynamic calculation gives reliable results. After all, the morphodynamic calculation is performed with the calculated hydrodynamic conditions. There is no usable hydrodynamic data obtained for the calibration area, so this hydrodynamic evaluation has been carried out on the basis of experience and

background knowledge. This involves looking at occurring water levels, flow velocities, wave heights and wave periods. After no more strange results have been obtained here, the morphological development can also be evaluated. The morphodynamic model results are compared against the observations from the data in various ways, all based on one of the three quality checks of Sutherland.

These different evaluations are described separately in the headings below and have been carried out parallel and iterative during the calibration. The different evaluations are (1) a visual comparison between the morphological development map by the numerical model and the morphological development map by the data, (2) the sediment import of the polder (bias), (3) the mean absolute error of in bed level of the grid cells (accuracy) and (4) the Brier Skill Score of the morphological development (skill). All methods were also performed for just the lower part or the upper part of the polder in order to properly assess the quality of the model between the front and back of the tidal area.

Visual check

First a visual test is done, in this subjective first test it is checked whether the morphological development within the calibration polder correspond with the morphological development in the data. It is important that the distribution of sedimentation in the model matches the visual observations at least partly. If not, the other evaluations are not required at all. The two most important distributions that were checked in this visual check are the distribution over the front and back of the polder and the distribution between the flats and the channels. For example, if all sediment settles near the boundary and none of the sediment reaches the back of the polder, it can immediately be concluded that the simulation results does not matches with the data analysis.

Sediment import

The total amount of sediment imported by the polder is an important criterion that the numerical model must meet since this comes in line with the aim of the research. In the data analysis (described in Section 3.1), the total volume of sediment import from August 2020 to August 2021 is determined. For every model result, the total imported sediment mass is compared to this volume to perform this 'bias' check. To properly compare these bulk quantities, the total volume increase in the polder is multiplied with the dry bed density of the mud, $\rho_b = 500 \text{ kg/m}^3$.

Mean absolute error

To assess the accuracy of a numerical model simulation, the mean absolute error (MAE) is calculated. By subtracting the change in bottom level according to the data from the change in bottom level according to the model results, the spatial varying errors of accumulation were obtained. By taking the mean of the absolute values of the spatially varying errors, the MAE is determined. In a perfect model, this value would be zero. When comparing model results, a lower value indicates a more accurate result.

$$MAE = \left\langle |\Delta z_{mod} - \Delta z_{meas}| \right\rangle \quad (3.1)$$

In this equation, Δz represents the change in bed level for a grid cell, *mod* stands for the modelled value and *meas* for the measured data. The $\langle \rangle$ denotes the spatial average value.

Brier Skill Score

To objectively assess the skill score of a morphodynamic model result, Sutherland et al. (2004) suggests using the Brier Skill Score (BSS). Sutherland et al. (2004) argues that the BSS is the best way to assess the behavior of a morphodynamic model because BSS is more 'honest' than measurements or accuracy. The BSS is calculated with equation 3.2. This gives a relative volume change. This definition of the BSS has been extracted from the assessment criteria in Van der Wegen et al. (2017).

$$BSS = 1 - \frac{\left\langle (\Delta vol_{mod} - \Delta vol_{meas})^2 \right\rangle}{\left\langle \Delta vol_{meas}^2 \right\rangle} \quad (3.2)$$

In this equation, Δvol represents the change in bed level volume for a grid cell, *mod* stands for the modelled value and *meas* for the measured data. The $\langle \rangle$ again denotes the spatial average value.

For the BSS, a score of 1 is a perfect model. Lower scores indicate a less good model and negative scores indicates results which are worse than the initial conditions. The assessments of the scores are shown in Table 3.1.

appreciation	BSS
Excellent	1.0 – 0.5
Good	0.5 – 0.2
Reasonable/fair	0.2 – 0.1
Poor	0.1 – 0.0
Bad	< 0.0

Table 3.1: Classification of Brier skill score

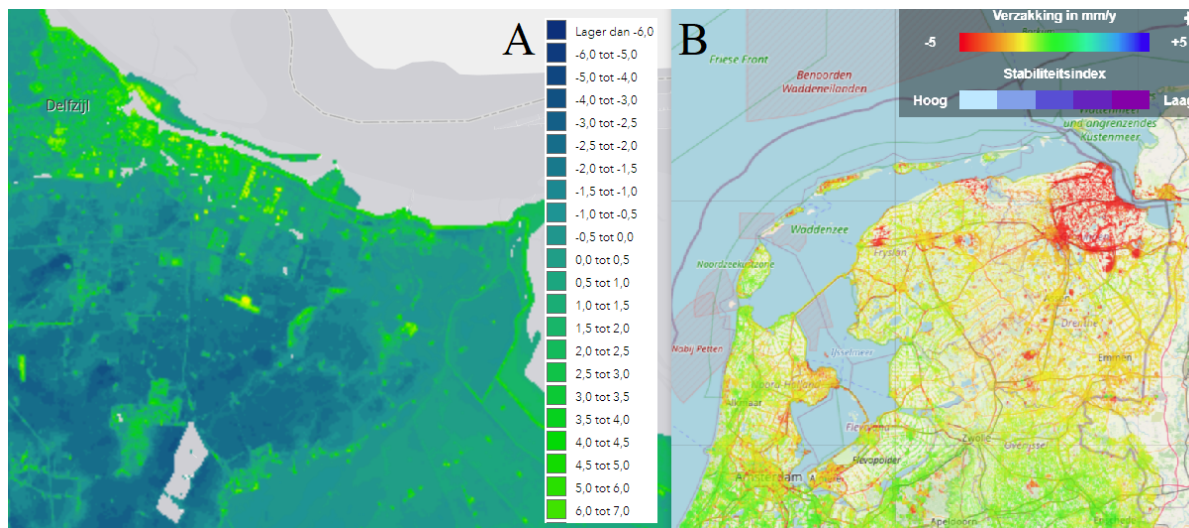


Figure 3.4: A: Elevation map of the project area. This figure shows that almost the entire area is below sea level (source: AHN, 2022). B: Subsidence map of the project area. This figure shows that the subsidence in northeast Groningen is very high compared to the rest of the country (source: NCG, 2022).

3.3. Model set-up application: Realignment project area

The model set up of the application of the calibrated numerical model is outlined in this section. As project area, a region located between the villages of Nieuwolda, Woldendorp and Borgsweer, and the N362 is determined. A comprehensive area analysis was conducted by Firet et al. (2018) and LAMA (2020), and this land was found to be suitable for the project. The area does not contain any villages, but there are some separate farms that should be removed. Additionally, there are many wind turbines and there is a solar park present. The majority of the area is composed of agricultural land. This region is also of interest to the province of Groningen (Matthijs Buurman, Coastal Development Program Manager in Groningen) and is identified as a potential intertidal area inside the dike in the report 'Ziel in Landschap' (van Paridon x de Groot | abe veenstra landschapsarchitect, 2020). Almost the entire area is below sea level (Figure 3.4A), making it suitable for allowing the tides to flow freely in this area. In addition, this area is also preferable for a pilot with the aim of raising the agricultural land since this area because this area is experiencing the highest subsidence in the Netherlands (Figure 3.4B).

This area is particularly interesting for this study as it borders the Ems Dollart region where high SSC still occurs and because of its location and bed heights. It creates an interesting realistic situation to focus on.

The most settings for the application are determined during the calibration phase with the model of Polder Breebaart. The domain, grid, bathymetry and some forcing conditions are different from the calibration phase. These are explained in this section. The aim of this research is to understand the underlying processes and the model of the project area is used to achieve this. The various scenarios drawn up to gain insight into the processes are discussed in section 3.3.5.

3.3.1. Grid schematization

Project domain

Four different domains were defined, each enclosing an area with a different surface area. The domains are based on current intentions of the province of Groningen, personal interpretation and the existing infrastructure and dike systems.

The domain of 'Bathymetry5' has the largest area and were determined with the advice of Matthijs Buurman, Program Manager for Coastal Development in Groningen, and derived from the inspiration report of LAMA (Fired et al., 2018; LAMA, 2020) (see Appendix 3.5). This area encloses an area of 2345 hectares, with its outline visualized in Figure 3.5. Bathymetry 5 also includes all smaller areas in Figure 3.5, so contains the total area of all black outlined areas of the realignment project area (i.e. Bat1 + Bat2 + Bat3 + Bat4 + Bat5).

The domain of 'Bathymetry3' has an average surface area and was determined with the advice of Albert Vos, Program Manager for IBP Vloed, and taken from the report 'Ziel in Landschap' (van Paridon x de Groot | abe veenstra landschapsarchitect, 2020) (see Appendix 3.5). This area is significantly smaller than Bathymetry5 and encloses an area of 790 hectares, with its outline visualized in Figure 3.5. Bathymetry 3 includes the area of Bat1, Bat2 and Bat3 in Figure 3.5.

In addition to these two domains, three more domains were designed, of which two were eventually used: 'Bathymetry2' and 'Bathymetry4'. Respectively, one being smaller than Bathymetry3, with an area of 366 hectares, and the other being in between Bathymetry3 and Bathymetry5 in terms of surface area with an area of 1653 hectares. The smallest domain, Bathymetry1, was found to be too small and is not included in the analysis.

All areas are significantly larger than the Breebaart polder, and efforts were made to adapt the domains to the local infrastructure and dike systems, considering the different intended enclosed areas. The different areas of the areas are listed again in Table 3.2.

Domain	Enclosed area [ha]
Polder Breebaart	63
Bathymetry2	366
Bathymetry3	790
Bathymetry4	1653
Bathymetry5	2345

Table 3.2: Surface area of all model domains which are used in the research

Computational grid project area

The primary focus of the research is the volume of extracted sediment, but the creation of natural values is also important. A coarse grid size is sufficient for total sediment extraction, but a finer grid size is preferable for evaluating the creation of a dynamic and diverse intertidal area. However, a too fine grid structure will significantly increase the calculation time. A minimal grid cell size of 35x35 meters captures most of the relevant transport processes while it remains realistic from a computational point of view. The four different created grids can be seen in Figure 3.6.

3.3.2. Bathymetry

In order to ensure realistic conditions, the initial bathymetry is based on the AHN (AHN, 2022). The main operations that have been performed are the removal of high areas and the creation of a channel system using a numerical simulation with the sediment transport formulations according to Engelund-Hansen, as explained below.

Removal of high areas

The study area includes several prominent features, such as a solar park, a sea dike and a grove. To accurately depict real-world conditions when opening the realignment site, the data points of the prominent features have been lowered till they are fitting in the height of the immediate area.



Figure 3.5: All the domain boundaries are visualised. Left in the map: the different domains of the realignment project area. Each larger domain contains also the area of the smaller domains. Bat1 is not further discussed in this thesis report. Right in the map: the location and domain boundary of Polder Breebaart.

Creation channel network

After opening, a tidal creek pattern is likely to develop. In this research the emphasis is on the mud deposition and not specifically on the development of this channel-shoal system. Because this creek pattern is highly unpredictable and dependent on the subsoil, for which there are no data, the channel-shoal system formation is greatly simplified, the same for all scenarios and based on the sand transport formulations of Engelund-Hansen.

The created channel patterns are used as the initial bathymetry for the Partheniades-Krone sediment transport calculation. The different bathymetries that are generated in this way can be seen in Figure 3.7.

3.3.3. External forcing conditions

The external forcing conditions are again tides, wind and the sediment concentration at the boundary. These are described separately below.

Tide

The tidal boundary conditions in the project area differ from those in the calibration area. The entrance to the project area is too large to be effectively managed using culverts. As a result, the project area will be open to the tidal signal of the Ems Dollart. The tidal time series starting from 2015 from Delfzijl, the nearest RWS measuring station, have been used as the tidal signal for the boundary condition of the project area.

Wind

The same data as in the calibration case can be used for the wind. For the application model of the realignment project area, the wind data since 2015 are used to include a larger time span. Appendix

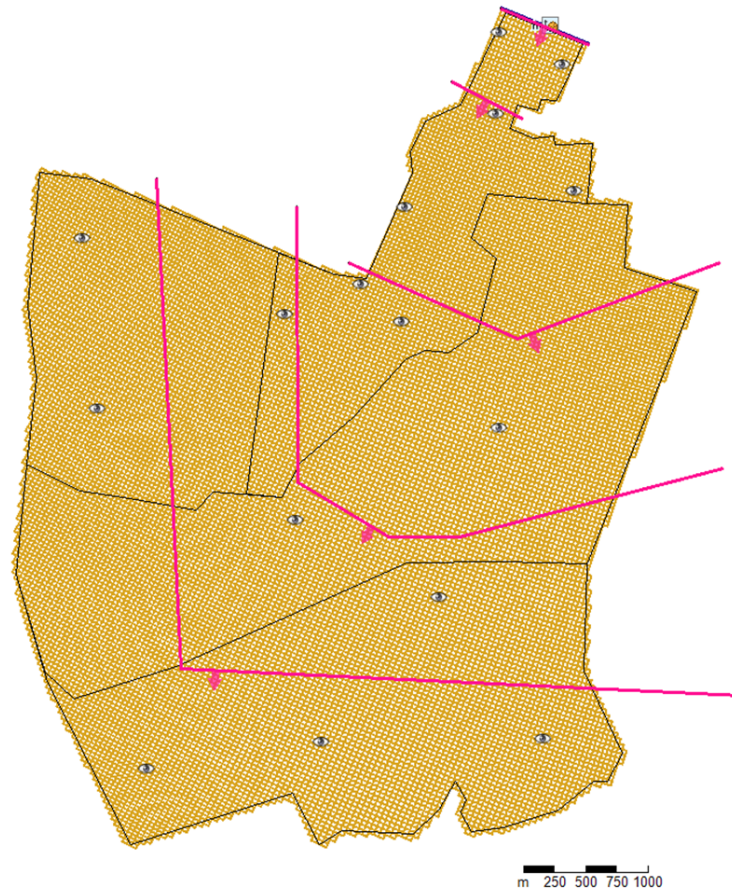


Figure 3.6: The grid of the four used domains. The 'eye' signs represents the observation stations in the numerical model and the red lines shows the observation cross-sections. The observation cross-sections are called crs1 to crs5, respectively from the entrance to the back of the polder. The larger domains includes also the area of the smaller domains towards the open boundary, upper right in the figure.

H further discusses how this data was obtained and processed.

Sediment concentration at open boundary

As in the calibration phase, the SSC that enters the boundary is a crucial forcing condition that determines the total volume of sediment that enters the area. From the Krone-equation (Equation 2.1) can be concluded that there exists a linear relationship between the SSC and the deposition flux. Even with a well-calibrated model, it is important to ensure that this value is adapted to the local conditions. However, the SSC in the Ems Dollart can vary a lot in both time and space, making it challenging to establish accurate values. For the project area, a constant SSC value of 0.15 kg/m^3 was chosen, based on the yearly average SSC reported by van Maren et al. (2015) in the Ems Dollart at measuring station S4 (see Appendix E for location). This value is considered to be a reasonable approximation of the SSC at the boundary and is used in the simulation of the project area. This forcing SSC is lower compared to the SSC for Polder Breebaart since the project area is located more seaward.

3.3.4. Design choices

The same choice was made for the bed roughness and the number of sediment fractions as in the calibration model. Calculations are based on a uniform Manning's roughness coefficient of $n = 0.015 \text{ s/m}^{1/3}$ and with one sediment fraction.

Simulation period

A simulation duration of 2 years is used in this study. This time frame is sufficient for certain sedimentation patterns to become apparent, while still being short enough to avoid unrealistic long-term behavior.

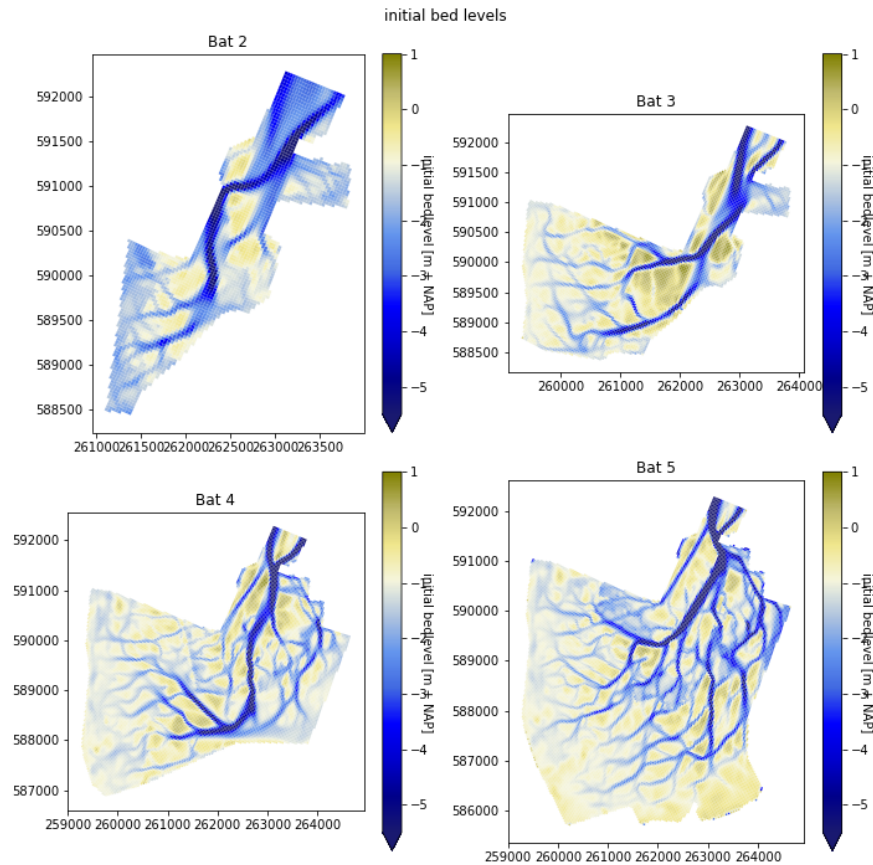


Figure 3.7: Initial bathymetry of the 4 domains. For all four domains, the bathymetry is created using the elevation data of AHN (AHN, 2022), and the transport formulations of Engelund-Hansen.

However, it is important to note that a 2-year simulation period may not provide a clear picture of the long-term behavior of the system, as the model would need to run for several decades in order to accurately predict long-term trends. Additionally, there are many uncertainties, even in the short-term, which can make it difficult to draw accurate conclusions about long-term behavior. By limiting the simulation period to 2 years, conclusions can still be drawn about the initial sediment extraction rate and the extent of the sedimentation patterns observed.

No initial bottom thickness

Starting with an initial bottom thickness leads initially to a significant sediment redistribution, which causes problems in the modeling. The bathymetry is not yet in balance and is created with sand and the Engelund-Hansen equation, instead of mud and the Parthediades Krone equations, leading to a discrepancy between the cross-sectional area and the O'Brien cross-sectional area. This sediment redistribution causes numerical instabilities and also makes it difficult to compare results. Erosion can greatly affect the total sediment flux in the different scenarios. To mitigate these problems, an initial bottom thickness of zero is chosen.

2D or 3D model

After careful considerations, it was determined that a 2D model would be the most efficient approach for this project. The primary reason for this decision is that a 2D model requires significantly less computational resources and thus produces results much more quickly. Though 3D models were also utilized during the calibration process to assess any potential differences in results, it was determined that these differences were negligible.

3.3.5. Model scenarios

During the application phase of the model, various scenarios are examined. As previously discussed in Section 3.3.1, multiple domains have been established, each with a different area. Each domain of the model has its own channel pattern that mimics the natural bathymetry. By utilizing these different models, the research questions, outlined in Section 2.5.9, are addressed. In this way, the aim of the research *to investigate the important factors of influence for sediment capturing efficiency in a managed realignment polder, to make the mud extraction from a turbid estuary as efficient as possible while creating new natural and agricultural value* is achieved.

Six distinct scenarios were conducted on each domain to gain a deeper understanding of the system, address the research questions, and ultimately create a seventh, final scenario that aligns with the research goal. The scenarios focuses on evaluating the impact of incoming tidal energy into the system, as this is a crucial factor to consider, particularly in relation to the calibration model, which had just a limited tidal range. By analyzing the results of these scenarios, it is aimed to offer an appropriate outcome to the research goal.

Scenario 1 - Reference model

No adjustments were made in the first model scenario. On this model, therefore, a completely undamped tidal signal is imposed at the open boundary.

Scenario 2 - Weir

The second scenario involves installing a non-erodible weir just inland of the open boundary. The weir has a height of $NAP + 0\text{ m}$, is supposed to be Mean Sea Level (MSL). The goal is to increase the settling time for suspended sediment particles by maintaining a deeper and temporarily stationary layer of water within the polder. This results in a reduced energy level for half of the tidal cycle. Additionally, this scenario significantly reduces the amount of incoming tidal energy by lowering the effective tidal range that enters the area.

Scenario 3 - Small weir

The concept behind the smaller weir in this scenario is similar to that of the weir in Scenario 2. The implementation of a weir extends the time for sediment to settle, while also reducing the energy flowing into the area. This scenario features a weir at a height of $NAP - 0.5\text{ m}$.

Scenario 4 - Half tidal range

This scenario focuses on limiting the incoming tidal energy. The tidal range is reduced by halving all data in the tidal time series. This approach allows for the observation of the effects of reduced energy without affecting the settling time. This scenario has less impact in practice because it can be challenging to implement. It can be achieved by introducing a flow resistance, such as a dense field of piles or a reduction in the cross-sectional area, thereby allowing only a portion of the tidal flow to pass into the area. The primary goal of this scenario is to enhance understanding.

Scenario 5 - Upper half tidal range

Scenario 5 serves as a comparison to scenario 2, which involves a weir up to $NAP + 0\text{ m}$. In scenario 5, only the upper half of the tide signal is retained by setting all the negative water level data to 0. Only the tidal signal is reduced, while in scenario 2 also the inflow area is also strongly reduced. In scenario 5, the lowest water depth will be reached much faster due to the larger cross-sectional area. As a result, the time with low flow velocities is longer. The settling time will increase compared to scenario 2, but the flow velocities will also increase.

Scenario 6 - Lower half tidal range

In scenario 6, the lower half of the tide signal is retained and therefore is the opposite of scenario 5. Similar to scenario 4 and 5, scenario 6 has less correlation with reality. It can be imagined as a huge culvert that closes as soon as the water level rises above $NAP + 0\text{ m}$. As this is not a realistic scenario, these model scenarios are solely for comparison with scenario 5 and to gain a deeper understanding of the processes.

Scenario 7 - Adjusted depth for the weir

This scenario was created after evaluating the results of scenarios 1-6. The outcomes of scenarios 2 and 3 indicate that the weir significantly restricts discharge, particularly for the largest areas, leading to excessive limitation of tidal energy. In scenario 7, the height of the weir is more closely tied to the surface area, resulting in a relative similar reduction of flow across different domains. The crest levels of these weirs are displayed in Table 3.3.

	Crest level of deep weir [$NAP + m$]
Bathymetry2	-0.6
Bathymetry3	-0.7
Bathymetry4	-1.1
Bathymetry5	-1.25

Table 3.3: The crest levels of weirs Scenario 7. The heights are determined such that the flow in the different domains is reduced in comparable ways.

3.3.6. Wave effect

In addition to the adjustments in the different scenarios, the effect of the wind-generated waves is also examined in the application area. To determine the effect of this waves, three scenarios are simulated twice again. Without the effect of wind-generated waves and with an extra large effect of wind-generated waves. This scaling of the wave-generated bottom shear stresses is done with the wave stirring scaling factor f_{tauw} . The three scenarios that are evaluated here are the reference case and the two scenarios that are judged to generate the best results.

3.4. Assessment of application results

Both the total sediment extraction from the estuary as the sediment distribution within the polder are important for the success of the project. The results of the application model of the realignment project area are therefore assessed by computing the total sediment import into the polder and the distribution of the imported sediment.

3.4.1. Total sediment extraction

Since the main goal of the Ems-Dollart 2050 program is to extract one million ton of dry matter per year from the estuary, the total sediment extraction of the polder is a crucial assessment criterion for evaluating the effectiveness in sediment extraction of the managed realignment polder. However, the sediment extraction can be investigated in various ways. Firstly, the total volumes that a scenario extracts from the estuary can be compared. Secondly, the extracted volume compared to the prism or the effective tidal range can be investigated. The gross transport is higher with a larger prism. By comparing the extracted sediment with the prism, the efficiency can be determined.

Because the SSC on the open boundary is constant, a comparison of the total accumulation with the gross sediment import will give the same results as the comparison with the prism. The comparison with the prism will therefore immediately reveal the scenarios with the highest capture efficiency.

3.4.2. Spatial sediment distribution

The sediment distribution can be analyzed both in terms of spatial distribution and elevation distribution of accumulation. Both perspectives are important, therefore they are examined separately.

In section 2.4 it was shown why a equal spatial distribution of sediment is important for nature development or raising agricultural. The elevation distribution of accumulation can also provide insight into the functioning of a scenario. When a scenario has a larger proportion of accumulation occurring at lower bed levels, likely more accumulation takes place in channels. For the nature development, it is important that sedimentation takes place especially within the tidal range.

4

Results

In this chapter the results of the research with the numerical model Delft3d FM are discussed. The chapter starts with a section where the insights from the data analysis are discussed. These insights form the targets to imitate with the simulation of the calibration model, discussed in section 2.5.9. This section concludes with the findings from the calibration phase, after which the application of the model is discussed in section 4.3, ending with a short summary of the key findings.

4.1. Insights from data analysis

4.1.1. General accumulation pattern

The morphological development is visualised in the bottom figures of 4.1. There has formed a general pattern of small-scale erosion near the inlet, with sedimentation occurring throughout the rest of the area, particularly in channels. Additionally, a sedimentation front can be observed migrating away from the inlet over time. Specifically, in August 2020, this front was located at about 25% of the polder, but by August 2021, it had advanced to approximately two-thirds of the polder. These findings provide insight into the dynamics of sedimentation in the area and the processes that govern the movement of sediment in the polder.

The middle bottom figure illustrates the difference between August 2020 and August 2021 and shows some erosion holes in the back of the study area. While it's challenging to identify the exact cause of this erosion, it appears that these holes may be temporary in nature, as they are not present in the map depicting the difference between March 2020 and August 2021. Due to this uncertainty and the limited duration of this erosion, it will not be further investigated in this study.

4.1.2. Total sediment import

The data analysis indicates that a total of 8255 m^3 of accumulation occurred between August 2020 and August 2021. This volume is determined by summing up all data points of the middle bottom figure in Figure 4.1. The sample frequency is every meter, so these data points are multiplied by one square meter to come to the total volume.

However, this data is interpolated over the grid in Figure 3.2 that is created in Section 3.2.1. Since the numerical model of Breebaart is build with the *WGS 84 / Pseudo-Mercator* projected coordinate system, the elevation data of Polder Breebaart is transformed from *Amersfoort / RD New* to *WGS 84 / Pseudo-Mercator*. Through this transformation, the distances in the area are scaled by approximately 1.5 and the accumulation is scaled by approximately $1.5^2 = 2.25$. Due to the interpolation to this coordinate system, the volume of the total accumulation to which the models must be calibrated is 18171 m^3 . The morphological change calculated with the numerical model will be compared to this volume for consistency. For more information about this transformation, see Appendix N.

4.1.3. Distribution between northern part and southern part of Polder Breebaart

A distinction can be made between the northern part of the polder, close to the entrance for the tide, and the southern part of the polder, below the bottleneck. In figure 4.1, the separation between these areas

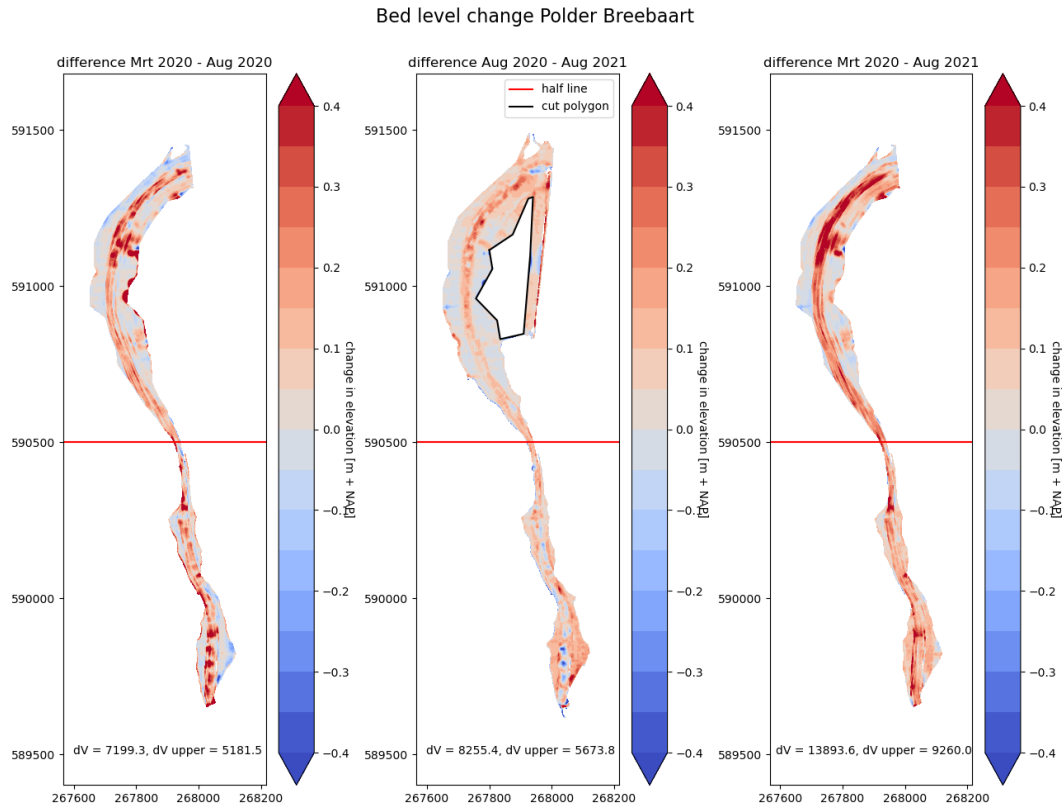


Figure 4.1: The difference in bed levels between data sets. At the bottom of the plots is the total volume change of sediment showed. The red line shows the divide between the upper part and lower part for the volume change calculation. The black polygon represents the data which is not included in the data analysis due to differences in reed height.

is visualized. Because there is only a small tidal difference in the polder and therefore low dynamics, it is not surprising that most of the sediment also initially settles near the entrance before partly being transported further by resuspension processes. This is also observed by the data, as approximately 2/3 of the sedimentation (5674 m^3 of the 8255 m^3 between August 2020 and August 2021) takes place in the upper part. This is further highlighted when the line used for the distinct calculation is moved northward, specifically at a quart the polder (i.e. at the height of $y = 591000$). More than half of the total sedimentation (4367 m^3 of the 8255 m^3 between August 2020 and August 2021) takes place northward of this line and therefore close to the entrance.

4.1.4. Distribution between tidal flat and channel

The data analysis presents a clear pattern of sedimentation taking place primarily in the channels. A separation is made in the bottleneck of the polder to distinguish the two parts of the polder that silted up differently. The northern part of the polder shows a noticeable difference in sediment accumulation between the channels and the shallow areas, whereas in the southern part of the polder, sedimentation rates are lower in the channels relative to the shallower parts. Overall, this finding highlights the significance of the channel dynamics in controlling the sedimentation patterns in the intertidal area.

4.2. Calibration phase of the model: Polder Breebaart

The Breebaart model is calibrated by varying different processes and settings in order to achieve the best results. The performance of the results from the calibration are mixed, with some success in the northern part of the polder, but a lack of sediment accumulation in the southern part. The results are analysed and evaluated with the methods described in Section 3.2.4. The conclusions of this analysis are described in Section 4.2.7. Overall, the Breebaart model serves as a valuable tool for understanding and addressing some sedimentation issues in the polder.

4.2.1. Parthediades-Krone parameters

The effect of varying different parameters in the Partheniades-Krone equations are illustrated in Figure 4.2. In this figure, the resulting flux (i.e., Deposition minus Erosion) is plotted against the bed shear stress. Each graph shows the variation of one of the three parameters that can be adjusted. This graph demonstrates the resulting flux that occurs with an increasing bed shear stress. It is evident from the figure that the deposition flux is minimal in comparison to the possible erosion flux at high bed shear stress. At the same time, it also shows that as long as the bed shear stress τ_b remains below the critical bed shear stress for erosion τ_{cr} , only deposition takes place. What is not shown in Figure 4.2 is the effect of the flux on the SSC, the flux directly influences the SSC. As a result, the deposition flux is also influenced and this dampens the effect on the total flux. Figure 4.2 only shows the initial flux, when the effect on the SSC and its feedback on the deposition flux is considered, you also have to deal with spatial varieties.

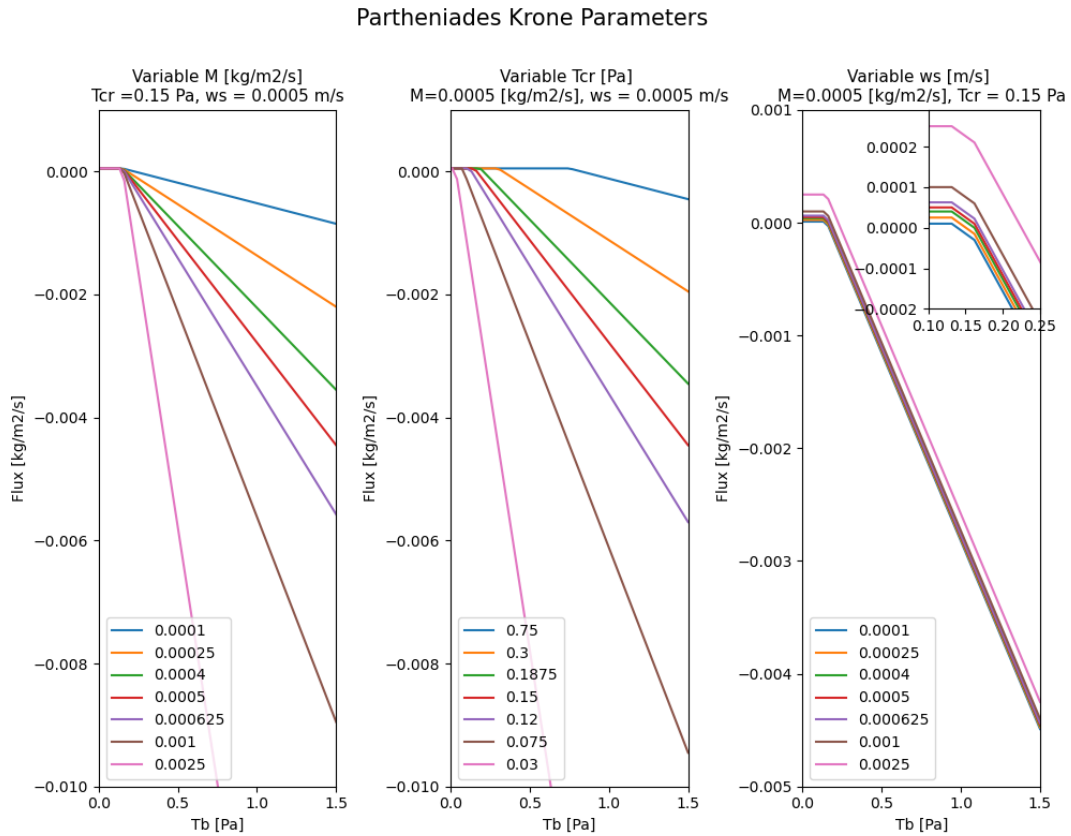


Figure 4.2: The effect of the Partheniades-Krone parameters on the flux. Only the horizontal piece at the top of the graph (where the flux is larger than 0) shows a flux where deposition exceeds erosion. This shows that the erosion flux at high shear stresses according to the Partheniades-Krone equations can become many times larger than the deposition flux. This research therefore mainly focuses on the small horizontal part at the top where net sedimentation can take place.

4.2.2. Only tide effect

The numerical simulations show that while importing sediment is successful, distribution within Polder Breebaart does not. Most accumulation occurs near the entrance and sediment movement is limited (Figure 4.3A). Even when sediment settling velocity is significantly reduced (order 10^{-5}), distribution remains uneven and the accumulation does not reach far enough into the polder. When decreasing the critical shear stress τ_{cr} to promote resuspension, the sediment is transported further into the polder. This results in erosion occurs particularly in the channels and sedimentation still occurs on the shallow parts, while the data shows the opposite (Figure 4.3B and Figure 4.3C). When the critical shear stress is further reduced, this becomes even more visible. With only the current-induced bed shear stresses, it is therefore not possible to get the distribution between front and rear as well as the distribution between

channel and mud flat.

This result is noticeable because it was expected from the conceptual model that the tidal current was largely responsible for the import of sediment and for its distribution within the polder. However, it seems that the amount of diffusion of suspended sediment in the polder is not sufficient. Therefore, the result is only successful in terms of imported sediment. For all other assessments (described in Section 3.2.4) it does not satisfy the requirements.

4.2.3. Wind effect

An effort was made to enhance the spread of SSC by adding the impact of wind in the calculation. The goal was for the wind to create a circulation current and transport the sediment deeper into the polder. To achieve this, a 3D calculation was performed. However, it was found that this approach did not achieve the desired outcome, sediment continued to settle near the entrance.

4.2.4. Wave effect

After running the simulation, which now takes into account the effects of waves, sedimentation can be observed further into the polder (Figure 4.3D). There is significant sedimentation in the channel at the back of the polder. Visually, the simulation appears to produce better results than previous simulations without wave effects. However, there is also significant erosion in the shallower areas of the polder. Analysis of the 5% exceedance values of the bed shear stresses shows that the shear stresses in the shallower areas are much higher than in the channels. This is likely due to the waves. By adjusting the parameter f_{tauw} , the influence of wave-induced shear stresses can be limited compared to current-induced bed shear stresses, resulting in lower erosion and sedimentation in the shallower areas. However, this also decreases sedimentation in the channels.

The Brier Skill Score (BSS) shows that the accumulation in the model is consistently worse than the initial bottom. Additionally, the sediment transport through the bottleneck of the area is virtually absent, and significant sediment transport to the south side of the polder has not yet been realized. Due to the resuspension, the waves mainly led to a redistribution between shallow and deep areas, and not enough for transport in the longitudinal direction of the polder.

4.2.5. Increased tidal energy

After multiple attempts, it is determined that it is not possible to reproduce significant sediment transport to the south side of the polder using the current parameters. Upon analysis, it is expected that this may be due to limitations in the model's ability to handle low-energy dynamics, as the tidal range in the area is only 20 cm.

To test this hypothesis, the model was run with the same parameters but with a tidal range boundary condition that is 6 times larger than the actual tidal range present. The results indicate that the simulation is much more successful in getting sediment to the back of the polder. The result of this model run can be seen in Figure 4.3E. This supports the hypothesis that the dynamics in the polder are too low to simulate the morphology with the created Delft3D FM model.

The model simulation with the increased tidal range is just for providing understanding of the underlying numerical processes and does not accurately reflect reality. The result is therefore not evaluated with the assessment methods. It shows that it is difficult to reproduce the accumulation of the data with the given preconditions boundary conditions.

4.2.6. Parameters from calibration

A wide range of parameters were evaluated during the calibration phase. The key parameters that were determined are discussed below. Additional information on some of these parameters and some extra parameters can be found in Appendix C.

Settling velocity w_s

The settling velocity, denoted by w_s , is a crucial calibration parameter. It has a direct impact on the volume of sediment that accumulates in an area. The deposition flux is described by Equation 2.1, and as shown in Figure 4.2, there is a linear relationship between the deposition flux and the settling velocity. This means that an increase in the settling velocity leads to an increase in total sedimentation. However, a higher settling velocity also results in more sediment settling near the entrance, which in turn leads to less sediment reaching the back of the polder. The model demonstrates improved spatial

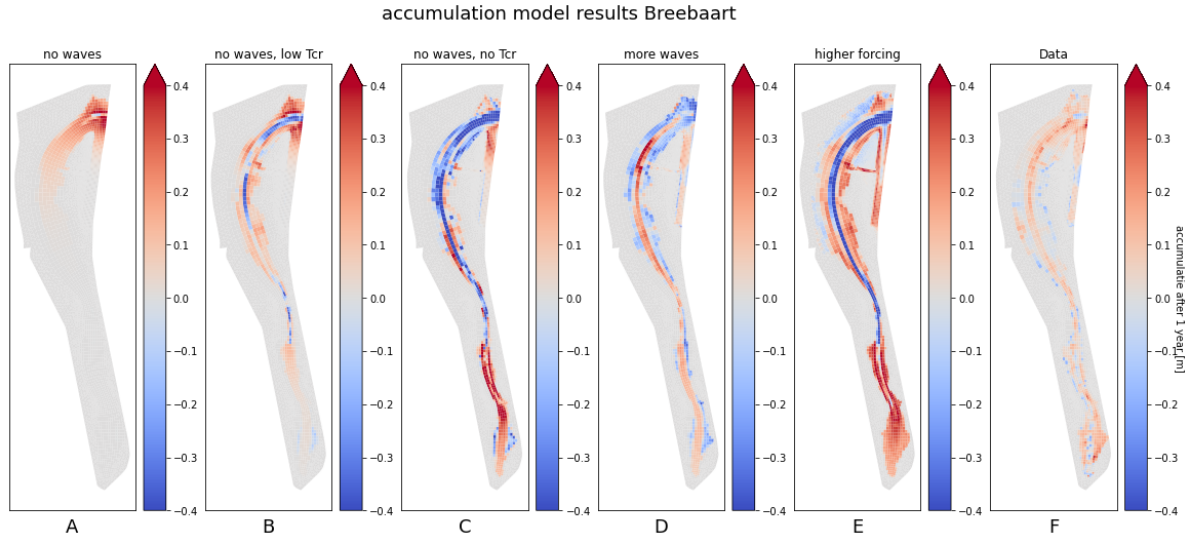


Figure 4.3: Some results during the calibration process. A: The result without waves and $\tau_{cr} = 0.15 Pa$. B: The result without waves and $\tau_{cr} = 0.04 Pa$. C: The result without waves and $\tau_{cr} = 0.01 Pa$. D: The result with waves. E: The result of a simulation with 6 times larger tidal forcing. F: The data which should be approximated with the numerical model.

distributions at lower settling velocities, however, these velocities may become unrealistic. Therefore, a lower limit of $w_s = 0.0001 m/s$ has been established to prevent the settling velocity from falling below a certain value.

The settling velocity used in the application model is $w_s = 0.0001 m/s$, or $0.1 mm/s$. This is the lower limit of the settling velocity. This is discussed in more detail in Appendix C.

Critical shear stress for erosion T_{cr}

As previously mentioned in Section 2.5.8, the critical shear stress is a key parameter whose magnitude is determined in the calibration of the model. Equation 2.2 and Figure 4.2 demonstrate that the critical shear stress plays a significant role in determining the amount of erosion that takes place and greatly influences the resulting sediment flux. The critical shear stress establishes the threshold for excess bed shear stress, erosion only begins when the shear stress exceeds this critical value. The erosion flux is therefore inversely dependent on the critical shear stress.

With the calibration model it is determined that the critical shear stress used in the application model is $T_{cr} = 0.21 Pa$. This is discussed in more detail in Appendix C.

Erosion parameter M

Similar to the critical shear stress, the erosion parameter M affects the erosion flux. However, unlike the critical shear stress, the erosion parameter has a linear positive relationship with the erosion flux. The erosion parameter scales all erosion that takes place, and therefore plays a significant role in determining the size of the erosion flux, which can quickly surpass the deposition flux.

With the calibration model it is determined that the Erosion parameter used in the application model is $M = 0.00025 kg/m^2/s$. This is discussed in more detail in Appendix C.

Wave stirring scaling factor f_{tauw}

During the calibration, it is determined that when accounting for the shear stress generated by wind waves, the generated shear stresses, especially in shallower areas, were excessively high and resulted in excessive erosion. This led to the conclusion that the shear stresses caused by wind waves has an disproportionately large impact on the total shear stresses. To address this, a parameter was introduced to limit the contribution of wave shear stress to the total shear stress. This is particularly effective in shallower areas, where the shear stress caused by flow is significantly smaller in comparison to that caused by waves.

With the calibration model it is determined that this parameter used in the application model is $f_{tauw} = 0.185$. This is discussed in more detail in Appendix C.

4.2.7. Assessment during calibration

The assessment of the model outcome is done as described in Section 3.2.4. These assessment methods are mainly applied on the northern half of the polder, since it is concluded that the sediment transport to the southern half of the polder through the bottleneck has not been successful in the numerical model.

Spatial distribution

The spatial distribution of the accumulation is done by a visual check. In Figure 4.4, the change in bed levels by the model is compared to the change in bed levels by the data. This immediately reveals that the northern part of the polder corresponds better with the data than the southern part. No emphasis was put on this because the assessment focuses on the northern part.

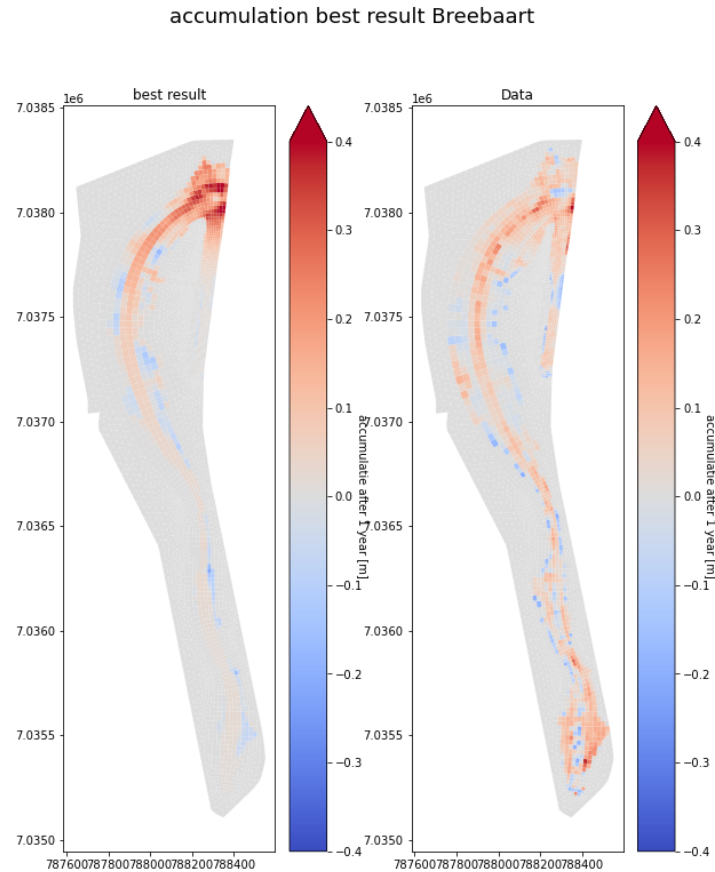


Figure 4.4: Calibration Breebaart. Erosion and accumulation according to model (left) and according to data (right)

Sediment import

The bias of the model is assessed with the total sediment import. The model overestimates the amount of incoming sediment. The data reveals a yearly sediment import of 18171 m^3 , whereas the best calibrated Breebaart model results in a total sediment import of 22635 m^3 . This represents an overestimation of 125%. With an imposed SSC at the open boundary and a settling velocity that has a realistic lower limit of $w_s = 0.0001 \text{ m/s}$, the deposition flux is according Krone's equation (equation 2.1) reasonably fixed. If the erosion flux is increased by using with a smaller critical shear stress (τ_{cr}) or with a larger erosion flux parameter (M), erosion increases significantly, particularly in the shallower areas. As a result, the total imported sediment quantitatively corresponds to the sediment import of the data, but the morphological development does not longer correspond with the data. The Brier Skill Score then quickly becomes negative (meaning that the morphological development of the model is worse than the initial bathymetry compared to the development in the data).

Mean absolute error

The Mean Absolute Error (MAE) is a measure of the model's accuracy. By analyzing only the northern half of the polder and calculating the MAE, the optimal score of $MAE = 0.079\text{ m}$ is obtained.

Brier Skill Score

The BSS is an analyse method that aims to provide an objective overall score for the model's skill. The BSS of $BSS = 0.057$ has been determined for the northern part of the polder. In addition to this BSS, the BSS is also calculated when only cells with accumulation are taken into account. When excluding cells with erosion, a BSS of $BSS = 0.42$ has been determined. This highlights the fact that the model is better at predicting the sedimentation patterns than the erosion patterns.

4.2.8. Overall assessment

Despite the model overestimating the total sediment import, it is decided to continue calculating with this parameter settings since this settings has result in the best scores for both the Mean Absolute Error and the Brier Skill Score. But it is important to keep in mind that these model settings overestimates the total sediment import.

The most important parameter setting of the calibration phase are previously discussed in Section 4.2.6. These parameters are summarised in Table 4.1. Other findings are explained in Appendix C and Appendix I.

Parameter	Value
Settling velocity	$w_s = 0.0001\text{ m/s}$
Critical shear stress	$\tau_{cr} = 0.21\text{ Pa}$
Erosion parameter	$M = 0.00025\text{ kg/m}^2/\text{s}$
Wave stirring scaling factor	$ftauw = 0.185$

Table 4.1: Parameters from calibration

4.3. Application phase: realignment project area

The numerical model of the realignment project area has been run with the parameter settings determined during the calibration. The forcing conditions which are used are described in Section 3.3. In Section 3.4 is described how the results are evaluated regarding the total sediment import into the polder and both the spatial and elevation distribution of the accumulated sediment. These evaluations are discussed separately below.

4.3.1. Sediment extraction

The goal of Ems-Dollart 2050 is to extract one million tons of dry matter from the estuary per year. Based solely on the results of the numerical model, it could be concluded that this objective could be achieved using a managed realignment polder (reference, half range and deepweir scenario in Figure 4.6). Because there are still many uncertainties in the model after calibration, the exact quantities will not be discussed further, but the focus will be on the mutual differences between the scenarios.

Total sediment extraction

The reference case imports the largest volume of sediment for all domains (Table 4.2 and Figure 4.5). The case with the weir at $NAP + 0\text{ m}$ is the least effective for almost all domains. The scenario with a halved tidal range, which limits incoming energy, and the scenario with a deep weir also result in a relatively large sediment import.

Sediment extraction compared to domain area

The sediment import is fairly linear in relation to the domain area. Figure 4.6 illustrates the sediment extraction in tons of dry matter per year for different domains of the polder. This linear relationship does not apply to all scenarios. It is noticeable that the graph of the 'weir' and 'smallweir' scenarios deflects enormously downwards from the bathymetry4 domain. This may have to do with the fact that the weir restricts the tidal prism that much that also the sediment import hardly rises further.

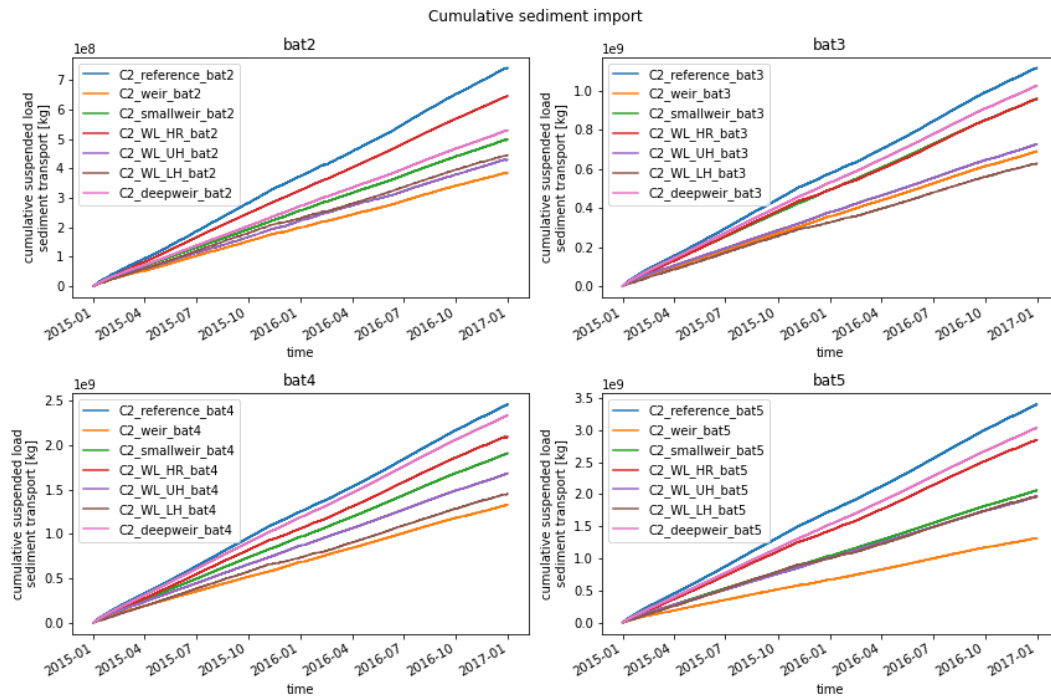


Figure 4.5: Sediment import of all model scenarios, measured by the cumulative sediment flux [kg], passing the boundary (i.e. crs1, see Figure 3.6).

[$10^6 m^3$]	Reference	Weir	Smallweir	Half range	Upper half	Lower half	Deepweir
Bat2	1.48	0.77	0.99	1.29	0.85	0.89	1.05
Bat3	2.22	1.37	1.91	1.91	1.44	1.25	2.04
Bat4	4.88	2.64	3.79	4.16	3.34	2.88	4.64
Bat5	6.75	2.61	4.09	5.66	3.90	3.91	6.03

Table 4.2: The sum of the total accumulation in the entire polder. The color range shows the highest net sediment import, relative to other scenarios for the same domain. Green indicates the highest imported volume [m^3] and in red the lowest imported volume [m^3].

Sediment extraction compared to prism

In Table 4.3 shows the tidal prism and the mean tidal range (MTR) for all the scenarios. The MTR and the tidal prism have a clear correlation (Figure 4.7). The reference case has the highest tidal prism and MTR. Because of the constant SSC at the open boundary, it has also the highest gross sediment import. This explains the high sediment import of the reference case.

Figure 4.8 shows the relation between the sedimentation and the tidal prism of the different scenarios. It is clear that the line of the reference case runs the lowest, which means the lowest sediment import relative to the tidal prism. Table 4.4 shows the total sediment extraction after two years divided by the prism. Scenario 5 and scenario 6 have been excluded from the table since they have such a low prism relative to the reference case that it would skew the comparison. From both Figure 4.8 and Table 4.4, it becomes clear that the reference case is the least efficient in capturing the incoming suspended sediment.

Table 4.4 also demonstrate that the efficiency for the scenario with the halved tidal range is the most efficient. When the tidal range is halved, the volume of sediment import relative to the prism is significantly higher. This is also evident in Figure 4.8, where the effect of halving the tidal range is visualised. It is clear that halving the tidal range does affect non-linearly the sediment import.

4.3.2. Spatial accumulation distribution

The spatial distribution of accumulation appears to be closely related to the occurring bed shear stresses. High incoming energy results in most accumulation at the back of the polder, while a limited amount

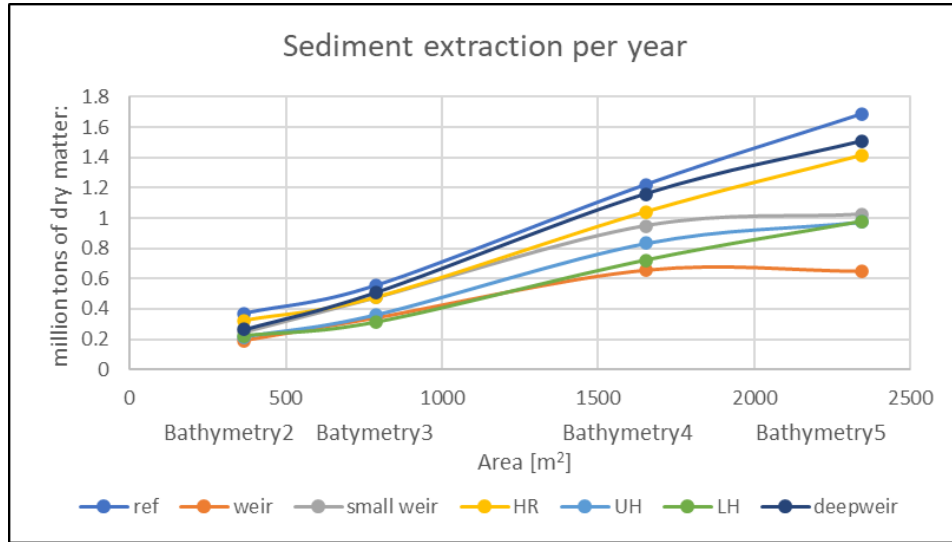


Figure 4.6: The sediment extractions per year in millions ton dry matter. The mass is calculated with $\rho_b = 500 \text{ kg/m}^3$

	Bat2		Bat3		Bat4		Bat5	
	MTR	Prism	MTR	Prism	MTR	Prism	MTR	Prism
	[m]	$[10^6 \text{ m}^3]$	[m]	$[10^6 \text{ m}^3]$	[m]	$[10^6 \text{ m}^3]$	[m]	$[10^6 \text{ m}^3]$
ref	3.0	8.7	3.0	16.2	3.0	34.3	3.0	50.7
weir	1.4	4.3	1.3	9.0	1.1	15.1	0.9	18.3
smallweir	1.8	6.1	1.7	11.6	1.4	21.6	1.3	27.7
HR	1.5	5.2	1.5	9.4	1.5	17.2	1.5	30.2
UH	0.9	3.3	0.7	4.3	0.8	11.1	0.8	16.9
LH	0.8	2.0	0.5	2.0	0.5	5.1	0.7	8.6
deepweir	1.9	6.3	1.9	12.7	1.8	27.6	1.8	39.0

Table 4.3: The mean tidal range (MTR) and tidal Prism for all scenarios. These two values are, of course, closely correlated. It is clear that the reference case in particular has high values. Higher values in the table have a deeper blue color to indicate the large numbers quickly.

of incoming energy hinders accumulation in the back of the polder. A comparison of model results is provided below where this finding is observed.

Reference case

The left four figures in Figure 4.9 shows mainly accumulation in the back of the polder for the reference scenarios. The majority of the area shows no accumulation. Figure 4.9 also shows the 95.83% percentile values for bed shear stress. This bed shear stress occurs on average for 1 hour per day. The map shows a clear relationship between the bed shear stress and the sedimentation patterns. The color limits of the bed shear stress maps are set to 0.21 and 0.51 Pa. These limits were chosen because erosion begins at 0.21 Pa (the critical shear stress) and at 0.51 Pa significant erosion is already taking place. A daily erosion flux of 1.29 kg/m^2 can be expected with an bed shear stress of 0.51 Pa for 1 hour per day (see equation 4.1). The deposition flux amounts to $1.30 \text{ kg/m}^2/\text{day}$ (see equation 4.2). It can be inferred that even if only this bed shear stress occurs for 1 hour per day, almost all deposition would erode away. Since lower bed shear stresses also occur for a larger part of the day, the high bed shear stress causing an erosion flux that exceeds the deposition flux in a large area. Therefore only accumulation takes place in areas of low bottom shear stresses.

$$E = M \left(\frac{\tau_b - \tau_{cr}}{\tau_{cr}} \right) = 0.00025 \left(\frac{0.51 - 0.21}{0.21} \right) = 0.00036 \text{ kg/m}^2/\text{s} \quad (4.1)$$

$$D = w_s C = 0.0001 * 0.15 = 0.000015 \text{ kg/m}^2/\text{s} \quad (4.2)$$

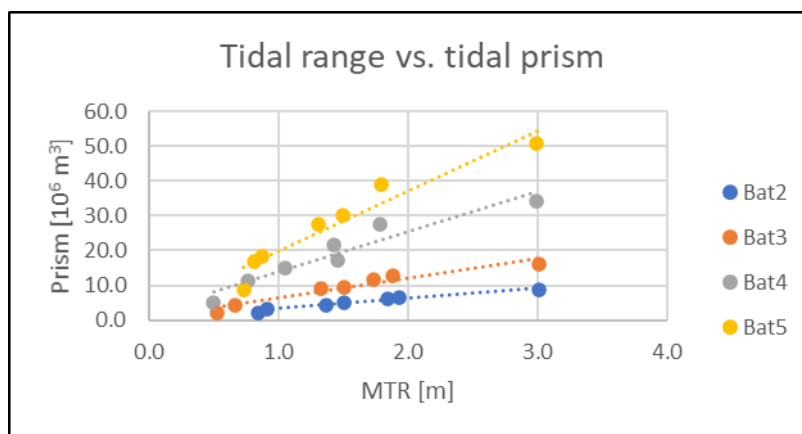


Figure 4.7: The tidal prism of all model scenarios is plotted against the mean tidal range (MTR). This shows a clear correlation. The angle at which the trend lines in the graph run, correspond to the area of the domains.

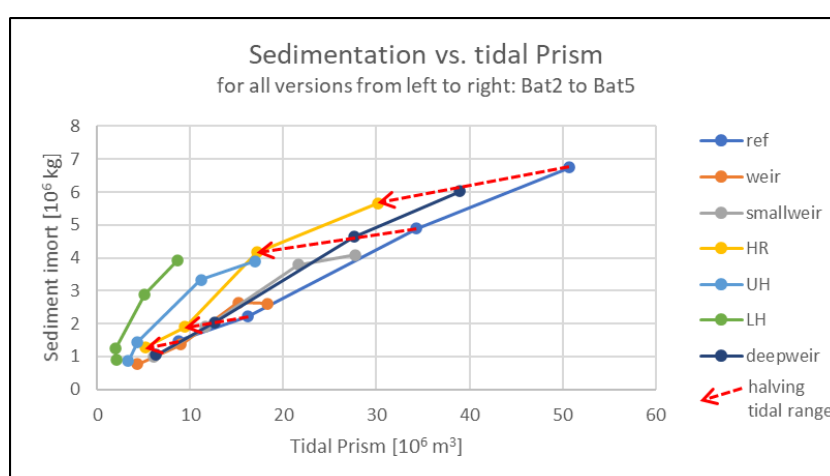


Figure 4.8: Accumulation as function of tidal prism. For all scenarios, markings from left to right, the domains Bat2 to Bat5. The effect of halving the tidal range is indicated in red dotted lines. It is clear that by halving the tidal range, the sediment import is not halved.

Half tidal range

The reference case has an excessive amount of energy in the system, showed by the high bed shear stresses and resulting in a lack of accumulation in a significant part of the area. By halving the tide range, the tidal prism is has decreased on average with 43.6%. Due to the tidal flats, this is not exactly the same as the decrease in tidal range. However, this still results in a significant reduction in incoming energy, which leads to another distribution of sediment. Figure 4.10 shows that for all domains, by halving the tidal range, the spatial distribution of accumulation is less centered in the back of the polder compared to the reference case.

Figure 4.10 shows that also the 95.83% percentile of bed shear stresses has been reduced in comparison with the reference case. In terms of spatial distribution, it appears that reducing the tidal prism results in a more favorable distribution of sediment in the polder.

When comparing the results of the scenarios halving the tidal range by using only the upper or lower half of the tide, the distribution of accumulation is very different. Both scenarios are importing comparable amounts of sediment (especially the largest area, as shown in Figure 4.5), the scenario with the lower half of the tide brings sediment more to the back of the polder. Additionally, in the scenario using the upper half of the tide, accumulation is more concentrated in channels then for the lower half (Figure 4.11). The same pattern emerges at bed shear stresses. The lower half scenario shows higher bed shear stresses in channels and till further into the polder than the upper half scenario. This suggests that water flows more through the channels in the lower half scenario and more evenly over the tidal flats, creating sheltered areas in the channels, in the upper half scenario.

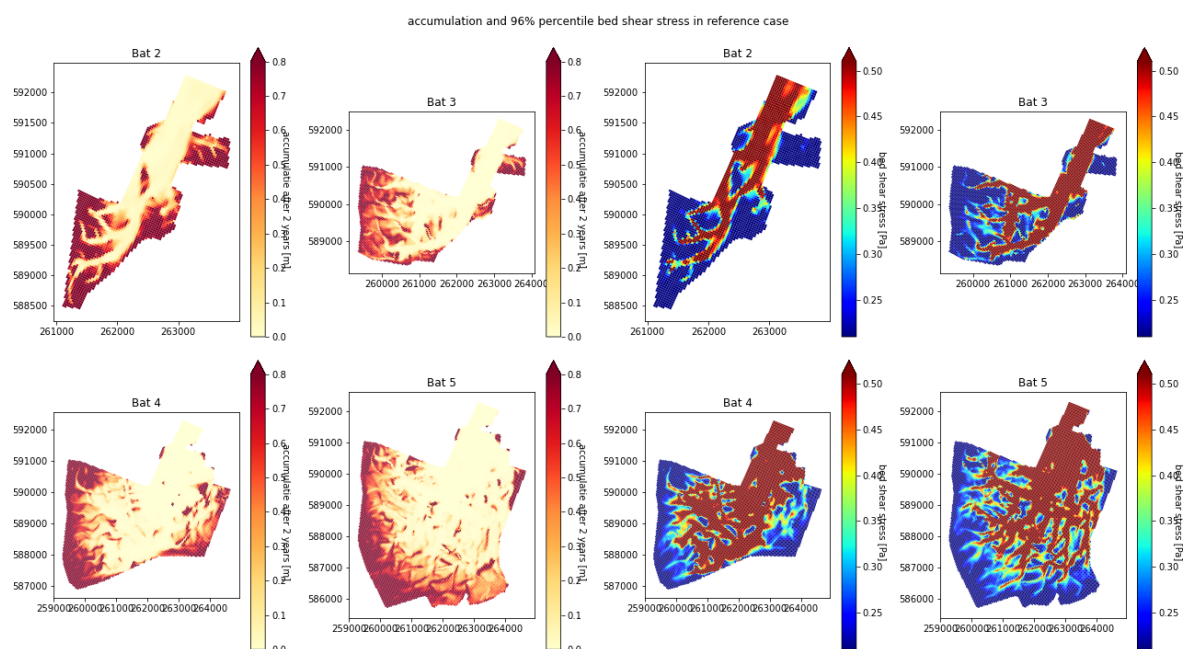


Figure 4.9: The accumulation after two years of the reference scenario and the 96% percentile of the occurring bed shear stress. This bed shear stress is occurring for 1 hour a day on average. The color bar limits starting from 0.21 Pa, which is the critical bed shear stress. Only excess bed shear stresses are colored therefore. There is a clear correspondence between the occurring bed shear stresses and accumulation patterns.

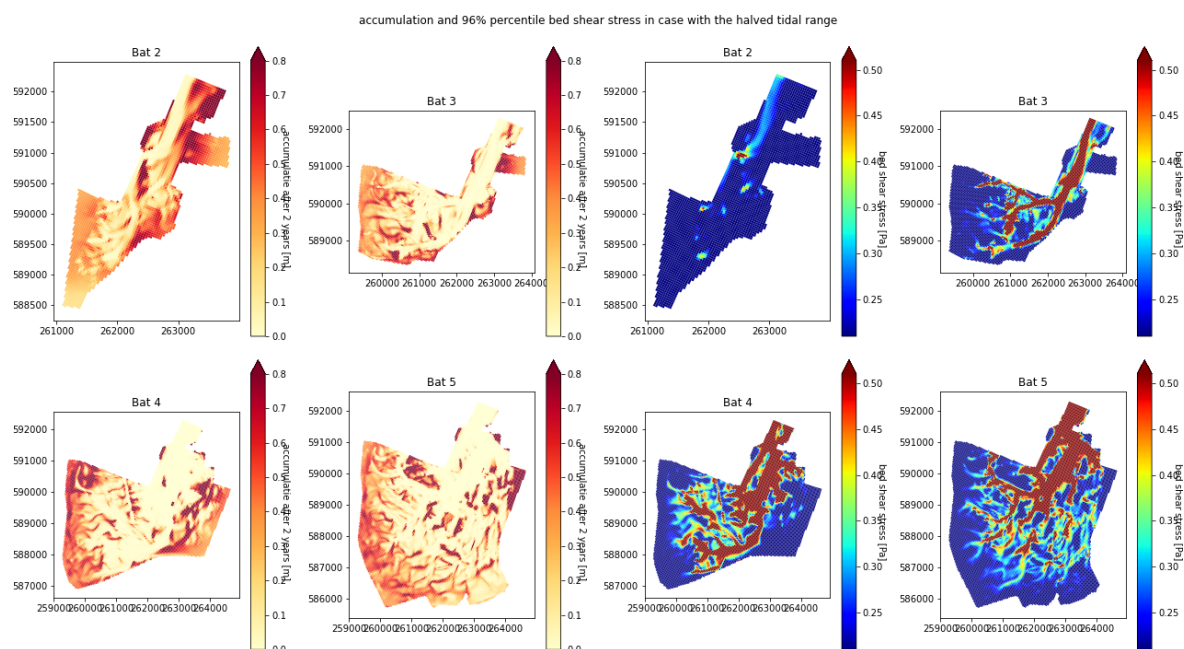


Figure 4.10: The accumulation after two years of the scenario with the halved tidal range and the 96% percentile of the occurring bed shear stress. This bed shear stress is occurring for 1 hour a day on average. The color bar limits starting from 0.21Pa, which is the critical bed shear stress, only the excess bed shear stresses are colored therefore.

	ref	weir	smallweir	HR	deepweir
Bat2	0.169	0.178	0.162	0.249	0.166
Bat3	0.137	0.153	0.164	0.202	0.161
Bat4	0.142	0.174	0.176	0.243	0.168
Bat5	0.133	0.142	0.148	0.188	0.155

Table 4.4: Total accumulation [m^3], divided by prism [m^3]. Scenario 5 and scenario 6 have been excluded from the table since they have such a low prism relative to the reference case that it would skew the comparison. Scenario HR (halved tidal range) shows significant higher sedimentation relative the tidal prism then the reference case. It should be noted that these numbers do not present the accumulation per tidal cycle, the numbers are only for comparison and to determine the relative efficiency of the scenarios.

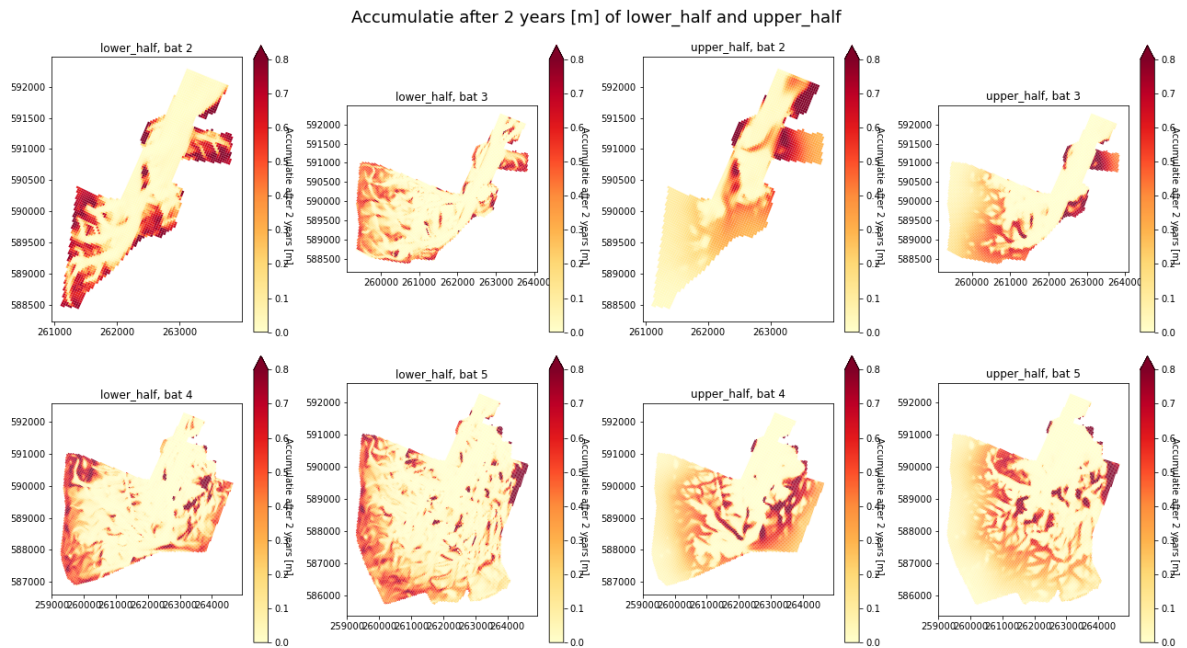


Figure 4.11: The accumulation after two years with the scenario using the lower half of the tidal range and the scenario using the upper half of the tidal range.

Weirs

The accumulation maps of the model simulations for the scenarios with the 'weir' (with a crest level at $NAP + 0\text{ m}$) and the 'smallweir' (with a crest level at $NAP - 0.5\text{ m}$) show that there is no accumulation at the back when using a weir (Figure 4.12). In the left figures (i.e. scenario 'weir'), the accumulation is centered further away from the back of the polder than in the right figures (i.e. scenario 'smallweir'). It seems that the suspended sediment does not reach the back of the polder. This is confirmed by the mean SSC values of these scenarios, shown in Figure 4.13. The distribution of accumulation is only reasonable for the scenario with she smallweir on the two smallest domains.

With the weirs, as with halving the tidal range, the incoming tidal prism is reduced. Table 4.3 shows that while the prism of scenario 'weir' and 'HR' is comparable, the occurring bed shear stresses are not. It seems that by using the weir, the incoming energy is limited too much to bring the sediment significant into the polder. This is supported by the observation that sediment is transported further into the polder in the scenario with the smallweir ($NAP - 0.5\text{ m}$) than in the scenario with the normal weir ($NAP + 0\text{ m}$).

The observation that reducing the incoming energy can have positive effects on the spatial distribution of accumulation and the observation that the weirs of scenario 'weir' and 'smallweir' reduces the incoming energy too much has lead to the creation of the seventh scenario, the scenario with the deep weir. In this scenario, the crest level of the weir is adjusted to the size of the domain, as listed in Table 3.3. This results in the sediment moving much further into the polder (Figure 4.14), creating a comparable pattern as the half tidal range scenario (Figure 4.10).

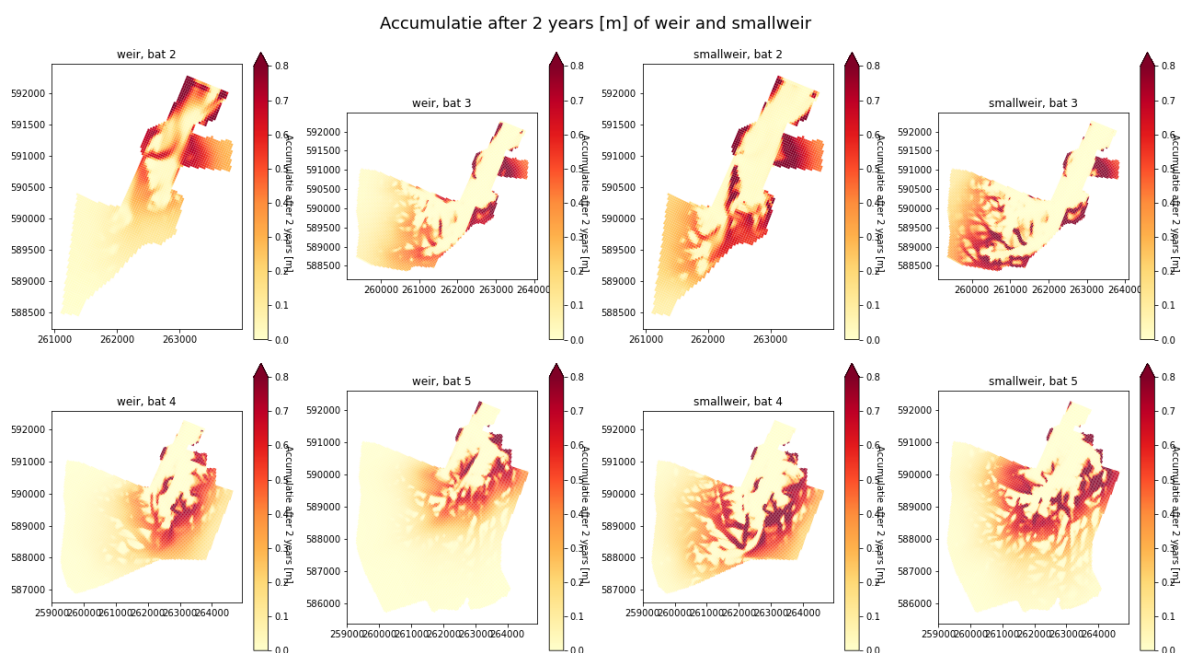


Figure 4.12: The accumulation after two years of the scenario with the weir (crest level at $NAP + 0\text{ m}$) and the scenario with the smallweir (crest level at $NAP - 0.5\text{ m}$).

In Section 3.3.5, it is noted that the scenario with the upper half of the tide is created to compare with the scenario that uses a weir with a crest level of $NAP + 0\text{ m}$. In Figure 4.15, the results of all water levels of Bathymetry 4 are plotted. The plot in the bottom right corner demonstrates that the tides of the weir and smallweir produce other water levels in the polder compared to the scenario using the upper half of the tide ('WL_UH'). This is also evident in the sedimentation patterns, where the difference between 'weir' and 'WL_UH' is significant. This is partly due to the delay in the lowering of the water level with the weir, resulting in a higher average water level.

Side basin accumulation

The two smallest domains of the model both contain a side basin close to the open boundary, with an area of approximately 37 ha. The simulations with these domains reveal that a relatively high net sedimentation occurs in this side basins. This accumulation is particularly notable because in the majority of the cases, no net sedimentation takes place in front of this side basin. This high accumulation can not be explained by higher sediment concentrations close to the entrance. The mean concentration deeper into the polder has the same values as close to the entrance. However, it can be explained by the occurring bed shear stresses in the side basin. The figures with the bed shear stresses confirm that this side basin contains very low energy, which explains the high net sedimentation in this area.

This result is particularly relevant when considering the aim of raising agricultural land. When creating several smaller basins along the edge of the area, with no flow through them, the net sedimentation can be stimulated. Furthermore, the results also indicate a fairly uniform accumulation, which is beneficial for the concept of the agricultural land raise. This rapid accumulation can also be interesting for creating higher elevated salt marsh nature or when mud has to be extracted for other applications such as making bio building blocks.

Part of accumulation in the back of the polder

In order to objectively assess the distribution of the accumulation, it is calculated for all scenarios which part of the accumulation takes place behind a certain observation cross-section. For the smallest domain (Bat2) this was calculated with crs3 and for the other domains this was calculated with crs5 (see Figure 3.6 for the observation cross-sections). The results of this calculation are shown in Table 4.5. In this table, the same scenarios create good results (i.e. an average percentage so that not too much and not too little sediment ends up in the back of the polder) as what was observed in the accumulation maps.

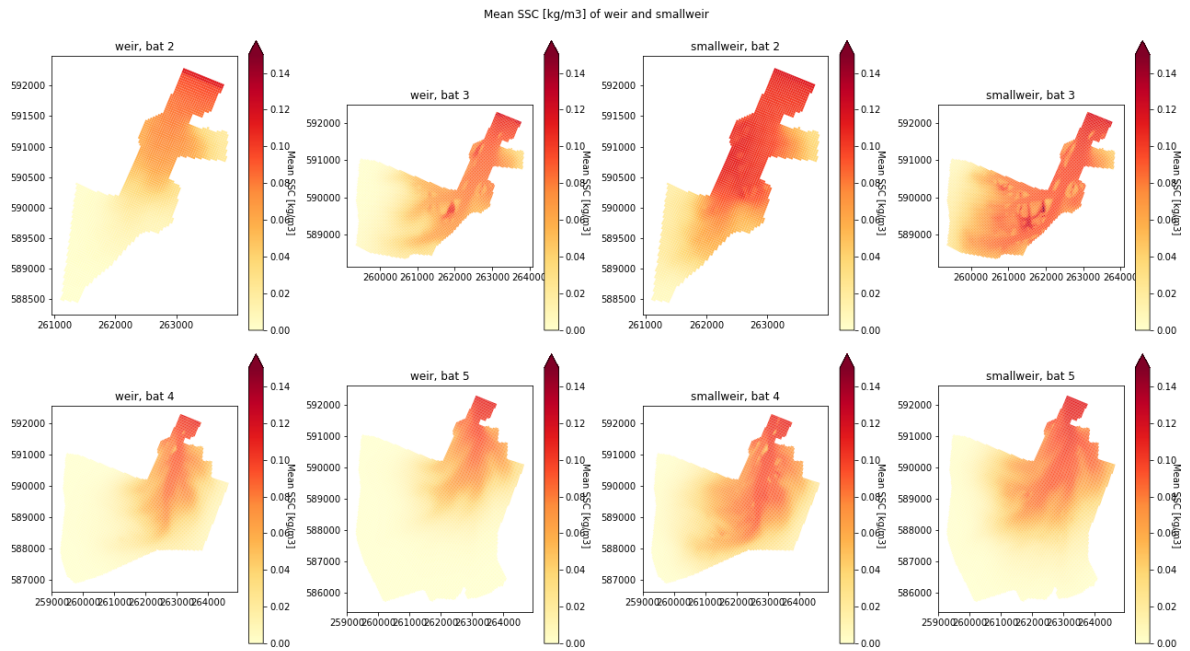


Figure 4.13: The mean SSC of the scenario with the weir (crest level at $NAP + 0\text{ m}$) and the scenario with the smallweir (crest level at $NAP - 0.5\text{ m}$).

	Reference	Weir	Smallweir	Half range	Upper half	Lower half	Deepweir
Bat 2	67.82%	8.04%	42.12%	38.95%	28.14%	63.92%	48.62%
Bat 3	60.22%	14.86%	41.88%	44.25%	29.75%	55.78%	49.97%
Bat 4	62.11%	1.64%	8.48%	45.29%	19.23%	52.79%	34.75%
Bat 5	77.24%	1.30%	6.22%	51.30%	25.93%	63.21%	46.11%

Table 4.5: The percentage of the accumulation which takes place behind a certain observation cross-section (crs3 for Bat2 and crs5 for the other domains). High percentages (i.e. much accumulation in the back of the polder) are indicated in blue and low percentages (i.e. little sediment reaching the back of the polder) in red. The reference case shows relatively the most accumulation behind these cross-sections and the weir the least. It is noticeable that the 'smallweir' scenario shows a completely different result for the two smaller domains compared to the two larger domains. This can be explained by the fairly good distribution of accumulation, already observed in Figure 4.12.

Explanation of observations

The maps of the accumulation and high shear stresses show a strong correlation. Where high shear stresses occur, no net sedimentation takes place, and vice versa. With large bed shear stresses, the erosion flux easily becomes larger than the deposition flux, so no accumulation occurs. In Figure 4.2 the sensitivity to high bed shear stresses already became apparent. The process is evident in the reference case, where the highest energy levels are present, resulting in high bed shear stresses and accumulation only takes place in the back of the polder.

The effect of the bed shear stresses on the accumulation also becomes clear when looking at the scenarios with the upper and lower half of the tidal range. In the scenario with the lower half of the tidal range, the tide mainly flows through the channels. This means that the energy can be distributed worse over the area, which ensures that high bed shear stresses occur much deeper into the polder, resulting in accumulation taking place mainly at the back of the polder. In the scenario with the upper half of the tide, the water flows more across the tidal flats and the incoming energy can be distributed much easier. As a result, the accumulation takes place less far in the polder. In this case, the channels function as sheltered areas with a low bed shear stress, so that most of the accumulation takes place there.

The best results regarding the spatial sediment distribution are achieved when the incoming energy is limited. However, the energy should not be limited too much, otherwise the suspended sediment will not reach the back of the polder, as can be seen in the scenarios with the weir. It is interesting that for all domains the accumulation pattern of the deepweir is quite similar to the accumulation pattern of the

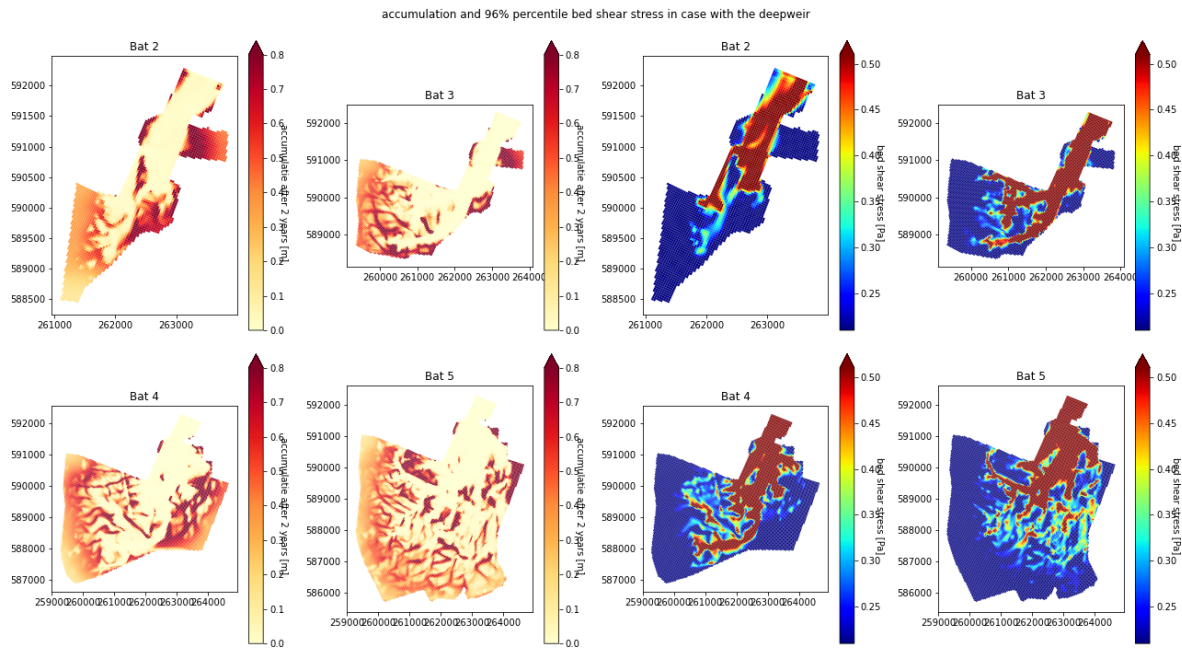


Figure 4.14: The accumulation after two years of the scenario with the deepweir (a weir with a submerged crest level dependent on size of the basin) and the 96% percentile of the occurring bed shear stress.

half range scenario. This seems to show that it is possible to positively influence the spatial distribution of accumulation by means of a weir. The results for all scenarios can be found in the Appendix D.

4.3.3. Elevation distribution of accumulation

Determination of elevation ranges

The elevation distribution of accumulation relatively to the tidal water levels is particularly relevant. That is why the average tidal levels are mapped first. Figure 4.16 shows the distribution of minimum and maximum tidal water levels. Here are the levels of the MLT, MSL and MHT indicated. It is clear that MSL is not at $NAP + 0\text{ m}$, but at $NAP + 0.16\text{ m}$. Furthermore, the level of MLT at $NAP - 1.62\text{ m}$ is relevant because this level is used as the elevation where the mudflats begin in the analysis.

An elevation range distribution has been made with the tidal boundaries in which the elevation level of the accumulation is divided. Table 4.6 shows what percentage of the total surface area of the polder falls within a certain range. It should be noted that the range sizes are doubled below MLT. It is clear that there is virtually no surface above MSL and that most of the surface is between $NAP - 0.2\text{ m}$ and $NAP - 1.25\text{ m}$. It is therefore not surprising that the majority of the accumulation also takes place in this elevation range, so the relative share of accumulation within an elevation range is more relevant.

	<-3m	<-2.3m	<-1.6m	<-1.25m	<-0.9m	<-0.55m	<-0.2m	<0.16m	>MSL
Bat 2	13.5%	12.8%	16.5%	13.5%	16.8%	14.9%	11.3%	0.7%	0.0%
Bat 3	10.2%	4.5%	9.2%	7.7%	13.1%	24.2%	18.0%	7.0%	6.1%
Bat 5	7.4%	4.4%	10.7%	9.7%	18.1%	29.1%	14.1%	4.8%	1.6%
Bat 5	8.4%	5.8%	11.2%	9.2%	13.8%	26.0%	18.0%	6.7%	0.9%
total	8.7%	5.7%	11.1%	9.4%	15.3%	25.9%	16.3%	5.7%	1.9%

Table 4.6: Percentage of the area per elevation range. The color indicate the higher percentages. Note that the ranges are not equal. Below $NAP - 1.6\text{ m}$ (i.e. MLT), the range sizes are doubled. According to the data, MSL is at $NAP + 0.16\text{ m}$. It is clear that the largest area surfaces are between $NAP - 0.55\text{ m}$ and $NAP - 0.9\text{ m}$.

General accumulation elevation distribution

In almost all cases, the majority of accumulation is between mean low tide (MLT) and mean sea level (MSL). The percentage of the accumulation what occurs on the tidal flats, ranges from 43% (in the case

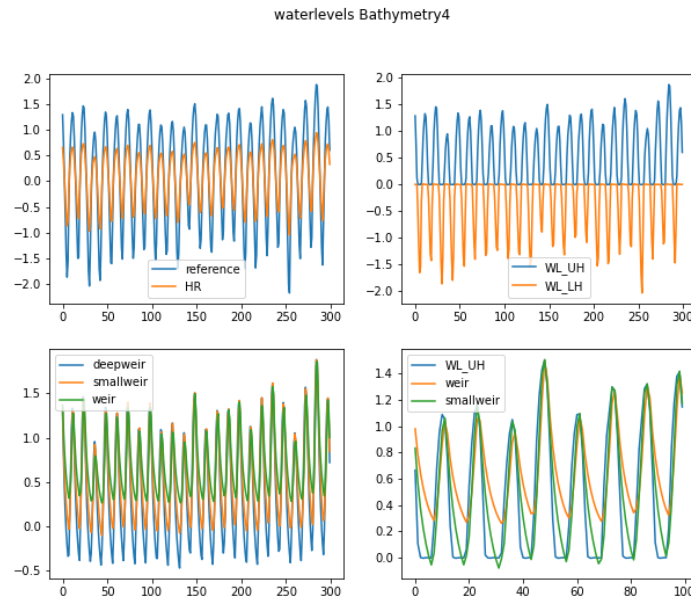


Figure 4.15: The water levels of all model scenarios in the domain of bathymetry 4.

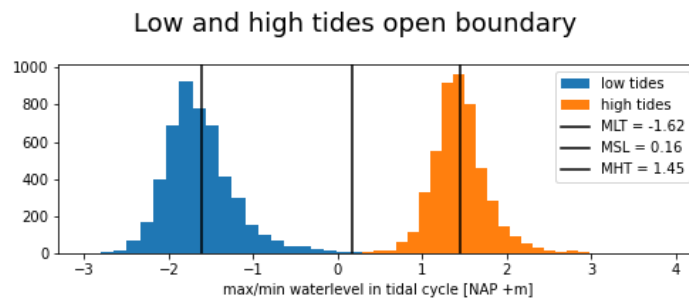


Figure 4.16: Distribution of minimum and maximum tidal water levels at the open boundary. The most relevant numbers here are MLT is at $NAP - 1.62\text{ m}$, since the mudflats begin at this elevation, and MSL is at $NAP + 0.16\text{ m}$

of bathymetry 2 with a weir) to 95% (in the reference case for bathymetry 3), with an average of 76%. In Figure 4.17 and Figure 4.18, the overall results of the elevation distribution of the accumulation of a scenario are visualised. Figure 4.17 shows the share of the accumulation within a range in the total sediment import. Figure 4.18 shows the distribution of accumulation, divided by the share in surface area of a elevation range. So there the relative share of the accumulation at a certain elevation is shown. This shows that the scenario with the weir, the smallweir and the upper half of the tide in particular show relatively more accumulation in the deeper parts of the area. This is also clear in Figure 4.19, where the cumulative accumulation distribution is shown.

In general it is concluded that in the reference scenario, the accumulation takes place on average on the highest elevation level. It should be noted that this elevation distribution can be explained by the fact that the spatial location where most accumulation takes place is also different for the scenarios. The location where most accumulation takes place in the scenario with the weir is generally deeper on average than it is further into the polder, where most of accumulation with the reference scenario takes place.

Half tidal range

The calculations with the halved tidal range show that using only the upper part of the tide results in almost four times more accumulation below 3 m than only using the lower half of the tide (490289 m^3 vs. 124597 m^3 when combining the four domains). When the share of this accumulation in the total

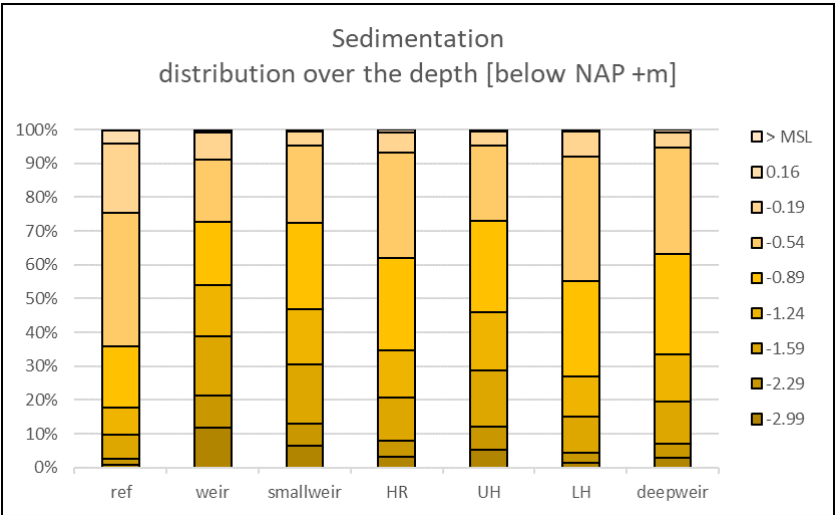


Figure 4.17: Distribution of sedimentation over height

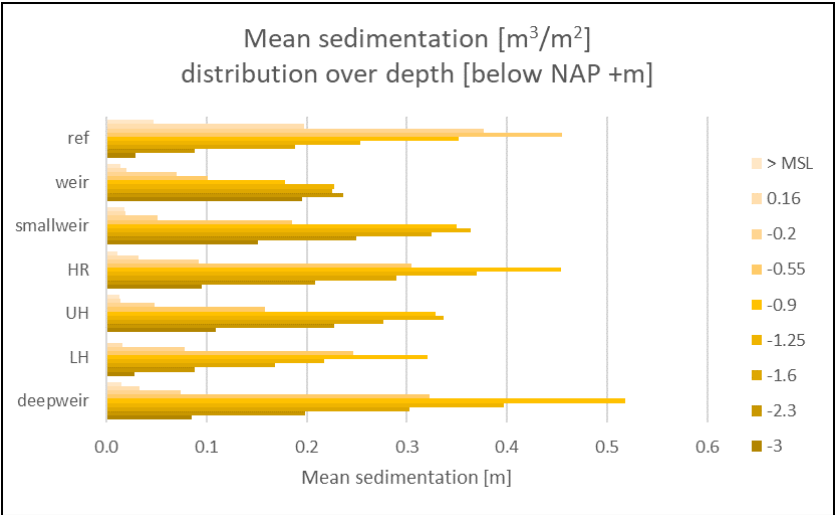


Figure 4.18: Distribution of sedimentation height per available squared meter for that height

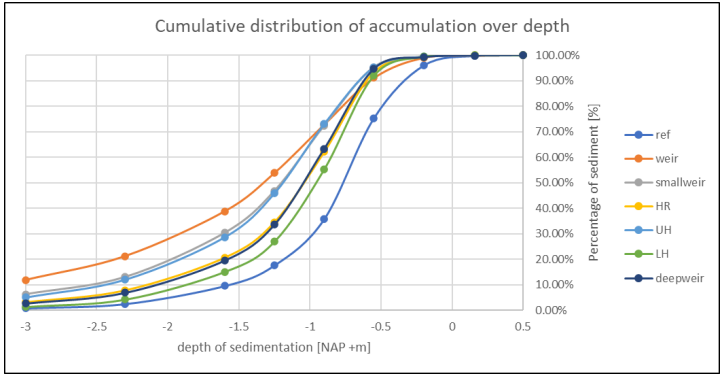


Figure 4.19: The percentage of accumulation that takes place lower

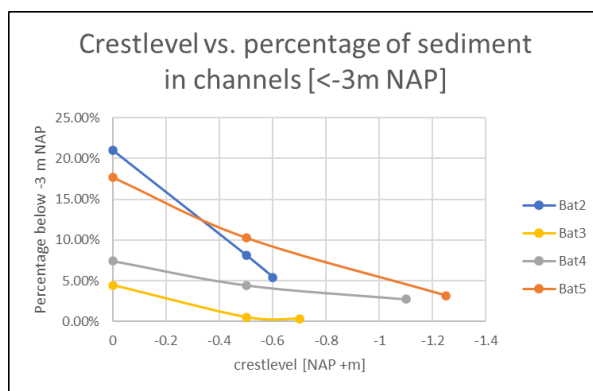


Figure 4.20: The percentage of accumulation that takes place below $NAP - 3\text{ m}$

sediment import per are compared, this difference is even stronger, namely 5.3 times higher when using the upperhalf of the tide (6.3% vs. 1.2% of the total accumulation when combining the four domains). With the scenario where the tidal range is halved in the middle part (i.e. scenario 4), the results are between the 'upper half tide' and the 'lower half tide' results. This agrees with the conclusion that water 'flushes' through the channels in the scenario with the lower half of the tide, while the scenario with the upper half of the tide flows across the flats, resulting in channels being more 'sheltered' places where sediment easier can settle.

Effect of weirs on deeper accumulation

An intriguing observation is that the percentage of sediment that accumulates in the deepest part (i.e. lower than 3 m) appears to have approximately a linear relationship with the crest level of the weir. This correlation is illustrated in Figure 4.20. The figure shows that this linear relationship appears to hold for all domains. This relationship would apply from a certain crest level of the weir where the incoming energy is no longer limited enough. This relationship requires further examination, but it could potentially assist in determining the optimal height of the crest level of the weir.

4.3.4. Wave effect

During the calibration phase, the importance of the effect of the waves became apparent. Waves are an important part of the resuspension of the sediment, bringing it further into the polder. To further investigate this conclusion, a simulation was performed without wave effect and with more wave effect (i.e. with $f_{tauw} = 0.5$) for the scenarios 'reference', 'half range' and 'deepweir' (i.e. scenario 1, 4 and 7) in domain bathymetry3 and Bat5. The results of this are very consistent and explained below.

Sediment import

In all cases, the total sediment extraction is higher without waves, and lower with more waves. The results of the simulations are shown in Figure 4.21 and Table 4.7. The effect of waves is the largest for the reference case and the smallest for scenario 'deepweir'. In addition, the effect in domain bathymetry3 is slightly bigger than in bathymetry5.

The decrease in total net sediment extraction when implementing waves is in line with the findings from the calibration phase. Waves provide extra resuspension so that sediment can be transported further, but it can also flow out of the area more easily.

Spatial accumulation distribution

When the effect of waves is not taken into account, less accumulation takes place in the channels and more on the tidal flats. When the effect of waves is increased, this effect is the opposite (Figure 4.22). In addition, when the wave effect increases, the accumulation is shifted more to back of the polder (Table 4.8). The average SSC values (Figure 4.23) show that particularly in the back of the polder the SSC values become higher when more wave effect is taken into account.

Both the shift of accumulation to the back of the polder and the shift of accumulation to the deeper areas are in line with the findings in the calibration phase and the expectations in the conceptual model. Waves cause more bed shear stresses, creating more resuspension and therefor allows sediment to be

		No waves	Normal [10 ⁶ m ³]	More waves
Bat 3	Reference	+13.40%	2.22	-22.23%
	Half range	+17.26%	1.91	-12.85%
	Deepweir	+8.60%	2.04	-8.92%
Bat 5	Reference	+11.52%	6.75	-18.84%
	Half range	+12.05%	5.66	-13.30%
	Deepweir	+5.21%	6.03	-7.93%

Table 4.7: The effect of waves on the total sediment extraction. The percentages indicating the increase or decrease when simulating without waves or with extra waves. The effect of waves is the largest for the reference case and the smallest for scenario 'deepweir'. In addition, the effect in domain bathymetry3 is slightly bigger than in bathymetry5.

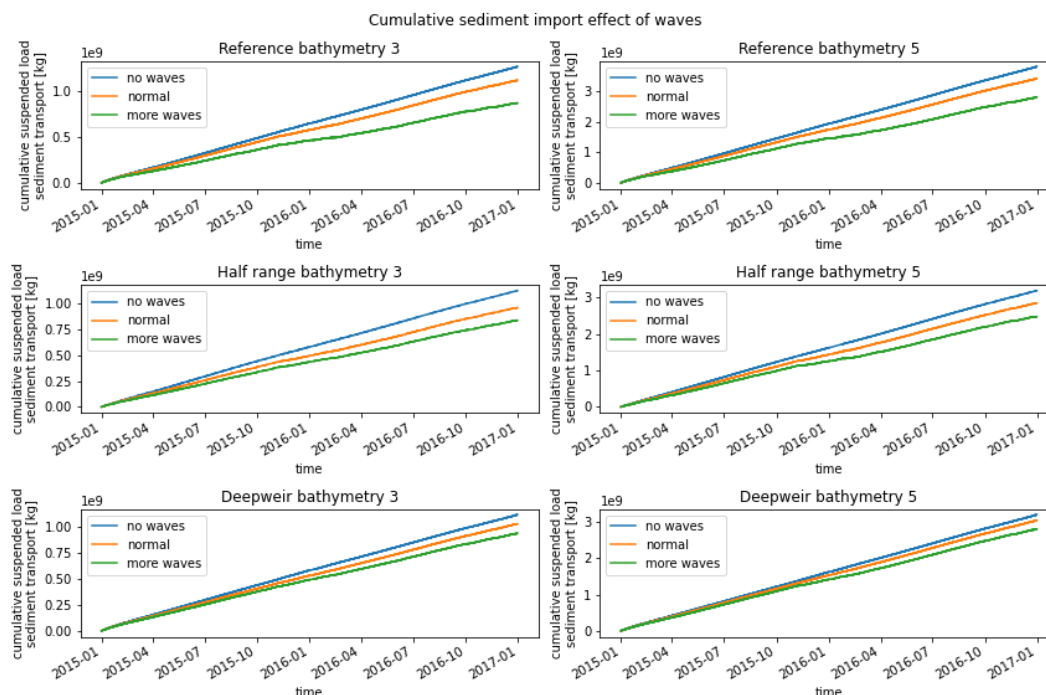


Figure 4.21: The influence of waves on the total sediment extraction volume of the polder. For all cases where waves have been simulated, this has a negative effect on the total extraction of sediment.

transported further. Because these wave-induced bed shear stresses mainly affect the shallow parts, the erosion flux particularly becomes higher on the flats and less accumulation takes place on the flats than the channels

Elevation distribution of accumulation

In figure 4.24, the cumulative accumulation distribution of the three scenarios without waves and with extra waves is shown. For all scenarios, it is clear that by increasing the wave effect, the distribution of accumulation is shifting to the deeper areas. This is in line with the findings in the calibration phase, the expectations after the spatial accumulation distribution and the expectation in the conceptual model. This supports the findings of the spatial accumulation distribution; wave induced bed shear stresses mainly affects the shallow areas. As a result, waves ensure that less accumulation takes place on the shallower areas and the eroded resuspended sediment can be deposited in the channels.

4.3.5. Key findings

The amount of sediment that enters a polder is largely determined by the incoming tidal prism. In our model, the concentration of suspended sediment at the boundary is constant, so a higher tidal prism results in more sediment entering the polder. Even if the trapping efficiency of the polder is lower, the

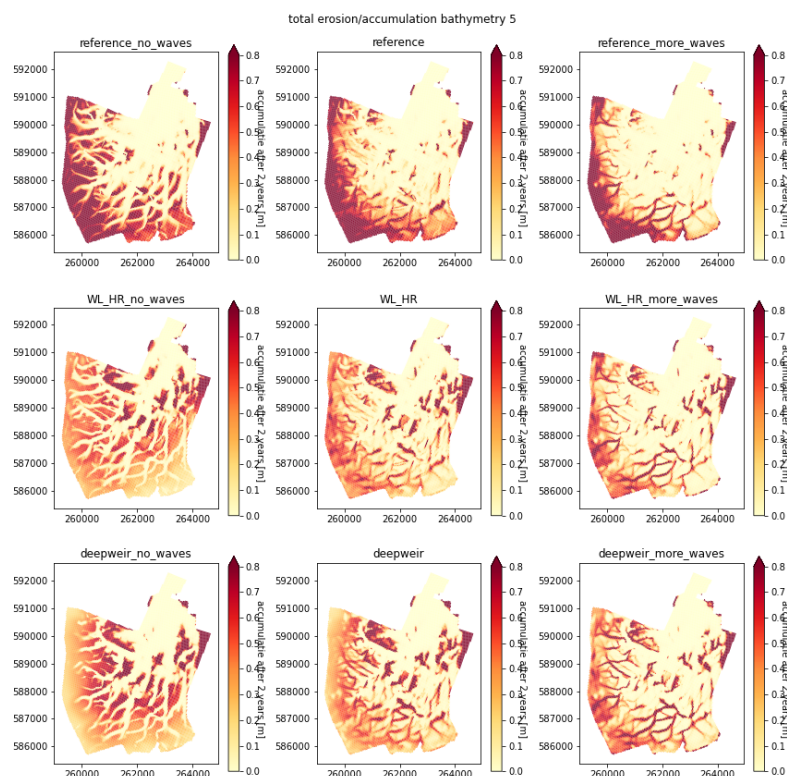


Figure 4.22: The effect of the waves on the accumulation patterns. When not taking into account the effect of waves (left figures), accumulation mainly occurs on the flats, while more wave effect results in the accumulation mainly occurs in the channels (right figures). Moreover, the sediment is transported further to the back of the polder by the influence of waves.

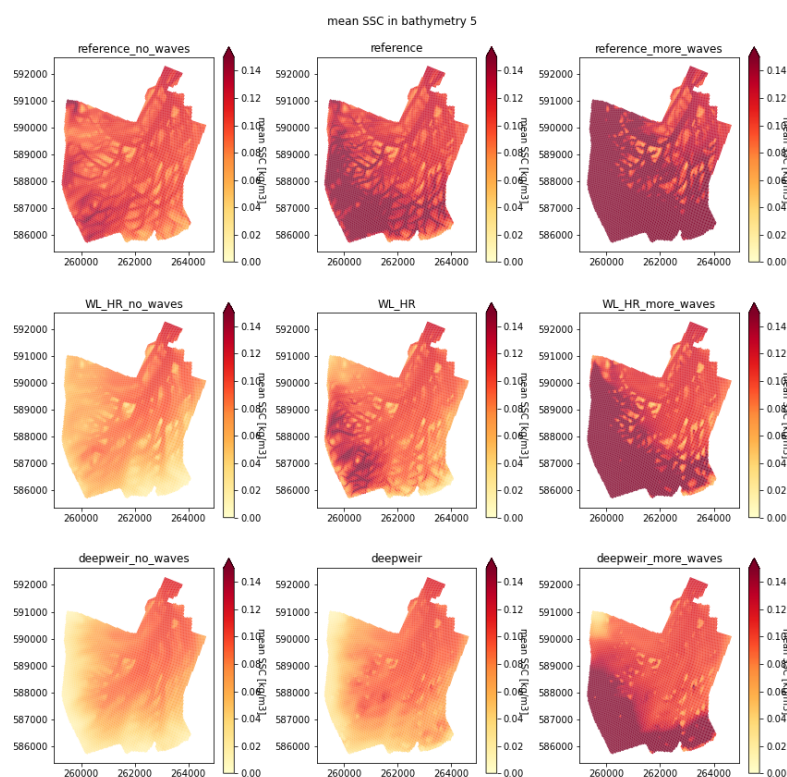


Figure 4.23: The effect of the waves on the accumulation patterns. It is clear that the waves cause higher sediment concentrations, especially in the back of the polder.

		No waves	Normal	More waves
Bat 3	Reference	53.30%	60.22%	73.33%
	Half range	31.46%	44.25%	59.95%
	Deepweir	43.77%	49.97%	60.06%
Bat 5	Reference	71.62%	77.24%	85.67%
	Half range	39.44%	51.30%	61.21%
	Deepweir	38.36%	46.11%	57.92%

Table 4.8: The percentage of the accumulation which takes place behind observation cross-section crs5 for the simulation of scenarios 'reference', 'half range' and 'deepweir' (i.e. scenario 1, 4 and 7) in domain Bat3 and Bat5 without wave effect and with more wave effect. Higher percentages (i.e. more accumulation in the back of the polder) are indicated in blue and lower percentages (i.e. little sediment reaching the back of the polder) in red. It is noticeable that in all cases a higher percentage of the accumulation takes place beyond this cross-section with more waves, and a lower percentage without waves.

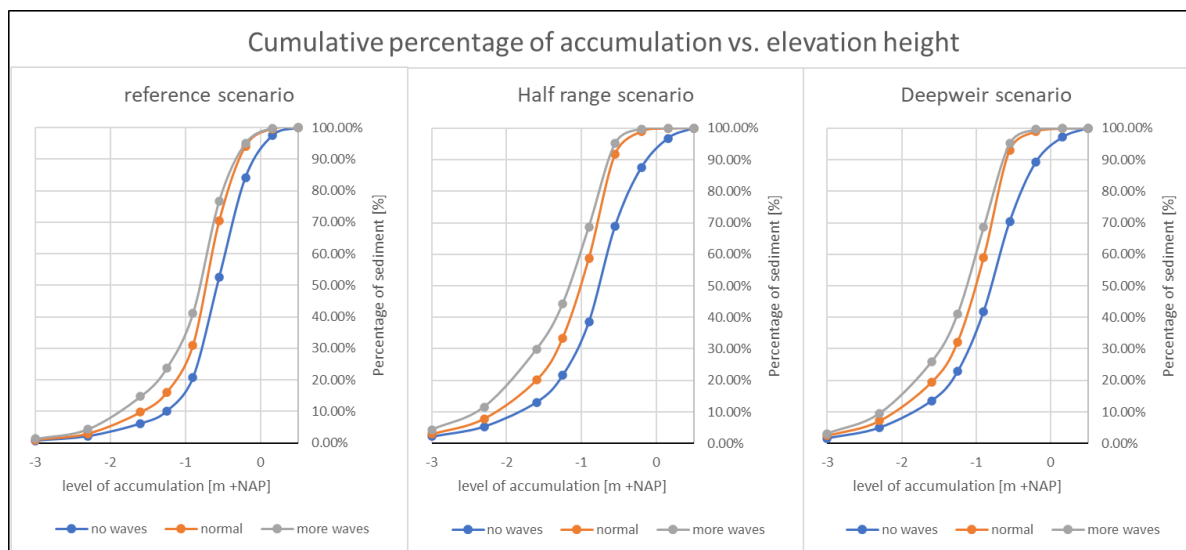


Figure 4.24: The influence of waves on the elevation distribution of accumulation. More waves result in accumulation on lower elevations. This is consistent with the observation that accumulation moves to the channels.

higher volume of incoming sediment means that more sediment is extracted overall.

The distribution of sediment accumulation within the polder is influenced by both waves and currents, which create energy that can either flush sediment out of the channels or promote accumulation. The simulations show that scenarios with high currents can induce high-energy flow in the channels, while scenarios with more wave activity tend to promote low-energy conditions in the channels and encourage sediment accumulation. Waves also create shear stresses on the shallow areas of the polder, which can lower the elevation of accumulation and cause sediment to accumulate further to the back of the polder.

However, elevation alone does not always provide a clear indicator of sediment accumulation, as the elevation of the area varies and affects the elevation of accumulation. Comparing scenarios with different levels of wave activity is useful because the effect of the waves both lower the elevation of accumulation, and accumulation takes place further to the back of the polder. This confirms that the accumulation mainly takes place in the channels when many waves are present.

Among our scenarios, 'half range' and 'deepweir' appear to be the most successful for achieving a balanced distribution of sediment across the polder, as they have good spatial and height distributions without significantly reducing the total sediment import. Of course, the stability of the weir, which is used to control water flow into and out of the polder, is also important. While this largely falls outside the scope of this study, the maximum flow velocity on top of the weir is determined to be 3.9 m/s, which should be manageable for a concrete weir.

Finally, the interesting sedimentation patterns in the side basins of the smallest two domains are observed, which could be explored further in the context of transitional polders, which are temporarily reopened to the tide to capture sediment before being returned to their original function Weisscher et al.

(2022)).

5

Discussion

The research conducted in this thesis study shows that the extraction of sediment from the estuary using a managed realignment polder is a successful approach. While this general conclusion can be drawn with reasonable certainty, the exact results are subject to some uncertainties due to the challenges encountered during calibration and the simplifications made to keep the study manageable (see Section 5.1). Additionally, certain complex processes not have been taken into account. Therefore, there are some limitations in drawing numerical conclusions, which raises some caveats about optimizing the design (see Section 5.2). It is worth noting that the model used in this study was calibrated to local conditions, and therefore, some results cannot be generalized broadly. However, findings regarding the effects of various processes may have broader applicability (see Section 5.3).

5.1. Uncertainty in the approach

5.1.1. Suitability of calibration location

Polder Breebaart has many similarities to the project area, but also some differences. An important difference one is the dampened tide. The tidal range within the dike in Polder Breebaart is roughly 15 times smaller than outside the dike (i.e. 20 cm compared to 3 m). This ensures that the effect of the tidal energy in the calibration area may be different than in the project area. However, since the area is close to the project area (i.e. similar sediment properties) and reliable elevation data is available, Polder Breebaart is estimated as most suitable for the calibration.

5.1.2. Possible limiting factors in Polder Breebaart model

The calibration of Polder Breebaart was not entirely successful. The model is not able to accurately replicate the entire morphological change. Specifically, the area southern of the bottleneck in Breebaart is not well represented in the numerical model. This can be attributed to several factors, which are explained below.

The low tidal dynamics

The low tidal dynamics in the polder results in a very low amount of discharge through the polder per tidal cycle. This also means that the current-related bed shear stresses are quite low. This may be a reason for a lack of resuspension, which in turn can limit the movement of sediment further into the polder. Furthermore, the low dynamics may also limit the horizontal diffusion, which affects the dispersion of sediment. Because sediment transport is successful when higher tidal dynamics act on the system (Figure 4.3E), this is the most likely cause. This is further supported by the spatial distribution of the accumulation in the application phase, where the accumulation takes place just at the back of the polder when using the largest tidal signal.

Consolidation

The mud in polder Breebaart has been modeled with a constant critical shear stress and without considering consolidation effects. However, prolonged stagnation of mud results in consolidation and higher critical shear stress, impacting resistance to resuspension. Incorporating this process in the model

could alter various parameters and alter the system dynamics. It's also important to account for the volume reduction due to consolidation when evaluating the sediment volume extracted from the estuary.

Reed bed

The Breebaart polder contains a significant amount of reed. This reed may influence the dynamics of the area in two ways. Firstly, the reed bed can reduce the effect of wind on waves by acting as a barrier. Secondly, the reed bed can have a dampening effect on wave action and currents. Particularly along the edges of the area, there is a significant amount of reed, which likely reduces the shear stresses. However, the effect of this vegetation was not included in the model.

5.1.3. Simplifications

Many simplifications and assumptions have been made. The most important of these are explained below. The first two apply to both the model of Polder Breebaart and the model of realignment project area, the other three only to the model of the realignment project area.

Only one sediment fraction

Only one sediment fraction with a single settling velocity is used in the model, while in reality there are a variety of mud and sand particles with varying settling velocities. These varying settling velocities can result in sediment settling easier in different zones of the intertidal area.

SSC levels on open boundary

The data used for the analysis of SSC contains a high degree of uncertainty. A constant SSC value was chosen based on an average, but due to a lack of usable data, this value is partly an estimation derived from overview maps. SSC is highly variable, both in the short-term, from hour to hour, and in the long-term, throughout the year, making it challenging to identify a representative value or time series. Additionally, the tidal component of SSC adds complexity as the values tend to be highest at increasing tide signal.

Additionally, there are also other factors that should be considered when analyzing SSC. One of these is the gradient in SSC with depth, where values tend to be higher closer to the bottom compared to near the water surface. This is particularly relevant when a weir is used, as it restricts mostly the bottom layers of the flow, and thus, the model may overestimate sediment import when not taking this into account.

Another important aspect that should be considered when analyzing the SSC value on the open boundary are the potential changes in SSC over time, as sediment is extracted from the estuary. As the aim of the research is to decrease SSC values, it is likely that these values will drop as a result of implementation of the polder. This in turn will lead to a decrease in sediment extraction and a lower accumulation rate in the polder.

No initial bottom thickness

In Section 3.3.4 is explained that starting without initial bottom thickness was done to properly compare scenarios of sediment redistribution. Moreover, the focus of this study is on accumulation within the intertidal area, not on the erosion. However, it should be noted that not allowing initial bed erosion may affect the behavior of the polder, such as preventing the formation of deeper channels or new channels. This should be taken into account when interpreting the results. The results show therefore only the initial accumulation and not the formation of the channel patterns in the intertidal area.

The model is run with an initial thickness of 0 m, so net erosion is not possible. If the model was started with an erodible bottom, the realignment area would probably first net export sediment, combined with a partially redistribution of the sediment. Only after this redistribution will the model of the area start to net import sediment.

The predefined channel pattern

The channel pattern is generated by calculations using the sand transport method of Engelund-Hansen and is created with sand, rather than mud. This creates an interesting bottom profile that appears natural, but it is important to note that it may not accurately reflect the bathymetry that would occur in reality. It should be noted that the Engelund-Hansen and Partheniades-Krone method are two different mathematical approaches that use different assumptions and equations to calculate the sediment

transport. The Engelund-Hansen model is based on the equilibrium condition of sediment transport and the Partheniades-Krone model is based on the kinetics of the sediment transport.

In this research the emphasis is on the mud deposition and not specifically on the development of this channel-shoal system. Because this creek pattern is highly unpredictable and among others dependent on the subsoil for which there are no data, the channel-shoal system formation is greatly simplified. Additionally, substantial erosion is required to occur close to the open boundary of the area when starting with just AHN data or an uniform depth as bathymetry. A preliminary calculation using the method of O'Brien (equation 2.4) indicates that the cross-sectional areas of the entrance channel must be significantly larger than the initial cross-sectional area with AHN data. An excessive amount of sediment would be initially washed away. The Partheniades-Krone equations are sensitive to high bed shear stresses, and when strong currents are present, large amounts of sediment are eroded. This not only causes numerical instability in the simulations, but it also does not accurately reflect reality. To overcome this issue, the model is first run using a sandy bottom with the Engelund-Hansen equations.

Incoming wave energy

The incoming wind waves at the open boundary are over estimated. The model calculates the wind waves in the open boundary with a fetch of 100 km, while the maximum fetch is just 10 km. It is found that waves can have a very important influence on the erosion. The overestimated incoming waves will probably mainly affect the erosion close to the entrance to the polder. Due to high shear stresses as a result of the flow, no net accumulation occurs in this area, so it has been estimated that the overestimation of these waves will not lead to significant extra erosion.

5.2. Optimization of the design

5.2.1. Reliability of the model results

The calibration phase revealed that the model struggles to accurately replicate results in low-dynamic systems, like Polder Breebaart. Despite higher dynamics being present at the realignment project area, considerable uncertainty remains due to the sensitivity of the parameters used to calculate the mud dynamics. The results of the application of the model must therefore been examined extra critically. Small variations in the parameters used to calculate the erosion flux can easily result in different outcomes. The model results indicate that local accumulations of more then 80 cm (i.e. 40 cm per year) may occur. Too much importance should not be attached to these kind of values and there is focused on the general behavior of the scenarios in relation to each other.

During the calibration it was seen that the numerical model realizes little sediment transport to the back of the polder, despite the fact that this does happen in the data. It could be that also in the scenarios in the realignment project area where the sediment transport does not reach the back of the polder, this will actually be in reality.

5.2.2. Elevations are dependent on spatial location

It is important to note that the distribution of elevation of accumulation is heavily influenced by the spatial location where the majority of the accumulation occurs in a simulation. If the accumulation predominantly takes place towards the back of the polder, the average elevation of accumulation would also be higher due to the presence of more tidal flats in that area. Therefore, it is only fair to compare the results of the elevation distribution of accumulation when the accumulation location is comparable. However, in the analysis of the effect of waves, this aspect strengthens the results, because the waves both carry sediment further to the back of the polder and create accumulation on lower elevations.

5.2.3. Important neglected complex processes

Simulating complex processes in numerical models can be challenging. Many of these complex processes have been omitted for the sake of simplicity, as described in Section 2.5.6. The two most important are explained below.

One of the neglected processes is consolidation, which causes higher critical shear stress values. The consolidation process is even accelerated on tidal flats, exposed to sunlight. It is not possible to use temporally varying critical shear stresses in Delft3D FM. Consolidation of mud can also cause a reduction in accumulated volume, the change in elevation of the accumulated areas could therefore be lower.

As described in Section 2.3.11, vegetation can influence morphological processes in several ways. Because vegetation involves a lot of uncertainty in both modeling and application, this has not been included. It is likely that when vegetation can be successfully applied, this will have a positive effect on the captured sediment volume.

5.2.4. Ecological benefits

It is challenging to assess the additional natural values of model results. A system, such as the one developed by Baptist et al. (2019), can be used to assess the diversity of different ecotopes and assign a score to the ecological conditions, but it is designed for existing ecotopes. Applying it to the results of a numerical morphological model is difficult. In Section 2.5.5 is stated that it would be profitable for nature development to create as much area within the tidal range and promote creek development and convex-up tidal flats. Most of the accumulation takes place within the tidal range, and therefore is concluded that the first of these criteria is met. It is hard to assess if the other criterias do to.

Additionally, most ecological benefits will take much longer to develop. Predicting how planted vegetation will evolve is highly uncertain and for micro biotics it needs time to develop in the system. It will take a while for the area to reach an healthy ecological balance. Therefore, assessing the ecological benefits in this context is largely subjective and not particularly decisive.

5.3. Generalizing the results

The research was specifically focused on a certain location, the Ems Dollart, and the parameters used were based on local conditions. Nonetheless, the modeled processes are generally applicable to other similar situations. The study found that creating a managed realignment polder can be effective in capturing sediment, but it should be noted that the application should not be replicated without considering local factors such as sediment properties and SSC values.

It is important to note that the model outcomes in this study, specifically the Partheniades-Krone equations, are highly sensitive to the parameters used. The research suggests that reducing the tidal range, for example by using a weir, can have a positive impact on sediment distribution, but this conclusion is based on a model that was calibrated to the conditions in Polder Breebaart. By calibrating the model in other locations, it will be possible to determine if this conclusion holds when using different parameters. This is crucial in determining whether limiting the tidal has a positive effect on the internal spatial distribution of accumulation.

6

Conclusions

In this thesis, the important factors of influence for the efficiency of sediment capturing in a managed realignment polder are examined. The goal of Ems-Dollart 2050 is to extract one million tons of dry matter from the estuary per year. Because there are uncertainties in the model, the exact quantities are of secondary importance compared to the obtained new insights in processes and key factors. The focus in the conclusion is therefore on these processes. The various research questions will also be answered in this chapter and are written in italics.

6.1. The general concept of sediment extraction with a managed realignment polder

How to optimize the efficiency of extracting sediment from a turbid estuary with a managed realignment polder?

In general, it can be concluded that extracting sediment with the managed realignment polder is successful, indicating that the concept is viable. The tidal prism, the shape of the polder, the incoming energy and wind generated waves are important factors influencing the total sediment extraction and spatial distribution of accumulation. The tidal prism determines together with the SSC the gross import of sediment. The shape of the polder partly determines how the energy can be distributed in the area, which determines where accumulation can occur or not. The incoming energy has an important influence on the sediment capture efficiency of the polder and the wind-generated waves ensure the resuspension of the sediment, allowing it to be transported further into the polder.

6.2. Effect of surface area of the managed realignment polder

What surface area of a managed realignment polder is the most efficient in capturing sediment?

The study has demonstrated that as long as there is no obstruction on the inflow, a linear correlation exists between the amount of imported sediment and the size of the area (Figure 4.6). The study did not reveal an optimal surface area in terms of efficiency. The amount of bed shear stress on a certain location is the most important factor in determining the possibility of sediment accumulation (see the sensitivity of the Partheniades-Krone equations to bed shear stresses in Figure 4.2). Therefore, a larger area is only beneficial as long as the energy can disperse rapidly.

6.3. Influence of shape of the managed realignment polder

What is the influence of the domain shape on the sediment distribution in the managed realigned polder?

It has already been stated above that the amount of bed shear stresses is the most important factor in determining whether accumulation can occur. Therefore, the shape of the managed realignment polder is important. A long and narrow area is likely to be less efficient in capturing sediment than a more round area where the tidal energy distributes easily in all directions.

In the two smallest domains, a rectangular basin was created close to the entrance. The model simulations clearly indicate that a significant amount of sedimentation occurs in this side-basin. This

accumulation can be explained by the low bed shear stresses in this area closed off on three sides. This notable accumulation near the entrance is particularly relevant for the secondary goal of raising agricultural land. It shows that it is possible to create suitable low energetic conditions close to high energetic areas. This raised land can result in higher salt marshes, raised agricultural land or it can be used for mud extraction for bio building blocks or raising agricultural land somewhere else.

6.4. Effect of incoming tidal energy

What is the influence of the tidal range on the spatial sediment distribution?

When the tidal prism is adjusted by decreasing the tidal range, the amount of imported sediment does not decrease proportionally, but much less (as seen in Figure 4.8). This is possibly because the tidal range of the Ems Dollart causes too much incoming energy, resulting in too high bed shear stresses for accumulation in a large part of the polder. Therefore, a larger tidal range ends up in a lower percentage of sediment being captured.

This hypothesis is supported by the fact that with the normal tidal range, accumulation only occurs close to the back of the polder. Halving the tidal prism by adjusting the tidal range leads to a more favorable sediment distribution in the polder. Model scenarios where too much incoming energy is blocked show spatial distributions not reaching the back at all. This is likely due to the strong influence of the occurring bed shear stresses on the net flux in the theory of the Partheniades-Krone. The location of sedimentation is strongly influenced by this bed shear stresses and therefore is dependent on the locations where the energy levels fall below a certain level.

Dampening the tidal range can be achieved by installing a submerged weir just behind the open boundary. However, a too high crest level of the weir blocks too much of the flow and leads to too much decrease in energy, causing sediment not to reach the back of the polder and restricting the import of sediment. The optimal crest level of the weir is dependent on the size of the area.

Is it possible to increase the total net sediment import by increasing the settlement time?

A weir was implemented to create a calm period in the polder for every tidal cycle, which extended the settlement time. Based on the results obtained in this study, this increase in settlement time does not appear to compensate for the decrease in sediment import.

6.5. Impact of waves

What is the influence of wind and waves on the erosion in an intertidal area?

The wave-induced bed shear stress appears to have a very important influence on the sediment distribution inside the polder. Waves generate extra bed shear stresses that ensure resuspension of sediment. This allows sediment to be transported further into the polder, but also to flow out of the polder. Waves thus ensure that the total sediment extraction decreases, but the distribution of sediment improves and moves further to the back of the polder.

At what bed level elevation relative to the tidal range does most accumulation take place?

Most of the accumulation takes place between mean low tide and mean sea level. However, this is also very dependent on the waves. The effect of the wave-induced bed shear stresses is most important in shallow areas. As a result, waves ensure that the resuspension mainly occurs on the tidal flats. Therefore, the accumulation will occur on higher levels when less wave impact is present, and move more to the channels when there is a more wave impact.

6.6. Additional natural and agricultural value

How can additional ecological values be stimulated?

The spatial distribution of the sediment is important for both the raising of agricultural land and the additional natural value, despite the fact that they have different interests. For raising agricultural land, it is especially important how quickly specific parts of the realignment area are raised. For high additional natural value it is important to have a well-distributed accumulation throughout the entire area. In addition, it is important to have convex-up tidal flats with a elevation between the tidal range. By decreasing the incoming energy and limiting the wave impact, both the spatial distribution and the elevation distribution of accumulation will be in favor of the additional natural value.

7

Recommendations

The primary focus of this master thesis is to investigate the distribution of total sediment import and accumulation within the project area. However, it is important to note that in order to make the research manageable, certain assumptions and simplifications have been made. To strengthen the conclusions of this study, further research on the project area is necessary. Additionally, the findings of this research have led to several general recommendations, which are relevant not only to this project area but also to similar locations. It is imperative to consider these recommendations for any future plans or actions related to this project.

7.1. Recommendation for further research on this project

Based on the research findings, a set of recommendations has been developed focusing on the project area. These recommendations address some of the concerns discussed in Chapter 5. Before implementing the project in the real world, it is advisable to conduct further research. This research should first continue with the model research. Certain aspects of the analysis could be verified in a physical model at a later stage. It is crucial to gain a thorough understanding of the sedimentation processes at the project site to ensure the implementation of effective and sustainable solutions.

7.1.1. Calibration

Calibrate model to area with comparable tidal range

The main difference between the calibration model and the application model is the tidal range. For this reason it is recommended to further calibrate the model in an area with a larger tidal range. This can be used to determine whether the calibrated parameters also apply with more tidal energy, or whether they need to be adjusted.

Others

The model's accuracy is affected by an important uncertainty related to the SSC, which is critical in determining the sediment import of the area. This is important in both the calibration phase and the application phase. One area of uncertainty pertains to the SSC values at the entrance of the polder, which can be resolved by collecting data with a minimum frequency of one hour to establish a correlation between tides and SSC values. This will allow for a more accurate estimate of the SSC that enters the polder and its effect on sediment import. In addition, calculations have been made with an assumed roughness in the model, which can also be determined more precisely.

7.1.2. Application

Long term accumulation and erodible bed

Ultimately, it is important to understand how the polder behaves in the long term. For the polder to continue to have a lasting impact on the SSC values in the estuary, it is crucial that it does not quickly reach a state of morphological equilibrium and stop extracting sediment. Therefore, it is recommended to also investigate the longer-term behavior of the polder in the model. It is assumed that an equal

distributed accumulation would benefit the long-term behavior with respect to mud extraction, but this assumption should be investigated.

To determine the long-term morphological behavior of the polder, it is essential to allow for significant morphological development in the area. It is important that erosion can take place to create new channels. In Chapter 5 is discussed what the effect of an erodible bottom could be, it is important to investigate this. It can also benefit the dynamics and diversity in the area when having different sediment fractions (and different settling velocities) present.

Others

To determine the best approach for implementing the sediment extraction project, there are several project-specific considerations that require further research. Firstly, the location of the entrance should be investigated. While the current focus is on locating the entrance next to Termunterzijl, it may be possible that a different location, such as in the Dollart where Polder Breebaart is located, could result in higher sediment extraction. Therefore, determining the locations with the highest SSC values can help make the best decision on the location of the entrance. However, it is also important to evaluate the potential impact on the surrounding ecosystem.

Secondly, the characteristics of the entrance to the polder require further research. This study suggests that limiting the incoming energy will benefit sediment distribution, which can be achieved by using a weir. The effect of a varying SSC over depth near the open boundary can be investigated in more detail, using a 3D model to provide a detailed and precise representation. This is important because the weir blocks mainly the deeper water layers. The reduction of tidal energy may be also achieved by limiting the width of the entrance or by creating flow resistance in the form of piles or large blocks in the inflow channel.

Thirdly, it is advisable to investigate the effect of a phased realignment process. This approach could help minimize the impact on existing land use and expropriating land from farmers while allowing for monitoring of sediment extraction over time. However, it is important to investigate potential pros and cons of this approach, as well as the cost and feasibility.

7.2. General research recommendations

In addition to the recommendations that focus on the project location, there is also a number of more general recommendations. All general recommendations can also be relevant for the project area.

Application of side basin

The model results showed that high sedimentation occurred in the side basin that was closed on three sides. This sedimentation was explainable by the low local bed shear stresses. Further research should be conducted to determine the potential benefits of creating different "sedimentation basins" in the design of managed realignment polders. If this concept proves effective, it could have significant implications for both sediment extraction and the raising of new agricultural land. Such an approach could provide a valuable tool to manage sediment extraction and help to adapt to sea level rise.

Modelling of a low dynamic system in Delft3D FM

The model was unable to sufficiently simulate the morphological development of Polder Breebaart. It had particular difficulty with the sediment transport to the back of the polder. Further investigation into the underlying processes that determine sediment dispersion could lead to a more complete understanding of the system. Finding ways to better incorporate them into the Delft3D FM model could lead to a better simulation of Polder Breebaart and comparable low-dynamic systems.

Vegetation

It has been highlighted that vegetation plays a crucial role in sedimentation and erosion. However, despite the existing knowledge on this subject, it remains challenging to accurately integrate this into models. Therefore, it is suggested to enhance the simulation of the impact of vegetation in models to achieve a more precise representation of the system and produce more dependable predictions.

Other factors of influence

Finally, there are always more factors that can influence the functioning of the polder where further research is recommended. Examples include the shape of the polder, the initial height of the bed or processes such as salt-driven transport and bioturbation.

References

- Adam, P. (1993). *Saltmarsh ecology*. Cambridge University Press.
- AHN. (2022). Actueel hoogtebestand nederland (ahn).
- Arcement, G. J., & Schneider, V. R. (1989). Guide for selecting manning's roughness coefficients for natural channels and flood plains.
- Baptist, M. J., Van Der Wal, J. T., Folmer, E. O., Gräwe, U., & Elschot, K. (2019). An ecotope map of the trilateral wadden sea. *Journal of Sea Research*, 152, 101761.
- Berlamont, J., Ockenden, M., Toorman, E., & Winterwerp, J. (1993a). The characterisation of cohesive sediment properties. *Coastal engineering*, 21(1-3), 105–128.
- Berlamont, J., Ockenden, M., Toorman, E., & Winterwerp, J. (1993b). The characterisation of cohesive sediment properties [Special Issue Coastal Morphodynamics: Processes and Modelling]. *Coastal Engineering*, 21(1), 105–128. [https://doi.org/https://doi.org/10.1016/0378-3839\(93\)90047-C](https://doi.org/https://doi.org/10.1016/0378-3839(93)90047-C)
- Brooks, H., Möller, I., Carr, S., Chirol, C., Christie, E., Evans, B., Spencer, K. L., Spencer, T., & Royse, K. (2021). Resistance of salt marsh substrates to near-instantaneous hydrodynamic forcing. *Earth Surface Processes and Landforms*, 46(1), 67–88.
- Chirol, C., Spencer, K. L., Carr, S. J., Möller, I., Evans, B., Lynch, J., Brooks, H., & Royse, K. R. (2021). Effect of vegetation cover and sediment type on 3d subsurface structure and shear strength in saltmarshes. *Earth surface processes and landforms*, 46(11), 2279–2297.
- Clapp, J. (2009). *Managed realignment in the humber estuary: Factors influencing sedimentation* (Doctoral dissertation). University of Hull.
- Colijn, F., & Cadée, G. C. (2003). Is phytoplankton growth in the wadden sea light or nitrogen limited? *Journal of Sea Research*, 49(2), 83–93. [https://doi.org/https://doi.org/10.1016/S1385-1101\(03\)00002-9](https://doi.org/https://doi.org/10.1016/S1385-1101(03)00002-9)
- courtesy of Rijkswaterstaat. (2022). Picture of polder breebaart.
- Cox, T., Maris, T., De Vleeschauwer, P., De Mulder, T., Soetaert, K., & Meire, P. (2006). Flood control areas as an opportunity to restore estuarine habitat. *Ecological Engineering*, 28(1), 55–63.
- D'Alpaos, A., Lanzoni, S., Marani, M., & Rinaldo, A. (2007). Landscape evolution in tidal embayments: Modeling the interplay of erosion, sedimentation, and vegetation dynamics. *Journal of Geophysical Research: Earth Surface*, 112(F1).
- Dalrymple, R., Choi, K., & Middleton, G. (2003). Sediment transport by tides. *Encyclopedia of sediments and sedimentary rocks: Dordrecht, Kluwer Academic Publishers*, 606–609.
- de Jonge, V. N. (1995). Wind-driven tidal and annual gross transport of mud and microphytobenthos in the ems estuary, and its importance for the ecosystem. *Changes in fluxes in estuaries. Olsen & Olsen, Fredensborg*, 29, 40.
- de Jonge, V. N., & Schückel, U. (2019). Exploring effects of dredging and organic waste on the functioning and the quantitative biomass structure of the ems estuary food web by applying input method balancing in ecological network analysis. *Ocean & Coastal Management*, 174, 38–55. <https://doi.org/https://doi.org/10.1016/j.ocecoaman.2019.03.013>
- de Jonge, V. N., Schuttelaars, H. M., van Beusekom, J. E. E., Talke, S. A., & de Swart, H. E. (2014). The influence of channel deepening on estuarine turbidity levels and dynamics, as exemplified by the ems estuary. *Estuarine, Coastal and Shelf Science*, 139, 46–59. <https://doi.org/https://doi.org/10.1016/j.ecss.2013.12.030>
- Deltares. (2021). *D-flow flexible mesh, user manual* (Version: 2022.02). Deltares.
- Dronkers, J. (1986). Tidal asymmetry and estuarine morphology. *Netherlands Journal of Sea Research*, 20(2-3), 117–131.
- Drylie, T. P., Lohrer, A. M., Needham, H. R., Bulmer, R. H., & Pilditch, C. A. (2018). Benthic primary production in emerged intertidal habitats provides resilience to high water column turbidity. *Journal of sea research*, 142, 101–112.
- Esselink, P. (2022).

- Esselink, P., & Berg, G. (2004). Hoogte-ontwikkeling en slibbalans van polder breebaart na invoering van een gedempt getijden-regime.
- Esselink, P., Tolman, M., & Veenstra, W. (2020). *Slibinvang polder breebaart na herinrichting: Datarapport eerste halfjaar* (tech. rep. PUCCIMAR rapport 20). PUCCIMAR Ecologisch Onderzoek & Advies.
- Esteves, L. S. (2013). Is managed realignment a sustainable long-term coastal management approach? *Journal of Coastal Research*, (65 (10065)), 933–938.
- Esteves, L. S. (2014). What is managed realignment? In *Managed realignment: A viable long-term coastal management strategy?* (pp. 19–31). Springer.
- Finkl, C. W. (2015). Managed realignment: A viable long-term coastal management strategy?; esteves, ls. *Journal of Coastal Research*, 31(3), 771–771.
- Firet, M., Hakvoort, F. H. E., Oterdoom, T., Muntjewerf, B., Snels, G., Noordhoff, I., & Braaksma, J. (2018). *Mooi werk mooi wad: Landmakers, slib als kans* (Unpublished Work), Programma naar een Rijke Waddenzee.
- French, P. (1999). Managed retreat: A natural analogue from the medway estuary, uk. *Ocean & Coastal Management*, 42(1), 49–62.
- Friedrichs, C. T. (2011). Tidal flat morphodynamics: A synthesis.
- Hanssen, J. L. J., van Prooijen, B. C., Volp, N. D., de Vet, P. L. M., & Herman, P. M. J. (2022). Where and why do creeks evolve on fringing and bare tidal flats? *Geomorphology*, 403, 108182.
- Hoogland, T., Van den Akker, J., & Brus, D. (2012). Modeling the subsidence of peat soils in the dutch coastal area. *Geoderma*, 171, 92–97.
- Hoven, K. v. d., Kroeze, C., & Loon-Steensma, J. M. v. (2021). How about the dikes? managed realignment in progress at the hedwige-prosperpolder. *FLOODrisk 2020-4th European Conference on Flood Risk Management*.
- Jongepier, I., Wang, C., Missiaen, T., Soens, T., & Temmerman, S. (2015). Intertidal landscape response time to dike breaching and stepwise re-embankment: A combined historical and geomorphological study. *Geomorphology*, 236, 64–78.
- Kearney, W. S., & Fagherazzi, S. (2016). Salt marsh vegetation promotes efficient tidal channel networks. *Nature communications*, 7(1), 1–7.
- Ketelaars M.B.G., M. M., Janssen S.K.H. (2022). Managed realignment. www.stowa.nl/deltafacts/waterveiligheid/het-kuststelsysteem/managed-realignment
- KNMI. (2022). Uurgegevens van het weer in nederland - nieuw beerta (286).
- Knutson, P. L., Ford, J. C., Inskeep, M. R., & Oyler, J. (1981). National survey of planted salt marshes (vegetative stabilization and wave stress). *Wetlands*, 1(1), 129–157.
- LAMA. (2020). *Slib het grijze goud. ontwerpend onderzoek naar het ophogen van landbouwgrond: Slib als motor voor regionale (landschaps)ontwikkeling*.
- Maggi, F. (2005). *Flocculation dynamics of cohesive sediment* (Thesis). Technische Universiteit Delft.
- Morris, R. K. (2012). Managed realignment: A sediment management perspective. *Ocean & coastal management*, 65, 59–66.
- Mu, T., & Wilcove, D. S. (2020). Upper tidal flats are disproportionately important for the conservation of migratory shorebirds. *Proceedings of the Royal Society B*, 287(1928), 20200278.
- NCG. (2022). Bodemdalingskaart 2.0.
- O'Brien, M. P. (1969). Equilibrium flow areas of inlets on sandy coasts. *Journal of the Waterways and Harbors Division*, 95(1), 43–52.
- Peletier, H., Wanningen, H., Speelman, B., & Esselink, P. (2004). Resultaten van een gedempt getijdenregime in polder breebaart. *De Levende Natuur*, 105(5), 191–194.
- Poggi, D., Porporato, A., Ridolfi, L., Albertson, J., & Katul, G. (2004). The effect of vegetation density on canopy sub-layer turbulence. *Boundary-Layer Meteorology*, 111(3), 565–587.
- Price, D. C. (2016). *Influence of vegetation on sediment accumulation in tidal saltmarshes: An integrated field and modelling study* (Doctoral dissertation). UCL (University College London).
- Reed, D., van Wesenbeeck, B., Herman, P. M., & Meselhe, E. (2018). Tidal flat-wetland systems as flood defenses: Understanding biogeomorphic controls. *Estuarine, Coastal and Shelf Science*, 213, 269–282.
- Schmidt, C., Iedema, W., van Es, K., Onwezen, M., & Haarman, F. (2019). *Monitoringsrapportage 2018* (Report).

- Schmidt, C., van Bentum, F., van Es, K., Onwezen, M., & Brenninkmeijer, A. (2021). *Monitoringsrapportage 2020* (Report). Eems Dollard 2050.
- Soulsby, R. L., Hamm, L., Klopman, G., Myrhaug, D., Simons, R., & Thomas, G. (1993). Wave-current interaction within and outside the bottom boundary layer. *Coastal engineering*, 21(1-3), 41–69.
- Stive, M. J., & Rakhorst, R. (2008). Review of empirical relationships between inlet cross-section and tidal prism. *Journal of Water Resources and Environmental Engineering*, 23(1), 89–95.
- Sutherland, J., Peet, A., & Soulsby, R. (2004). Evaluating the performance of morphological models. *Coastal engineering*, 51(8-9), 917–939.
- Symonds, A. M., Vijverberg, T., Post, S., Van Der Spek, B.-J., Henrotte, J., & Sokolewicz, M. (2016). Comparison between mike 21 fm, delft3d and delft3d fm flow models of western port bay, australia. *Coast. Eng.*, 2, 1–12.
- Taal, M., Schmidt, C., Brinkman, A., Stolte, W., & Van Maren, D. (2015). *Slib en primaire productie in het eems-estuarium: Een samenvatting van vier jaar meten, modelleren, kennis bundelen en verwerven* (Report).
- Talke, S. A., de Swart, H. E., & De Jonge, V. (2009). An idealized model and systematic process study of oxygen depletion in highly turbid estuaries. *Estuaries and coasts*, 32(4), 602–620.
- Temmerman, S., Moonen, P., Schoelynck, J., Govers, G., & Bouma, T. J. (2012). Impact of vegetation die-off on spatial flow patterns over a tidal marsh. *Geophysical Research Letters*, 39(3).
- Tydemans, P. (2005). De polder breebaart: De ontwikkelingen in de polder breebaart resultaten van de monitoring in 2003 en 2004 en een vergelijking met 2001 en 2002. *Rapportnr.: 2005.030*.
- Van de Kreeke, J., Day, C. M., & Mulder, H. P. J. (1997). Tidal variations in suspended sediment concentration in the ems estuary: Origin and resulting sediment flux. *Journal of Sea Research*, 38(1), 1–16. [https://doi.org/https://doi.org/10.1016/S1385-1101\(97\)00040-3](https://doi.org/https://doi.org/10.1016/S1385-1101(97)00040-3)
- van den Hoven, K., Kroeze, C., & van Loon-Steensma, J. M. (2022). Characteristics of realigned dikes in coastal europe: Overview and opportunities for nature-based flood protection. *Ocean & Coastal Management*, 222, 106116.
- Van der Wegen, M., Van der Werf, J., De Vet, P., & R bke, B. (2017). Hindcasting westerschelde mouth morphodynamics (1963-2011).
- Van Maren, D., & Winterwerp, J. (2013). The role of flow asymmetry and mud properties on tidal flat sedimentation. *Continental Shelf Research*, 60, S71–S84.
- van Es, K. (2021). *Programmaplan 2021-2026* (Report). Eems-Dollard-2050, Province Groningen.
- van Maren, D. S., Oost, A. P., Wang, Z. B., & Vos, P. C. (2016). The effect of land reclamations and sediment extraction on the suspended sediment concentration in the ems estuary. *Marine Geology*, 376, 147–157. <https://doi.org/https://doi.org/10.1016/j.margeo.2016.03.007>
- van Maren, D. S., Pierik, H. J., Dankers, P. J. T., & Schmidt, C. (2020). De verslibbing van het eems-estuarium. *Landschap : tijdschrift voor landschapsecologie en milieukunde*, 37(3), 112–121. <https://edepot.wur.nl/532285>
- van Maren, D. S., van Kessel, T., Cronin, K., & Sittoni, L. (2015). The impact of channel deepening and dredging on estuarine sediment concentration. *Continental Shelf Research*, 95, 1–14. <https://doi.org/https://doi.org/10.1016/j.csr.2014.12.010>
- van Paridon x de Groot | abe veenstra landschapsarchitect. (2020). *Ziel in landschap - koersverkenning delfzijl* (Report). van Paridon x de Groot | abe veenstra landschapsarchitect.
- Vos, P., & Knol, E. (2013a). De ontstaansgeschiedenis van het dollardlandschap; natuurlijke en antropogene processen. *K. Essink (Red.), Stormvloed*, 31–43.
- Vos, P., & Knol, E. (2013b). De ontstaansgeschiedenis van het dollardlandschap; natuurlijke en antropogene processen. *K. Essink (Red.), Stormvloed*, 31–43.
- Vos, P. C., & Knol, E. (2015). Holocene landscape reconstruction of the wadden sea area between marsdiep and wester: Explanation of the coastal evolution and visualisation of the landscape development of the northern netherlands and niedersachsen in five palaeogeographical maps from 500 bc to present. *Netherlands Journal of Geosciences*, 94(2), 157–183.
- Weisscher, S. A., Baar, A. W., van Belzen, J., Bouma, T. J., & Kleinhans, M. G. (2022). Transitional polders along estuaries: Driving land-level rise and reducing flood propagation. *Nature-Based Solutions*, 2, 100022. <https://doi.org/https://doi.org/10.1016/j.nbsj.2022.100022>
- Winterwerp, J. C. (2011). Fine sediment transport by tidal asymmetry in the high-concentrated ems river: Indications for a regime shift in response to channel deepening. *Ocean Dynamics*, 61(2), 203–215.

- Winterwerp, J. C., Van Kessel, T., van Maren, D. S., & Van Prooijen, B. C. (2022). *Fine sediment in open water: From fundamentals to modeling*. World Scientific.
- Winterwerp, J. C., & Wang, Z. B. (2013). Man-induced regime shifts in small estuaries—i: Theory. *Ocean Dynamics*, 63(11), 1279–1292. <https://doi.org/https://doi.org/10.1007/s10236-013-0662-9>
- Zhou, Z., Coco, G., van der Wegen, M., Gong, Z., Zhang, C., & Townend, I. (2015). Modeling sorting dynamics of cohesive and non-cohesive sediments on intertidal flats under the effect of tides and wind waves. *Continental Shelf Research*, 104, 76–91.
- Zhou, Z., Liang, M.-j., Chen, L., Xu, M.-p., Chen, X., Geng, L., Li, H., Serrano, D., Zhang, H.-y., Gong, Z., et al. (2022). Processes, feedbacks, and morphodynamic evolution of tidal flat–marsh systems: Progress and challenges. *Water Science and Engineering*.

List of Figures

2.1	A: The Ems estuary around 1250 AD. All brown areas are peat, the green areas are embanked salt marshes with the red lines along the ems representing some of the first dikes. Due to the absence of the Dollart, the Ems estuary was much more narrow than it is today (P. Vos and Knol, 2013a). B: The development of the Dollart since its largest size. Since 1550, the surface of the Dollart has been greatly reduced. (van Maren et al., 2016)	5
2.2	Schematic diagram with the most important processes affecting SPM levels. Human influence affects all facets. (Winterwerp et al., 2022)	6
2.3	The concept of a managed realignment polder. (Ketelaars M.B.G., 2022)	7
2.4	Polder Breebaart, a small polder, open to the tide in the Dollart through a culvert, indicated by the red line. (courtesy of Rijkswaterstaat, 2022)	8
2.5	Cycle of deposition and resuspension of clay particles (Maggi, 2005)	9
2.6	Bed load transport of sediment in a symmetrical tidal current (A) and a asymmetrical current (B). In the asymmetrical case is the volume of transported sediment lower in the second phase of the tide (with lower flow velocities) than in the first phase of the tide, due to the required critical flow velocity for erosion. Even if the second phase would take longer. (Dalrymple et al., 2003)	11
2.7	Mud flocs transported during flood (left) and during ebb (right). As a result of higher flow velocities, the water is more turbulent, which leads to the formation of larger and more flocs that are dispersed higher in the water column. This increases the transport of flocs. (Winterwerp, 2011)	11
2.8	Effect of only settling lag (A) and combined settling lag with scour lag (B). The maximum current speeds decrease toward the land (dashed diagonal line). A sediment travels from 1) (where threshold velocity is exceeded) to 4) (after the threshold velocity becomes below the threshold at 3) during flood. The particle travels back to point 7 during ebb. This creates a landward migration of the particle due to the inequality between the time it needs to reach the threshold velocity due to the landward decreasing current velocities. Due to the scour lag, this effect becomes even larger (Dalrymple et al., 2003).	12
2.9	schematic representation of bed shear stress with non-linear Wave-current interaction. The bed shear stress of the current (τ_c) in (a), the bed shear stress of the waves (τ_w) in (b) and the combined mean bed shear (τ_m) and combined maximum bed shear stress (τ_{max}) in (c) (Soulsby et al., 1993).	14
2.10	The reduction of flow velocity over regular (left) and irregular (right) vegetation. (Winterwerp et al., 2022)	15
2.11	Convex-up and concave-up tidal flats. Convex-up tidal flats have a larger area within the tidal range, where the most ecologic value is present. Convex-up tidal flats are therefore preferable for nature development. Additionally, more creek development occurs in convex-up tidal flats, which is also preferable for nature development (Hanssen et al., 2022).	16
2.12	The concept of the sediment import in the managed realignment polder. The tidal inflow in the polder has a higher SSC than the outflow because a part of the suspended mud particles settles.	17
3.1	The bed levels in Mrt 2020 (with measurement cross-sections in red), Aug 2020 and Aug 2021. The black polygon represents the data which is not included in the data analysis due to differences in reed height.	21
3.2	Projected topographic data of Polder Breebaart (left) and grid schematisation (right). The crosses in the right figure show the model measurement stations and the lines show the model measurement cross sections.	22

3.3	Tidal forcing in Polder Breebaart on open boundary	23
3.4	A: Elevation map of the project area. This figure shows that almost the entire area is below sea level (source: AHN, 2022). B: Subsidence map of the project area. This figure shows that the subsidence in northeast Groningen is very high compared to the rest of the country (source: NCG, 2022).	25
3.5	All the domain boundaries are visualised. Left in the map: the different domains of the realignment project area. Each larger domain contains also the area of the smaller domains. Bat1 is not further discussed in this thesis report. Right in the map: the location and domain boundary of Polder Breebaart.	27
3.6	The grid of the four used domains. The 'eye' signs represents the observation stations in the numerical model and the red lines shows the observation cross-sections. The observation cross-sections are called crs1 to crs5, respectively from the entrance to the back of the polder. The larger domains includes also the area of the smaller domains towards the open boundary, upper right in the figure.	28
3.7	Initial bathymetry of the 4 domains. For all four domains, the bathymetry is created using the elevation data of AHN (AHN, 2022), and the transport formulations of Engelund-Hansen.	29
4.1	The difference in bed levels between data sets. At the bottom of the plots is the total volume change of sediment showed. The red line shows the divide between the upper part and lower part for the volume change calculation. The black polygon represents the data which is not included in the data analysis due to differences in reed height.	33
4.2	The effect of the Partheniades-Krone parameters on the flux. Only the horizontal piece at the top of the graph (where the flux is larger then 0) shows a flux where deposition exceeds erosion. This shows that the erosion flux at high shear stresses according to the Partheniades-Krone equations can become many times larger than the deposition flux. This research therefore mainly focuses on the small horizontal part at the top where net sedimentation can take place.	34
4.3	Some results during the calibration process. A: The result without waves and $\tau_{cr} = 0.15 \text{ Pa}$. B: The result without waves and $\tau_{cr} = 0.04 \text{ Pa}$. C: The result without waves and $\tau_{cr} = 0.01 \text{ Pa}$. D: The result with waves. E: The result of a simulation with 6 times larger tidal forcing. F: The data which should be approximated with the numerical model.	36
4.4	Calibration Breebaart. Erosion and accumulation according to model (left) and according to data (right)	37
4.5	Sediment import of all model scenarios, measured by the cumulative sediment flux $[\text{kg}]$, passing the boundary (i.e. crs1, see Figure 3.6).	39
4.6	The sediment extractions per year in millions ton dry matter. The mass is calculated with $\rho_b = 500 \text{ kg/m}^3$	40
4.7	The tidal prism of all model scenarios is plotted against the mean tidal range (MTR). This shows a clear correlation. The angle at which the trend lines in the graph run, correspond to the area of the domains.	41
4.8	Accumulation as function of tidal prism. For all scenarios, markings from left to right, the domains Bat2 to Bat5. The effect of halving the tidal range is indicated in red dotted lines. It is clear that by halving the tidal range, the sediment import is not halved.	41
4.9	The accumulation after two years of the reference scenario and the 96% percentile of the occurring bed shear stress. This bed shear stress is occurring for 1 hour a day on average. The color bar limits starting from 0.21 Pa, which is the critical bed shear stress. Only excess bed shear stresses are colored therefore. There is a clear correspondence between the occurring bed shear stresses and accumulation patterns.	42
4.10	The accumulation after two years of the scenario with the halved tidal range and the 96% percentile of the occurring bed shear stress. This bed shear stress is occurring for 1 hour a day on average. The color bar limits starting from 0.21Pa, which is the critical bed shear stress, only the excess bed shear stresses are colored therefore.	42
4.11	The accumulation after two years with the scenario using the lower half of the tidal range and the scenario using the upper half of the tidal range.	43

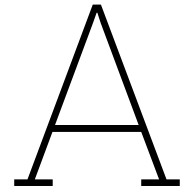
4.12	The accumulation after two years of the scenario with the weir (crest level at $NAP + 0\text{ m}$) and the scenario with the smallweir (crest level at $NAP - 0.5\text{ m}$).	44
4.13	The mean SSC of the scenario with the weir (crest level at $NAP + 0\text{ m}$) and the scenario with the smallweir (crest level at $NAP - 0.5\text{ m}$).	45
4.14	The accumulation after two years of the scenario with the deepweir (a weir with a submerged crest level dependent on size of the basin) and the 96% percentile of the occurring bed shear stress.	46
4.15	The water levels of all model scenarios in the domain of bathymetry 4.	47
4.16	Distribution of minimum and maximum tidal water levels at the open boundary. The most relevant numbers here are MLT is at $NAP - 1.62\text{ m}$, since the mudflats begin at this elevation, and MSL is at $NAP + 0.16\text{ m}$	47
4.17	Distribution of sedimentation over height	48
4.18	Distribution of sedimentation height per available squared meter for that height	48
4.19	The percentage of accumulation that takes place lower	48
4.20	The percentage of accumulation that takes place below $NAP - 3\text{ m}$	49
4.21	The influence of waves on the total sediment extraction volume of the polder. For all cases where waves have been simulated, this has a negative effect on the total extraction of sediment.	50
4.22	The effect of the waves on the accumulation patterns. When not taking into account the effect of waves (left figures), accumulation mainly occurs on the flats, while more wave effect results in the accumulation mainly occurs in the channels (right figures). Moreover, the sediment is transported further to the back of the polder by the influence of waves.	51
4.23	The effect of the waves on the accumulation patterns. It is clear that the waves cause higher sediment concentrations, especially in the back of the polder.	51
4.24	The influence of waves on the elevation distribution of accumulation. More waves result in accumulation on lower elevations. This is consistent with the observation that accumulation moves to the channels.	52
A.1	visualisation of the methodology	73
B.1	The Ems estuary around 1250 AD. All brown areas are peat, the green areas are embanked salt marshes (P. Vos and Knol, 2013a)	75
B.2	The development of the Dollart since its largest size around 1550 (van Maren et al., 2016)	75
B.3	The bottom development between 1000 and 2000 AD across cross-section A-B of Figure B.2 (P. C. Vos and Knol, 2015)	76
B.4	The observed suspended sediment concentrations in the Ems Dollart from 5 november till 10 november 1990. The measurements are taken in the middle reaches of the estuary. For the exact location see B.7. From the measurements becomes clear that the SSC varied a lot over the tidal cycle. (Van de Kreeke et al., 1997)	77
B.5	Annual change in sediment concentration C (in mg/l/year) for Huibertgat (S1), Groote Gat Noord (S6), Bocht van Watum (S7) and Bocht van Watum Noord (S8). The blue lines represent the 95% uncertainty interval and the dashed lines represent the relative yearly increase as function of the concentration in 2010. (van Maren et al., 2016).	78
B.6	The observed suspended sediment concentrations in the Ems Dollart from 5 november till 10 november 1990. The measurements are taken in the middle reaches of the estuary. For the exact location see B.7. From the measurements becomes clear that the SSC varied a lot over the tidal cycle. (Van de Kreeke et al., 1997)	79
B.7	Map of the Ems-Dollart Estuary with the three reaches. The red line shows the measurement location of the SSC measurements of Kreeke in 1990, shown in Figure B.4.(de Jonge and Schückel, 2019)	79
B.8	Trends in primary production based in changes in the turbidity. (the + and – signs stand for a calculation with- and without the organic waste load from the Westerwoldsche Aa).(de Jonge and Schückel, 2019)	81
B.9	Relative changes in the biomasses of the functional groups for period 1955+ (including organic waste load) to 2005- (excluding organic waste load) for the three reaches.(de Jonge and Schückel, 2019)	82

B.10 Mean annual suspended sediment in the Ems estuary and Ems river de Jonge et al., 2014	83
B.11 Dredging volumes in the Ems Dollart estuary van Maren et al., 2015	84
B.12 Tidal amplitude changes in the Ems estuary and Ems River Taal et al., 2015	85
B.13 Computed increase in suspended sediment concentration due to bottom changes between 1985 and 2005 (van Maren et al., 2015)	85
B.14 An tidal flat – saltmarsch system is accreting (upper figure) or retreating (lower figure). The retreating salt marshes shows also lower and less tidal flats. They lose their convex-up shape, resulting in a smaller surface area between the tidal range, while that is precisely the elevation that has the highest ecological value and where the most biomass is located. (Reed et al., 2018)	87
C.1 model results after 1 month with 2 sediment fractions (left) and with both sediment fractions separately	90
C.2 Occurring wave height/water depth ratios with different γ_b 's.	92
C.3 Occurring 95% value of bed shear stresses with different γ_b 's.	93
C.4 Distribution of occurring bottom shear stresses with $\gamma_b = 0.8$.	94
C.5 Distribution of occurring bottom shear stresses with $\gamma_b = 0.6$.	94
C.6 Distribution of occurring bottom shear stresses with $\gamma_b = 0.5$.	95
C.7 Distribution of occurring bottom shear stresses with $\gamma_b = 0.35$.	95
D.1 Model results of all scenarios with bathymetry 2. Upper left: accumulation after two year. Upper right: mean SSC. Lower left: 83.3 percentile of occurring bed shear stresses. Lower right: 95.8 percentile of occurring bed shear stresses.	97
D.2 Model results of all scenarios with bathymetry 3. Upper left: accumulation after two year. Upper right: mean SSC. Lower left: 83.3 percentile of occurring bed shear stresses. Lower right: 95.8 percentile of occurring bed shear stresses.	98
D.3 Model results of all scenarios with bathymetry 4. Upper left: accumulation after two year. Upper right: mean SSC. Lower left: 83.3 percentile of occurring bed shear stresses. Lower right: 95.8 percentile of occurring bed shear stresses.	99
D.4 Model results of all scenarios with bathymetry 5. Upper left: accumulation after two year. Upper right: mean SSC. Lower left: 83.3 percentile of occurring bed shear stresses. Lower right: 95.8 percentile of occurring bed shear stresses.	100
D.5 Model results of the wave effect on scenarios 'reference' (upper), 'half range' (middle) and 'deepweir' (lower) in bathymetry 3. Upper three: accumulation after two year. lower three: 95.8 percentile of occurring bed shear stresses.	101
D.6 Model results of the wave effect on scenarios 'reference' (upper), 'half range' (middle) and 'deepweir' (lower) in bathymetry 5. Upper three: accumulation after two year. lower three: 95.8 percentile of occurring bed shear stresses.	102
D.7 Mean SSC results of the wave effect on scenarios 'reference' (upper), 'half range' (middle) and 'deepweir' (lower) in bathymetry 3 (upper three) and bathymetry 5 (lower three).	103
D.8 The accumulation of the scenarios 'half range' (left four) and 'deepweir' (right four). The results are quite similar when speaking of accumulation distribution, particularly for Bat4 and Bat5.	104
D.9 The accumulation of the scenarios 'lower half' (left four) and 'upper half' (right four). The results are completely different when speaking of accumulation distribution. In 'lower half' the sediment is transported much further into the polder and the channels are 'flushed'. In 'upper half' the accumulation takes place less deeply in the polder and mainly in the channels.	104
D.10 The accumulation of the scenarios 'weir' (left four) and 'smallweir' (right four). Both results of the accumulation distribution show that most of the accumulation occurs too close to the entrance. Only the results of 'smallweir' for Bat2 and Bat3 show good results.	105
D.11 In contrast to the accumulation of 'half range' and 'deepweir', the maps with mean SSC values do not match each other. The mean SSC of the scenarios 'half range' (left four) and 'deepweir' (right four) show some differences. 'Half range' shows higher SSC in particularly the channels, while the distribution in scenario 'deep weir' has a more equal SSC field. This is explainable by the higher mean water level in the area for 'deepweir'.	105

D.12	The mean SSC of the scenarios 'lower half' (left four) and 'upper half' (right four). In the results it is clear that high SSC values are at same areas as high accumulation (Figure D.9. 'Lower half' shows higher SSC values especially in the channels, which supports the conclusion that high flow velocities (with high shear stresses) occur in the channels.	106
D.13	The occurring bed shear stresses of the scenarios 'lower half' (left four) and 'upper half' (right four) are completely different, but in line with the accumulation and mean SSC of these scenarios. In the results it is clear that higher bed shear stresses occur in deeper parts of the polder for 'lower half', while close to the entrance on the tidal flats 'upper half' generates higher bed shear stresses.	106
E.1	Location of SSC measuring stations. (van Maren et al., 2015)	108
E.2	Computed average SSC levels according van Maren et al., 2016	108
F.1	The steps of the conceptual model, schematically displayed (Winterwerp et al., 2022)	110
G.1	Waterlevels in Polder Breebaart, oktober 2003 (Esselink and Berg, 2004)	112
G.2	Tidal boundary condition of Polder Breebaart	112
H.1	KNMI weather stations of the Netherlands with a red triangle on the location of the project (source: https://www.logboekweer.nl/)	113
K.1	Upper three: the bed levels in Mrt 2020 (with measurement cross-sections in red), Aug 2020 and Aug 2021. Bottom three: the difference in bed levels between data sets. At the bottom of the plots is the total volume change of sediment showed. The red line shows the divide between the upper part and lower part for the volume change calculation. The black polygon represents the data which is not included in the data analysis due to differences in reed height.	121
K.2	The area which is not taken in consideration, shown on a map with bed level change	122
M.1	The possible domain of the project area according Firt et al. (2018) and LAMA (2020)	127
M.2	The possible domain of the project area according van Paridon x de Groot abe veenstra landschapsarchitect (2020)	127
M.3	All the domains, each larger domain contains the area of the smaller domains. Bathymetry5 (the outer lines) and Bathymetry3 (outlined with the black-red line) are designed using the domains in Figure M.1 and M.2 respectively.	128

List of Tables

3.1	Classification of Brier skill score	25
3.2	Surface area of all model domains which are used in the research	26
3.3	The crest levels of weirs Scenario 7. The heights are determined such that the flow in the different domains is reduced in comparable ways.	31
4.1	Parameters from calibration	38
4.2	The sum of the total accumulation in the entire polder. The color range shows the highest net sediment import, relative to other scenarios for the same domain. Green indicates the highest imported volume [m^3] and in red the lowest imported volume [m^3].	39
4.3	The mean tidal range (MTR) and tidal Prism for all scenarios. These two values are, of course, closely correlated. It is clear that the reference case in particular has high values. Higher values in the table have a deeper blue color to indicate the large numbers quickly.	40
4.4	Total accumulation [m^3], divided by prism [m^3]. Scenario 5 and scenario 6 have been excluded from the table since they have such a low prism relative to the reference case that it would skew the comparison. Scenario HR (halved tidal range) shows significant higher sedimentation relative the tidal prism then the reference case. It should be noted that these numbers do not present the accumulation per tidal cycle, the numbers are only for comparison and to determine the relative efficiency of the scenarios.	43
4.5	The percentage of the accumulation which takes place behind a certain observation cross-section (crs3 for Bat2 and crs5 for the other domains). High percentages (i.e. much accumulation in the back of the polder) are indicated in blue and low percentages (i.e. little sediment reaching the back of the polder) in red. The reference case shows relatively the most accumulation behind these cross-sections and the weir the least. It is noticeable that the 'smallweir' scenario shows a completely different result for the two smaller domains compared to the two larger domains. This can be explained by the fairly good distribution of accumulation, already observed in Figure 4.12.	45
4.6	Percentage of the area per elevation range. The color indicate the higher percentages. Note that the ranges are not equal. Below $NAP - 1.6\ m$ (i.e. MLT), the range sizes are doubled. According to the data, MSL is at $NAP + 0.16\ m$. It is clear that the largest area surfaces are between $NAP - 0.55\ m$ and $NAP - 0.9\ m$	46
4.7	The effect of waves on the total sediment extraction. The percentages indicating the increase or decrease when simulating without waves or with extra waves. The effect of waves is the largest for the reference case and the smallest for scenario 'deepweir'. In addition, the effect in domain bathymetry3 is slightly bigger than in bathymetry5.	50
4.8	The percentage of the accumulation which takes place behind observation cross-section crs5 for the simulation of scenarios 'reference', 'half range' and 'deepweir' (i.e. scenario 1, 4 and 7) in domain Bat3 and Bat5 without wave effect and with more wave effect. Higher percentages (i.e. more accumulation in the back of the polder) are indicated in blue and lower percentages (i.e. little sediment reaching the back of the polder) in red. It is noticeable that in all cases a higher percentage of the accumulation takes place beyond this cross-section with more waves, and a lower percentage without waves.	52
B.1	Annual production of algae in the Ems Estuary from 1976-1980. (de Jonge, 1995)	80
G.1	Tidal constituents with their periods and amplitudes	111



Methodology overview

The methodology used in this research is thoroughly explained in chapter 3. To provide a clear understanding of the process, a schematic representation of the different steps taken within the research is illustrated in Figure A.1. This figure highlights that the foundation of the research begins with the development of a conceptual model and how feedback loops are incorporated to refine and improve the model.

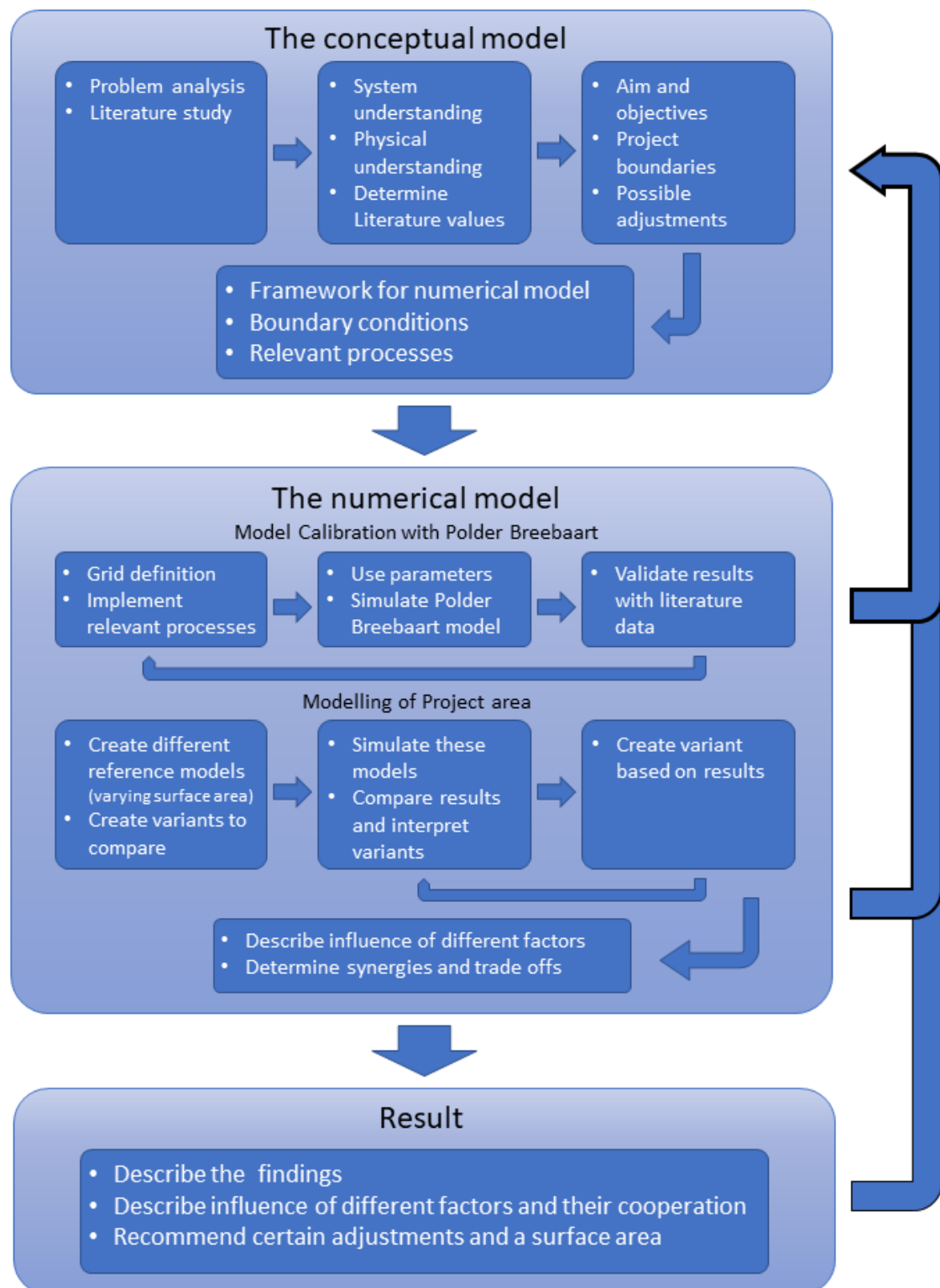


Figure A.1: visualisation of the methodology

B

Literature study

B.1. Historical development of Ems Dollart

In order to understand the current mud dynamics in the Ems-Dollart, it is important to consider the origin of the shape of the Ems-Dollart Estuary. The Ems-Dollart estuary has undergone significant changes throughout its history, both due to natural factors and human activity. Using paleogeographic maps, researchers have been able to reconstruct the landscape of the Ems estuary area between 500 BC and 2000 AD (Figure B.3). Because the changes in the landscape are only relevant from about 1500 AD, only this development has been discussed.

Until the 15th century, the estuary had a completely different shape. The Ems delta was much slimmer, and the entire Dollart had not yet been developed (figure B.1). The land surrounding the Ems delta mainly consisted of peat (the brown areas in Figure B.1). Before humans started exploiting the extensive coastal peatlands, the ground level was well above sea level with salt marshes on the coast (the green areas in Figure B.1). Since the peat land has been drained with ditches for agriculture purposes in the Middle Ages, the area subsided. This leads together with the reclamation of marshlands, to an increased flood risk. This led to the need for building and maintaining dikes to protect the area from flooding.

The natural factors that have played a role in the development of the Ems Dollart estuary are sea level rise and storm surges. Sea level rise has been a natural process that has occurred over a long period of time, but the human interventions in the area have made the area more vulnerable to the effects of sea level rise. The whole Ems delta was embanked, but two major floods (in 1412 and 1509) ensured that a large piece of peat land was swept away, forming the Dollart. Around 1550 the Dollart had reached its maximum size (Figure B.2). From then on, the Dollart was increasingly dammed up and reclaimed until it took its current shape in 1924 P. Vos and Knol, 2013b.

B.2. observed changes in turbidity and biomass in the Ems Dollart

There is a relationship between the turbidity and the biomass of algae (Colijn and Cadée, 2003). It therefore is useful to look at the changes over time of both aspects. These two aspects are discussed separately below.

B.2.1. The increase of turbidity

The Ems Dollart is naturally very turbid and large spatial and temporal variations occur in the Estuary. These variations are caused by continuous changing flow velocities. Because the concentrations vary so much over time, a single measurement to measure turbidity makes little sense. This has been shown with continuous measurements in November 1990 where the large variations in turbidity were visible (Van de Kreeke et al., 1997). The variations of this turbidity is shown in Figure B.4.

Unfortunately, there are no continuous measurements over a long period and only the data from Rijkswaterstaat can be used. Rijkswaterstaat has been monitoring four locations in the Ems-Dollart estuary in the MWTL program since 1972. In 1990, the measurement method is changed, therefore only the data starting from 1990 is useful. A sample is taken every month at these four locations

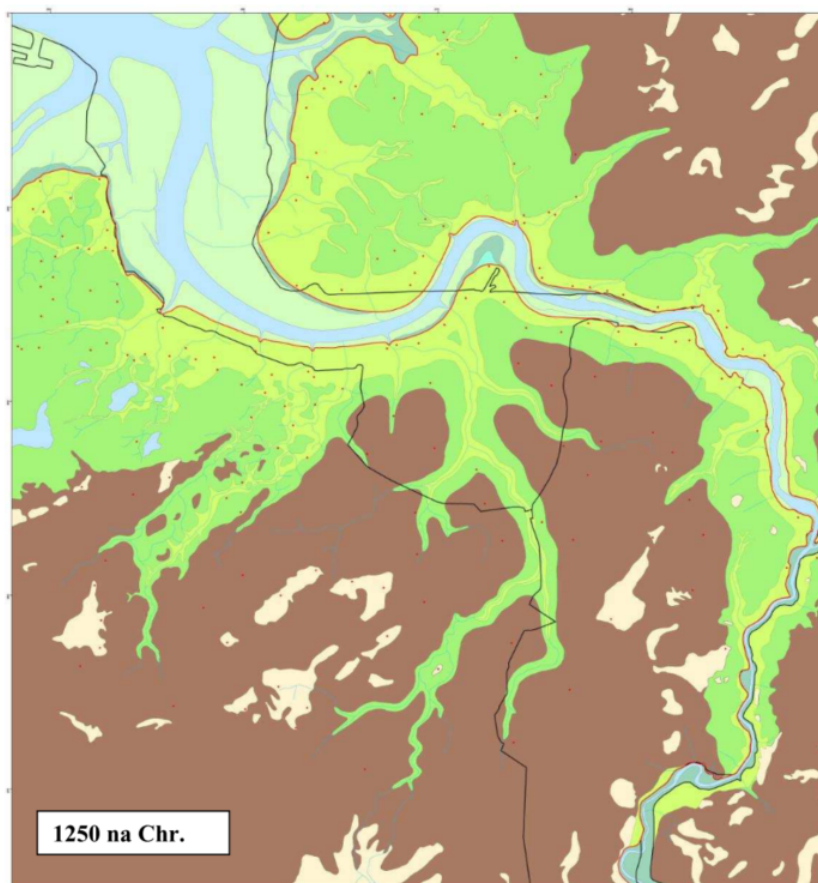


Figure B.1: The Ems estuary around 1250 AD. All brown areas are peat, the green areas are embanked salt marshes (P. Vos and Knol, 2013a)

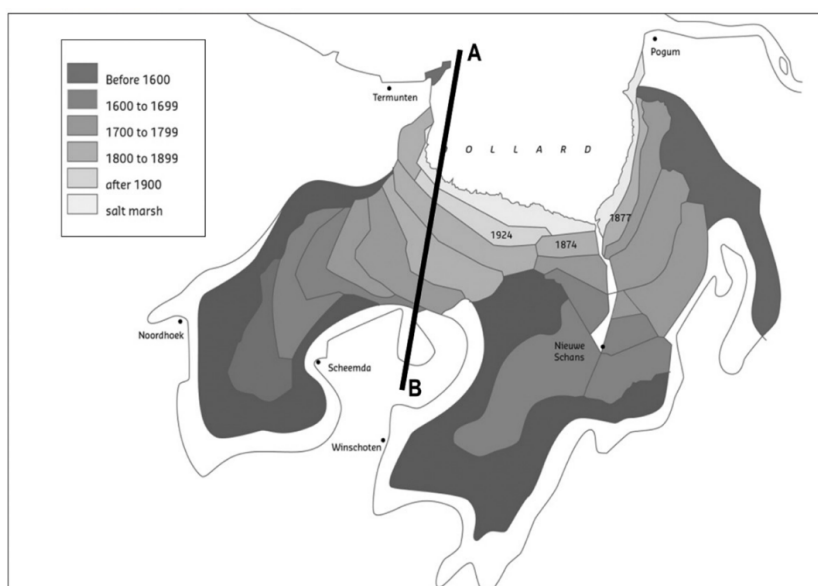


Figure B.2: The development of the Dollart since its largest size around 1550 (van Maren et al., 2016)

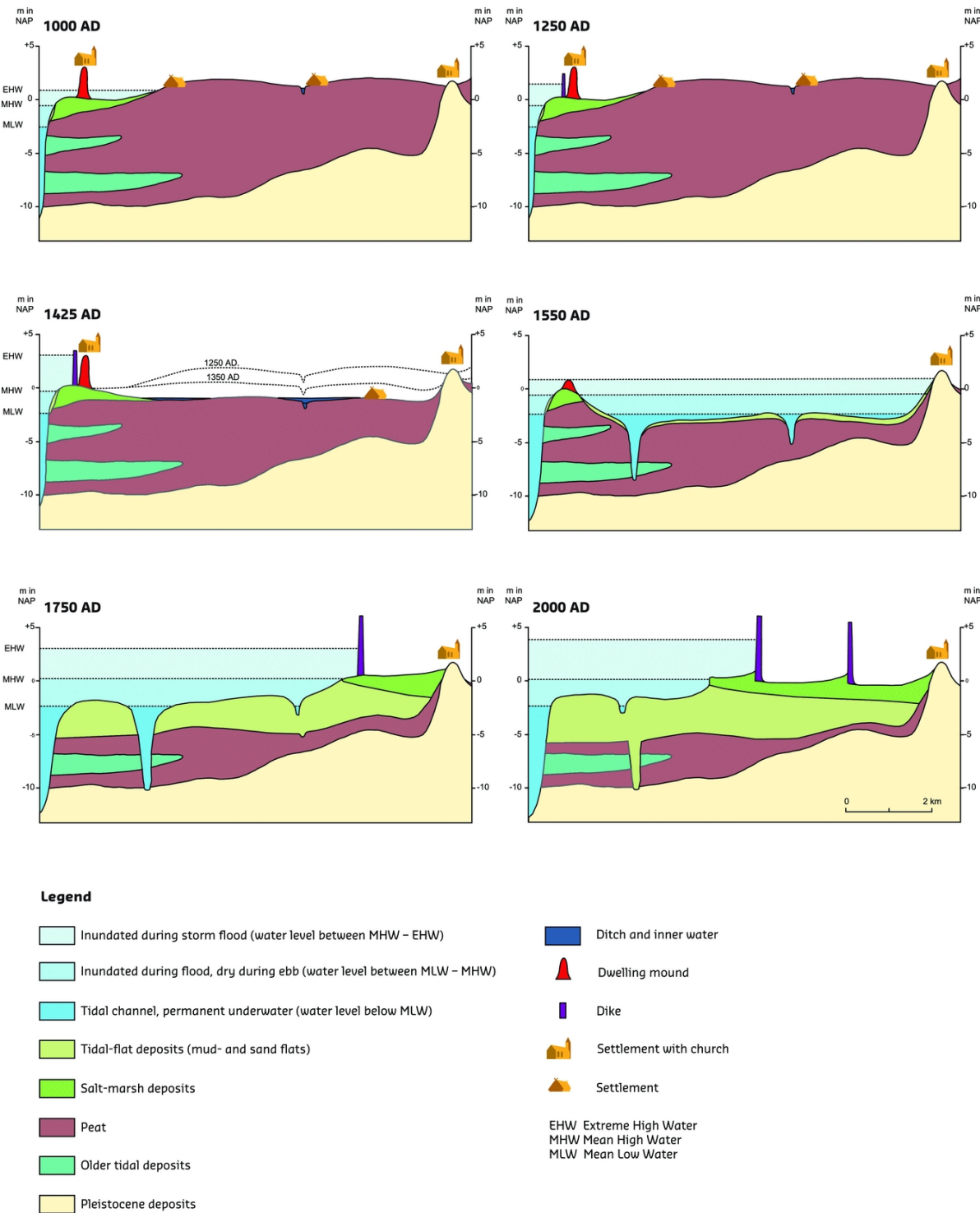


Figure B.3: The bottom development between 1000 and 2000 AD across cross-section A-B of Figure B.2 (P. C. Vos and Knol, 2015)

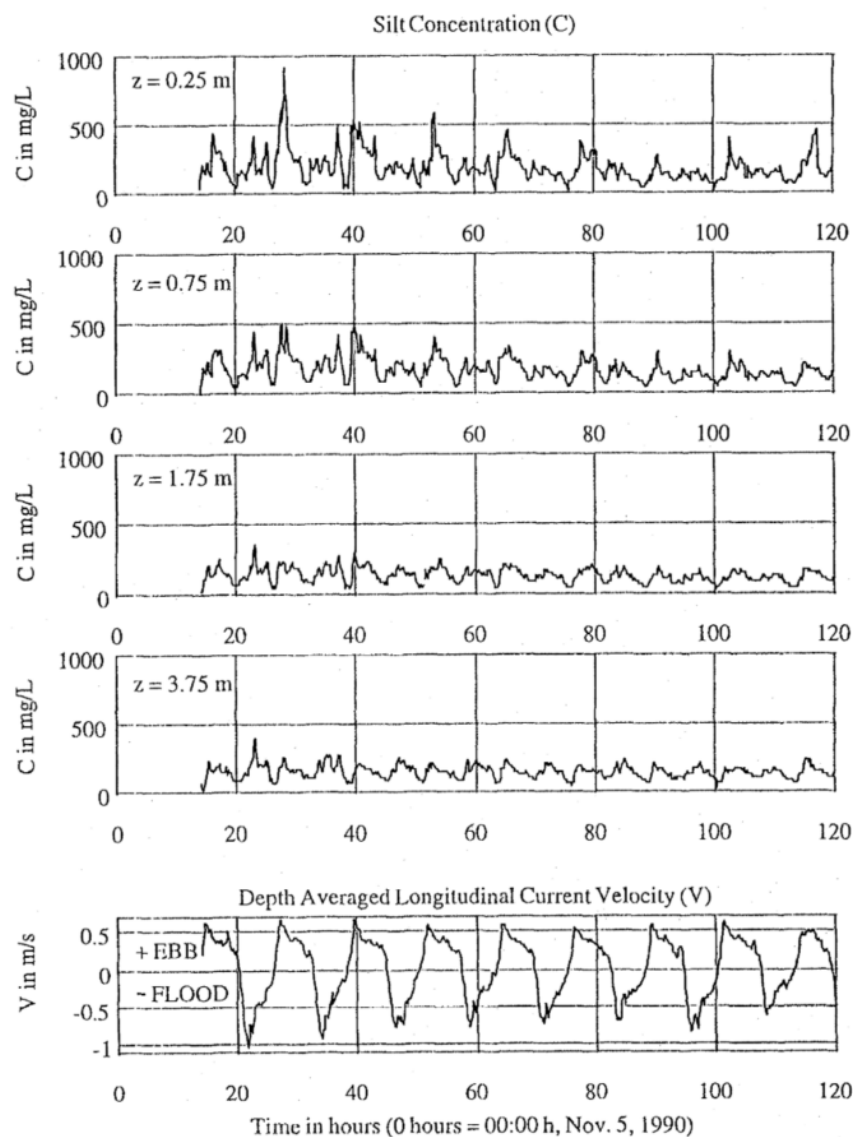


Figure B.4: The observed suspended sediment concentrations in the Ems Dollart from 5 november till 10 november 1990. The measurements are taken in the middle reaches of the estuary. For the exact location see B.7. From the measurements becomes clear that the SSC varied a lot over the tidal cycle. (Van de Kreeke et al., 1997)

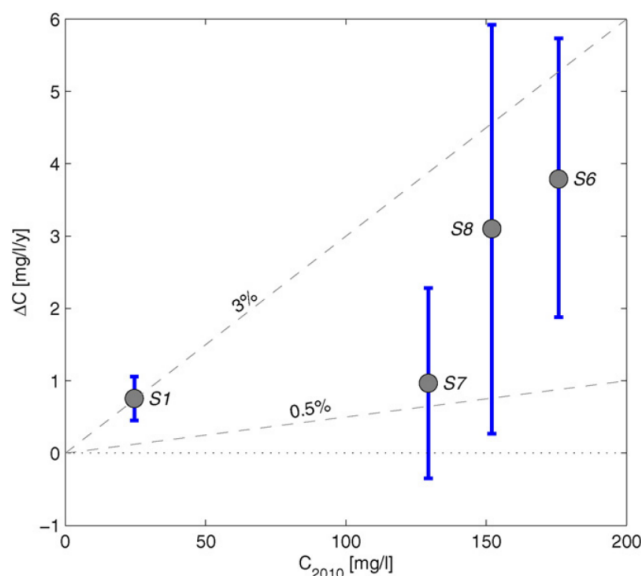


Figure B.5: Annual change in sediment concentration C (in mg/l/year) for Huibertgat (S1), Groote Gat Noord (S6), Bocht van Watum (S7) and Bocht van Watum Noord (S8). The blue lines represent the 95% uncertainty interval and the dashed lines represent the relative yearly increase as function of the concentration in 2010. (van Maren et al., 2016).

where the suspended sediment concentration is measured. In the estuary (at Huibertgat) an increase of between 2 and 5% per year is visible between 1990 and 2010, and an increase between 1 and 3% per year has also been observed at the measuring point in the Dollart (Groote Gat Noord) (van Maren et al., 2016). This increase is shown in Figure B.5.

The measurements between 1972 and 1990 also show a strong increase in suspended sediment concentration, see Figure 4 B.6 (de Jonge et al., 2014). Finally, the increase in SSC in the Ems River is even 100 times greater than it was in the 1950s (de Jonge et al., 2014). This is probably due to the deepening of the Ems River, which has made it flood dominant (Winterwerp and Wang, 2013).

B.2.2. The decrease in algae biomass

There is a strong link between the turbidity and the decrease of production of algae (Colijn and Cadée, 2003). By nature, estuaries are areas of high algae production, which form the basis of the marine food web (de Jonge and Schückel, 2019). When this production deteriorates, this influences the entire food web in a negative way. Besides to the fact that less food is available, the decline in algae production also causes a higher oxygen deficiency in the water Talke et al., 2009. The algae production is expressed in Primary Production and is determined by the availability of phosphate, nitrogen, silicate and light. A distinction must be made between different algae. The algae that are important can be divided into the floating algae (Phytoplankton), the microalgae on the tidal flats (Microphytobenthos) and the resuspended microphytobenthos (Tychoplankton). Together with the seagrass, these algae form the total primary production. Because there is virtually no more seagrass in the Ems-Dollart estuary, this is no longer included.

There is a large spatial variation in the estuary for algae growth. In different parts of the Ems Dollart estuary the share in the production of the different algae is different. In the lower and middle reaches (see Figure B.7), the production is dominated by the phytoplankton (respectively 57% and 59% of the total production per reach) while the production in the Dollart is dominated by microphytobenthos (72% of the total production in the Dollart) (de Jonge, 1995). The total area of the lower reaches ($1300 \cdot 10^3 m^2$) and the middle reaches ($460 \cdot 10^6 m^2$) are both larger than the area of the Dollart ($220 \cdot 10^6 m^2$) and contribute more to the total production. The share of the production of phytoplankton in the total Ems Dollart estuary is 53%. All these values can be seen in Table B.1. These proportions may vary slightly from year to year.

In particular, the total biomass of the phytoplankton has decreased. Figure B.8 shows the clear decrease of the different algae in the three different reaches between 1955 and 2005. Here it can be

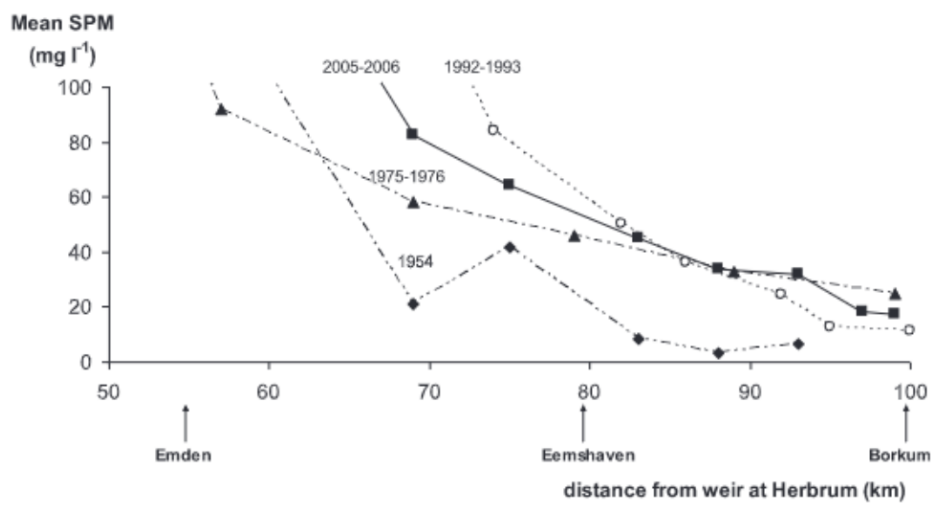


Figure B.6: The observed suspended sediment concentrations in the Ems Dollart from 5 november till 10 november 1990. The measurements are taken in the middle reaches of the estuary. For the exact location see B.7. From the measurements becomes clear that the SSC varied a lot over the tidal cycle. (Van de Kreeke et al., 1997)

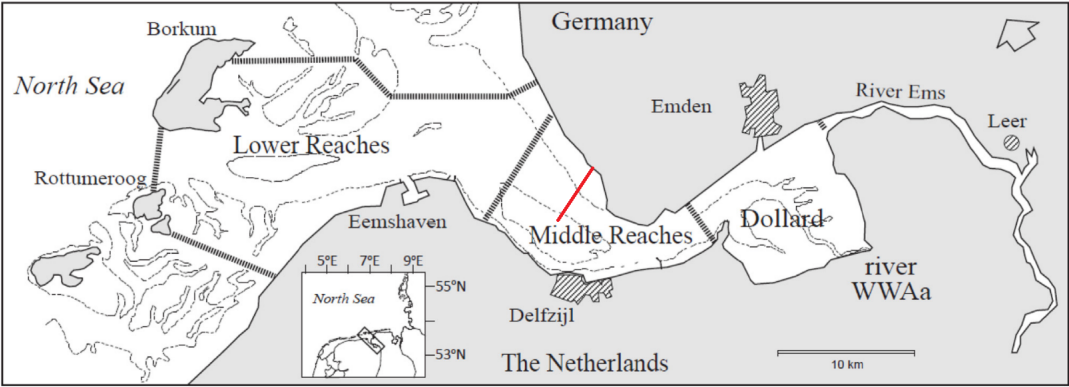


Figure B.7: Map of the Ems-Dollart Estuary with the three reaches. The red line shows the measurement location of the SSC measurements of Kreeke in 1990, shown in Figure B.4.(de Jonge and Schückel, 2019)

total annual production (tonnes/year)	Lower reaches	Middle reaches	Dollart	Total
Phytoplankton	48224	8598	205	57027
(share of total)	44.5%	7.9%	0.2%	52.6%
(share of reach)	5.3%	59%	2.1%	
Tychoplankton	20825	3348	2560	26733
(share of total)	19.2%	3.1%	2.4%	24.7%
(share of reach)	24.8%	23%	26.3%	
Microphytobenthos	15070	2624	6956	24650
(share of total)	13.9%	2.4%	6.4%	22.7%
(share of reach)	17.9%	18%	71.6%	
Total	84119	14570	9721	108410
(share of total)	77.6%	13.4%	9%	100%
Area ($10^6 m^2$)	1300	460	220	1980
Production ($gC m^{-2} y^{-1}$)	64.7	31.7	44.2	54.8

Table B.1: Annual production of algae in the Ems Estuary from 1976-1980. (de Jonge, 1995)

seen that the phytoplankton in particular is undergoing an enormous decrease (de Jonge and Schückel, 2019). As a result of the decrease in primary production of the algae, an enormous decrease in almost all other ecological groups is also visible. This can be seen in Figure B.9.

B.3. Causes of turbidity increase in Ems Dollart

There are several causes of the increase in turbidity possible. According van Maren (van Maren et al., 2016; van Maren et al., 2020) is this increase mainly because the number of sediment sinks has decreased enormously. Other causes that are put forward for the increase in turbidity in the estuary are the leaching of the extremely turbid river Ems, an increase in suspended sediment in the Wadden Sea due to a decrease in sediment sinks elsewhere, dredging with the associated dredging releases and the deepening of the navigation channels. The different possible causes are discussed separately below.

B.3.1. Decrease of sinks

Much land reclamation took place over the past 500 years in the entire Ems-Dollart Estuary, as already explained in Section B.1. This has required a constant supply of sediment. In addition, there used to be a lot of room for natural accretion in salt marshes. The last reclamation took place in 1924, but since then, a lot of dredging has been done in the estuary and in the Ems River (see Figure B.11). This dredging has also acted as a sediment sink. A large part of the dredging work took place in the port of Emden (1.5 million m³/year), but here they stopped extracting dredging sludge in 1994 and started regular re-aeration to prevent consolidation. This has resulted in a further decline in sediment sinks.

Taken together, until 1994 a total volume of 2.3 million m³/year of sediment could be extracted from the Dollart in various sinks. Since 1994 this is only 1.3 m³/year (which is mainly extracted in the Ems-river). As a result, the total volume of sinks has drastically decreased. The remaining mud remains in suspension in the estuary (van Maren et al., 2016). This is probably the main cause of the massive increase in turbidity and can explain 90% of the increase in turbidity (Taal et al., 2015).

B.3.2. Turbidity of Ems River

As stated at the end of Section B.2.1, the Ems-River in particular has become more turbid. A study from de Jonge et al., 2014 showed that the suspended mud concentration in the parts of the Ems River is 100 times greater than it was in the 1950s (de Jonge et al., 2014). The increase in turbidity in the Ems River leads to an increase in the Ems-Dollart Estuary due to leaching through river runoff and tidal current causing turbid water to wash into the estuary. The increase in turbidity is shown in Figure B.10, the Ems River in this plot is from the left side till Emden (55 km). The cause of the higher turbidity in the Ems River is explained in section .

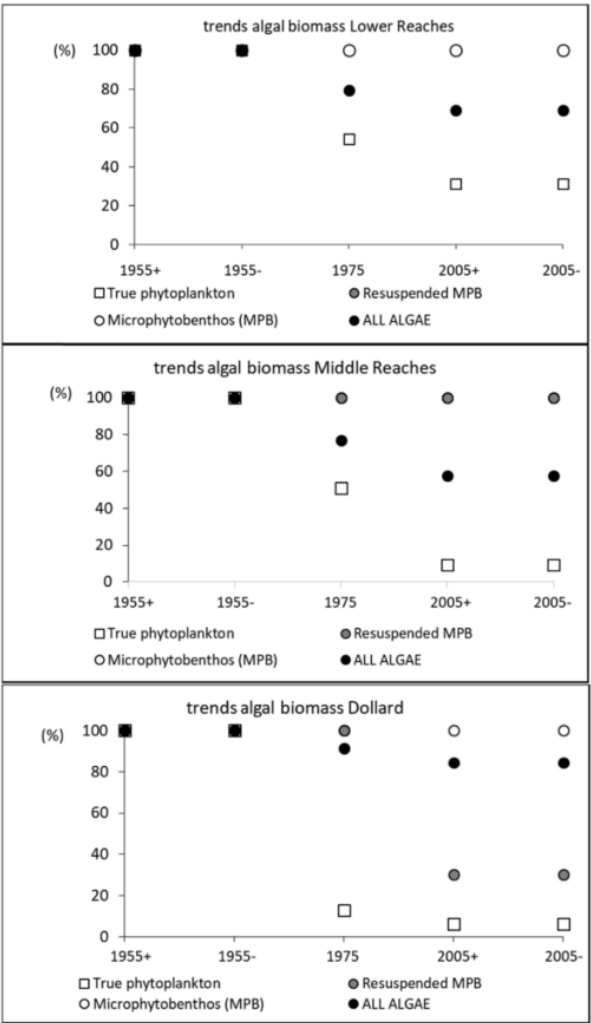


Figure B.8: Trends in primary production based in changes in the turbidity. (the + and – signs stand for a calculation with- and without the organic waste load from the Westerwoldsche Aa).(de Jonge and Schückel, 2019)

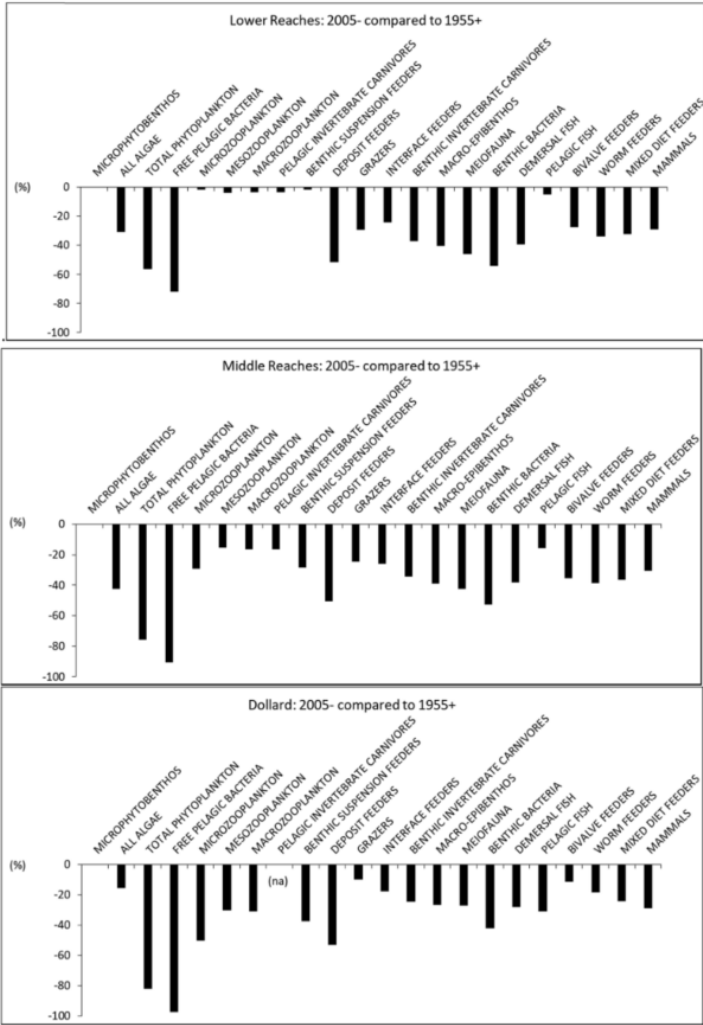


Figure B.9: Relative changes in the biomasses of the functional groups for period 1955+ (including organic waste load) to 2005- (excluding organic waste load) for the three reaches.(de Jonge and Schückel, 2019)

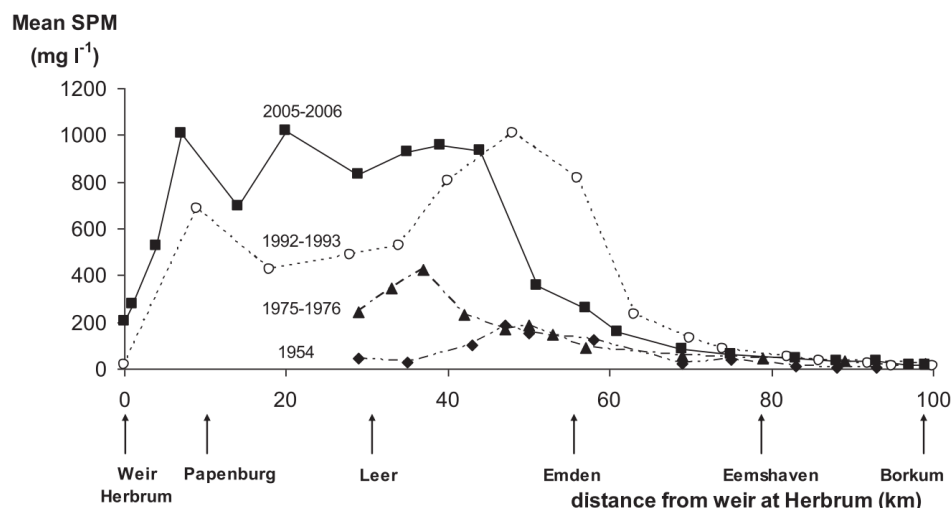


Figure B.10: Mean annual suspended sediment in the Ems estuary and Ems river de Jonge et al., 2014

B.3.3. Increase in suspended sediment in the Wadden

It is plausible that the concentration of suspended sediment has also increased in the Wadden Sea because several sediment sinks have also been removed here. In 1929 the Zuiderzee was closed and in 1969 the Lauwerszee was also closed. Moreover, the land reclamation works along the Groningen and Frisian coast have disappeared. The increase in the concentration of suspended sediment here is many times lower than in the Ems-Dollart Estuary, but may have resulted in extra concentration building up in the estuary.

B.3.4. Dredging activities

Due to the increase in the draft of ships, the fairway has also been further deepened over the years. Particularly since the 1970s, a great deal of dredging has taken place in the Ems Estuary (see Figure B.11). Every year, approximately 10 million m³ is dredged, of which approximately 8 million m³ is dispersed to specially designated release locations in the estuary (van Maren et al., 2015). These deposits create a lot of turbidity and suspended sediment in the estuary and the dredging activities could therefore play an important role in the increased turbidity (de Jonge et al., 2014).

B.3.5. Channel Deepening

As indicated in Section B.3.4 above, the fairways have been deepened. This deepening has several consequences. Firstly, the deepening ensures that a greater salinity gradient flow occurs. Upstream in the Ems River, the salinity is lower, and the density of the water is therefore smaller. Due to this density difference, a down-estuary oriented flow occurs at the surface and an up-estuary oriented flow at the bottom. Because the sediment concentrations at the bottom are normally higher than at the surface, a net up-estuary sediment transport is generated. Because the depth in the Ems River has increased, there is a greater difference in salinity at the bottom and the water surface and less friction. This leads to a greater up-estuary sediment transport (van Maren et al., 2015). Second, the tide encounters less resistance when the channels are deeper. This makes it easier for the tide to flow in and increases the horizontal tide, which also increases the upstream vertical tide. This can also be clearly seen in Figure B.12 (Taal et al., 2015). The larger tidal velocities lead to larger suspended sediment concentrations in the estuary due to higher friction. Thirdly, the channel deepening in the middle reaches of the Ems Dollart estuary has ensured that a lot of sedimentation takes place in the 'Bocht van Watum' and the system has changed from a two-channel system into a single-channel system. In a model study the effect of the changed bathymetry between 1985 and 2005 investigated (van Maren et al., 2015). The results of this study shows that this change in bathymetry has also an effect on the turbidity in different parts of the Ems Dollart estuary (Figure B.13).

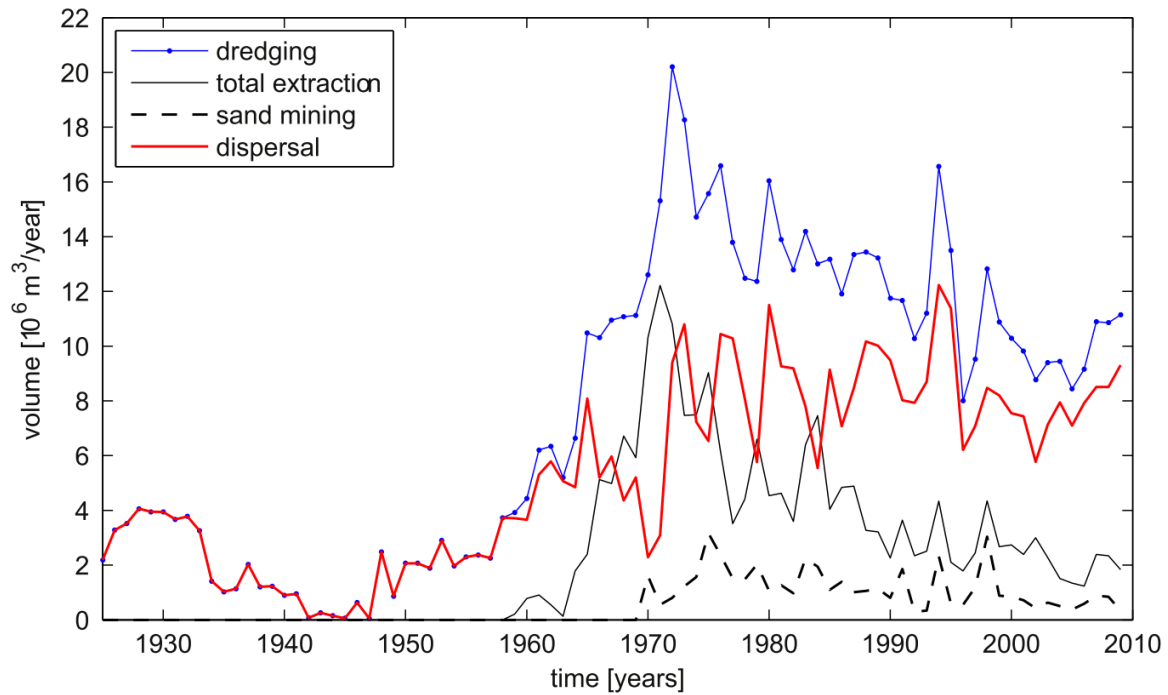


Figure B.11: Dredging volumes in the Ems Dollart estuary van Maren et al., 2015

B.4. managed realignment

B.4.1. The Medway Estuary

The Medway Estuary in Kent, UK is an example of a successful implementation of managed realignment in a muddy environment. Located in the southeast of England, the Medway Estuary is a tidal system with a large tidal range and a history of flooding and erosion. In the early 2000s, the UK government implemented a managed realignment project in the Medway Estuary to reduce the risk of flooding and erosion and restore valuable habitats such as salt marshes and mud flats (Clapp, 2009).

The Medway Estuary managed realignment project involved breaching and removing sea defenses, creating new tidal channels, and restoring existing habitats. The project was designed to create a wider and more natural coastal floodplain that could better absorb the energy of incoming waves and tides. The project also involved the restoration of salt marshes and mud flats, which provide important ecological and economic benefits.

The Medway Estuary managed realignment project has been highly successful in terms of both coastal protection and habitat restoration. The project has helped to reduce the risk of flooding and erosion in the area and has created a more natural and sustainable approach to coastal defense. The project has also contributed to the restoration and expansion of valuable habitats, such as salt marshes and mud flats, which provide important ecological and economic benefits. According to French (1999), it could be argued that the salt marshes behind the breached sites have been more resistant to natural erosion processes compared to the surrounding open salt marshes. This successful example demonstrates the effectiveness of managed realignment in creating more sustainable and dynamic coastal systems in muddy environments French, 1999.

B.4.2. The Hedwige-Prosper Polder

The Hedwige-Prosper Polder, located in the Scheldt estuary between the Netherlands and Belgium, is an ongoing managed realignment project that involves opening up parts of the area to the sea and creating new nature reserves. The area consists of the Dutch Hertogin Hedwige polder and the Northern part of the Belgian Hertog Prosper polder. With rising sea levels and the extension of the port of Antwerp, the project is a response to the increasing difficulty and expense of maintaining the old flood defenses (Hoven et al., 2021).

The project has not been without controversy, as some local residents and farmers have raised

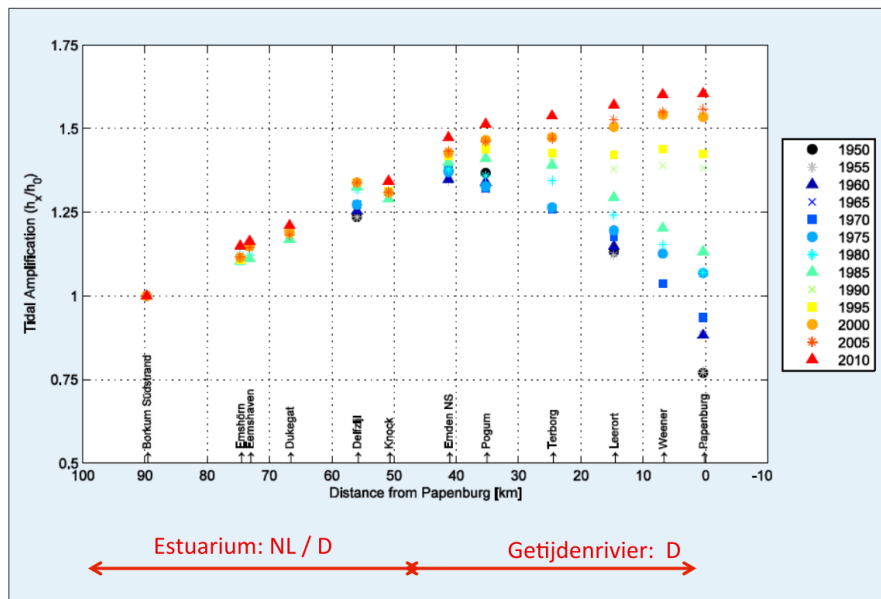


Figure B.12: Tidal amplitude changes in the Ems estuary and Ems River Taal et al., 2015

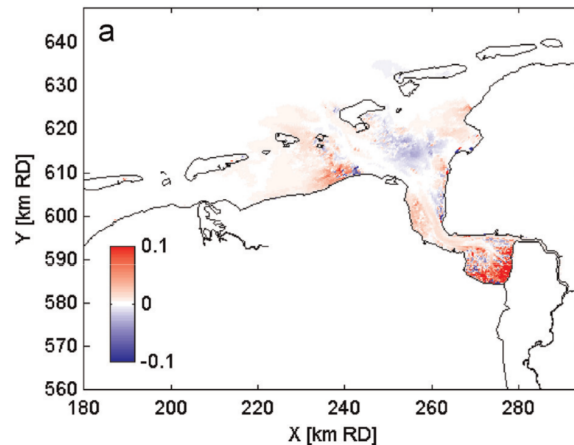


Figure B.13: Computed increase in suspended sediment concentration due to bottom changes between 1985 and 2005 (van Maren et al., 2015)

concerns about the impact on their land and livelihoods. Despite the opposition, the Dutch government has moved ahead with the plan, citing the need to protect the area from flooding and to comply with European Union regulations. The project involves the construction of a new dike to protect existing homes and infrastructure, while also allowing for controlled flooding of the new nature reserves. The flooded areas will act as natural barriers against rising sea levels, while also providing habitats for a range of plant and animal species.

The realignment of the polders involves lowering and breaching the old primary dikes along the Scheldt estuary and excavating creeks to facilitate tidal flow and stimulate saltmarsh restoration. The project aims to create a dynamic intertidal landscape with high ecological values and a natural flood protection function, which will benefit the local ecology, economy, and society. While the project is ongoing, initial reports suggest that it has been successful in achieving its goals, with new nature reserves attracting a variety of birds and other wildlife and managed flooding helping to mitigate the risks of flooding and sea level rise (van den Hoven et al., 2022).

B.5. Tidal flat and salt marsh morphodynamics

Tidal flats and salt marshes are coastal ecosystems that are highly influenced by the movement of water with the tides. Tidal flats are flat, shallow areas that are covered by water at high tide and exposed at low tide, and are typically found in areas with low wave energy and a large tidal range. Salt marshes are wetlands that are characterized by their salt-tolerant vegetation, which includes grasses, shrubs, and other plants that are adapted to survive in both wet and dry conditions. Both tidal flats and salt marshes are found in low-lying areas along the coast and are flooded and drained by the tide on a daily basis (Adam, 1993). These ecosystems provide a range of ecological and economic benefits, such as acting as a buffer against storms and coastal erosion and providing habitat for a diverse range of plants and animals.

Understanding the processes and factors that influence tidal flat and salt marsh morphodynamics is important for predicting and managing the changes that these ecosystems may undergo over time. This includes identifying potential impacts of human activities on these ecosystems and developing strategies to minimize those impacts and promote the health and resilience of these important coastal habitats.

Tidal flat morphodynamics are driven by several processes, including tidal flat accretion, settling lag, and tidal asymmetry. Tidal flat accretion refers to the process by which sediment is deposited and builds up on tidal flats, while settling lag is the delay in the settlement of sediment particles to the bottom of the tidal flat. Tidal asymmetry refers to the difference in the strength and duration of the tidal currents on the flood and ebb tides. These processes are described in more detail in Section 2.3.

Other factors that influence tidal flat and salt marsh morphodynamics include the presence of tidal channels, the influx of nutrients from nearby estuaries, and the impact of human activities such as land development and pollution. The flow of water and sediment in and out of the tidal flat and salt marsh can be affected by the presence of tidal channels, while the influx of nutrients can affect the growth and productivity of salt marsh vegetation. Human activities can also have a significant impact on these ecosystems, through activities such as land development, pollution, and the construction of coastal defenses.

One principle that can be taken into consideration in research aimed at promoting sedimentation is the following: sediment (especially mud) tends to move from areas of high energy to areas of low energy (Friedrichs, 2011). Waves create high energy in shallow areas, resulting in a net sediment flux towards deeper areas. Therefore, the formation of tidal flats and salt marshes is promoted in areas influenced by tides.

The morphodynamics of salt marshes, or the way in which they change and develop over time, are influenced by a variety of factors. One important factor is the movement of water with the rise and fall of the tide, which leads to daily flooding and draining of the marsh. The presence of vegetation can also have a significant impact on salt marsh morphodynamics. The vegetation first gives a positive feedback on the amount of sediment that is fixed in a salt marsh. Due to the presence of pioneer vegetation, the wave energy and current energy are dissipated. This creates an area with little energy which increases net sedimentation. This raises the bed level, allowing more types of vegetation to grow. Due to the elevation change, however, the area is flooded less frequently, until it is only inundated during spring tides, storm events or a combination of the two. As a result, less sediment is supplied and the net sedimentation decreases considerably (Brooks et al., 2021). On the other hand, a reduction of vegetation can lead to erosion and a lowering of the marsh surface (Temmerman et al., 2012). The rooted salt marsh plants can cause bumps that are difficult to erode. If the flow around such a bulge accelerates, extra erosion can also take place locally (Winterwerp et al., 2022). Erosion of the salt marshes causes mud flats to disappear as well. This is clarified in Figure B.14. Erosion causes the tidal flats to lose their convex-up shape, resulting in a smaller surface area between the tidal range, while that is precisely the elevation that has the highest ecological value and where the most biomass is located (Mu and Wilcove, 2020; Zhou et al., 2022).

Other factors that influence salt marsh morphodynamics include the availability of sediment and nutrients, sea level changes, and the intensity and frequency of storms. The high availability of nutrients in channels leads to a relative rapid growth of vegetation along channels and therefore also in sedimentation (D'Alpaos et al., 2007). On the other hand, the growth of salt marsh vegetation also contributes to the formation of a channel network. The formation of this channel network involves not only the salt marshes, but also the mudflats and the rest of the intertidal area (Kearney and Fagherazzi, 2016). The formation of a salt marsh area along the edge of the intertidal zone therefore contributes to a dynamic

and varied ecosystem (Cox et al., 2006).

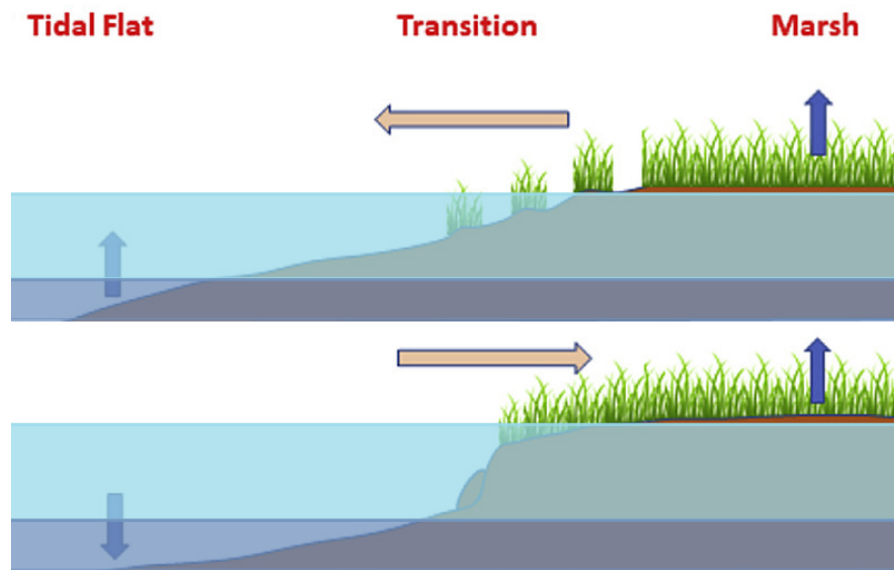
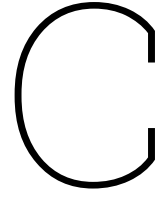


Figure B.14: An tidal flat – saltmarsh system is accreting (upper figure) or retreating (lower figure). The retreating salt marshes shows also lower and less tidal flats. They lose their convex-up shape, resulting in a smaller surface area between the tidal range, while that is precisely the elevation that has the highest ecological value and where the most biomass is located. (Reed et al., 2018)



Calibration findings

This appendix presents the findings of the calibration process for Delft3D, the numerical model used in this study. The key parameters considered include settling velocity, critical shear stress, erosion parameter, and the consideration to use one or two sediment fractions. The results of the calibration process are discussed in detail, with a focus on how they were determined and their implications for the overall modeling approach. Additionally, the limitations and uncertainties associated with the calibrated parameters are also discussed.

C.1. Settling velocity

The settling velocity, denoted by w_s , is a crucial calibration parameter. It has a direct impact on the volume of sediment that accumulates in an area. The deposition flux is described by Equation 2.1, and as shown in Figure 4.2, there is a linear relationship between the deposition flux and the settling velocity. This means that an increase in the settling velocity leads to an increase in total sedimentation. However, a higher settling velocity also results in more sediment settling near the entrance, which in turn leads to less sediment reaching the back of the polder.

The different iterations during the calibration phase show that the accuracy of the numerical model simulations constantly improves at a lower settling velocity. By making the settling velocity smaller, it always takes longer before the sediment settles, which means that even with the low dynamics of Polder Breebaart, the dispersal of the incoming sediment is more successful. The best results are obtained with higher SSC values on the boundary and extremely low settling velocities. Because this only showed better results very slowly, it required higher SSC values and such a low settling velocity is no longer realistic, the lowest realistic value is assumed for the settling velocity. The settling velocity used in the application model is $w_s = 0.0001m/s$, or $0.1mm/s$.

C.2. Critical shear stress

As previously mentioned in Section 2.5.8, the critical shear stress is a key parameter whose magnitude is determined in the calibration of the model. Equation 2.2 and Figure 4.2 demonstrate that the critical shear stress plays a significant role in determining the amount of erosion that takes place and greatly influences the resulting sediment flux. The critical shear stress establishes the threshold for excess bed shear stress, erosion only begins when the shear stress exceeds this critical value. The erosion flux is therefore inversely dependent on the critical shear stress.

Increasing the critical shear stress reduces the erosion flux. In the iterations before waves were added, this value had to be extremely low to not just generate deposition. After wind-generated waves were added, this parameter could be set higher, but a higher critical shear stress always causes the location where most accumulation takes place to shift towards the entrance of the polder. With this parameter is mainly the distribution between the front and the back influenced, more then the channel-flat distribution. With the calibration model is determined that the critical shear stress used in the application model is $T_{cr} = 0.21Pa$.

C.3. Erosion Parameter

Another important calibration parameter is the Erosion parameter M . Similar to the critical shear stress, the erosion parameter affects the erosion flux. However, unlike the critical shear stress, the erosion parameter has a linear positive relationship with the erosion flux. The erosion parameter scales all erosion that takes place, and therefore plays a significant role in determining the size of the erosion flux, which can quickly surpass the deposition flux.

By sliding with both the critical shear stress and the erosion parameter, a balance must be found. By also playing with parameter f_{tauw} , this equilibrium is determined in such a way that there is an equilibrium. This parameter both influences the distribution between the front and the back as between the channel and the flat. With the calibration model is determined that the Erosion parameter used in the application model is $M = 0.00025$.

C.4. Wave-stirring parameter

During the calibration, it is determined that when accounting for the shear stress generated by wind waves, the generated shear stresses, especially in shallower areas, were excessively high and resulted in excessive erosion. This led to the conclusion that the shear stresses caused by wind waves has an disproportionately large impact on the total shear stresses. To address this, a parameter was introduced to limit the contribution of wave shear stress to the total shear stress. This is particularly effective in shallower areas, where the shear stress caused by flow is significantly smaller in comparison to that caused by waves.

This parameter scales with forcing instead of in the Erosion-Deposition models. This parameter scales the influence of the wave-generated bed shear stress. Because the wave-generated bed shear stress, in contrast to the current-induced bed shear stress, has the greatest influence on the shallow parts, this allows scaling between the occurring bed shear stresses on the shallow parts and the channels. This mainly affects the distribution between these two parts. With the calibration model it is determined that this parameter used in the application model is $f_{tauw} = 0.185$.

C.5. One or two sediment fractions

During the research, the idea arose to work with two different sediment fractions. This idea stems from the fact that consolidated mud has a different critical shear stress τ_{cr} than unconsolidated mud. The critical shear stress is defined as the shear, stress value when the sediment starts to erode from the mud bed. When the mud is deposited for a longer time, the mud will consolidate more and more. With the consolidation of the mud, some of its sediment properties starts to improve. One of these improved properties is a higher resistance to erosion (Berlamont et al., 1993b).

By giving one sediment fraction in the numerical model the parameters of the consolidated mud and another sediment fraction the parameters of the suspended mud an attempt has been made to approach reality better. The idea is to create an base bed layer which is more difficult to erode than the new deposited sediment. The deposition of the new sediment will be on top of the stronger sediment in the model and should not be affected by the stronger (more consolidated) layer below. The stronger base bed layer ensures that erosion compared to the starting bathymetry only occurs in places with structurally high shear stresses.

The model is set up with an initial bottom thickness of 1 meter, consisting exclusively of the sediment fraction with the bigger critical shear stress ($\tau_{cr,bed} = 15Pa$). On the tidal boundary, on the other hand, only the other sediment fraction has been applied to the sediment concentration ($C = 0.2kg/m^3$, this sediment fraction is given a much lower critical shear stress ($\tau_{cr,susp} = 0.15Pa$). Other sediment parameters are kept the same ($M = 0.0001$, $w_s = 0.0001m/s$, $\rho_s = 2650kg/m^3$ and $\rho_b = 500kg/m^3$).

In order to properly map out the elaboration of these model settings, two control model simulations were performed to compare the model results. Both control simulations contained only one of the sediment fractions of the model which is tested here. Both control model simulations contained a initial thickness of 0, a boundary concentration value of $C = 0.2kg/m^3$ and both control model simulations has further the same settings as the tested model.

The model performed a one-month simulation. From the results of this simulation it becomes clear that the model does not function as designed. The results of the three model simulations can be seen in fig C.1. In the left-hand result, it was the intention to create a stronger base layer (with a larger τ_{cr})

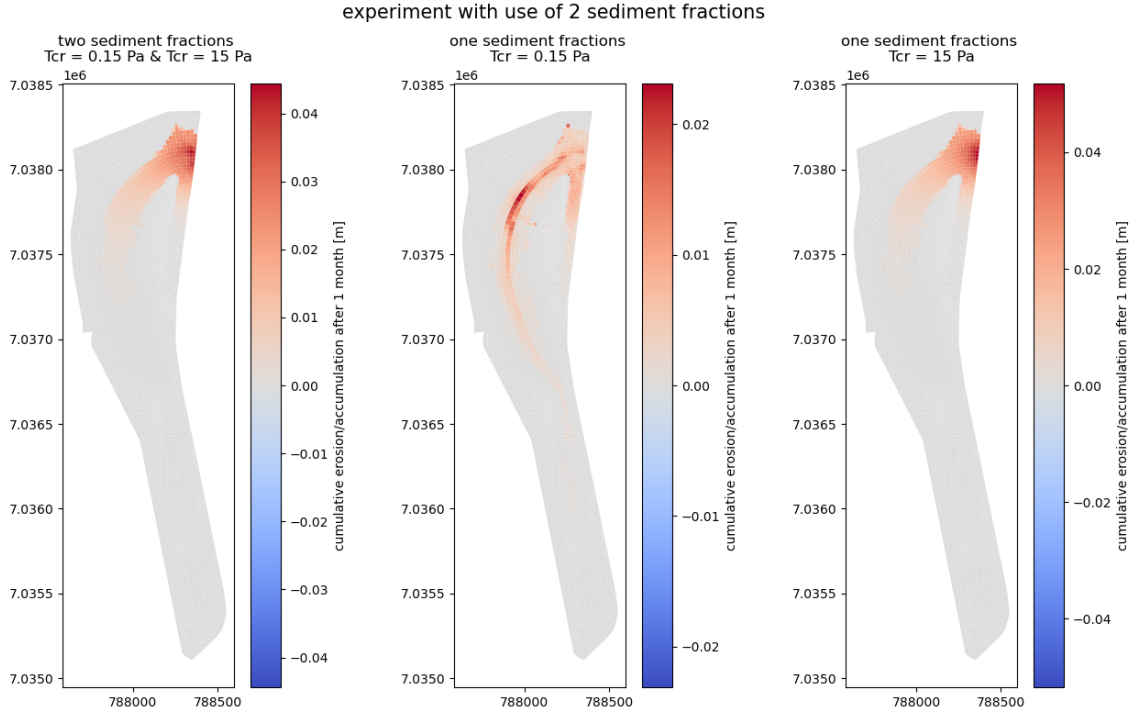


Figure C.1: model results after 1 month with 2 sediment fractions (left) and with both sediment fractions separately

where on top of it, the weaker suspended sediment (with a smaller τ_{cr}) could settle. In that case, the result should look a bit like the result in the middle, where the same weak suspended sediment is used. Contrary to this intended result, the left result is very similar to the right result. In both the left and right situations almost no re-suspension occurs. This is intended in the right-hand result, where the suspended sediment has been given a high critical shear stress with the aim that little erosion takes place and in particular the sedimentation is visible after an initial settlement. But in the left map is the 'weak' suspended sediment used.

The model produces these result due to it uses only one sediment layer. This ensures that the sediment which is settled, perfectly mixes with the sediment that is already present in the bed layer. The 4 centimeter of settled sediment with $\tau_{cr,susp} = 0.15$ is therefore perfectly mixed with the 1 meter of sediment with $\tau_{cr,bed} = 15$ which is already present in the bed. Due to this mixing, it is almost impossible to re-suspend due to high shear stresses. Therefore there will not be made use of two sediment fractions.

C.6. Breaker index

By adding wind waves it is important to take into account the maximum wave height in relation to the water depth. When the wave height exceeds a certain factor times the water depth, the wave breaks. This factor is called the Breaker index γ_b . This parameter is first used to scale the wave effect, but later this is done with the ftauw-parameter instead of the breaker index. This is less important therefore.

$$\gamma_b = \frac{H_b}{h_b} \quad (C.1)$$

This process of wave breaking plays an important role for the morphodynamics because the this breaker index limits the occurring wave heights, especially on the shallow parts of the area. By limiting the occurring wave heights, the wave-induced bed shear stress is also limited. As determined, this wave induced bed shear stress has a major influence on the re-suspension of the sediment and distribution over all the parts of the area. It is therefore important that this parameter is determined accurately.

In Figure C.2 are the maximum occurring wave height divided by water depth's visualised. The maximum occurring wave heights in every map are larger than the breaker index γ_b . This is because

the breaker index puts a limit on the root mean square wave height H_{RMS} , which is approximately equal to the significant wave height H_s divided by 1.4. The different maps of Figure C.2 clearly show that the relative wave height decreases, especially in the shallower parts of the area when the γ_b is reduced. This is because the fetch length is not long enough to develop larger waves in the area.

Figure C.3 shows the occurring bed shear stresses for the same varying breaker indexes γ_b as in figure C.2. Here you can clearly see the effect of the waves on the bed shear stresses. In the same grid cells with a high relative wave height, a high shear stress can also be seen.

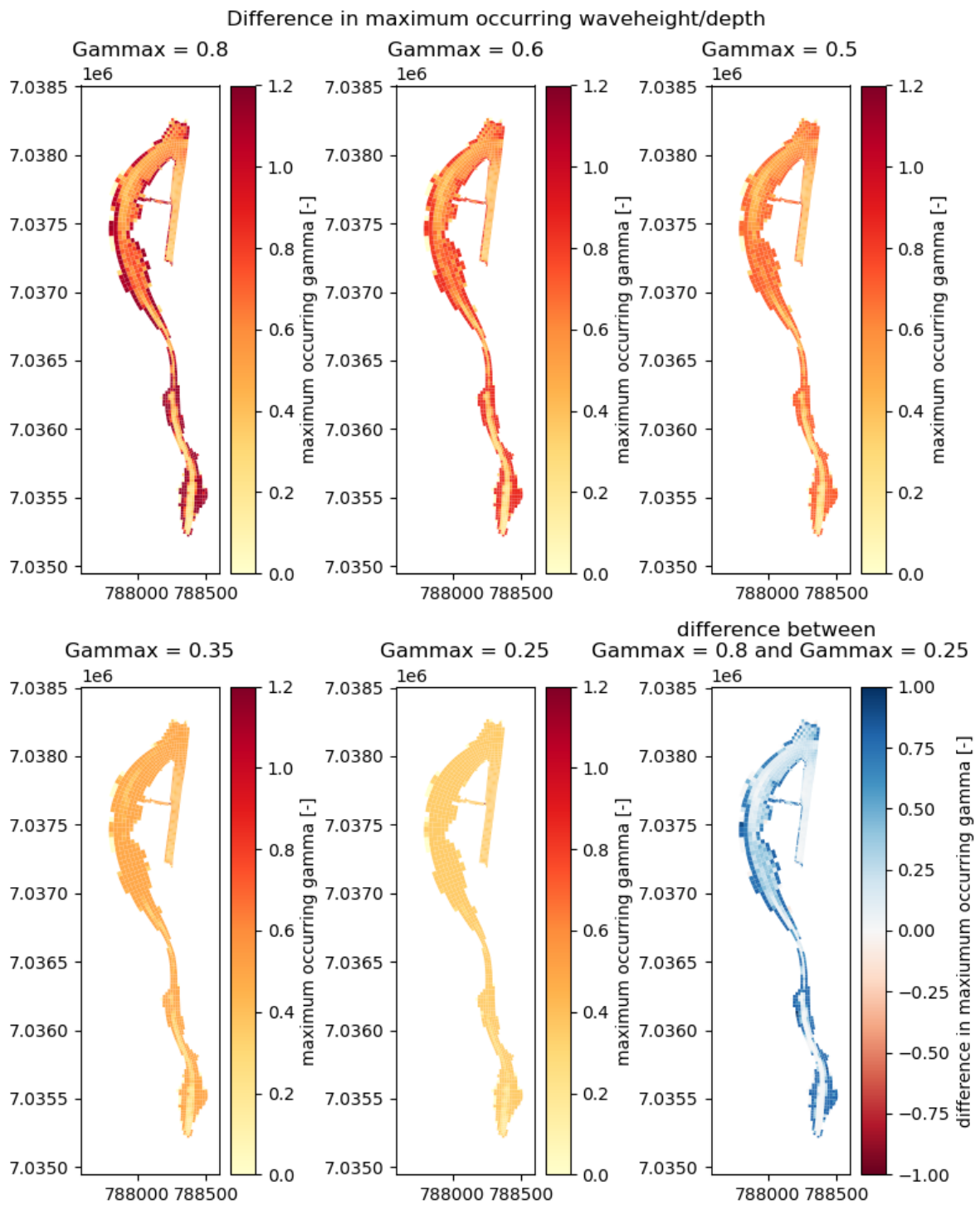


Figure C.2: Occurring wave height/water depth ratios with different γ_b 's.

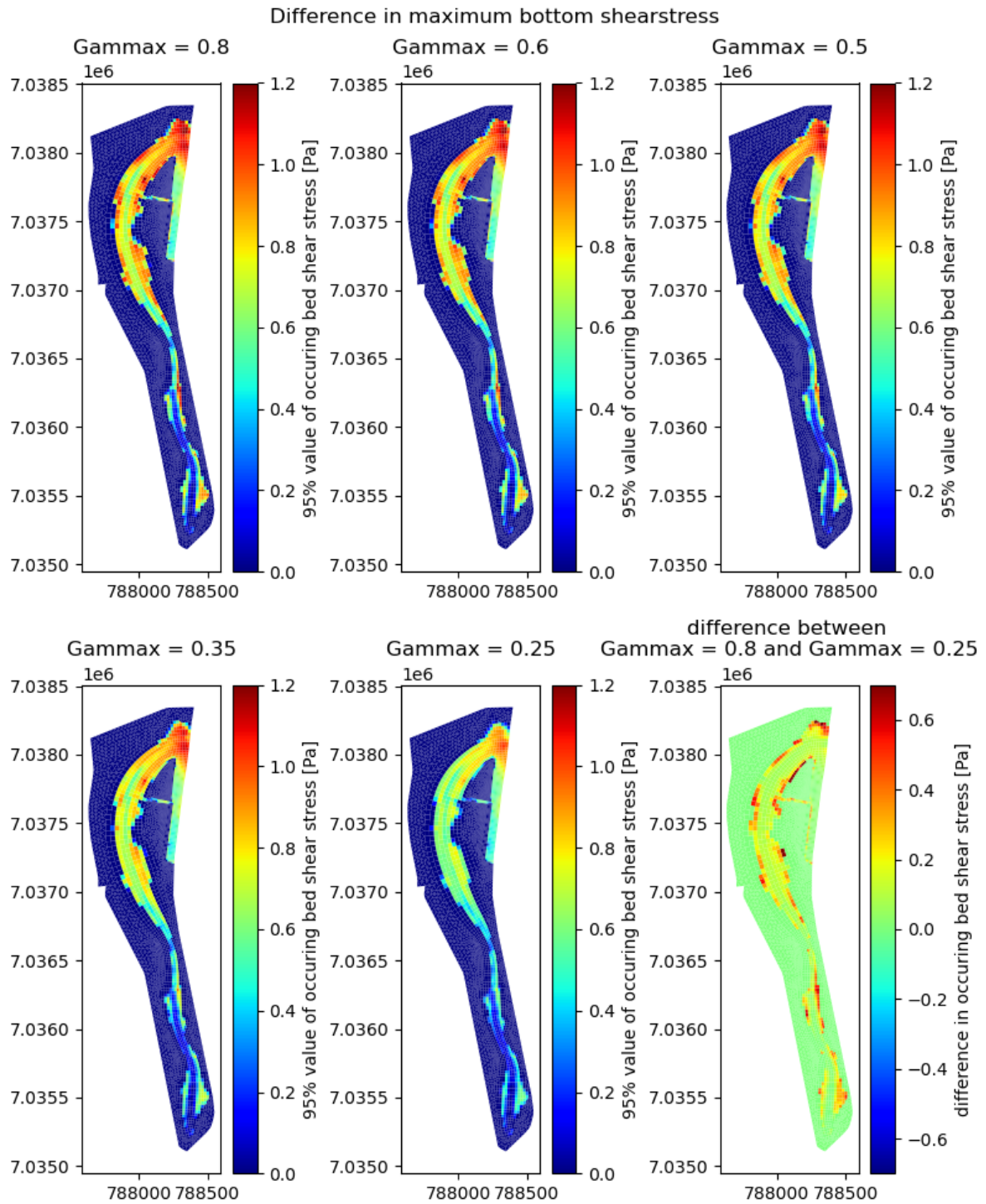


Figure C.3: Occurring 95% value of bed shear stresses with different γ_b 's.

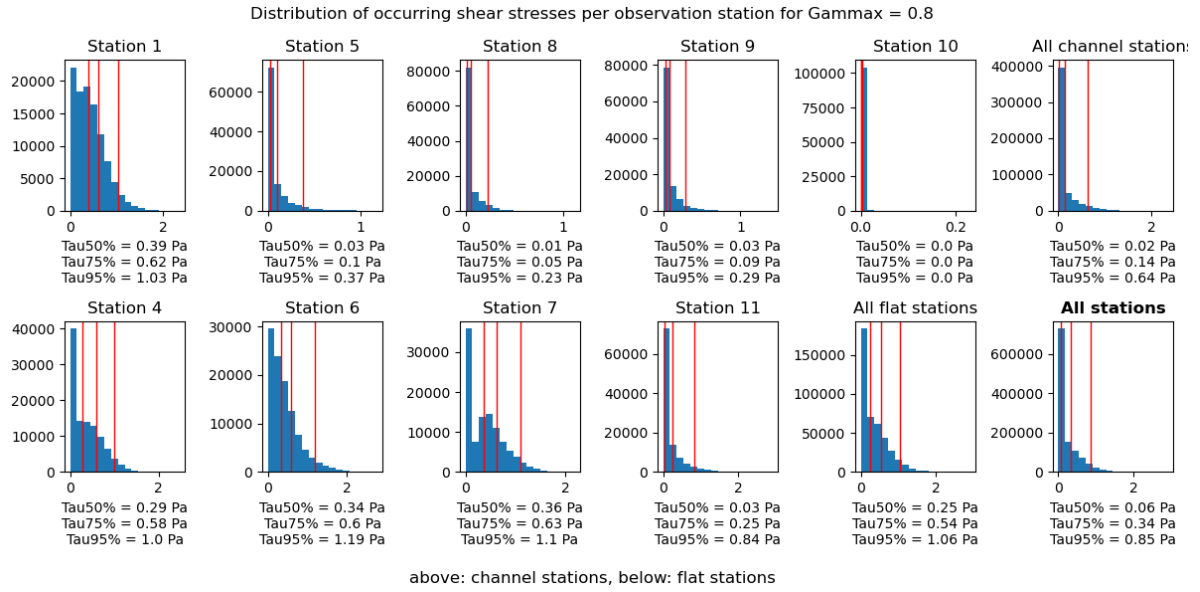


Figure C.4: Distribution of occurring bottom shear stresses with $\gamma_b = 0.8$.

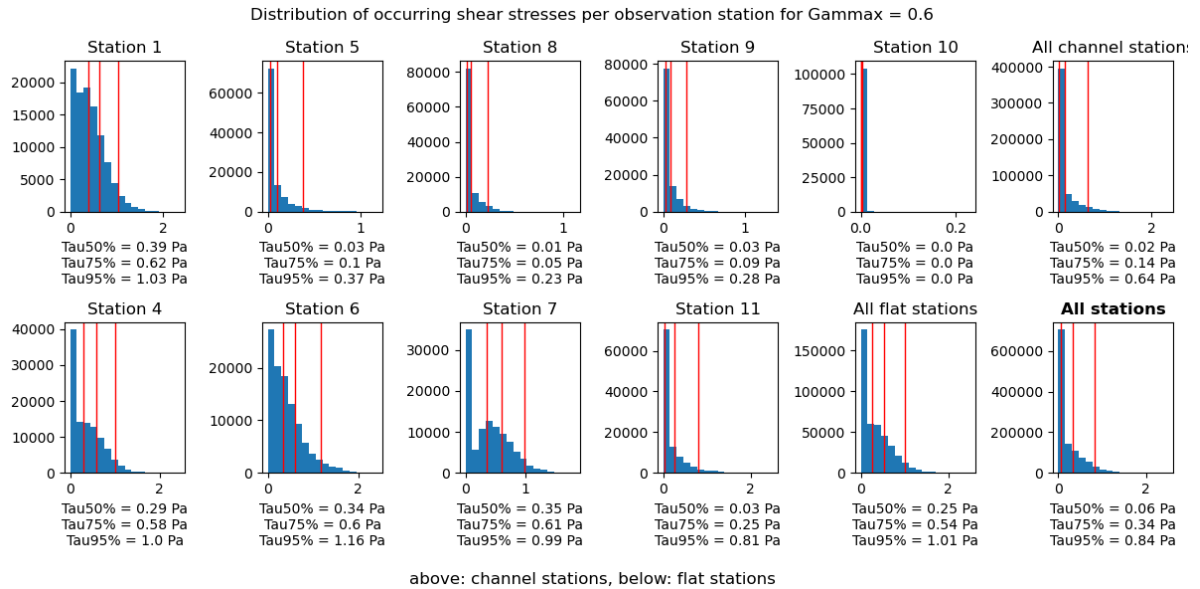


Figure C.5: Distribution of occurring bottom shear stresses with $\gamma_b = 0.6$.

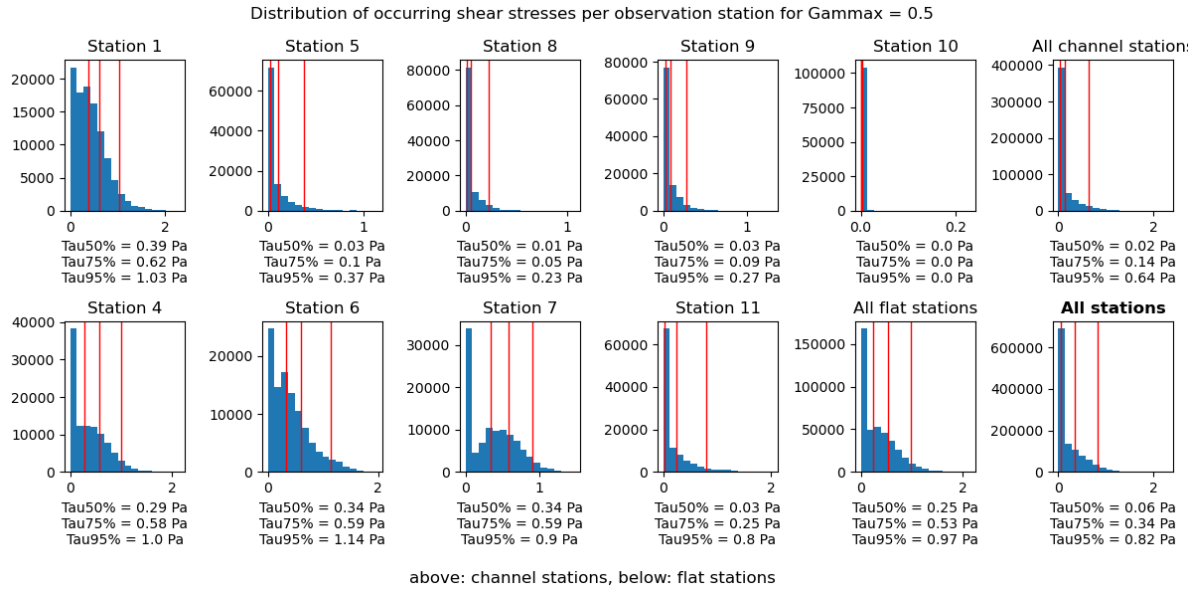


Figure C.6: Distribution of occurring bottom shear stresses with $\gamma_b = 0.5$.

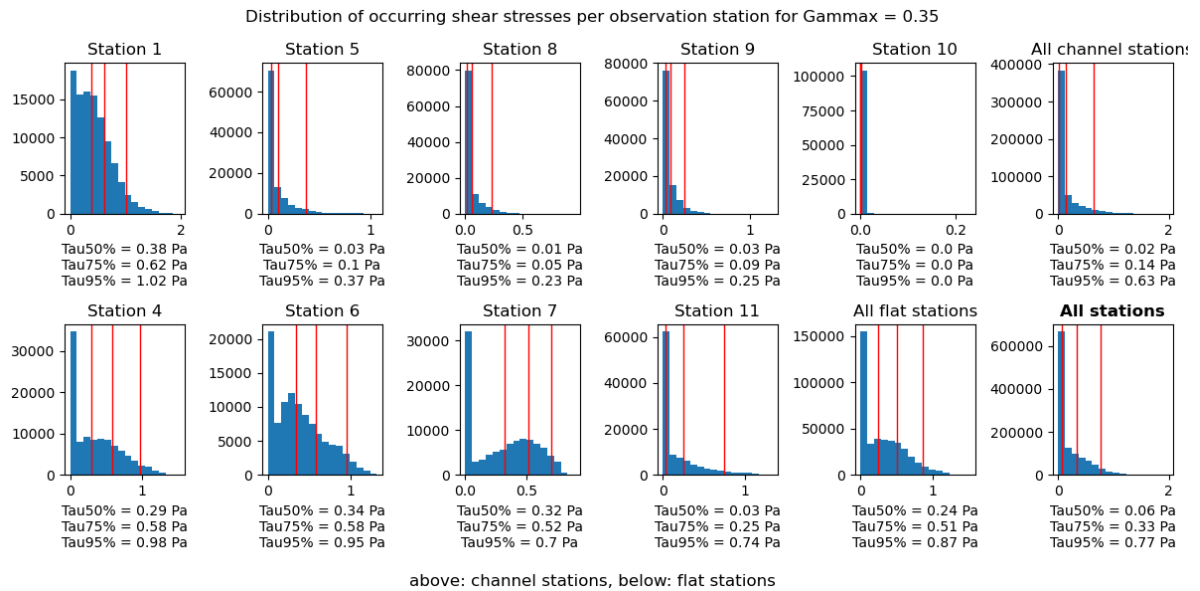


Figure C.7: Distribution of occurring bottom shear stresses with $\gamma_b = 0.35$.

D

Model results project area

Of all scenario results, the accumulation, the mean SSC values, the 83.3 percentile of occurring bed shear stresses (i.e. one hour a day on average) and the 95.8 percentile of occurring bed shear stresses (i.e. 4 hours a day on average) are shown (Figure D.1, Figure D.2, Figure D.3 and Figure D.4). Subsequently, the results of the simulations are shown without waves and with extra wave effect (Figure D.5, Figure D.6 and Figure D.7). Finally, a number of scenarios have been displayed opposite each other to clearly display differences.

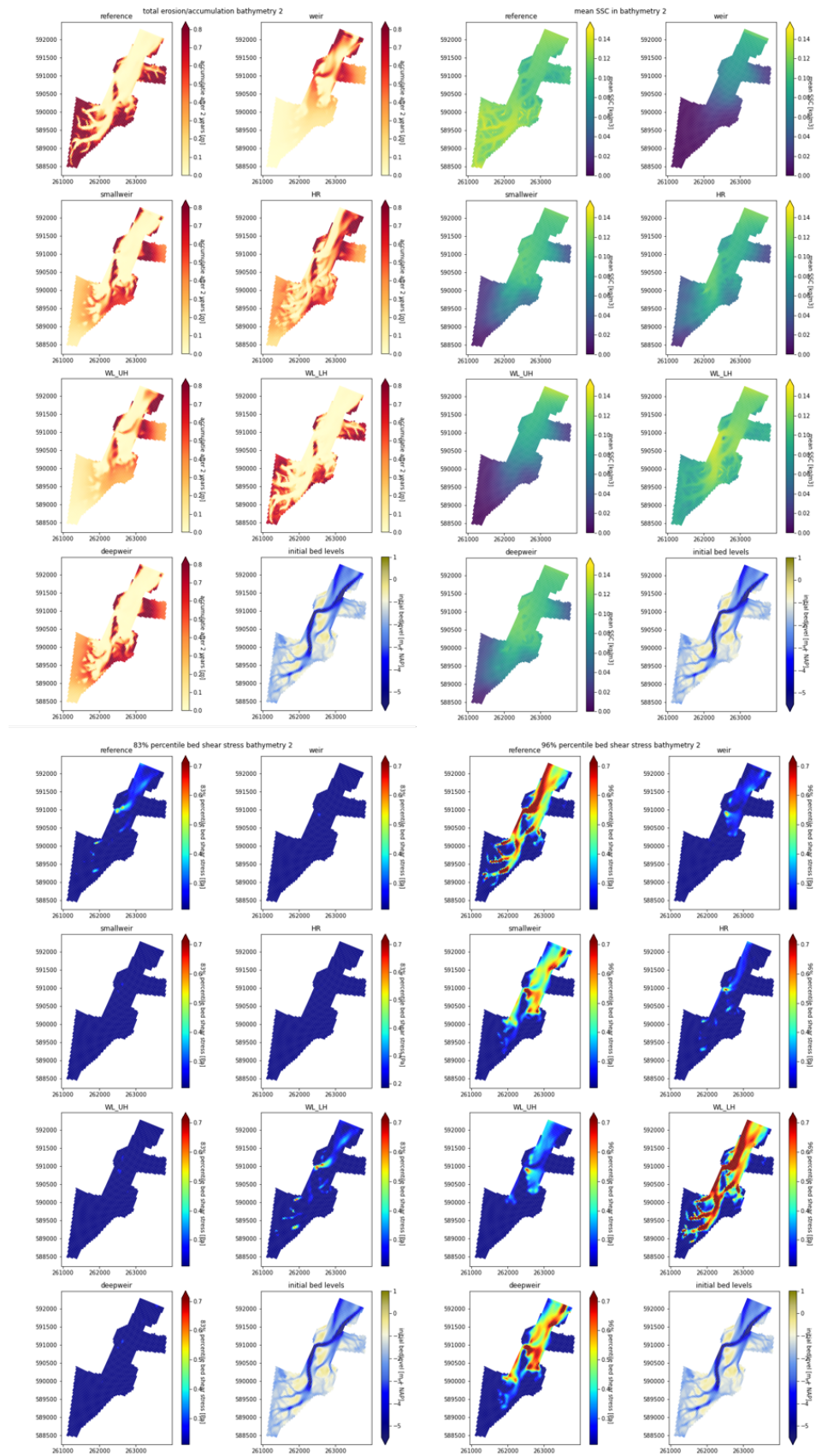


Figure D.1: Model results of all scenarios with bathymetry 2. Upper left: accumulation after two year. Upper right: mean SSC. Lower left: 83.3 percentile of occurring bed shear stresses. Lower right: 95.8 percentile of occurring bed shear stresses.

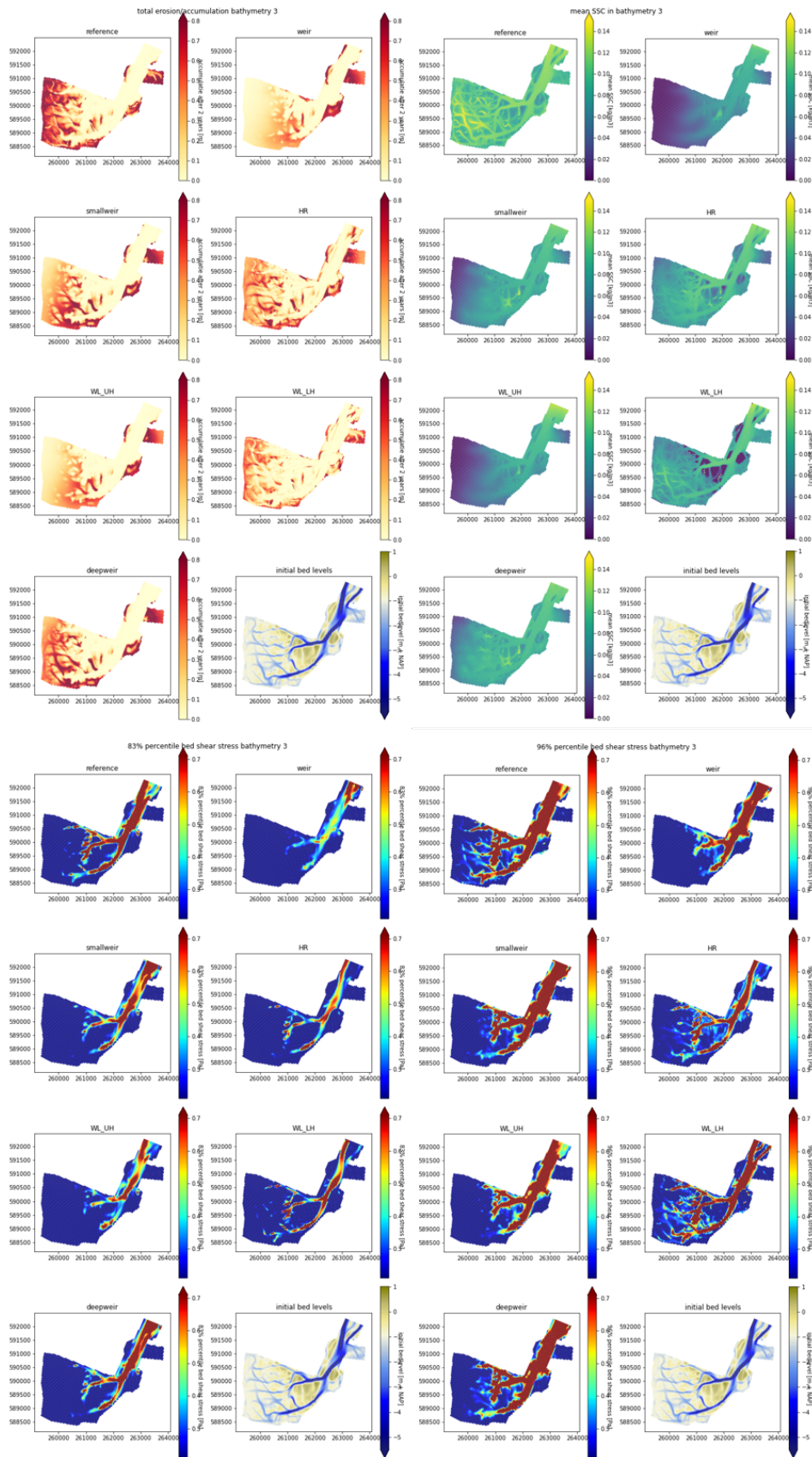


Figure D.2: Model results of all scenarios with bathymetry 3. Upper left: accumulation after two year. Upper right: mean SSC. Lower left: 83.3 percentile of occurring bed shear stresses. Lower right: 95.8 percentile of occurring bed shear stresses.

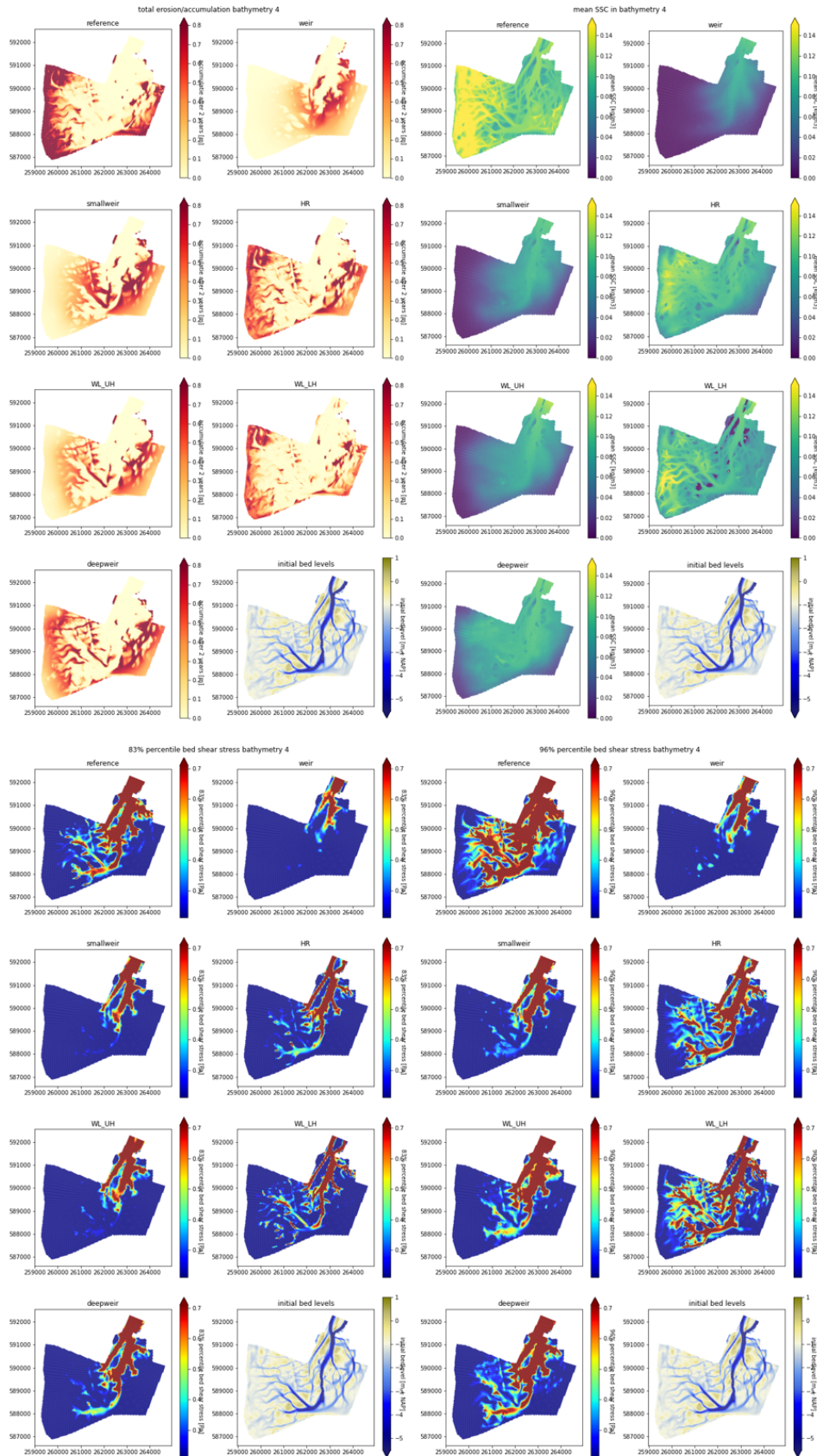


Figure D.3: Model results of all scenarios with bathymetry 4. Upper left: accumulation after two year. Upper right: mean SSC. Lower left: 83.3 percentile of occurring bed shear stresses. Lower right: 95.8 percentile of occurring bed shear stresses.

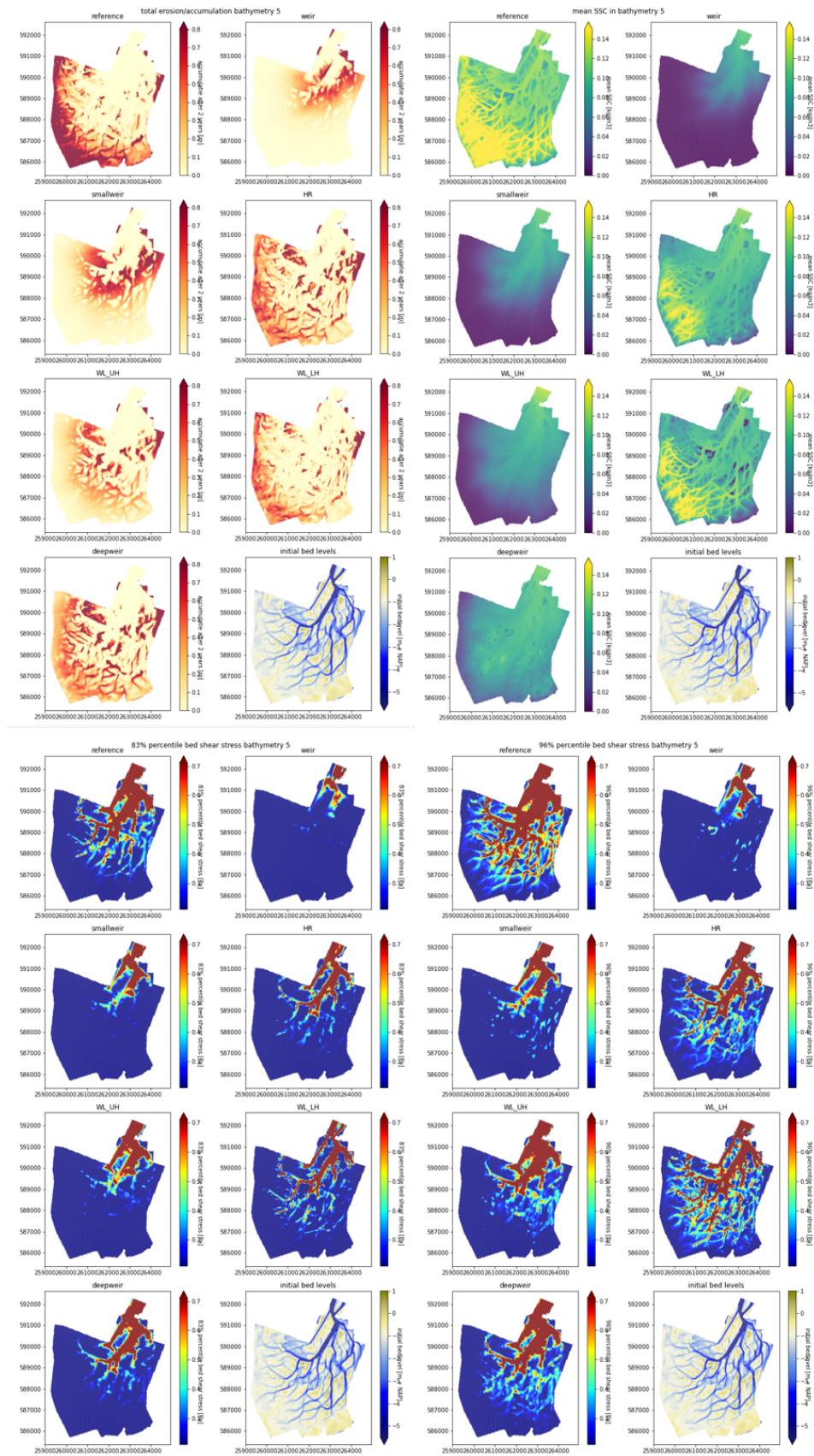


Figure D.4: Model results of all scenarios with bathymetry 5. Upper left: accumulation after two year. Upper right: mean SSC. Lower left: 83.3 percentile of occurring bed shear stresses. Lower right: 95.8 percentile of occurring bed shear stresses.

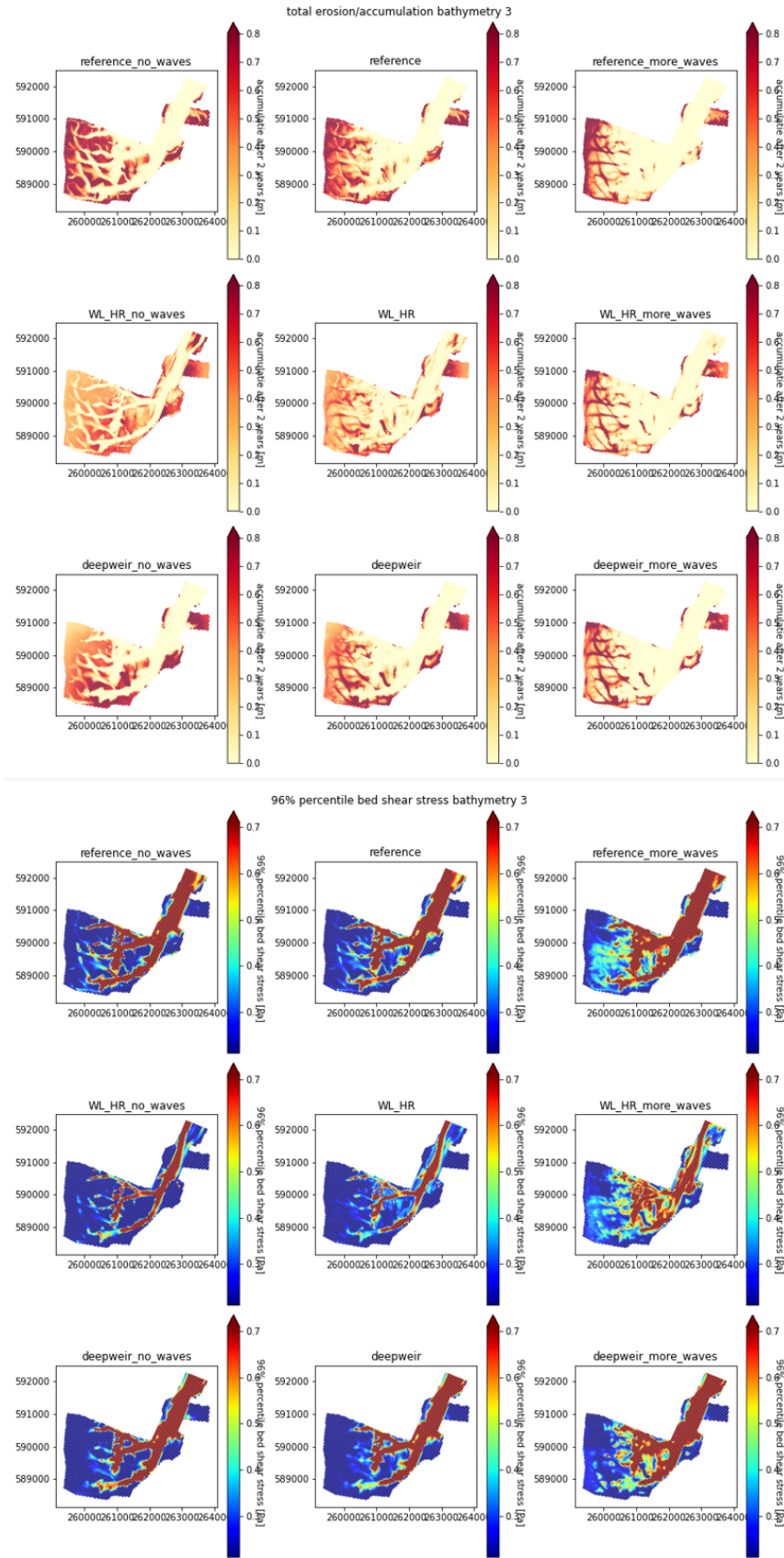


Figure D.5: Model results of the wave effect on scenarios 'reference' (upper), 'half range' (middle) and 'deepweir' (lower) in bathymetry 3. Upper three: accumulation after two year. lower three: 95.8 percentile of occurring bed shear stresses.

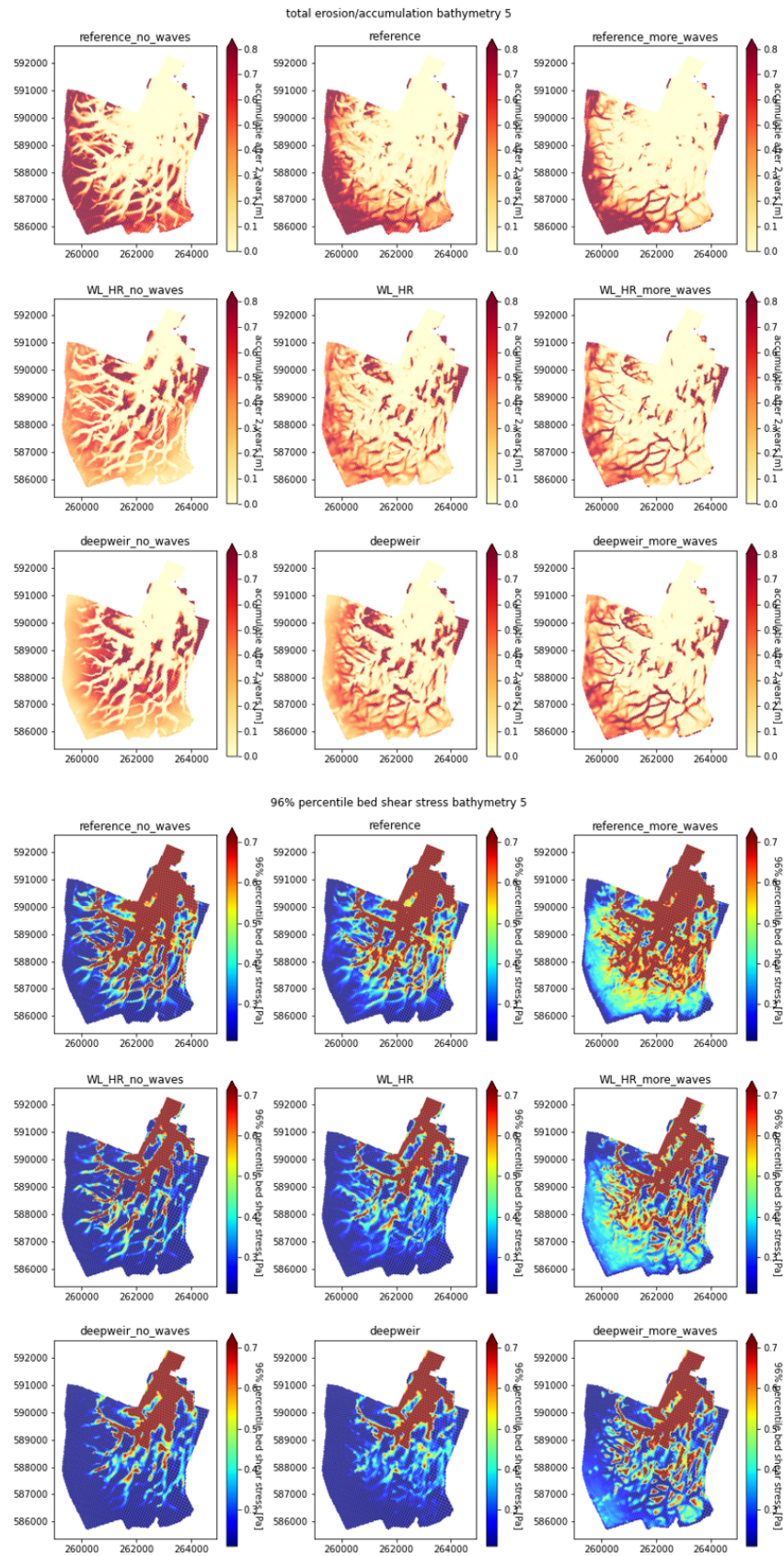


Figure D.6: Model results of the wave effect on scenarios 'reference' (upper), 'half range' (middle) and 'deepweir' (lower) in bathymetry 5. Upper three: accumulation after two year. lower three: 95.8 percentile of occurring bed shear stresses.

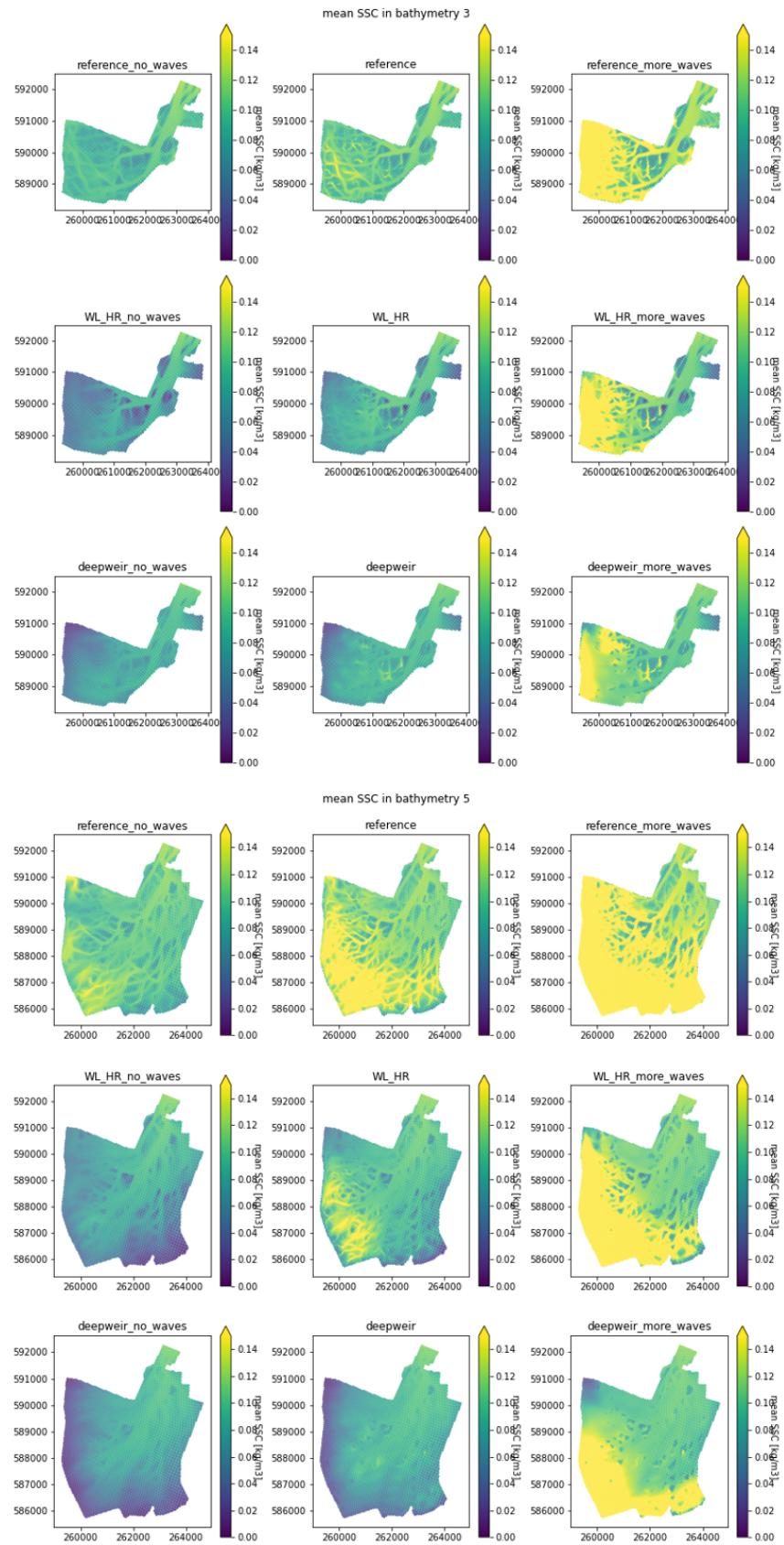


Figure D.7: Mean SSC results of the wave effect on scenarios 'reference' (upper), 'half range' (middle) and 'deepweir' (lower) in bathymetry 3 (upper three) and bathymetry 5 (lower three).

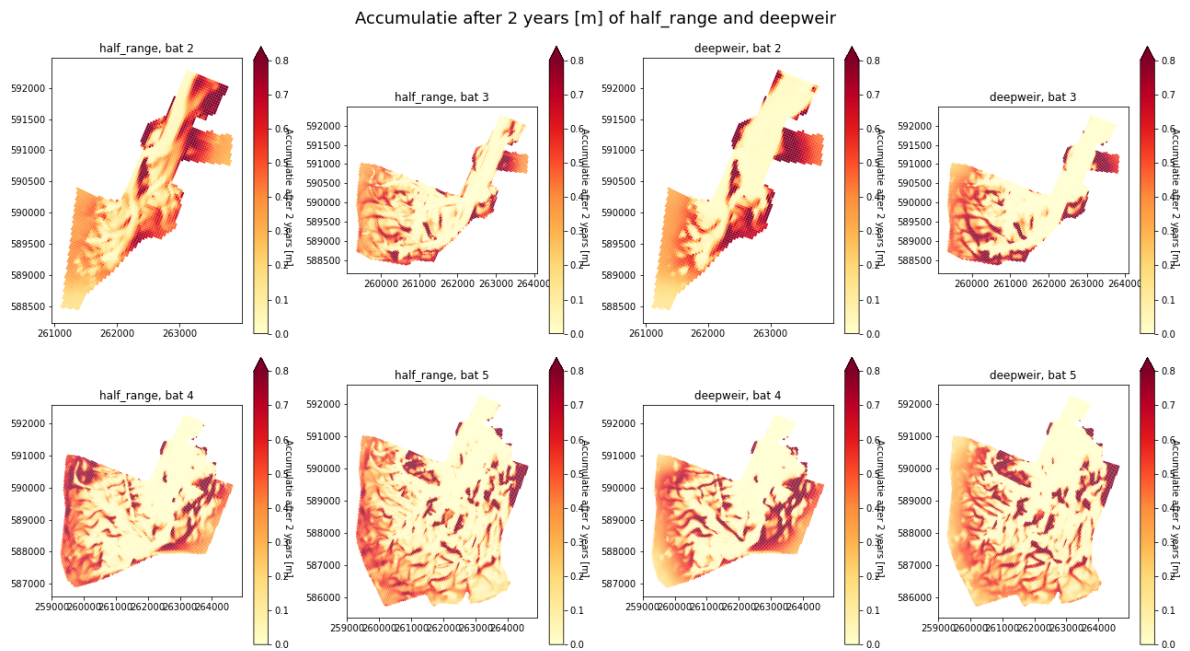


Figure D.8: The accumulation of the scenarios 'half range' (left four) and 'deepweir' (right four). The results are quite similar when speaking of accumulation distribution, particularly for Bat4 and Bat5.

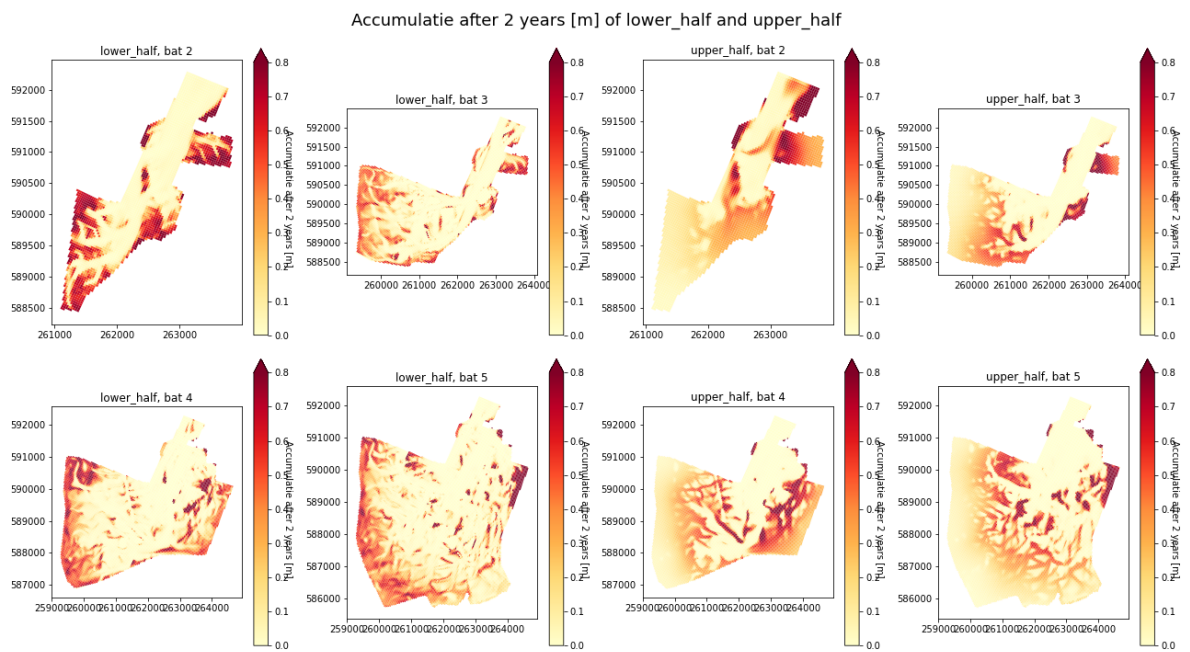


Figure D.9: The accumulation of the scenarios 'lower half' (left four) and 'upper half' (right four). The results are completely different when speaking of accumulation distribution. In 'lower half' the sediment is transported much further into the polder and the channels are 'flushed'. In 'upper half' the accumulation takes place less deeply in the polder and mainly in the channels.

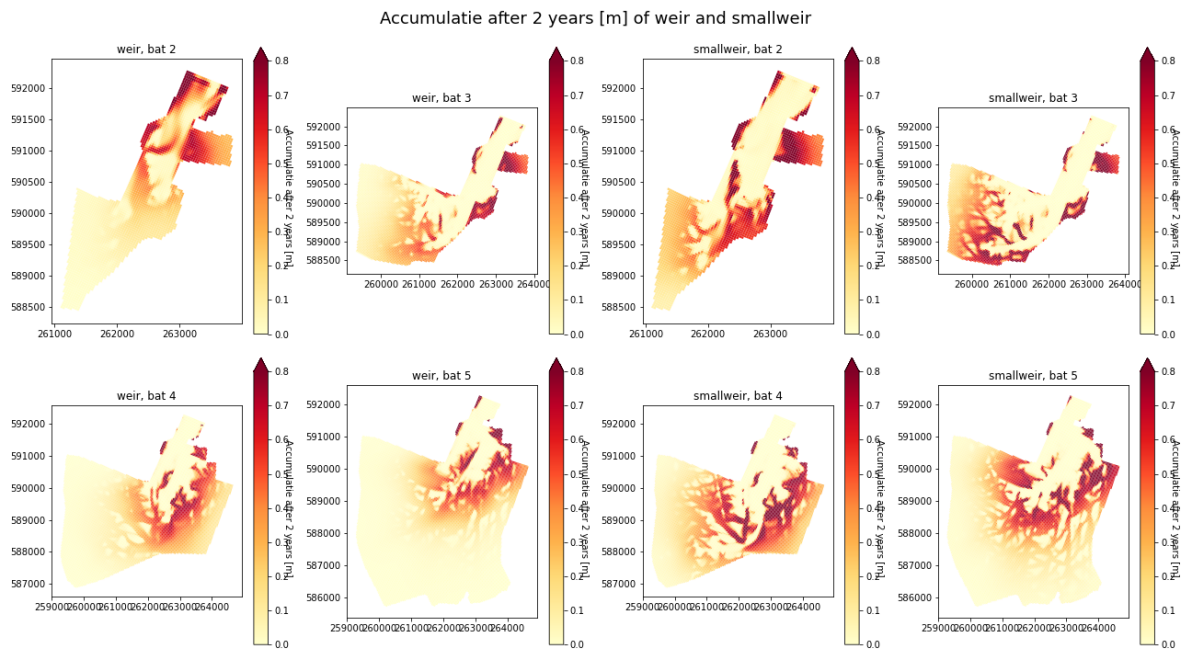


Figure D.10: The accumulation of the scenarios 'weir' (left four) and 'smallweir' (right four). Both results of the accumulation distribution show that most of the accumulation occurs too close to the entrance. Only the results of 'smallweir' for Bat2 and Bat3 show good results.

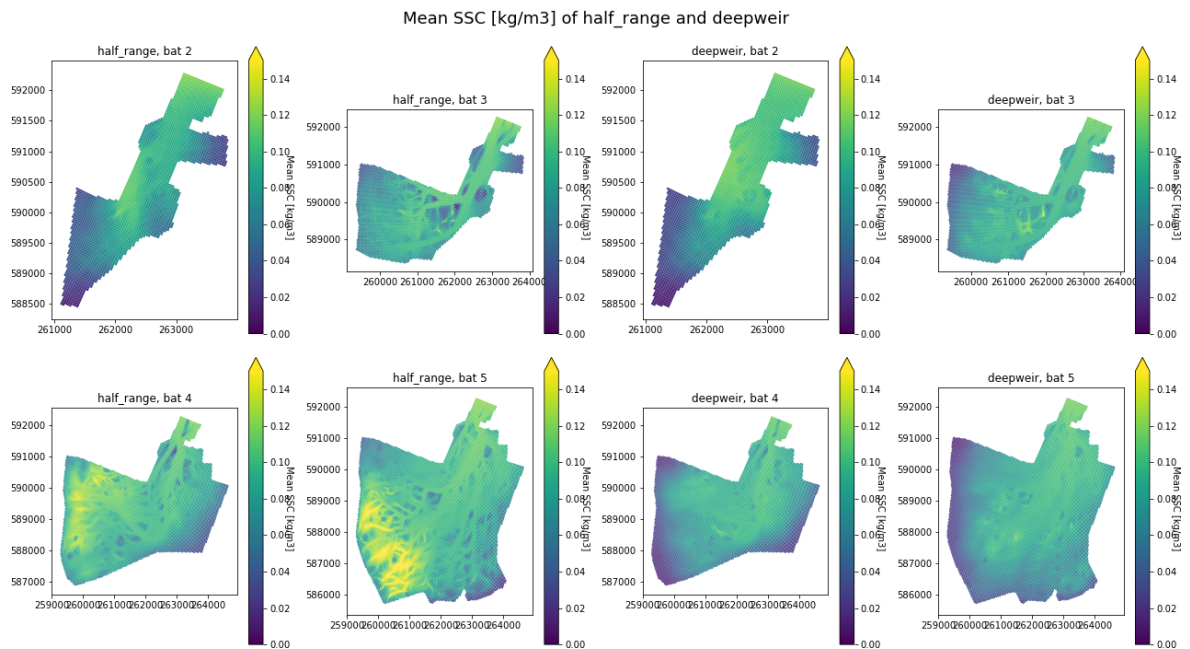


Figure D.11: In contrast to the accumulation of 'half range' and 'deepweir', the maps with mean SSC values do not match each other. The mean SSC of the scenarios 'half range' (left four) and 'deepweir' (right four) show some differences. 'Half range' shows higher SSC in particularly the channels, while the distribution in scenario 'deep weir' has a more equal SSC field. This is explainable by the higher mean water level in the area for 'deepweir'.

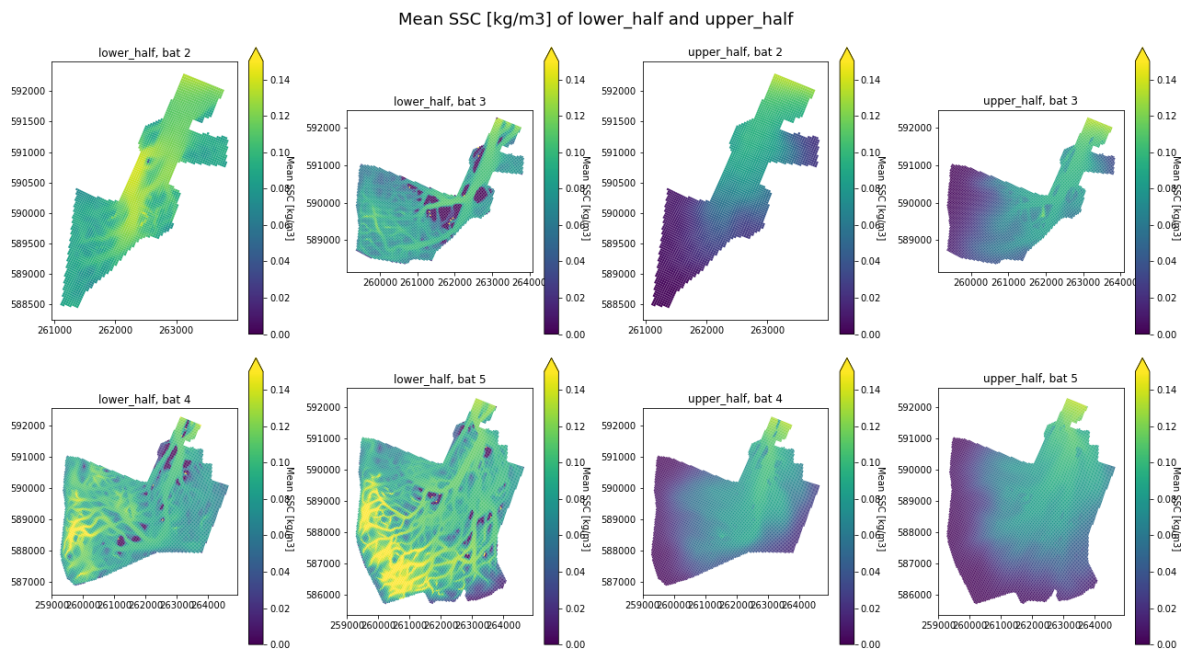


Figure D.12: The mean SSC of the scenarios 'lower half' (left four) and 'upper half' (right four). In the results it is clear that high SSC values are at same areas as high accumulation (Figure D.9). 'Lower half' shows higher SSC values especially in the channels, which supports the conclusion that high flow velocities (with high shear stresses) occur in the channels.

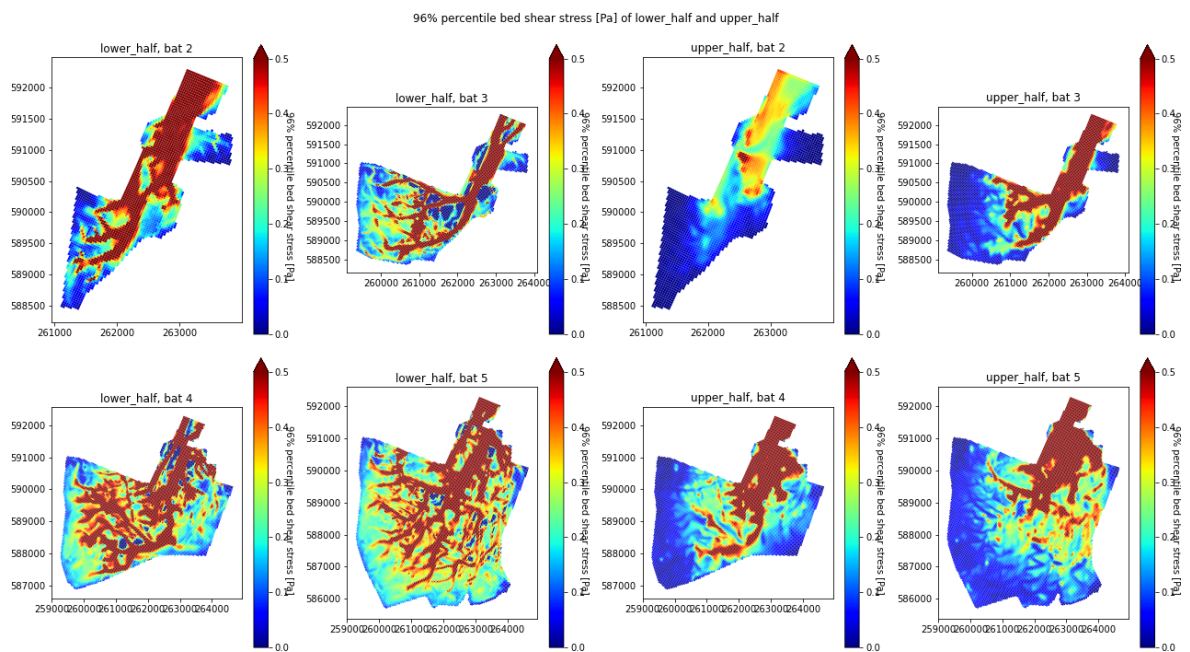
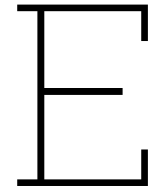


Figure D.13: The occurring bed shear stresses of the scenarios 'lower half' (left four) and 'upper half' (right four) are completely different, but in line with the accumulation and mean SSC of these scenarios. In the results it is clear that higher bed shear stresses occur in deeper parts of the polder for 'lower half', while close to the entrance on the tidal flats 'upper half' generates higher bed shear stresses.



SSC measuring stations

This appendix contains an overview map of the measurement stations of the SSC in the Eems Dollard. This overview map can be seen in Figure E.1. In this figure, the top two images show the location of the Eems Dollard within the Netherlands, together with two salt measurement stations (BC) and a wave measurement station (SON). At the bottom figure is an overview of all measuring points with the suspended sediment concentration measuring stations in yellow. In green are the water level measurement stations shown, of which WL3 (near Delfzijl) has been used as a time series for the tides on the open boundary in the application phase of the research. Current velocity observation points are indicated in red and Eems kilometers are indicated in blue, this is a standard reference in the Ems river (van Maren et al., 2015).

Figure E.2 shows the calculated annual average sediment concentration in the estuary in 2012 (van Maren et al., 2016).

van Maren et al., 2016

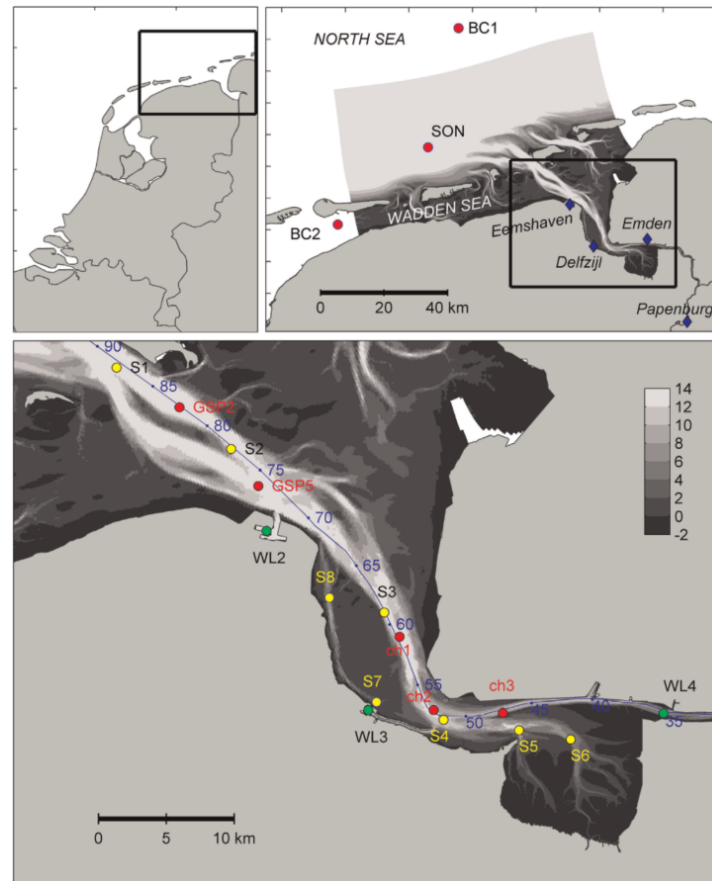


Figure E.1: Location of SSC measuring stations. (van Maren et al., 2015)

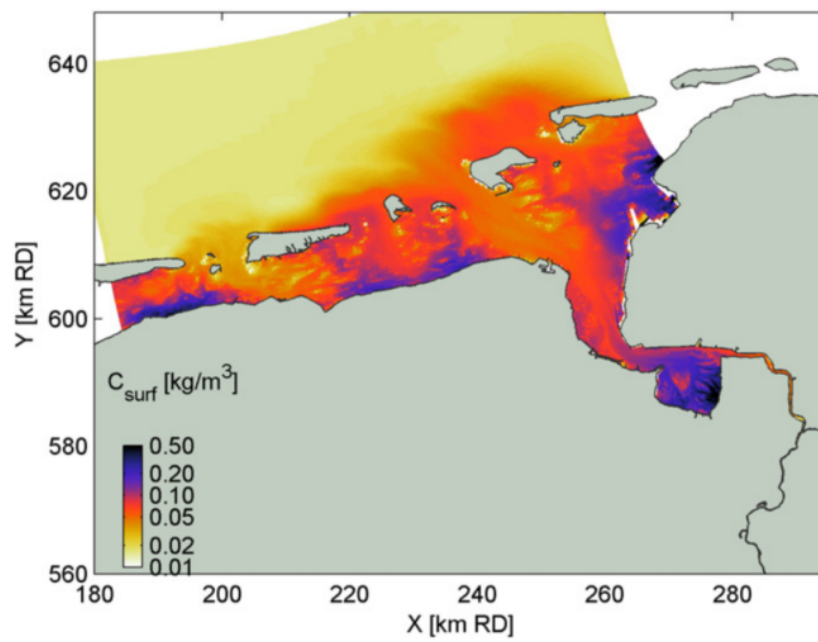
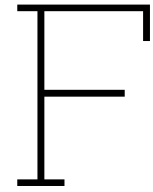


Figure E.2: Computed average SSC levels according van Maren et al., 2016



The conceptual model

When using a numerical model, it is important to first have a clear idea of what your goal is when using the model. To properly determine the aim of the research, a good analysis must be made. This analysis results in the conceptual model. The conceptual model describes how the system functions and which processes are important to include and which processes can be ignored. In addition, it describes other preconditions of the research and how certain validation can be obtained. It forms the framework of the numerical model. The used numerical model is only a tool for the conceptual model.

Figure F.1 shows the position of the conceptual model within the study. Here it can be seen that the conceptual model follows from the problem analysis and a good system understanding. Only when the conceptual model is in order, the numerical model and the numerical simulations can be performed well (Winterwerp et al., 2022). The outcomes of this numerical simulations subsequently contributes to the improvement of the conceptual model.

A common way to set up the conceptual model is in a flowchart with the different processes and variables, but it can also be drawn up purely textually or visually. However, it is important that the conceptual model is not fixed. It is not a static concept, but it can develop during research. The results of the numerical model can contribute to the understanding of the system and thus to the improvement of the conceptual model. New insights can therefore always improve the model to subsequently achieve even better insights (Winterwerp et al., 2022).

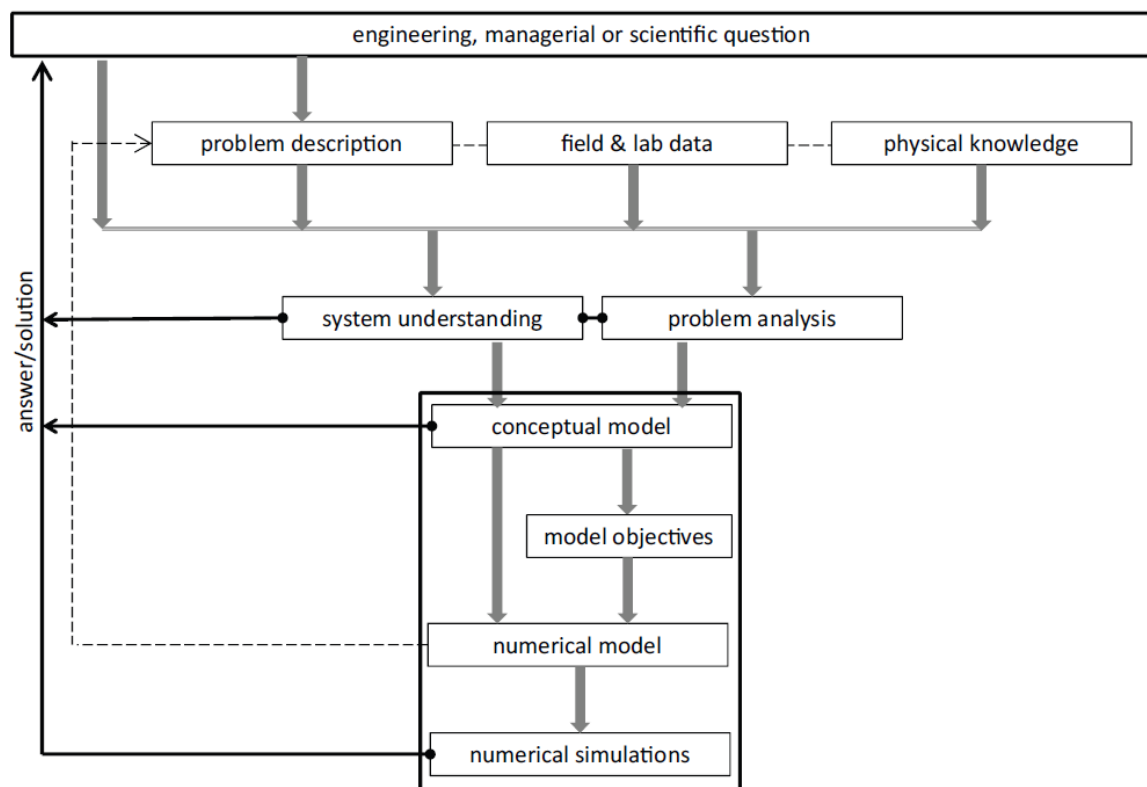


Figure F.1: The steps of the conceptual model, schematically displayed (Winterwerp et al., 2022)



Creation tidal boundary Polder Breebaart

Because a damped tidal regime operates on Polder Breebaart, a standard harmonic tidal signal cannot simply be used for the boundary condition. The tides in Polder Breebaart enter through a culvert in the sea dike. The maximum water level in the polder can be regulated with sliders in the culvert (Peletier et al., 2004). In the early years after the opening, experiments were carried out with the position of these gates in order to maximize the tidal difference in the polder. This experiment shows that when the maximum water level is lowered, the tidal range increases. However, a lower HW means that a smaller part of the polder will be flooded and influenced by the tidal movement. At the end of the experiment, the gates were set to a maximum level of 0.15 m +NAP. At that time the average tidal difference turned out to be approximately 35 cm (Esselink and Berg, 2004). Over time, this tidal difference has become smaller due to other sliding positions, together with morphological processes such as accumulation and a smaller tidal prism. Actual water level measurements show that the water level currently varies from -0.1 m +NAP to +0.1 m +NAP (Esselink, 2022).

By combining different harmonic components, an attempt has been made to create a tidal signal that corresponds in terms of amplitude and asymmetry with the signal that occurs in Polder Breebaart according to Esselink and Berg, 2004, showed in Figure G.1. This signal is created in python and the code is showed below. This code result in a tidal signal which is showed in Figure G.2. Only lunar tidal constituents are used to create this tidal signal. The amplitudes of the used tidal constituents are showed in table G.1.

Tidal constituent	Period [s]	Amplitude [m]
A	-	0
M2	44100	0.09
M4	22050	-0.025
M6	14700	0.011
M8	11025	0.004
M10	8820	-

Table G.1: Tidal constituents with their periods and amplitudes

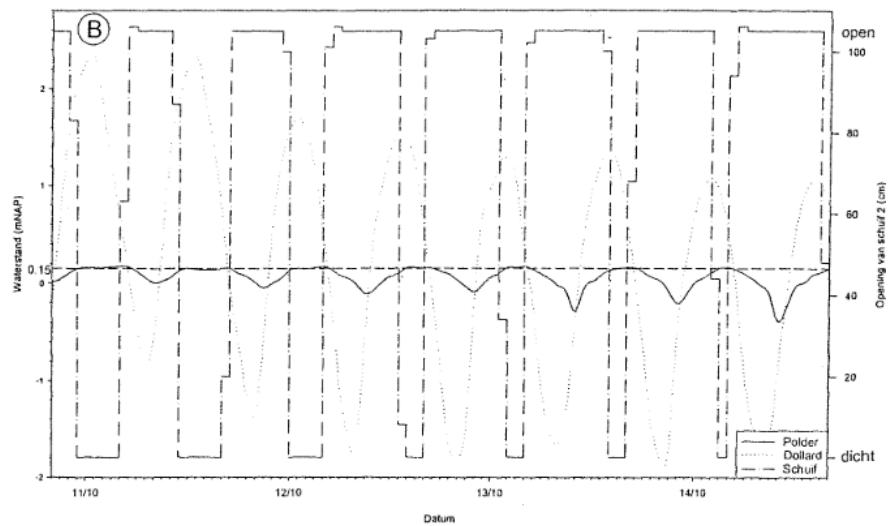
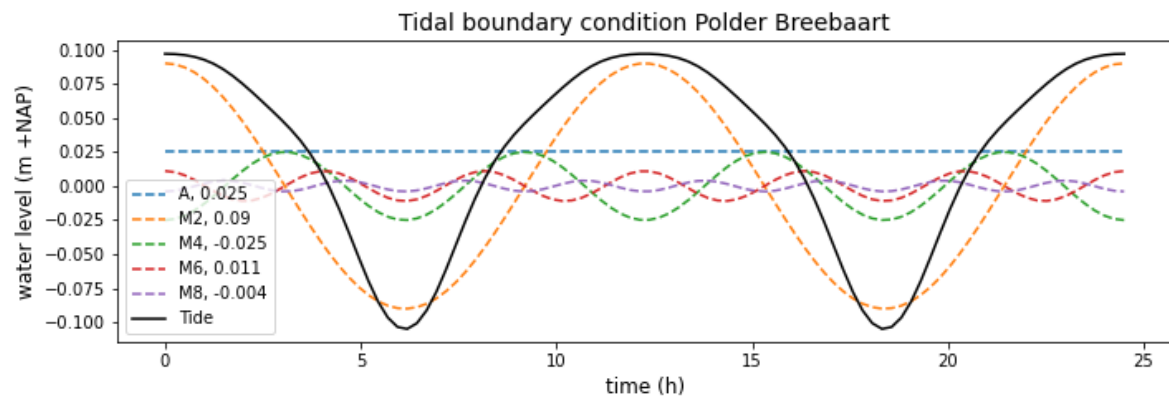


Figure G.1: Waterlevels in Polder Breebaart, oktober 2003 (Esselink and Berg, 2004)



tidal minimum = -0.105 m, tidal maximum = 0.097 m, tidal range = 0.202 m

Figure G.2: Tidal boundary condition of Polder Breebaart

H

Meteorological forcing condition

Because wind-generated waves have an important influence on the bed shear stresses and thus influence the resuspension, it is important that realistic wind data is obtained and processed. To obtain wind data, the database of the Royal Netherlands Meteorological Institute (KNMI) is used. The data from station Nieuw Beerta (weather station number 286) is used since this is the nearest weather station to the location of the project. Figure H.1 shows the Dutch weather stations of the KNMI and the project location.

From this data the wind data is extracted and used as boundary condition for the model. The data When the wind direction in the data was variable, the direction in the data indicates 990. Since this is not a useful direction for the D3D model, these data lines have been removed. For the calibration model of Polder Breebaart is the data used since August 2020, since this is the starting time of the used bed levels. For the realignment project area is the data since 2015 used, to have a longer time span of weather data.



Figure H.1: KNMI weather stations of the Netherlands with a red triangle on the location of the project (source: <https://www.logboekweer.nl/>)

The python code which is used to extract the wind data from the KNMI .txt file and make the D3D .tim wind input file is the following:

```

1 import numpy as np
2 # import matplotlib.pyplot as plt
3 import pandas as pd
4
5 #importing data
6 weerdata1120 = pd.read_csv('uurgeg_286_2011-2020.txt', delimiter=',', skiprows=30,
7                             parse_dates=True, index_col=1)
8 weerdata2130 = pd.read_csv('uurgeg_286_2021-2030.txt', delimiter=',', skiprows=30,
9                             parse_dates=True, index_col=1)
10 weerdata = pd.concat([weerdata1120, weerdata2130])
11 weerdata = weerdata.drop(weerdata.index[weerdata.index < '2020-08-01'])
12
13 #editting data & count minutes
14 weerdata.index.name = 'date'
15 weerdata['time'] = weerdata.index + pd.to_timedelta(weerdata['HH'], unit='h')
16 weerdata['minutes'] = (weerdata.time - pd.to_datetime('2020-08-01 01:00:00')).astype('
17     timedelta64[m]').astype(int)
18 weerdata['speed'] = (weerdata['FF'] / 10).astype(int)
19 weerdata['dir'] = weerdata['DD']
20 weerdata = weerdata.drop(['# STN', 'HH', 'DD', 'FH', 'FF', 'FX', 'T', 'T10N',
21     'TD', 'SQ', 'Q', 'DR', 'RH', 'P', 'VV', 'N', 'U', 'WW', 'IX',
22     'M', 'R', 'S', 'O', 'Y', 'time'], axis=1)
23
24 # delete wrong directions
25 weerdata = weerdata[weerdata.dir < 990]
26
27 # print(weerdata)
28 # weerdata.reset_index()
29 # # weerdata.set_index('minutes')
30 # print(weerdata)
31
32 np.savetxt(r'real_winddata_since_1aug2020.tim', weerdata.values, fmt='% d')

```



Main calibration problems and solutions

A large number of different problems and challenges have arisen during the calibration phase. The main issues are outlined below, along with the solutions that fixed them. Part of the problems boiled down to software imperfections. These problems have been fixed in updated versions of the software in collaboration with the software development team.

problem

Incoming sediment settles only close to the entrance

solution

by adding the effects of wind and especially the wind-generated waves, there is more resuspension of sediment and the sediment is transported further into the polder.

problem

Wind and waves do not create the right results, but almost all the sediment is eroded away

solution

Calculating with newer versions of the software solves this problem

problem

The fetch length and fetch depth are calculated at the beginning of the simulation (for all points and all directions), but when the circumstances change (tide etc.), the fetch doesn't change, creating unrealistic fetch lengths and depths.

solution

By adding keyword 'Tifetchcomp', the fetch conditions are recalculated according this statement (in seconds). Tifetchcomp is set to 7200 s

problem

At some cells, the wave height was, despite a set value of $\gamma_{max} = 0.7$, very height compared to the water depth. For example, at some cells, a wave height of 0.2 meter occurs, while the local depth was just 0.05 meter. This waves result in very high shear stresses

solution

This problem is solved by the software develop team. The γ_{max} parameter was not applied correctly in the numerical calculation. This problem is fixed starting from Delft3D FM DIMR set version 2.21.11.76524

problem

In some very shallow grid cells, extremely high bed shear stresses occur, causing a lot of erosion to take place here.

solution

By adding the keyword $E_{pshu} = 0.1$ no morphological calculations are performed for cells shallower

than 10 cm (= 0.1 m). As a result, these shear stresses have no effect on the morphology.

problem

At certain moments in the simulation, an extremely high concentration (million kg/m³) occurs in certain grid cells without a cause being identified (no high flow/waves, not shallow cells). This concentration then spreads to surrounding cells, resulting in extremely high sedimentation.

solution

this has been solved by the software development team and the keyword 'testdryingflooding' has been created for this. To prevent this, testdryingflooding = 2 can be added in newer software versions.

problem

The SSC of a few single cells continues to rise endlessly to insane concentrations.

solution

There is a manual upper limit on what SSC values one can get. This limit is set at $UpperLimitSSC = 20 \text{ kg/m}^3$. This is 100 times higher than the incoming concentration on the boundary conditions

problem

Extreme and inexplicably high shear stresses occur in some cells.

solution

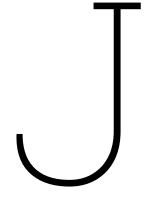
This problem has been solved because it has been raised with software development and they have resolved it in newer software versions.

problem

The shear stresses in the shallow cells are much too high, so that only erosion can take place here.

solution

In the shallow cells, the relative influence of wave-induced bed shear stress is quite high. By adding the parameter 'ftauw' the influence of the wave-induced bed shear stresses is limited. As a result, it scales better with the height of the current-induced bed shear stresses



Assessment methods

Evaluating the results obtained from the numerical models is an essential part of developing a credible morphological model. The data is used to create the starting conditions, but also to compare the model results with, to determine whether the model gives reliable results. This evaluation must be done on a reliable basis and may not be done just subjectively. Sutherland et al. (2004) have described how different model quantification methods can be used to quantify morphological models. In their paper they show that the quality of a morphodynamic model can be judged on the basis of bias, accuracy and skill. In this research study, it is attempted to assess the quality of the calibration in all three ways.

A python function is written to evaluate the model results with these different methods. These different evaluations are described separately in the headings below. All methods were also performed for just the southern part or the northern part of the polder in order to properly assess the quality of the model between the front and back of the area.

J.1. Sediment import

The total amount of sediment imported by the polder is an important criterion that the numerical model must meet since this comes in line with the aim of the research. This method is in line with the 'bias' method of Sutherland et al. (2004). For every model result, the total imported sediment volume is compared to the volume. In the python function, these method is calculated as 'bias', 'bias_onder' and 'bias_boven'. Here, '_onder' or '_boven' calculates the rating for only the bottom or top part. In the data, a difference can be observe rd between the accumulation in the southern part and the northern part of the polder. With 'sed_part_under' in the python function it is determined which percentage of the total sedimentation takes place southern of the bottleneck in the polder. With 'sed_part_50' is determined which percentage of the total sedimentation takes place southern of the cross-section where in the data is the divide of 50% of the total accumulation volume in the polder.

J.2. Mean absolute error

To assess the accuracy of a numerical model simulation, the mean absolute error (MAE) is calculated. By subtracting the change in bottom level according to the data from the change in bottom level according to the model results, the spatial varying errors of accumulation were obtained. By taking the mean of the absolute values of the spatially varying errors, the MAE is determined. In a perfect model, this value would be zero. When comparing model results, a lower value indicates a more accurate result.

$$MAE = \langle |\Delta z_{mod} - \Delta z_{meas}| \rangle \quad (J.1)$$

In this equation, Δz represents the change in bed level for a grid cell, *mod* stands for the modelled value and *meas* for the measured data. The $\langle \rangle$ denotes the spatial average value. In the python function, these method is calculated with 'mean_abs_err', 'mean_abs_err_onder' and 'mean_abs_err_boven'.

J.3. Brier Skill Score

The skill of the model result is calculated with the Brier Skill Score (BSS) according to Sutherland et al. (2004). Sutherland argues that the BSS is the best way to assess the behavior of a morphodynamic model because BSS is the most 'honest'. The BSS is calculated with equation J.2. This gives a relative volume change. This definition of the BSS has been extracted from the assessment criteria in Van der Wegen et al. (2017).

$$BSS = 1 - \frac{\langle (\Delta vol_{mod} - \Delta vol_{meas})^2 \rangle}{\langle \Delta vol_{meas}^2 \rangle} \quad (J.2)$$

In this equation, Δvol represents the change in bed level volume for a grid cell, *mod* stands for the modelled value and *meas* for the measured data. The $\langle \rangle$ again denotes the spatial average value. In the python function, these method is calculated with 'BSS', 'BSS_ponder', 'BSS_boven', 'BSS_accu' and 'BSS_accu_boven'.

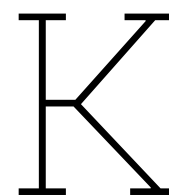
J.4. The python function

```

1 def BrierSkillScore(file, loc=-1, devide = 7036580, devide50 = 7037780):
2     #return BSS, BSS_ponder, BSS_boven, BSS_accu, BSS_accu_boven, mean_abs_err,
3     mean_abs_err_ponder, mean_abs_err_boven, bias, bias_ponder, bias_boven, sed_part_ponder,
4     sed_part_50
5     dvol_mod = (file.mesh2d_cum_ero_accu[loc,:]-file.mesh2d_cum_ero_accu[0,:]) * file.
6     mesh2d_flowelem_ba
7     dvol_meas = data_xr_dz * file.mesh2d_flowelem_ba
8     BSS = (1-((dvol_mod - dvol_meas)**2).mean() / (dvol_meas**2).mean())
9
10    dvol_mod_ponder = xr.where(file.mesh2d_face_y < devide, dvol_mod, np.nan)
11    dvol_meas_ponder = xr.where(file.mesh2d_face_y < devide, dvol_meas, np.nan)
12    BSS_ponder = (1-((dvol_mod_ponder - dvol_meas_ponder)**2).mean() / (dvol_meas_ponder**2).mean()
13    ())
14
15    dvol_mod_boven = xr.where(file.mesh2d_face_y > devide, dvol_mod, np.nan)
16    dvol_meas_boven = xr.where(file.mesh2d_face_y > devide, dvol_meas, np.nan)
17    BSS_boven = (1-((dvol_mod_boven - dvol_meas_boven)**2).mean() / (dvol_meas_boven**2).mean()
18    ())
19
20    dvol_mod_accu = xr.where(data_xr_dz > 0, dvol_mod, np.nan)
21    dvol_meas_accu = xr.where(data_xr_dz > 0, dvol_meas, np.nan)
22    BSS_accu = (1-((dvol_mod_accu - dvol_meas_accu)**2).mean() / (dvol_meas_accu**2).mean())
23
24    dvol_mod_accu_boven = xr.where(data_xr_dz > 0, dvol_mod_boven, np.nan)
25    dvol_meas_accu_boven = xr.where(data_xr_dz > 0, dvol_meas_boven, np.nan)
26    BSS_accu_boven = (1-((dvol_mod_accu_boven - dvol_meas_accu_boven)**2).mean() / (
27    dvol_meas_accu_boven**2).mean())
28
29    abs_err = abs((file.mesh2d_cum_ero_accu[loc,:]-data_xr_dz))
30    mean_abs_err = abs_err.mean()
31
32    abs_err_ponder = xr.where(file.mesh2d_face_y < devide, abs_err, np.nan)
33    mean_abs_err_ponder = abs_err_ponder.mean()
34
35    abs_err_boven = xr.where(file.mesh2d_face_y > devide, abs_err, np.nan)
36    mean_abs_err_boven = abs_err_boven.mean()
37
38    bias = (dvol_mod-dvol_meas).sum()
39
40    bias_ponder = (dvol_mod_ponder-dvol_meas_ponder).sum()
41
42    bias_boven = (dvol_mod_boven-dvol_meas_boven).sum()
43
44    sed_part_ponder = (dvol_mod_ponder.sum()/dvol_mod.sum())
45
46    dvol_mod_50 = xr.where(file.mesh2d_face_y < devide50, dvol_mod, np.nan)
47    sed_part_50 = (dvol_mod_50.sum()/dvol_mod.sum())

```

```
42 #     return np.round(BSS.data,4),np.round(BSS_onder.data,4),np.round(BSS_accu.data,4),np.  
    round(rel_abs_err.data,4), np.round(rel_abs_err_onder.data,4), np.round(sed_part_onder.  
    data,4)  
43 return BSS.data, BSS_onder.data, BSS_boven.data, BSS_accu.data, BSS_accu_boven.data,  
    mean_abs_err.data, mean_abs_err_onder.data, mean_abs_err_boven.data, bias.data,  
    bias_onder.data, bias_boven.data, sed_part_onder.data, sed_part_50.data
```



Creation bed level change map Polder Breebaart

For calibration it is important that the change in bed levels in Polder Breebaart is mapped. Bed level data from various measurement moments has been made available by Peter Esselink (Esselink, P, March 2022). The data consists of three different measurement moments, namely the measurement by the contractor in March 2020 and two measurements with an RTK-drone in August 2020 and August 2021. The March 2020 data set has a different structure than the two other data sets. The March 2020 data set consists of a number of cross-sections that have been measured. The two other data sets consist of bed level data covering the entire area with a resolution of 1 m x 1 m.

To compare the data from March 2020 with the other two, an interpolation is performed between the cross-sections. These cross-sections and interpolation of this data are shown in the upper left figure from Figure K.1. In the upper middle and upper right figure of Figure K.1 you can see that although the data of August 2020 and August 2021 were obtained in the same way, they are not directly of the same format. The August 2020 data covers a much larger area than the August 2021 data. In addition, there is a large piece of land that was a lot higher in 2020 than in 2021. After inquiry it appears that this is because in 2021 the reeds had already been mowed before the measurement was taken. This creates an inequality in the measured height data. This difference in the data should therefore not be included in the calculation because otherwise the calculation would not be representative.

The area with the mown reed has been manually cut from the data. A polygon has been made which encloses the data to be removed as well as possible. Subsequently, only the data that lies outside that polygon has been subtracted from each other. Figure K.2 shows which data has been left out of consideration. By subtracting data sets with each other, the maps of Figure K.1 are created. The map in the middle of this figure is used to calibrate the model since this map shows the change in bed level between two comparable data sets over a year.

The python code which is used to analyse the data sets and to create the maps in Figure K.1 and K.2 is the following:

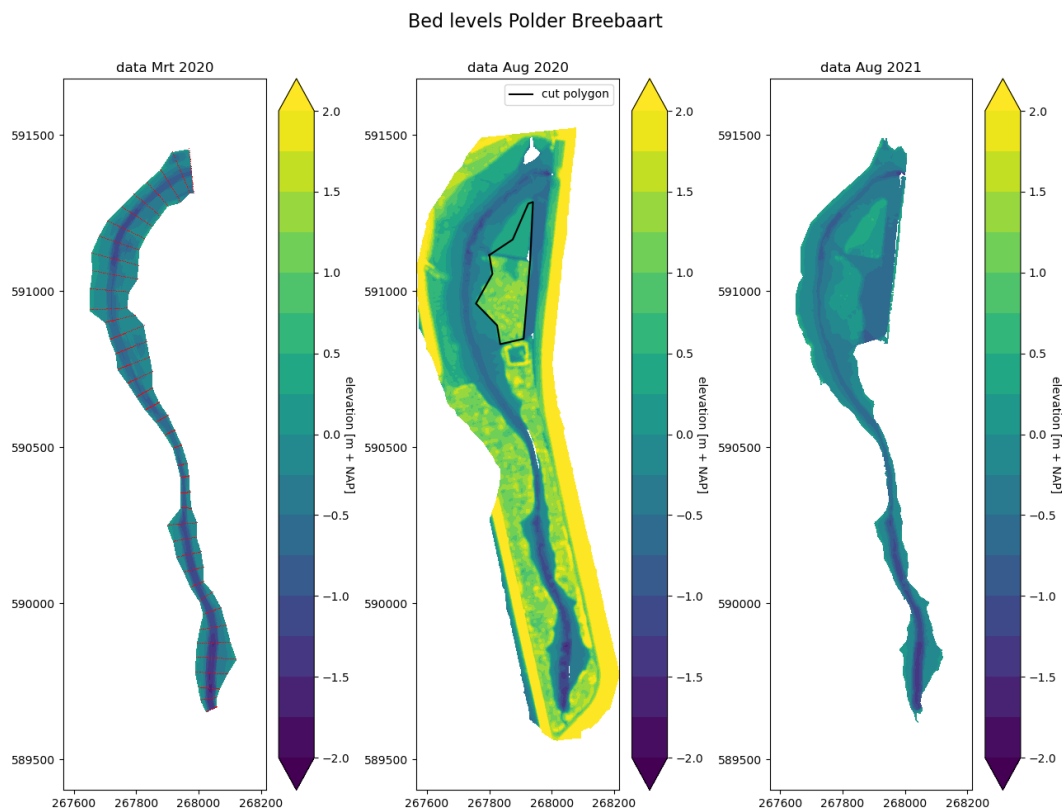


Figure K.1: Upper three: the bed levels in Mrt 2020 (with measurement cross-sections in red), Aug 2020 and Aug 2021. Bottom three: the difference in bed levels between data sets. At the bottom of the plots is the total volume change of sediment showed. The red line shows the divide between the upper part and lower part for the volume change calculation. The black polygon represents the data which is not included in the data analysis due to differences in reed height.

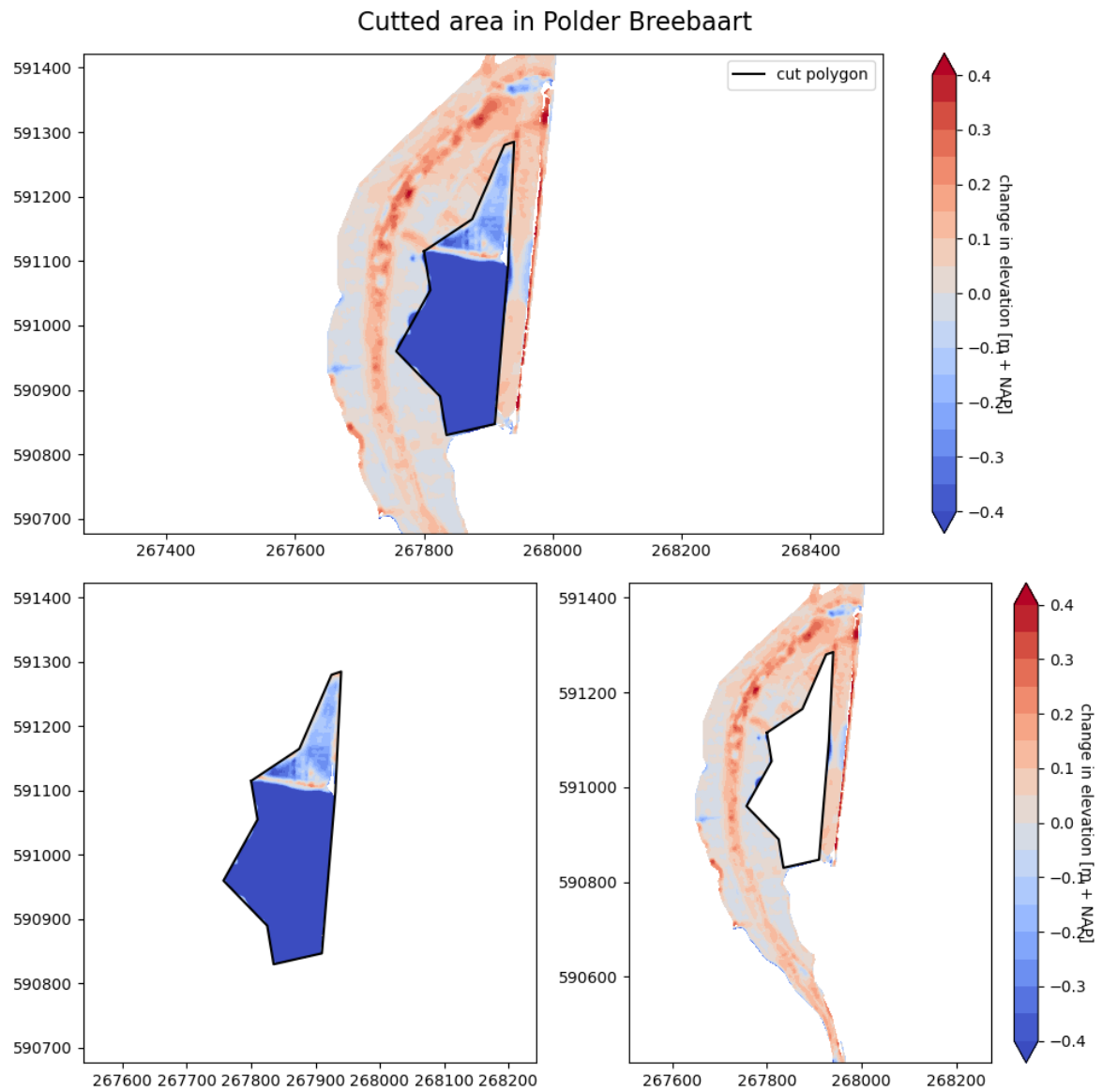


Figure K.2: The area which is not taken in consideration, shown on a map with bed level change



Numerical model choice

In this appendix, the choice of the numerical model is explained briefly. First, some general explanation of a numerical coastal model is presented, followed by some explanation how this is implemented in this thesis research and finally some elaboration about the differences between a rectangular grid and a triangular grid.

L.1. Numerical coastal model

Coastal models are numerical models used to simulate or analyse the physical processes occurring in coastal areas. These models can be used to predict or analyse and get more insight about the movement of water, sediment, and pollutants, as well as the resulting changes in the shape of the coastline and the bathymetry. There are different types of coastal models, including empirical models, process-based models, and coupled models. Empirical models use statistical relationships to describe the behavior of the coastal system, while process-based models simulate the physical processes occurring in the coastal environment. Coupled models combine both empirical and process-based approaches. In addition, coastal models can focus on hydrodynamics, waves and morphodynamics.

Hydrodynamic models are used to simulate the movement of water in the coastal zone, including currents, tides, and other water movements. These models can help predict the transport of sediments as well as the effects of storms and other natural events on the coast. Wave models, on the other hand, are used to simulate the behavior of waves in the coastal zone. These models can help predict the height and direction of waves, as well as their effects on the coast, such as erosion and flooding. Morphological models are used to simulate the long-term evolution of the bathymetry. These models can help predict how the bed will change over time due to natural processes such as erosion and sediment transport.

Each type of coastal model has its own strengths and limitations, and different models are best suited for different types of applications. For example, hydrodynamic models are best suited for simulating short-term water movements, while morphological models are best suited for simulating long-term coastal evolution or bed formation.

Delft3D is a process-based numerical model that can be used for simulating a wide range of coastal and estuarine processes, including water flow, wave propagation, and sediment transport. It is a coupled model that combines hydrodynamic, wave, and sediment transport models to simulate the behavior of the coastal system in a comprehensive and physically-realistic way.

L.1.1. Model calibration

Model calibration is the process of adjusting the model parameters and inputs to better match the observed data from the real-world system being modeled. This is a necessary step in the use of numerical coastal models because all models are simplifications of the real world and therefore cannot perfectly reproduce the behavior of the system. Calibration improves the accuracy of predictions and identifies any limitations or biases in the model. By comparing the model's predictions to observed data, it can be ensured that the model accurately represents the real-world system being modeled, and can make necessary adjustments to improve the accuracy of predictions. Additionally, identifying

any limitations or biases in the model through calibration allows for improvements to be made, making the model more useful and reliable for a variety of applications. Overall, calibration is a crucial step in ensuring that morphodynamic models are accurate and effective tools for understanding and predicting the behavior of coastal systems.

As the model needs to predict future conditions for an area yet to be developed, it cannot be calibrated using data from the project location itself. To ensure the most accurate results, it is important to find a location that is as comparable as possible to the project location for the model's calibration.

L.1.2. Polder Breebaart for calibration

The Breebaart calibration is subsequently used to develop a model for the project area. It should be realized however that the main goal of Polder Breebaarts design is to create nature reserve. In contrast, the main purpose of the project area is to extract mud from the Ems Dollard estuary to reduce turbidity. However, the creation of nature in the design area is also an important aspect that is promoted as much as possible.

In Polder Breebaart, the tide flows into the polder through a culvert, which reduces the maximum tidal range and results in a small tidal range. Due to the large size of the design area, the entrance for water flow must have a larger cross-sectional area than a culvert. A calculation using O'Brien's equations (see Section 2.3.8) shows that with a forecast area of 750 hectares, a tidal range of 3 meters, and assuming that 1/4th of the calculated prism is limited by tidal flats, the cross-section must be more than 1300 m^2 for equilibrium. This is calculated with $a = 7.75 * 10^{-5}$, according to Stive and Rakhorst (2008).

$$A_c = 750 * 10000 * 3/4 * 3 * a \quad (\text{L.1})$$

Another important difference between Polder Breebaart and the new project area is the approach to create the intertidal area. Polder Breebaart was actively created and a creek was excavated, while the intention for the new project area is to rely on natural dynamics as much as possible. Additionally, the new area is too large for extensive engineering work without incurring high costs. The last major difference is the size of the area, with Polder Breebaart covering 63 hectares and the new project area being 10 to 35 times larger.

L.1.3. Grid and bed schematization

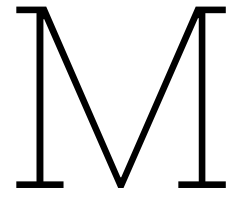
The grid and bed schematization in numerical modeling is important because it determines the resolution and accuracy of the model. A well-defined grid allows for a more accurate representation of the physical processes being simulated, while a poorly defined grid can lead to numerical errors and inaccurate results. In addition, the bed schematization is important because it determines the geometry of the modeled domain and how the various physical processes, such as flow and sediment transport, are represented within the model. Proper bed schematization is crucial for accurately predicting the evolution of the system over time.

L.2. Rectangular grid vs. triangular grid

In numerical coastal modeling, the choice of grid can significantly affect the efficiency and accuracy of the simulation. A rectangular grid is often considered more efficient than a triangular grid for several reasons. First, rectangular grids have a higher degree of orthogonality, meaning that the grid lines are perpendicular to each other. This orthogonality leads to a smoother and more uniform grid, which can help reduce numerical errors and improve the accuracy of the simulation. In contrast, triangular grids can have more irregular shapes and angles, which can result in less smoothness and greater numerical errors (Deltares, 2021).

Moreover, rectangular grids are often easier to generate and manipulate computationally. Because the edges of a rectangular grid are parallel to the x and y axes, they can be more easily aligned with the boundaries and coastlines of the simulation domain. This alignment can lead to faster computation times and better convergence properties, as the rectangular grid can more accurately capture the shape and dynamics of the coastline. Triangular grids, on the other hand, can require more complex algorithms to generate and manipulate, and may result in higher computation times and lower simulation accuracy. Overall, the efficiency and accuracy advantages of rectangular grids determines the

choice for a rectangular grid for the numerical coastal modeling with Delft3D FM of the project location (Symonds et al., 2016).



Domain boundary of realignment project area

As location for the realignment project area, a region located between the villages of Nieuwolda, Woldendorp and Borgsweer, and the N362 is determined. A comprehensive area analysis was conducted by Fiet et al. (2018) and LAMA (2020), and this land was found to be suitable for the project. The area does not contain any villages, but there are some separate farms that should be removed. Additionally, there are many wind turbines and there is a solar park present. The majority of the area is composed of agricultural land.

The domain of 'Bathymetry5' has the largest area and were determined with the advice of Matthijs Buurman, Program Manager for Coastal Development in Groningen, and derived from the inspiration report of LAMA (Fiet et al., 2018; LAMA, 2020). Figure M.1 shows the domain in this inspiration report. This domain corresponds to the domain of Bat5 in Figure M.3.

The domain of 'Bathymetry3' has a smaller surface area and was determined with the advice of Albert Vos, Program Manager for IBP Vloed, and taken from the report 'Ziel in Landschap' (van Paridon x de Groot | abe veenstra landschapsarchitect, 2020). Figure M.2 shows the domain in this report. This domain corresponds to the domain of Bat3 in Figure M.3.



Figure M.1: The possible domain of the project area according Fiet et al. (2018) and LAMA (2020)

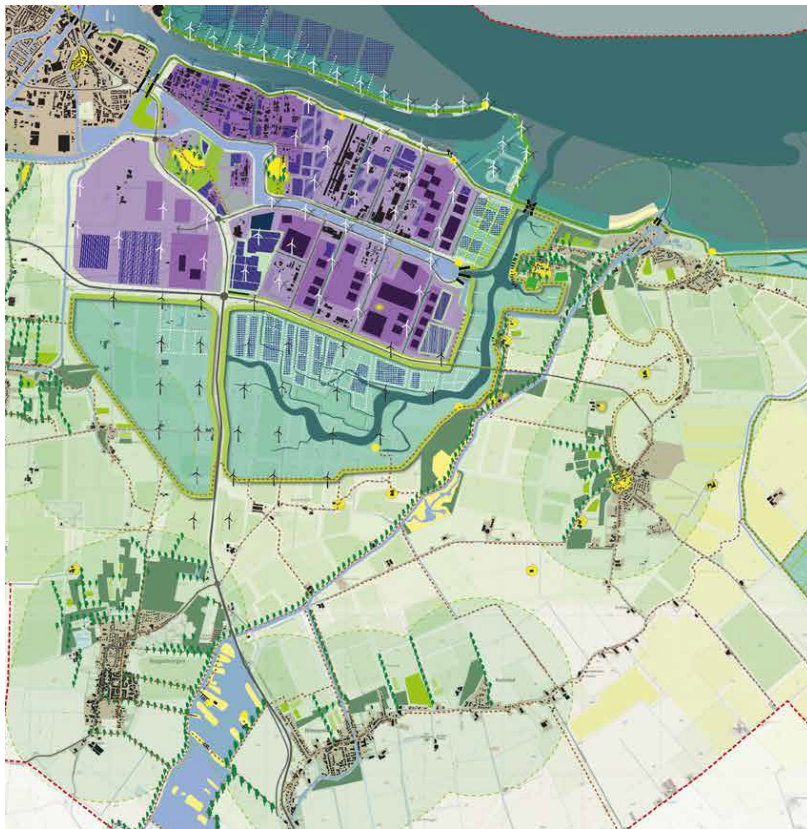


Figure M.2: The possible domain of the project area according van Paridon x de Groot | abe veenstra landschapsarchitect (2020)

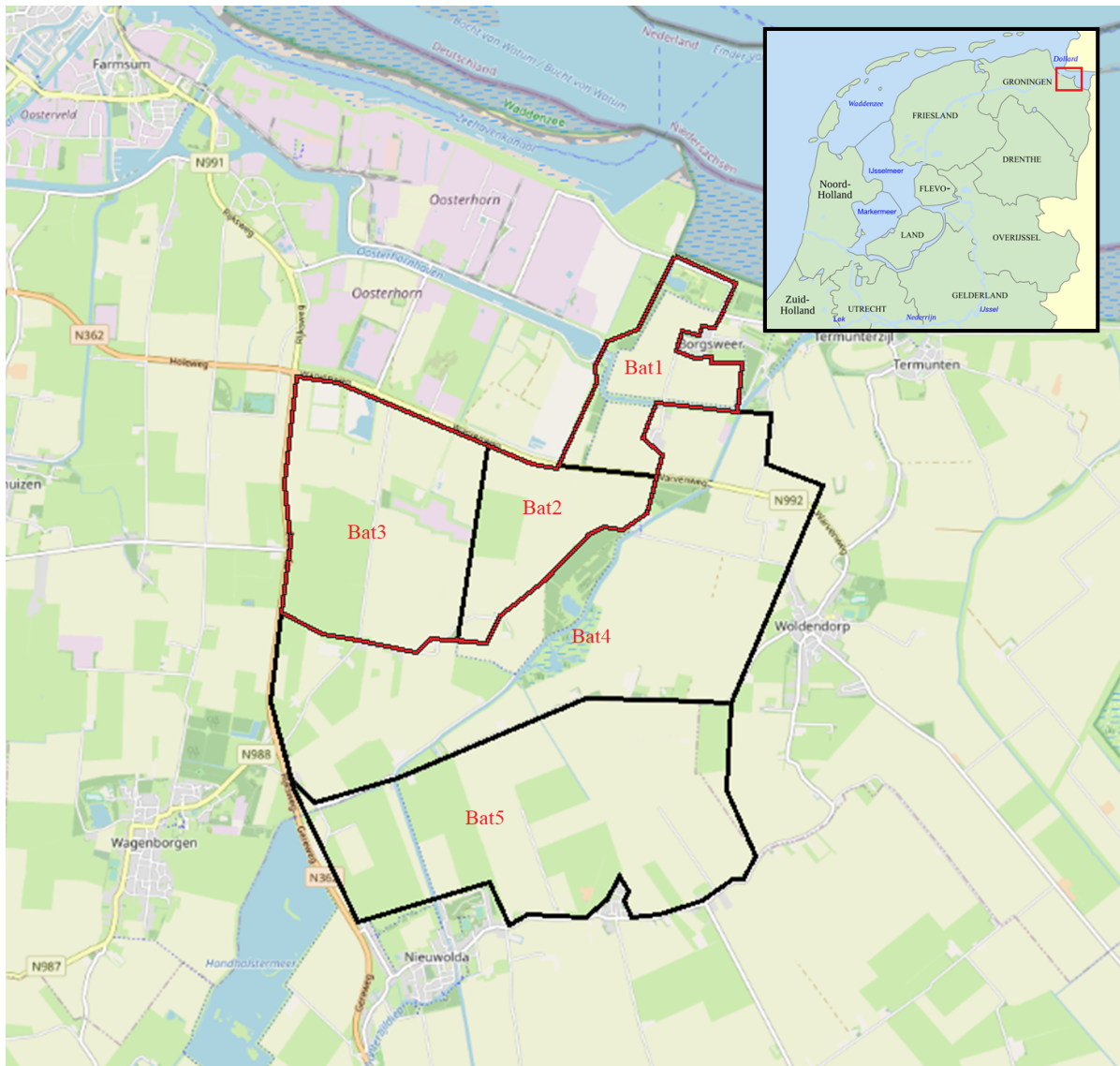


Figure M.3: All the domains, each larger domain contains the area of the smaller domains. Bathymetry5 (the outer lines) and Bathymetry3 (outlined with the black-red line) are designed using the domains in Figure M.1 and M.2 respectively.



Impact of coordinate system on Polder Breebaart model

The influence of using the wrong coordinate system for the Polder Breebaart model is an important consideration in this study. The model was originally created using OpenStreetMap in the coordinate system *EPSG:3857 WGS 84 / Pseudo-Mercator*. However, the elevation data used in the study was obtained in the coordinate system *EPSG:28992 Amersfoort / RD New*, which required the elevation data to be projected onto the model's coordinate system. This projection resulted in scaling all x and y directions by a factor of approximately 1.5, which increased the surface area and volume of the accumulation by a factor of 2.25. As a consequence, there was a discrepancy of about a factor of 2.25 between the data analysis and the calibration model.

The scaling of the surface area could affect the system's response to incoming sediment, as the sediment needs to be transported further to spatially match the effect of the data. However, the study found that the sediment import is approximately linearly related to the polder's surface area, which limits the impact of the scaling on the system's response. In addition, the research found that the sediment import is not linearly related to the tidal range, suggesting that the water levels should not be scaled. Nevertheless, it is important to consider this when working with the model further. It is worth noting that the water level boundary condition was kept constant despite the scaling of the surface area, which resulted in the prism being scaled to the same extent as the polder's surface area.

Impact of Coordinate System on Polder Breebaart Model

The Polder Breebaart grid was created using OpenStreetMap in the coordinate system *EPSG:3857 WGS 84 / Pseudo-Mercator*. However, the elevation data obtained was in the coordinate system *EPSG:28992 Amersfoort / RD New*. To match this, the elevation data was projected onto the model's coordinate system. This projection resulted in scaling of all x and y directions by a factor of approximately 1.5, which in turn scaled the surfaces by a factor of $1.5^2 = 2.25$. As a result, the volume of accumulation was also increased by a factor of 2.25, leading to a difference of about 2.25 between the data analysis and the calibration model. It is worth noting that while the surface area has been scaled, the water level boundary condition remains the same. Consequently, the prism is scaled to the same degree as the polders surface area.

The scaling of the surface area could cause the system to respond slightly differently to incoming sediment, as the sediment must be transported further to spatially match the distribution of the data. However, the research has shown that the sediment import is approximately linearly related to the size of the polder, and therefore, this scaling would only have a limited influence. It is worth noting that the sediment import is not linearly related to the tidal range. If this is accurate, the water levels should not be scaled. Nevertheless, it is important to consider this factor when working with the model further.